ANGIOTENSIN-CONVERTING ENZYME CLEAVAGE OF THE ALZHEIMER'S BETA-AMYLOID PEPTIDE

Kate Larmuth

Thesis Presented for the Degree of

DOCTOR OF PHILOSOPHY

In the Division of Medical Biochemistry

University of Cape Town

November 2015

To my family in memory of

Betty Larmuth

DECLARATION

This dissertation is the result of my own work and includes nothing, which is the outcome of work done in collaboration except where specifically indicated in the text. It has not been previously submitted, in part or whole, to any university of institution for any degree, diploma, or other qualification.

Signed: Signed by candidate

Signature removed

Date: 19.07.2015

Kate Larmuth

University of Cape Town

ABSTRACT

Angiotensin-1 converting enzyme (ACE) is a zinc metallopeptidase that consists of two homologous catalytic domains (N and C) with different substrate specificities. ACE is a central component of the intrinsic brain renin angiotensin-aldosterone system (BRAAS), well renowned as the regulator of blood pressure. The BRAAS has alternate functions that extend beyond fluid and blood pressure homeostasis into areas such as neurological function. As a result, it is implicated in many neurodegenerative diseases including Alzheimer's disease (AD). ACE's specific mechanistic role in AD is not entirely clear and is somewhat controversial. However, it has been shown that ACE hydrolyses the amyloid beta (Aβ) peptide, the putative causative agent of AD.

This study aimed to investigate the molecular basis of ACE hydrolysis of Aβ by determining: 1) the kinetic parameters of five different forms of human ACE with various N-terminal amyloid beta (Aβ) substrates; 2) the specific active site determinants of Aβ-domain selectivity; and 3) the high-resolution crystal structures of the N-domain of ACE in complex with Aβ(1-16), Aβ(10-16), Aβ(4-10), the FRET Aβ(4-10)Y and Aβ(35-42) peptides. For the physiological Aβ(1-16) peptide, a novel ACE cleavage site was found at His14/Gln15. Furthermore, Aβ(1-16) was preferentially cleaved by the truncated N-domain; however, the presence of an inactive C-domain in full-length ACE greatly reduced enzyme activity and affected domain-selectivity. Two fluorogenic substrates, designed specifically to assess ACE's mechanism of Aβ hydrolysis Aβ(4-10)Q and Aβ(4-10)Y, underwent endoproteolytic cleavage at the Asp7/Ser8 bond. The Aβ(4-10)Q peptide was a poor substrate of ACE but was N-selective, with a selectivity driven largely by interactions with the domain-specific residues of the S2 and S2' pockets. The selectivity of the S2' residues were confirmed with a similar, more physiological, fluorogenic Aβ(4-10)Y peptide. This work provides further understanding towards the substrate determinants of N-selectivity, highlighting the importance of the S2' Ser357. ACE C-domain hydrolysed Aβ(4-10)Y with modest efficiency compared to the other substrates, where hydrolysis under the same conditions did not occur. Moreover, Aβ(4-10)Y also displayed N-domain selectivity. In contrast to Aβ(1-16) and Aβ(410)Q, both sACE and the double C-domain (CC-sACE) construct showed positive domain cooperativity towards Aβ(4-10)Y. The high-resolution crystal structures of the N-domain in complex with five Aβ peptide fragments provided an overlapping, conserved, molecular mechanism of peptide binding and evidence of the enzyme's broad exoprotease activity. In addition to the kinetic and structural studies, ACE's signalling response to the N-selective Aβ(1-16) and Aβ(1-42) was investigated using immunodetection and mass spectrometry. Similar to the ACE inhibitor lisinopril, the Aβ peptides elicited ACE signalling by phosphorylation of the cytoplasmic Ser1270 residue and JNK activation. The signalling response of ACE was coupled to increased ACE activity and expression on treatment with Aβ(1-42). These studies allowed us to rationalise the increased ACE activity and expression found in AD, may arise through direct interactions with Aβ.

This work provides a kinetic, structural and mechanistic understanding of the selective cleavage of Aβ by the N and C catalytic sites of ACE. Due to the broad substrate specificity of the two domains of ACE, and the overarching N-selectivity of Aβ hydrolysis, these findings provide rationale for further *in vivo* pharmacological studies on the mechanism of action C-domain-selective inhibitors, in the context of AD

ACKNOWLEDGEMENTS

I would like to give my heart-felt thanks to Ed the-Iron-man Sturrock, for all your support both scientifically and as a friend, mentor, hero and a supervisor. Ed has made our lab not only a place of work but also an ACE family home. His persistence and steadfastness forms a pillar of support allowing us as students to explore science broadly. Thank you Ed, for your eloquence, honest critique and for knowing exactly when it was time for a long run in the forest or some serious swimming.

To Sylva, the ACE mother, my friend and confidante, who has my back in many, experimental and life, situations. Thank you for the runs, the lunchtime swimming laps and for all your support in so many ways! Without you, I would have been lost on many an occasion.

Then to my parents, Girvan (Da) and Lucielle (Mem), you are heroes to me on many fronts. I am so grateful for your existence, love and support throughout my scientific pursuits. You have and still do provide a safe haven for me whenever the mental and emotional demands of science and life take its toll. Thank you!

To Uncle John and Aunt Angela for your support and generosity, and love, I am so grateful that you have come into our lives! To Jacky and Wayne, your support, love and awesomeness I cannot do without I thank you both! James, my one and only brother! Good luck with your further scientific pursuits, and thank you for being there through mine!

This work would not have been completed without the help of some amazing people who happen to be my best friends. These folk kept me on course and sane:

Dunja, you have taught me so much in so many ways I cannot thank you enough. You helped ease the struggle of this work with our many mountain, climbing, tea, cake, pancake and costume dress up adventures. Thank you for your friendship and constant support again, on ALL fronts.

Charl meeting you in honours at Stellenbosch was pretty life changing. Through thick and thin you call me up, when I was crawling into a hole somewhere, to inspire me to carry on and heal. Thank you dude, for everything! I also have to include all the awesome surf missions, which helped me stay sane.

Jerome, you were my first big city friend! Your laid back (yet somehow still angry looking) and decisive take on life and surfing is seriously impressive and inspiring. Thank you for the beer, chicken and veggies dinners, the epic surf sessions and for your awesome company. All of which made the pursuit of this PhD so much easier.

Kapokkie! Isa! Van Nekkies tot UCT, climbing, banting en debattering maatjie! Baie baie dankie vir alles! You are always there to listen and give sound constructive advice and support, including gloves for the late night cold finger typing sessions. You are super special to me and again were integral in helping me through this process.

Adrian my love, I cannot quite explain how fantastic you have been motivationally. Taking on my troubles with a keen critical ear and supporting me with lots of love all the way from the Amazon. For this and for other reasons, too many to count, I thank you.

To my oldest friends, Theresa, Elsa, Bridgette and CJ, thank you for all the love, moments of crying, laughter and crazy adventures once more keeping me sane and supported. To Heather and Niel thank you so much for giving me a home and a cat on loan.

Then to the people intrinsically connected to the work contained in this thesis, the members of the Blackburn Lab, I thank you. A special thanks to Brandon for his expertise and Kate-calming ability, helping focus and overcome all those signalling optimisations. Then to Nelson for his expertise and support towards the mass spectrometry experiments.

To all the members of the ACE lab from the old guard (Ross, Riyad, Wendy, Chris, Tony, Colin, Kerry, Ayesha and Nailah) to the new (Karabelo, Dale, Albert and Afolake) with a special mention to Vinasha and Lizelle, my deepest thanks for all our escapades both scientific and not.

Then final thanks to my funders over the years: the NRF, DAAD, UCT and the Ernst and Ethel Eriksen trust.

CONTENTS

LIST OF TABLES

LIST OF FIGURES

LIST OF ABBREVIATIONS AND ACRONYMS

Å	Angstrom
ABC	Ammonium bicarbonate
Abz	o-aminobenzoic acid
ACE	Angiotensin-converting enzyme
ACEi	ACE inhibitors
ACN	Acetonitrile
AcSDKP	N-acetyl-Ser-Asp-Lys-Pro
AD	Alzheimer's disease
ADAM	A Disintegrin and Metalloproteinase
ADDLs	Aβ-derived diffusible ligands
AGC	Automatic gain control
AICD	APP intracellular cytoplasmic domain
AMPK	Adenosine monophosphate-activated protein kinase
ANG(1-7)	Angiotensin (1-7)
ANG(1-9)	Angiotensin (1-9)
ANGI	Angiotensin I
ANGII	Angiotensin II
ANGIII	Angiotensin III
ANGIV	Angiotensin IV
AP-1	Apoprotein-1
ApoE	Apolipoprotein E
APP	Amyloid precursor protein
ARB	Angiotensin receptor blocker
AST	Active site titration
AT_1R	Angiotensin 1 Receptor

ABBREVIATIONS

AT_2R	Angiotensin 2 Receptor
AT_4R	Angiotensin 4 Receptor
Aβ	Amyloid beta
B_2R	Bradykinin-2 receptor
BACE	Beta-site APP-cleaving enzyme
BBB	Blood-brain barrier
BDNF	Brain-derived neurotrophic factor
BK	Bradykinin
BMP7	Bone morphogenetic protein-7
BPPb	Bradykinin potentiating peptide b
BRAAS	Brain renin-angiotensin-aldosterone-system
CAA	Cerebral amyloid angiopathy
CC-sACE	Double C-domain sACE construct
Cdom	Wild type C-domain truncated construct
CHO	Chinese hamster ovary
CID	Collision induced dissociation
CK2	Casein kinase 2
CNS	Central nervous system
COX-2	Cyclooxygenase-2
CRB1	Cellular retinol-binding protein
CREB	cAMP response element binding protein
C-sACE	N-domain sACE active site knockout
CSF	Cerebral spinal fluid
CVD	Cardiovascular disease
dH_2O	Double distilled deionised water
DIA	Data independent acquisition

DMEM	Dulbecco's Modified Eagle Medium
DNA	Deoxyribonucleic acid
DS	Down's syndrome
DTT	Dithiothreitol
ECE	Endothelin-converting enzyme
EDDnp	ethylenediamine 2, 4-dinitrophenyl
EDTA	Ethylenediaminetetraacetic acid
ETD	Electron transfer dissociation
FACS	Fluorescence-activated cell sorting
FAD	Familial Alzheimer's disease
FCS	Foetal calf serum
FITC	Fluorescein isothiocyanate
FRET	Fluorescence resonance energy transfer
FWHM	Full width at half maximum
$GLUT_4$	Glucose transporter type 4
GSK-3β	Glycogen synthase kinase-3
HCD	High energy collision dissociation
HDAC	Histone deacetylase
HEPES	4-(2-hydroxyethyl)-1-piperazineethanesulfonic acid
HHL	Hippuryl-L-histidyl-L-leucine
HL	His-Leu
HPLC	High-pressure liquid chromatography
HR/AM	High-resolution and accurate mass
HUVEC	Human umbilical vein endothelial cells
IAA	Iodoacetamide
Icv	Intracerebralventricular

ABBREVIATIONS

IDE	Insulin degrading enzyme
IFE	Inner filter effect
IRAP	Insulin-regulated membrane aminopeptidase
ISF	Interstitial fluid
JNK	c-Jun NH2-terminal kinase
LC	Liquid chromatography
LRP1	Lipoprotein receptor-related protein-1
LTP	Long term potentiation
MALDI TOF	Matrix Assisted Laser Desorption Ionization Time-of-Flight
MAPK	Mitogen-activated protein kinase
MAPKK	Mitogen-activated protein kinase kinase
MCI	Mild cognitive impairment
miR	Micro RNA
MMP-9	Matrix metalloproteinase-9
MRM	Multiple reaction monitoring
MYH9	Myosin heavy chain IIA
NCE	Normalized collision dissociation
Ndom	Wild type N-domain truncated construct
NEP	Neprilysin
NF-κB	Nuclear factor-κB
NO	Nitric oxide
N-sACE	C-domain sACE active site knockout
NSAID	Non-steroidal anti-inflammatory drug
NT-4	Neurotrophin-4
O-GlcNA	O-GlcNAcylation
PAGE	Polyacrylamide gel electrophoresis

PBS	Phosphate-buffered saline
pG	Pyroglutamate
pJNK	Activated c-Jun NH2-terminal kinase
PKA	Protein kinase A
PKC	Protein kinase C
PMSF	Phenylmethylsulfonyl fluoride
PPAR	Peroxisome proliferator-activated receptor
PRM	Parallel reaction moitoring
pSer1270	Phosphorylated Ser1270
PTMs	Post translational modifications
RAAS	Renin-angiotensin-aldosterone-system
RAGE	Advanced glycation endproducts
RE	Restriction enzyme
ROS	Reactive oxygen species
sACE	Somatic ACE
SAD	Sporadic Alzheimer's disease
SDS	Sodium dodecylsulphate
SIM	Single ion monitoring
sRAGE	Soluble Advanced Glycation Endproducts
T2DM	Type-2 diabetes mellitus
tACE	Testis ACE
TBS-T	Tris-buffered saline with Tween
TFA	Trifluoroacetic acid
TGFβ-1	Transforming growth factor β
TM	Transmembrane
TNFα	Tumor necrosis factor α

ABBREVIATIONS

TZD	Thiazolidinedione
WHO	World Health Organisation
$Y3NO_2$	3-nitrotyrosine
ZPHL	Benzyloxycarbonyl-Phe-L-His-Leu
α2M	α2-macroglobulin

1 CHAPTER

Literature Review

1.1 Alzheimer's disease.

In an aging world population, developments in healthcare are prolonging our life span and improving quality of life. Today in most developed countries, life expectancy is above 80 years of age.

There is however, a yin to this yang: non-communicable diseases are more prevalent due to increased life span and stand out as huge financial and health care burdens to society. One such major contributor is Alzheimer's disease (AD). AD is an extremely debilitating disease that destroys its victim's personality, and motor and cognitive abilities. It is the most common form of dementia (60-80 %) and in these cases, the final manifestation of aging (Alzheimer's Association, 2013). Dementia is a term used to describe a broad spectrum of diseases and conditions that arise from neuronal loss of normal function or cell death. In AD, neuronal cells die off gradually, slowly impairing an individual's ability to carry out basic bodily functions such as walking and swallowing, and is ultimately fatal (Braak and Braak, 1991).

The World Health Organisation (WHO) estimates that 35.6 million people live with dementia worldwide. It is projected that by 2030, the incidence will double and by 2050 more than triple (World Health Organization, 2012). The current global cost of dementia is approximately US$ 604 billion, of which 89 % is incurred in high-income countries. Predictions for low-income countries, whose financial status are dependent on and converge with high-income countries, are more severe. Here, the immediate families bear the largest brunt emotionally and financially, as there are poor community services and little institutionalization. WHO's prerogatives are to seek out a cure and to identify and improve the knowledge surrounding primary prevention indicators. Evidence to date has pointed out a number of risk factors. These are largely related to life style, genetic predisposition and cardiovascular disease (CVD). Changes need to be implemented to decrease the risk of CVD, and thus AD, by improving access to education and countering risk factors for vascular disease, including diabetes, midlife hypertension, midlife obesity, smoking, and physical inactivity. For humanity to have hope of finding a cure, the underlying mechanism and primary causes of AD development need to be elucidated.

1.2 The amyloid hypothesis.

The most prominent pathology of AD is the presence of intercellular neurofibrillary tangles of hyperphosphorylated tau protein and large extracellular masses of β-amyloid (Aβ) protein plaques (Grundke-Iqbal *et al*., 1986; Masters *et al*., 1985). Aβ was first observed, without

causality, by Alois Alzheimer in 1907 in the brain of a middle aged woman who displayed, what we now know as, classic symptoms of AD (Alzheimer, 1907). The amyloid beta peptide itself was only isolated and biochemically characterised almost 80 years later with the development of new protein isolation and extraction techniques (Glenner and Wong, 1984; Masters *et al*., 1985; Roher *et al*., 1993b).

Through the pioneering work of Glenner and Wong (1984) on brain tissue from Down´s syndrome (DS) patients, the foundations for what we now know as the amyloid hypothesis were laid (Glenner and Wong, 1984). These scientists first described and named the 4kDa "amyloid β protein", isolated from meningeal vasculature and, later the same year, linked it to AD by mapping the gene encoding the amyloid precursor protein (APP) to chromosome 21 (Kang *et al*., 1987). Due to the observation that most DS patients develop the neuropathological criteria for AD by the age of 40 (Zigman *et al*., 2008) and that DS patients have two extra copies of APP (Tanzi *et al*., 1987) a causal link was thus established between AD and Aβ. This, taken together with the hallmark Aβ plaque observed in post mortem analysis of both DS and AD patients, lead to the formation of a hypothesis that the accumulation, oligomerization and eventual fibril and plaque formation of Aβ, is the primary causative factor in AD pathologies (Hardy and Selkoe, 2002; Hardy and Higgins, 1992). These pathologies are facilitated via tau neurofibrillary tangle formation, leading to synaptic loss and neuronal cell death (Jin *et al*., 2011; Pooler *et al*., 2014; Rapoport *et al*., 2002; Roberson *et al*., 2007; Vishnu, 2013). Thus, it was proposed that alleviating the accumulation and plaque formation of Aβ would cure AD. This hypothesis propelled research around AD and the Aβ peptide for many years. Although recently under great scrutiny, this hypothesis is fundamental to on-going research efforts as more light is shed on the molecular and biological mechanisms of AD.

The discovery of the amino acid sequence of Aβ from the analysis of fibrils deposited in vasculature (Glenner and Wong 1984) and neuronal plaques (Masters *et al*. 1985) led to a movement of several different research groups to isolate APP (Goldgaber *et al*., 1987; Kang *et al*., 1987; Tanzi *et al*., 1987). Genetics, fundamental in teasing apart initial and seemingly unrelated molecules, led to further understanding of the mechanism of Aβ in neurodegeneration. Autosomal dominant mutations are linked to familial Alzheimer's disease (FAD), which has an early onset with the youngest diagnosis from age 40. These genetic mutations provided greater insight into the disease, as most FAD mutations are found in genes related to the processing of APP that ultimately lead to increased production of Aβ. The mechanism of production and breakdown of the Aβ peptide has since been elucidated. The peptide itself is linked to the disruption of calcium homeostasis, apoptosis and to the generation of cell membrane pores (Carvalho *et al*., 2009; Curtain *et al*., 2001; De Felice *et al*., 2007; Morishima *et al*., 2001). It also activates the complement immune response, is associated with oxidative stress and many other neurotoxic processes (Varadarajan *et al*. 2000; Velazquez *et al*. 1997; Johnstone *et al*. 1999; Amor *et al*. 2010; Larson *et al*. 2012; Fu *et al*. 2012).

1.2.1 Processing of APP and production of the Aβ peptide.

The accumulation of Aβ occurs from an imbalance between its anabolism and catabolism, resulting in the characteristic neuron-coating amyloid plaques. The Aβ peptide is a cleavage product of protease activity on the transmembrane protein APP and this process has been comprehensively reviewed by numerous groups (Annaert and De Strooper, 2002; De Strooper, 2010; Haass *et al*., 2012; Nalivaeva and Turner, 2013). APP is a naturally occurring glycoprotein expressed in both somatic tissues as well as neuronal tissue. It is a type-1 membrane protein with a large, heavily glycosylated, extracellular N-terminal region, a transmembrane region and a relatively short cytoplasmic C-terminus (Kang *et al*., 1987). Several isoforms of APP exist, however, APP695 is the most abundant form found in neuronal tissue and it is the shortest isoform, lacking a kunitz-type protease inhibitor sequence (Hardy, 1997; Mattson, 1997). All APPs generally enter into the secretion pathway where they can form homodimers and be processed once on the cell membrane (Ben Khalifa *et al*., 2012). APP695, however, preferentially undergoes proteolytic processing within the slightly acidic endosomal compartment.

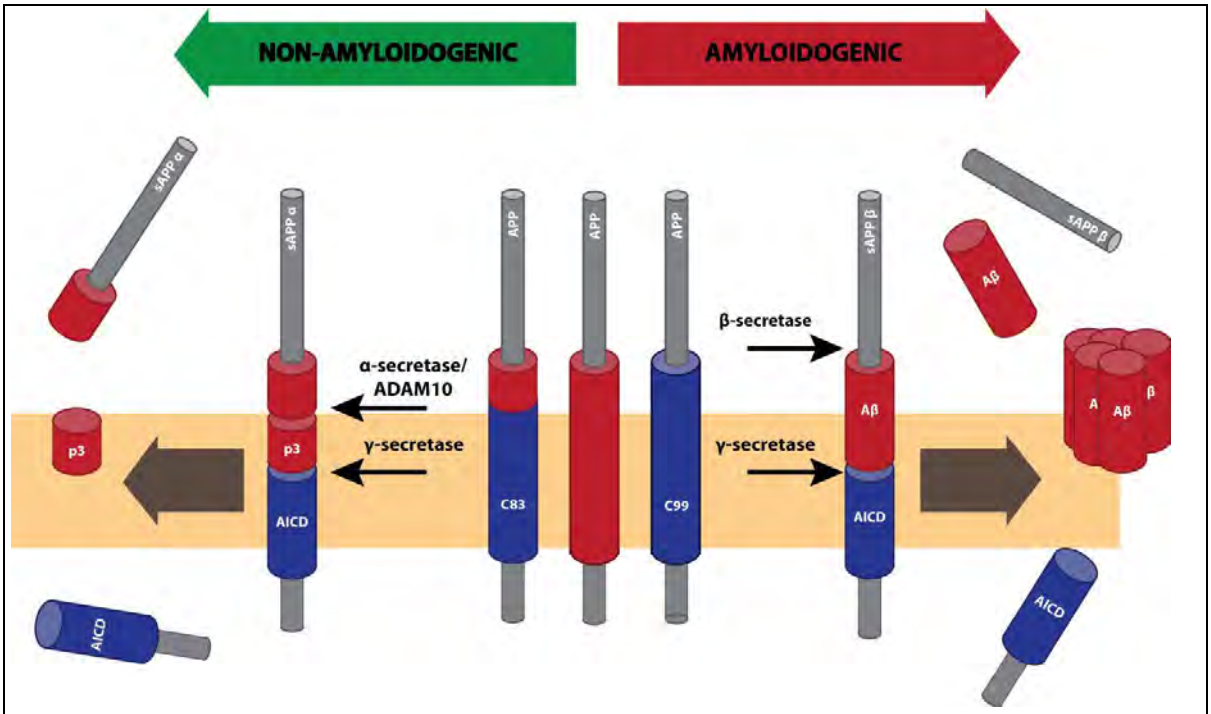

Figure 1.1 **The traditional APP processing pathways.** The non-amyloidogenic pathway is initiated by α-secretase cleavage, whereas amyloidogenic processing pathway is initiated by β-secretase cleavage. Both pathways generate soluble, functional ectodomains of APP (sAPP α and sAPP β) and two transmembrane C-terminal fragments (C83 and C99, respectively). Subsequent γ-secretase cleavage within the transmembrane domain yields the 3 kDa p3 peptide and the roughly 4 kDa Aβ, respectively. The signalling cytoplasmic polypeptide AICD is released simultaneously.

There are two distinct pathways by which APP undergoes processing: The minor amyloidogenic pathway, which leads to the generation of Aβ; and the major non-amyloidogenic pathway, which does not liberate Aβ (Figure 1.1). Dysregulation of the amyloidogenic pathway via environmental or genetic predisposition causes Aβ accumulation and is associated with development of AD.

Only 10% of all APP enters the amyloidogenic pathway. The other 90% enters the non-amyloidogenic processing pathway, initiated by the α-secretase, now known as A Disintegrin And Metalloproteinase (ADAM) 10 (Donmez *et al*., 2010; Parkin *et al*., 2011), followed by cleavage by the γ-secretase. ADAM 10 hydrolyses APP at a site within the Aβ region liberating Aβ(17-X) peptides (X, refers to multiple C-termini positions), sAPP α and the p3 peptide (Figure 1.1) (Annaert and De Strooper, 2002; Dulin *et al*., 2008).

Aβ production occurs via the constitutive action of two aspartyl proteases, namely β and γ-secretases (Nalivaeva and Turner, 2013; Seubert *et al*., 1993; Shoji *et al*., 1992; Wilquet and Strooper, 2004). Cleavage by β-secretase, beta-site APP-cleaving enzyme (BACE-1), results in the formation of the N-terminus of Aβ and initiates its production. This enzyme liberates the large ectodomain (sAPP β) of APP into the extracellular fluid. Left behind within the cell membrane is the carboxy-fragment known as C99 (Cai *et al*., 2001; Vassar *et al*., 1999). C99 is then cleaved by the γ-secretase within the hydrophobic membrane of the cell which ultimately releases the Aβ peptide into serum or cerebral spinal fluid (CSF) (Ehehalt *et al*., 2003; Lichtenthaler *et al*., 2011). The cytoplasmic fragment, also known as the APP intracellular cytoplasmic domain (AICD) (Figure 1.1), has both protective and detrimental contributions to the pathology of AD and is liberated from both pathways (Beckett *et al*., 2012; Gao and Pimplikar, 2001). APP695 and its endosomal pathway enable a preferential association with BACE-1 thus liberating Aβ and ACID in an amyloidogenic mechanism mediated by cholesterol and lipid rafts (Ehehalt *et al*., 2003; Nalivaeva and Turner, 2013). APP belongs to a highly conserved protein family however, knockouts of APP alone are not lethal but double null mutants with APP-like-Protein-2 lead to early postnatal lethality in mammals, suggesting a functional redundancy between the two (von Koch *et al*., 1997). Furthermore mice homozygous for APP null mutation have abnormal forebrain commissures, and reduced neuromuscular function (Magara et al., 1999; Zheng et al., 1995). Several knock in, mouse lines expressing various sections of APP have provided further evidence of APPs multifaceted function (reviewed in Guo *et al*., 2012). Specifically with regard to the Aβ fragment, the pathology related to AD proceeds independently of the C-terminus of APP (H. Li *et al*., 2010). Thus, hinting that the two functions could possibly be uncoupled genetically.

1.2.1.1 **Aβ structure and aggregation.**

Despite intensive research on the Aβ peptide, once liberated from APP its natural role and pathological mechanisms are not clear. Aβ appears to influence numerous systems including: kinase activation (Tabaton *et al*., 2009); scavenging metal ions and protecting against metal–induced oxidative damage through regulation of cholesterol transport (Fantini and Yahi, 2010; Igbavboa *et al*., 2009); and affecting glutamatergic neurotransmission (Govoni *et al*., 2014). Interestingly, Aβ has been shown to cycle with wakefulness and sleep. Wakefulness is associated with high synaptic activity, extensive long term potentiation (LTP) of neurons and low interstitial fluid levels of Aβ while sleep is generally accompanied by the opposite conditions (Kang *et al*., 2009; Vyazovskiy *et al*., 2008). As Aβ is known to dampen LTP and neuron excitation, the accumulation of Aβ could possibly play an important role in sleep (Kang *et al*., 2009; Musiek *et al*., 2015).

Amyloid β toxicity appears to be dependent on the structural conformations adopted by varying forms of Aβ. Aβ isolated from soluble, fibrillar masses and plaques has a large amount

of heterogeneity at both N-and C-termini (Hardy *et al*., 2014; Nhan *et al*., 2014; Portelius *et al*., 2010a). The toxicity and biochemical properties of this molecule have been shown to be dependent on the length and composition of the terminal residues which dictate its secondary, tertiary and quaternary structure (Glabe, 2008; Lindgren and Hammarström, 2010; Nhan *et al*., 2014; Sakono and Zako, 2010; Youssef *et al*., 2008). Mature fibril formation can be described as an uncharacterised, nucleation-dependent polymerization reaction. The exact mechanistic process of the aggregation into fibrils is as yet unknown. It is largely due to the stochastic accumulation of various Aβ forms leading to a heterogeneous mix. Fibril and plaque deposits are relatively, but not permanently, stable and uniform. The dissolution of plaques into oligomers is one way in which plaques may generate a perpetual toxicity (Broersen *et al*., 2010; Serpell, 2000). Amyloid fibrils are at the core of dense and diffuse amyloid plaques. These can be found within the brain parenchyma and/or accumulate in the cerebral blood vessel walls in the form of cerebral amyloid angiopathy. These fibrils are the end-point of Aβ oligomerization. They develop via numerous molecular signals that induce sequential modification, binding and stacking of monomeric forms of Aβ.

Central to the theory of Aβ aggregation are monomeric peptides, activating through conformational changes into either α-helices or anti-parallel β-sheet secondary structures, which recruit more Aβ and stack to form protofibrils (Bartolini *et al*., 2007; Taylor *et al*., 2003). These soluble protofibrils then associate to form fibres and fibres associate to form plaques (Ahmed *et al*., 2010; Benseny-Cases *et al*., 2007; Chimon *et al*., 2007). However, recently Cohen *et al.* have shown that monomers require fibrils in order to induce activation and subsequent aggregation (Cohen *et al*., 2013).

Soluble globular oligomers of Aβ or Aβ-derived diffusible ligands (ADDLs) are well-renowned for their low-dosage, extreme and specific synaptotoxicity (Haass and Selkoe, 2007; S. Li *et al*., 2010; Mattson, 2004; Rosenblum, 2014; Tomic *et al*., 2009). The fibril form of amyloid plaque has been proposed as a molecular sink for soluble forms of Aβ, like ADDLs, acting as Aβ scavengers of oligomeric and soluble forms in a protective manner (Hane, 2013). Soluble Aβ oligomers correlate better with disease progression, loss of synaptic density and cognitive decline (Haass and Selkoe, 2007; Lesné *et al*., 2013; S. Li *et al*., 2010; McLean *et al*., 1999; Rosenblum, 2014; Tomic *et al*., 2009). These species of soluble oligomers, globular and protofibrillar amyloid are now considered the first toxic species as they present presymptomatically and prior to any neurofibrillary tangles (with their associated toxicity) and plaque deposition (Hane, 2013; Larson *et al*., 2012; Sakono and Zako, 2010; Tomic *et al*., 2009). The very nature of soluble Aβ-intermediates makes them difficult to characterise structurally and in terms of toxicity profiles. Numerous studies have indicated many different forms as causative of AD. Some of the more important forms of Aβ species are discussed in this chapter.

1.2.1.2 **Aβ derived from C-terminal secretase action on APP**

In almost every case of FAD the genetic mutations (in APP, or components of the γ-secretase) induce an increase in the production of long Aβ (Aβ(1-42) – Aβ(1-52)) (De Strooper, 2010; Haass *et al*., 2012; Lesné *et al*., 2006). The most studied variations are those of the carboxy terminus, where two peptides have been the focus in AD research, namely Aβ(1-40) and Aβ(1-

42). Aβ(1-40) is by far the most abundantly produced, yet longer C-terminal residues are known for their increasing aggregation and toxicity.

The production of all Aβ peptides greater than Aβ(1-17) is dependent on γ-secretase activity. However, the exact molecular mechanism by which γ-secretase accesses this Aβ(1-17) cleavage site, located on the extracellular side of the membrane, is currently unknown (Beher *et al*., 2002). A number of elegant studies led to the proposed mechanism of γ-secretase processing of the α- and β-secretase cytoplasmic fragments (Qi-Takahara *et al*., 2005; Sato *et al*., 2003; Takami *et al*., 2009; Yagishita *et al*., 2008). If primary cleavage occurs at the ε site to release AICD 50 and Aβ(1-49), then the subsequent cleavage, at three residue intervals in each turn of the APP helix would release 46, 43 and 40 residue Aβ peptides. If cleavage initiates the release of AICD 51 and Aβ(1-48), then Aβ peptides of 45, 42 and 40 residues would follow generating C-terminal Aβ heterogeneity (Figure 1.). An alternate processing pathway, independent of γ-secretase action, also exists whereby the C99 fragment is processed further by the α-secretase leading to the release of Aβ(1-15) and Aβ(1-14) (Beher *et al*., 2002). Thus, Aβ(1-14) and Aβ(1-15) are specific products of α- and β-secretase concerted cleavage (Figure 1.). These short isoforms are present in CSF along with Aβ(1-40) and Aβ(1-42) in AD patients and are used as diagnostic markers of both FAD and sporadic AD (SAD) (Pannee *et al*., 2014).

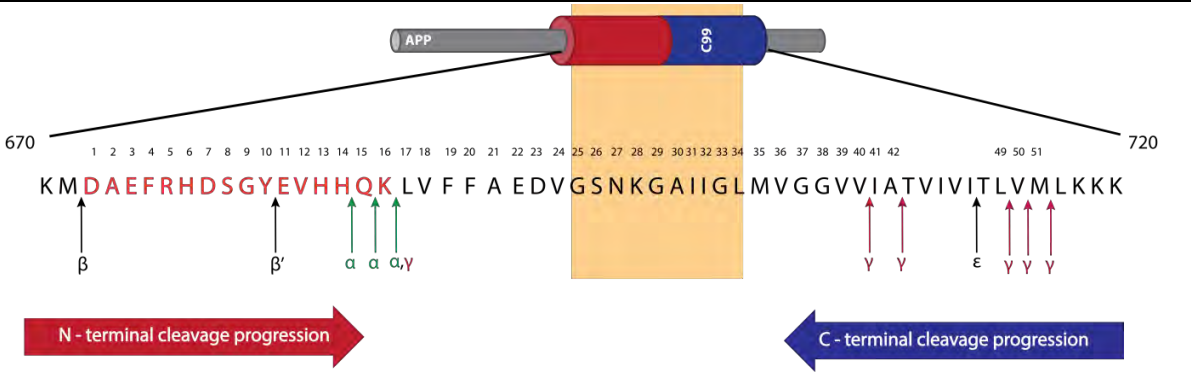

Figure 1.2. **Secretase cleavage sites of Aβ**. The amino acid sequences (with numbering based on the APP695 isoform) are shown incorporating the largest Aβ sequence found between APP670-APP720. The cleavage sites for both N- and C-terminal secretase-truncations are indicated along with the ε-site (black) of γ-secretase (red) association. The β and β' are shown in black and the α-secretase alternate processing sites are indicated in green. The amino acid numbers are indicated for the full-length Aβ(1-42), as well as the position of Aβ(1-49/50/51). The orange highlighted amino acids from Aβ(1-16) indicate the region of metal binding and posttranslational modification.

Aβ(1-16) production appears to be dependent on all three secretases. The mechanism behind this is still unclear (Pannee *et al*., 2014; Portelius *et al*., 2010a, 2010b, 2006). A natural function has been assigned to the Aβ(1-16) fragment, as it has recently been shown to amplify and induce fear conditioning via the nicotinic receptors. Also, its activity is regulated by the metal binding domain YEVHHQ (Lawrence *et al*., 2014). With regard to toxicity in AD, Aβ(1-16) has a controversial role, implicated as both inert and cytotoxic (Du *et al*., 2011; Liao *et al*., 2007; Ramteke *et al*., 2014). The potential cytotoxic properties of Aβ(1-16) are linked to the metal binding domain, known for its role in producing detrimental reactive oxygen species (ROS) and aiding oligomerization on its own and within the full-length Aβ(1-42) (Bush, 2003; Curtain *et al*., 2001; Du *et al*., 2011; Minicozzi *et al*., 2008; Ramteke *et al*., 2014). This peptide,

however, occurs at higher concentrations in AD patients' CSF in comparison to controls (Portelius *et al*., 2010a, 2010b). The reason for the upregulation of the Aβ(1-16) generating pathway in AD is unknown. One proposed possibility is that there is an increase in α-secretase activity in an attempt to counteract the dysregulation of APP processing (Portelius *et al*., 2011).

1.2.1.3 **N-terminally truncated Aβ peptides derived from APP.**

The formation of the N-terminus of Aβ (position Asp 1) normally occurs via BACE-1 cleavage (Figure 1.). Truncations of the N-terminal region are extremely prevalent and are toxic, as are most forms of Aβ (Pike *et al*., 1995). N-terminal truncations also make up a large portion of the aggregated and stable plaques of AD patients (Bayer and Wirths, 2014; Guzmán *et al*., 2014; Portelius *et al*., 2006; Youssef *et al*., 2008).

There are a number of different N-terminal truncations of the full-length Aβ(1-40/42). These include peptides beginning with Ala-2, Glu-3, pyroglutamate Glu-3 (pG3), Phe-4, Arg-5, His-6, Asp-7, Ser-8, Gly-9, Tyr-10 and pyroglutamate Glu-11 (pG11). BACE-1 is responsible for the formation of Aβ(11-X) at the β'-site (Figure 1.) which, in older deposits and in AD, Aβ undergoes post-translational modification to form pG11. Aside from this cleavage site it is unclear exactly what pathways and enzymes are responsible for other N-terminal truncations, most of which arise independently of BACE-1 (Bayer and Wirths, 2014).

Aβ(2-X), increases in the brain tissue from AD patients but decreases in CSF (Bibl *et al*., 2012). The formation of this peptide is not entirely independent of BACE-1 cleavage. It has been suggested that Aβ(2-X) occurs via the combined action of BACE-1 and aminopeptidase A. Meprin-β, however, sheds APP independent of BACE-1, generating the same cleavage sites until APP is overexpressed. Only then does meprin-β produce a large amount of Aβ(2-X) (Bien *et al*., 2012; Broder and Becker-Pauly, 2013). The zinc metalloprotease neprilysin (NEP) is a major Aβ degrading enzyme. It does, however, also produce the truncations Aβ(3/4/6-X) (Leissring *et al*., 2003b) which are all BACE-1 independent sites. The Aβ(3-X) species undergo pyroglutamylation over time to form pG3 (Jawhar S, Wirths O, 2011). This along with Aβ(4-X) are the two N-terminal truncations most consistently reported in AD (Bayer and Wirths, 2014). They also have severe toxicity associated with their rapid, low dose aggregation into soluble oligomers (Bayer and Wirths, 2014; Jawhar S, Wirths O, 2011; Kummer and Heneka, 2014; Youssef *et al*., 2008). The Aβ(5-X) site corresponds to cleavage by another amyloid degrading enzyme, the serine protease plasmin (Carson and Turner, 2002; Tucker *et al*., 2000). A different metalloprotease and the focus of this study, angiotensin converting enzyme (ACE), has been shown to hydrolyse Aβ between residues Asp7-Ser8 and is a candidate protease for the formation of Aβ(8-X) (Hu *et al*., 2001; Kumar *et al*., 2012; Oba *et al*., 2005). In the search for early diagnostics of AD, the N-truncated Aβ variants Aβ(2/pG3/4/5/8/9-X) provide good correlations to disease onset and severity in both SAD and FAD (Bayer and Wirths, 2014; Guzmán *et al*., 2014; Kummer and Heneka, 2014; Moore *et al*., 2012; Pannee *et al*., 2014; Sergeant *et al*., 2003).

1.2.2 Modifications to the N-terminus of Aβ induce greater toxicity.

The N-terminal region of Aβ, between residues 1-16, constitutes the minimal metal ion binding site (Inoue *et al*., 2009; Minicozzi *et al*., 2008; Uversky, 2010). Metals like Cu^{+}, Cu^{2+}, Zn^{2+} and Fe^{2+} bind to soluble, monomeric or oligomerized forms of the peptide and co-precipitate in AD (Caragounis *et al*., 2007; Hureau, 2012; Karr *et al*., 2004; Kowalik-Jankowska *et al*., 2001; Minicozzi *et al*., 2008; Shi *et al*., 2014; Zirah *et al*., 2006). Both Zn^{2+} and Cu^{2+} are produced from active synapses during normal neural transmission and are essential for normal brain development and function (Assaf and Chung, 1984; Bush, 2003; Hartter and Barnea, 1988; Howell *et al*., 1984).

The Aβ peptide may interfere with iron homeostasis as it has a strong affinity for iron, both Fe^{2+} and Fe^{3+}, that is 8 orders of magnitude greater than that of transferrin (Jiang *et al*., 2009). In mouse models of AD, regardless of Aβ, over expression of APP decreases the level of metal ions at a constant rate throughout the animals' lifespan (Bush, 2003). Based on this, it has been suggested that Aβ and APP are upregulated in response to the metal ion increase (Bush, 2003; Maynard *et al*., 2002). APP indeed is regulated by a novel iron-regulatory element (IRE-Type II) within the 5'-untranslated region upstream of its gene (Rogers *et al*., 2008). In addition, APP exhibits Fe^{2+} oxidizing activity mediated by a conserved H-ferritin-like active site (Duce *et al*., 2010). This active site is inhibited by Zn^{2+}. APP oxidizes Fe^{2+} to Fe^{3+} and loads Fe^{2+} into transferrin promoting Fe export from the neuron. In AD, Fe detrimentally accumulates in the cell cytoplasm (Duce *et al*., 2010). The excessive Zn present in Aβ aggregates in AD neural tissue inhibits ferroxidase activity of APP. This in turn inhibits the efflux of Fe^{2+}, which promotes pathology.

Zn^{2+} has a far greater affinity for Aβ than either Cu or Fe. Binding of low micro molar amounts of Zn^{2+} induces rapid precipitation of soluble Aβ into aggregated fibres; furthermore, plaques appear to be Zn sinks as abnormally high levels are found within them. This is because Zn coordinates intermolecular interactions between two molecules and/or fibres of Aβ by His(Nτ)-Zn^{2+}–His(Nτ) bridges. Similar coordination of Cu^{+} occurs to His13 and His14 in a linear fashion in monomeric forms of Aβ, whereas in soluble oligomeric forms Cu^{2+} has been described in a tetrahedral coordination, inducing increased reactivity towards O_2 (Karr *et al*., 2004; Nhan *et al*., 2014). In this way, the toxicity of Cu ions is two pronged. After binding and inducing aggregation they also induce enhanced ROS production (Bush, 2003; Hureau, 2012). Overall, Cu ions have an exacerbating effect on AD (Deshpande *et al*., 2006; Dolev and Michaelson, 2006; Jiang *et al*., 2009).Binding of Aβ to Fe and Zn, similar to Cu, regulates their redox cycling which produces more ROS (Bush, 2003; Huang *et al*., 1999; Nishino and Nishida, 2001). This then causes more oxidation of reducing agents and an overall imbalance in the cellular environment by further production of ROS and depletion of reducing agents and O_2 (Bush, 2003; Hureau, 2012; Jiang *et al*., 2009). The Aβ(1-16) peptide has been used as a model for metal binding and peptide aging in NMR studies (Figure 1.3) (Zirah *et al*., 2006). This peptide was able to undergo Zn-induced helix formation and isomerization related to aging (Figure 1.3 A). Specifically, Zn binding stabilized the apo-structure (Figure 1.3 B) and induced N-terminal folding into an α-helix (Figure 1.3 C) (Zirah *et al*., 2006). This could be a possible mechanism for the molecular switch of Aβ from the innocuous to the toxic form.

Isomerization and racemization of N-terminal Aβ, are modifications which occur in older plaque cores, where the Asp1 and 7 residues are converted from D to L-isoforms (Inoue *et al*., 2014; Roher *et al*., 1993a; Tambo *et al*., 2013). These modifications occur more frequently in brain parenchyma than in vascular deposits (Fabian *et al*., 1994). It is thought that these changes can be induced by ROS and exposure to free radicals (Huang *et al*., 1999) and may adversely affect clearance and proteolysis.

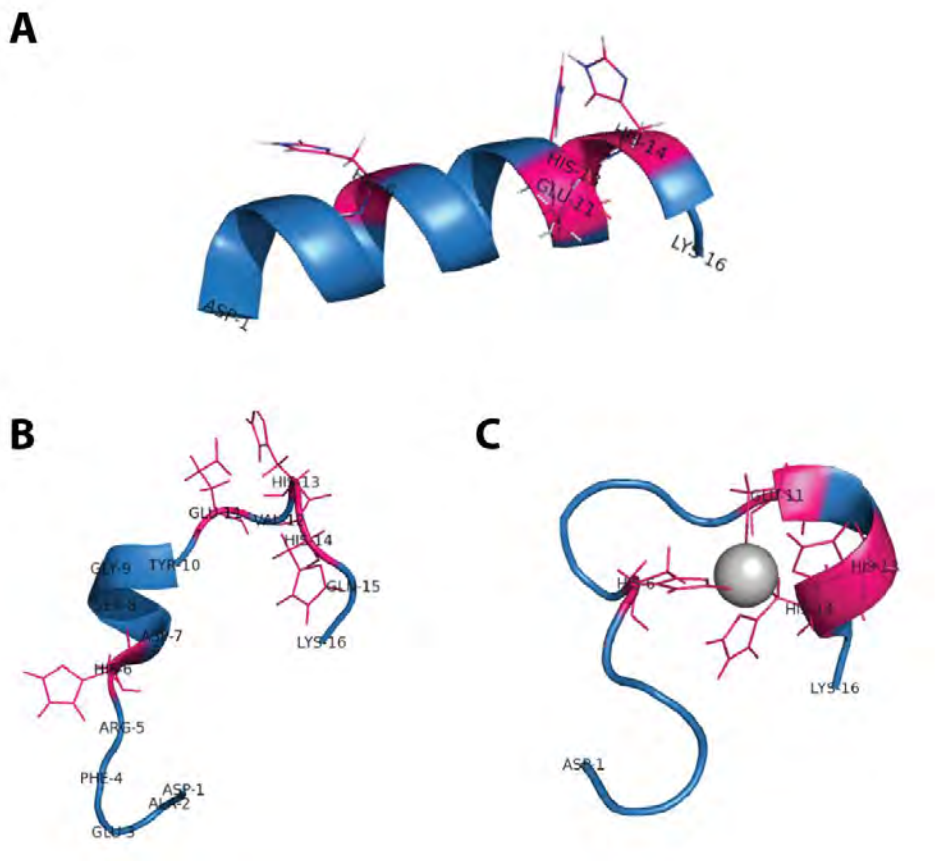

Figure 1.3 **The Zn coordination of Aβ(1-16).** The peptide backbone is indicated in blue and the metal binding residues are coloured pink and labelled. All structures are modified from Zirah *et al*. (2006). **A)** Alpha-helical structure of Aβ(1-16) in solution of tetrafluoroethylene (80 %) and water (20%). **B)** Aβ(1-16) apo structure unbound PDB 1ZE7 in aqueous solution . **C)** The Zn^{2+} bound Aβ(1-16) in aqueous solution, PDB 1ZE9. Here coordination of all three His residues as well as the Glu11 to the Zn^{2+} ion occurs, inducing structural stabilization. These images were generated using PyMOL software (v 0.99, DeLano Scientific).

Dysregulated brain glucose metabolism is a downstream effect of Aβ toxicity, and type-2 diabetes mellitus exacerbates Aβ pathology in AD models. One example is that of glucose hypometabolism and its influence on the progression of AD, which occurs through the nutrient-responsive post-translational O-GlcNAcylation (O-GlcNA) of nucleo-cytoplasmic proteins (Hart, 1999; Zhu *et al*., 2014). Thus, impaired O-GlcNA in the brain could, in principle, contribute to Aβ toxicity (Zhu *et al*., 2014). Furthermore glucose metabolism may affect APP processing, as a mass spectrometry study on AD patients revealed multiple N-terminal Aβ(1-15/16/17/18/19/20) and Aβ(3/4-15), Aβ(4/5-17) peptides were *O*-glycosylated (Halim *et al*., 2011). The predominant glycosylated peptides being Aβ(1-15/17) to which glycosylation occurred at Tyr10. As there appeared to be no glycosylation on the full-length Aβ(1-40/42)

peptide it was theorised that Tyr10 glycosylation of APP is protective as it is very close to the membrane and may prevent γ-secretase cleavage (Halim *et al*., 2011).

Phosphorylation acts as a molecular recognition switch. There are many examples of extracellular kinases that could facilitate such a posttranslational modification of Aβ (Kummer and Heneka, 2014). There are three residues in Aβ that could act as potential phosphorylation sites: Ser8, Ser26 and Try10. In studies on NT2 neurons, phosphorylation of Ser26 was described as inducing greater toxicity to Aβ (Milton, 2001). This toxicity was again linked to a lack of fibril formation and an increase in soluble oligomers. Phosphorylation of Aβ at Ser8 is more prevalent and slightly more is known about it. Immunohistochemical studies indicated that Ser8 phosphorylated Aβ was localised to plaques in AD patients and transgenic mice (Kumar *et al*., 2011). Phosphorylation of this site promotes oligomerization, thought to nucleate fibrils, yet may paradoxically be protective. However, toxicity was increased in *Drosophila* models compared to the un-phosphorylated Ser6 Aβ molecule (Kumar *et al*., 2011). Interestingly, this site affects proteolysis by both ACE and insulin degrading enzyme (IDE) and could reduce its clearance.

The increased inflammation, found in AD, leads to the upregulation of nitric oxide synthase which creates more nitric oxide (NO) leading to an increase in NO-induced post translational modifications (PTMs). These modifications include the formation of S-nitrothiols at Cys residues and Tyr modifications, like nitration and dinitrotyrosine formation (Radi, 2004). The conversion of Aβ Tyr10 to nitrotyrosine was found at the core of Aβ plaque in mouse AD models and in human AD brains (Kummer *et al*., 2011). This same modification of Aβ, favoured by oxidative stress, has been shown to increase Aβ aggregation, inhibit LTP to a larger degree than the unmodified form and stabilize Aβ dimers (Varadarajan *et al*. 2000; Kummer *et al*. 2011; Kummer and Heneka 2014). As discussed, all PTMs whether by proteolysis, metal binding, isomerization, nitration, or pyroglutamylation all appear to accelerate Aβ nucleation and increase Aβ's toxicity. The N-terminal region of Aβ, overall, has a dramatic influence on the pathogenesis of Aβ and often determines if these peptides precipitate into the proverbial fibril sink or form more toxic species like loose soluble protofibrils, dimers, ADDLs and circular structures that induce pore formations within cell membranes. All of these alterations have implications on clearance and processing of Aβ.

1.3 Aβ Clearance and Degradation.

AD is a complex disease that, in the majority of cases, has a more syndrome-like nature of onset. The more common sporadic form of AD has been linked to inefficient removal or increased influx of Aβ (Mawuenyega *et al*., 2010). Over the last two decades, it has become evident that AD is a result of disequilibrium between production and clearance of Aβ. This implicates tissues, outside of neurons and microglia, now considered important when addressing causation of AD, specifically: the status of the blood-brain barrier (BBB) (Bell and Zlokovic, 2009), the choroid plexus (Serot *et al*., 2012) and hepatic function (Kang and Rivest, 2012). There are several mechanisms implicated in the influx and clearance of Aβ that fall into three categories, known as the 3Ds: (1) perivascular **d**rainage, (2) transcytotic **d**elivery and (3) enzymatic/glial **d**egradation.

1.3.1 Perivascular drainage.

The immunologically privileged central nervous system is devoid of conventional lymphatic vessels. This leaves only the perivascular drainage system to deal with all the functions normally assigned to lymphatic vessels and nodes (Weller *et al*., 2010). It is theorised that perivascular drainage occurs as a result of blood vessel pulsations (Schley *et al*., 2006). These pulsations supply a motive force to the interstitial fluid (ISF), a fluid almost completely separate from CSF, and its solutes (Szentistványi *et al*., 1984). Drainage begins as a process of diffusion of ISF from grey matter where its rate is influenced by the composition of solutes and metabolites, including the presence of Aβ, in the extracellular space (Syková and Nicholson, 2008; Weller *et al*., 2009). ISF then flows more rapidly along white matter tracts and perivascular drainage routes (Abbott, 2004; Weller *et al*., 2010). Aβ toxicity extends beyond soluble oligomers and plaque formation; it also accumulates in the walls of cerebral arteries and capillaries creating the prominent vascular pathology in AD, cerebral amyloid angiopathy (CAA) (Vasilevko *et al*., 2010). As neurons, astrocytes and other cells in the brain produce Aβ, it is expected to be cleared via perivascular drainage. Indeed, perivascular congestion has been linked to the pathogenesis of CAA, as its drainage route corresponds to the distribution of Aβ immunofluorescence in CAA (Preston *et al*., 2003). This phenomenon is further evidenced through the analysis of CSF, where, as more plaques form and sequester Aβ, CSF Aβ levels drop in AD (Sunderland *et al*., 2003). The levels of Aβ(1-40) in CSF however, are higher in AD patients and control groups compared to CAA groups (Verbeek *et al*., 2009). The level of Aβ(1-40) in CSF is a distinguishing factor between AD and CAA, as it drains better but paradoxically, if in excess deposits in the perivasculature. CAA is accelerated in immunized AD patients, whose Aβ plaques become solubilised, and the decrease in CSF Aβ concentrations in general are indicative of impaired perivascular drainage (Patton *et al*., 2006; Verbeek *et al*., 2009). Overall amyloid flows from the extracellular space, through perivascular drainage routes, out of the brain to the cervical lymph nodes. Following this, smooth muscle cells and perivascular macrophages take up Aβ for degradation and, in capillary endothelia, it is transported into the blood periphery as part of the Aβ elimination pathway. Aging stiffens arteries lowering the pulsative force causing CAA and, in AD, drainage is further hampered by the clogging effect of excessive Aβ (Hawkes *et al*., 2013, 2011). Thus, cardiovascular health is imperative in order to maintain suitable pulsation amplitudes and drainage (Arbel-Ornath *et al*., 2013). Inefficient perivascular drainage of Aβ and/or pre-existing CAA will induce either intracerebral haemorrhage or AD.

1.3.2 Transcytotic delivery.

Peripheral Aβ enters the central nervous system (CNS) via the receptor for advanced glycation endproducts (RAGE) receptor-mediated transport across the BBB (Deane *et al*., 2003) and exits via binding to the lipoprotein receptor-related protein-1 (LRP1) (Shibata *et al*., 2000). RAGE is a receptor and a member of the immunoglobulin superfamily with wide array of ligands (Stern *et al*., 2002). RAGE, unlike other receptors, can create and sustain positive feed-back loops of expression in response to its ligands (Lue *et al*., 2001). Thus the expression of RAGE on cerebral vessels, neurons and microglia is increased in response to Aβ production (Deane *et al*., 2003). Aβ binding to RAGE induces oxidative stress, apoptosis, synaptic

dysfunction and microglial activation (Origlia *et al*., 2010; Yan *et al*., 1996). On the endothelial surface of capillaries, Aβ stimulated RAGE induced the production of pro-inflammatory cytokines and endothelin-1 (Deane *et al*., 2003) promoting vasoconstriction and aggravating pathology (Girouard and Iadecola, 2006; Kisanuki *et al*., 2010). RAGE also occurs in a soluble isoform (sRAGE) which scavenges and competes with membrane bound RAGE for ligands. sRAGE promotes the removal of circulating ligands like Aβ and its levels in AD are reduced (Emanuele *et al*., 2005). Higher concentrations of sRAGE correlate protectively against cardiovascular disease, hypertension, arthritis and AD (Emanuele *et al*., 2005; Falcone *et al*., 2005; Geroldi *et al*., 2006).

LRP1 is a receptor member of the LDLR family, like many LDLRs it is multifunctional, acting as both a scavenger and signalling receptor. It is expressed widely from neural cells to cerebral microvasculature (Kanekiyo and Bu, 2014; Wolf *et al*., 1992). LRP1 has multifaceted roles in AD in that it significantly regulates Aβ trafficking, endocytosis and subsequent lysosomal degradation. The trafficking of Aβ out of the CNS across the BBB occurs post Aβ binding to the ligands for several of the LDLR family, like apolipoprotein E (ApoE) or α2-macroglobulin (α2M), to be delivered to peripheral sites of degradation (Bu, 2009; Pflanzner *et al*., 2011; Shibata *et al*., 2000). There are three allelic polymorphisms of *APOE* (ε2, ε3 and ε4) with subtle protein structural differences defining their altered roles (Mahley *et al*., 2009; Zhu *et al*., 2012). The ApoE ε4 isoform has strong links to AD being the isoform most deficient at Aβ clearance via LRP-1 (Ladu *et al*., 2000; Riddell *et al*., 2008; Shibata *et al*., 2000) and associated with aggravated CAA with intracranial haemorrhaging (Biffi *et al*., 2010; Fryer *et al*., 2005).

1.3.3 Metalloproteases and Aβ proteolysis.

Degradation of Aβ occurs in the brain parenchyma by microglia and numerous proteases and is another major clearance mechanism for Aβ. Regardless of where the accumulation of Aβ occurs within the brain (in the interstitial extracellular space or within cells), glial cells are central to AD in that they both secrete ApoE and phagocytise Aβ (LaDu *et al*., 2000; LaFerla *et al*., 2007; Zhu *et al*., 2012). Glial cells accompany amyloid plaques and have both beneficial and aggravating effects towards the pathology of AD. Apart from glial phagocytosis there are many enzymes which have proven capable of hydrolysing Aβ both *in vitro* and *in vivo* (James Scott Miners *et al*., 2008; Nalivaeva *et al*., 2012). Generally, it is thought that these peptidases reduce the aggregating potential and toxicity of Aβ. The most well-known Aβ degrading proteases include insulin degrading enzyme (IDE) (Qiu *et al*., 1998; Vekrellis *et al*., 2000), neprilysin (NEP) (Iwata *et al*., 2000), endothelin-converting enzyme (ECE) (Eckman *et al*., 2003), matrix metalloproteinase-9 (MMP-9) (Backstrom *et al*., 1996; Yan *et al*., 2006), plasmin (Tucker *et al*., 2000) and ACE (Hu *et al*., 2001; Scott Miners *et al*., 2011; Zou *et al*., 2007). In this literature review, I will focus on the metalloproteases NEP and IDE (discussed below) and ACE (section 1.4).

1.3.3.1 **Neprilysin**

The most renowned Aβ-protease is neprilysin (neutral endopeptidase-24.11, enkephalinase, neutrophil cluster-differentiation antigen 10 or common acute lymphoblastic leukaemia antigen). In the brain NEP is found on pre- and post-synaptic membranes, within the tunica media and in cortical and leptomeningeal blood vessels endothelium where it is involved in synaptic signalling (Barnes *et al*., 1988) and the regulation of vascular tone. NEP expression patterns, all along perivascular drainage routes as well as in vessels, position it well as a major degrading enzyme of Aβ. NEP's Aβ-degrading ability has been indicated both *in vitro* (Howell *et al*., 1995) and *in vivo* (Iwata *et al*., 2001, 2000). Over the years, Saido *et al* have proved that NEP is capable of reducing Aβ levels and is a major Aβ-degrading enzyme. They found that in mice lacking NEP AD pathology was exacerbated (Iwata *et al*., 2001) and, in turn, reversed by human NEP-targeted gene delivery to the brain of AD transgenic mice (Iwata *et al*., 2013, 2004; Marr *et al*., 2003). The first clinical association of NEP with AD was revealed on analysis of mRNA levels in hippocampal and Aβ-burdened cortical tissues (Yasojima *et al*., 2001). NEP mRNA levels in AD were significantly lower compared to non-demented control patients. NEP was not only found to reduce plaque burden but also CAA pathology (Miners *et al*., 2006). In AD with CAA, both activity and expression of NEP were reduced and NEP was shown to protect cerebrovascular smooth muscle cells from Aβ-induced cell death (Miners *et al*., 2011). Furthermore the ApoE genotypes correlated to NEP activity as they do towards AD: NEP activity being greatest in *APOE* ε2/3 genotype > *APOE* ε3/3 > ε3/4, and lowest NEP and greatest risk levels associated with ε4/4 genotypes (Miners *et al*., 2011, 2006).

On examination of the aging brain, NEP expression in AD affected tissue, both neuronal and vascular, decreased with age (Iwata *et al*., 2002; Nalivaeva *et al*., 2012). Although brain tissue expression appears to decrease astrocytic NEP, NEP expression has been shown to increase in astrocytes around Aβ plaques in an age-dependent manner (Apelt *et al*., 2003). NEP expression has recently been found to be regulated by AICD, a product of APP secretion (Figure 1.1), thought to negatively regulate the production of Aβ (Pardossi-Piquard *et al*. 2005). AICD upregulates NEP expression and competes with histone deacetylase (HDAC)1 for binding to the NEP promoter region. HDAC inhibitors such as trichostatin A and valproic acid could upregulate NEP activity as well as expression (Beckett *et al*., 2012; Nalivaeva *et al*., 2012). The upregulation of NEP makes for an interesting therapeutic advancement towards the treatment of AD. However, there are complications associated with NEP overexpression. These complications are most likely due to NEP's cleavage and hydrolysis of many physiologically relevant peptides such as enkephalins, tachykinins and natriuretic peptides (Kenny *et al*., 1993; Turner *et al*., 2001). In hypertensive rat models, inhibition of NEP induces lower mean arterial blood pressure and increased natriuresis (Potter, 2011; Webb *et al*., 1989). Thus, upregulation of NEP would exacerbate any cardiovascular pathology. Further in-depth studies on transgenic mice indicated that NEP overexpression failed to ameliorate cognitive functions yet reduced the more pathogenic Aβ oligomers (Meilandt *et al*. 2009). Most NEP substrates are found within the mill molar range (Vijayaraghavan *et al*., 1990), subsequently it has been proposed that low (nano molar) Aβ concentrations, to which NEP has a K_M of 2.5 micro molar (Iwata *et al*., 2000), make the physiological significance of this enzyme questionable (Shibata *et al*., 2000).

The crystal structure of NEP complexed with phosphoramidon has improved our understanding of substrate specificity and the catalytic mechanism for this enzyme (Oefner *et al*., 2000). A recent paper endeavoured to enhance NEP's Aβ specificity and activity over its more natural substrates by directed evolution. They successfully mutated two amino acid residues which altered the active site accessibility to better accommodate the large Aβ substrate (Webster *et al*., 2014). These alterations generated a variant of NEP that has a 20-fold increased catalytic efficiency for Aβ(1–40) and up to 3000-fold reduction in its ability to process a range of alternative substrates (Webster *et al*., 2014). Although these data lend themselves to the development of NEP overexpression or activation, further investigation is required to validate this enzyme as a drug target for AD.

1.3.3.2 **Insulin degrading enzyme**

Of the amyloid proteases, IDE (insulysin, insulinase, , EC 3.4.24.56) was the first identified as capable of Aβ-degradation and this has since been confirmed in both cell and animal models of AD (reviewed in Leissring, 2008; Nalivaeva *et al*., 2012). IDE overexpression has been shown to ameliorate any Aβ pathology induced by IDE knockout mice (Farris *et al*., 2003; Leissring *et al*., 2003a). IDE has a very interesting substrate specificity, in that its substrates share almost no homology other than their β-sheet-rich, amyloidogenic nature (Kurochkin and Goto, 1994; Kurochkin, 1998; McCord *et al*., 2013). These, often peptide hormone, substrates are also hydrolysed completely at multiple cleavage sites to ensure inactivation.

IDE is most well-known for its role in diabetes, as the enzyme primarily responsible for the breakdown of insulin (Abdul-Hay *et al*., 2011; Maianti *et al*., 2014). However, AD has been implicated by some as a type-3 diabetes, due to the growing body of evidence implicating hyperinsulinemia as the cause of Aβ accumulation and associated pathologies (de la Monte and Wands, 2008). This theory was based on IDE's specific substrate preference for large amyloid fibrils such as Aβ, whose catalysis is competitively inhibited by insulin (Craft and Watson, 2004; de Tullio *et al*., 2008; Farris *et al*., 2003). Furthermore, diabetes generates neuronal insulin resistance in response to hyperinsulemia, which causes local hypoinsulemia. This increases inflammation and could induce neuronal dysfunction. IDE is interesting in that its high affinity substrates, like insulin, bind directly to its active site (unlike most of its small substrates which bind to allosteric sites which induce inhibition rapidly) and induce substrate inhibition at higher concentrations (Noinaj *et al*., 2011; Shen *et al*., 2006). In contrast, small molecules that bind allosterically induce a conformational change that opens up the clam-like structure generally activating IDE. Insulin has been shown to regulate the levels of IDE, with insulin resistance blocking any positive feedback of IDE expression and causing an increase in Aβ, which is a result of both competitive substrate inhibition and a decrease of IDE levels in AD patients (Cook *et al*., 2003; Leissring *et al*., 2003b). Aβ oligomers disrupt insulin receptor signalling and reduce insulin binding to them, thus down regulating neuronal insulin receptors and promoting insulin resistance (Xie *et al*., 2002; Zhao *et al*., 2008). This provides further support for the link between type-3 diabetes and AD.

Like NEP, IDE has a large repertoire of substrates other than insulin and Aβ. Interestingly, it is the main protease responsible for the degradation of AICD (Edbauer *et al*., 2002) thus potentially negatively regulating NEP cytosolically. Counteracting this, a well-known neuropeptide somatostatin regulated by NEP (Saito *et al*., 2005), binds allosterically to

activate and enhance IDE activity towards Aβ (Ciaccio *et al*., 2009; Tundo *et al*., 2012). Unlike NEP, IDE is primarily located in the cell cytosol, however, it is secreted in significant amounts into the extracellular milieu and CSF (Zhao *et al*., 2009). More importantly, it is found in the mitochondria of neurons, where Aβ induces irrevocable damage and, furthermore, the secreted form of IDE co-localised with Aβ in endosomes (Bulloj *et al*., 2010; Leissring *et al*., 2004). The data implicating IDE as a major Aβ degrading enzyme *in vivo* are convincing (Farris *et al*., 2003; Leissring *et al*., 2003a). Like NEP, overexpression or activation of IDE is a tempting potential therapy for the treatment of AD, although not without its caveats.

1.4 Angiotensin I-converting enzyme.

The contribution of ACE and its fellow Aβ degrading proteases has been extensively reviewed before (Hooper & Turner 2000; Carson & Turner 2002; Turner 2003; Wang *et al*. 2006; Miners *et al*. 2008; Rosenberg 2009; Strooper 2010; Gough *et al*. 2011; Nalivaeva *et al*. 2012; Miners *et al*. 2014). The exact role of ACE in AD pathology however, remains undefined (discussed below).

ACE is most renowned for its dicarboxypeptidase conversion of angiotensin I (ANGI) to the vasoconstrictive angiotensin II (ANGII) and the breakdown of bradykinin (BK) (reviewed in Acharya *et al*., 2003; Riordan, 2003; Sturrock *et al*., 2012). This hydrolytic function places ACE as a central component of the renin-angiotensin-aldosterone-system (RAAS) - the hormonal system responsible for the maintenance and homeostasis of blood pressure (Ehlers and Riordan, 1989; Sancho *et al*., 1976; Shapiro and Riordan, 1984). Like NEP and IDE, ACE cleaves a wide range of physiological substrates and has many functions (for a thorough review see Bernstein *et al*. 2013); however the production of ANGII and breakdown of BK (major effectors of the RAAS) associate ACE activity primarily with cardiovascular disorders (reviewed in Zaman *et al*., 2002). Physiologically ACE is implicated in a multitude of functions and is also responsible for the breakdown of the tetrapeptide N-acetyl-Ser-Asp-Lys-Pro (AcSDKP) (P. Li *et al*., 2010; Peng *et al*., 2005). Ac-SDKP was first described as a natural regulator of hematopoietic stem cell proliferation (Bonnet *et al*., 1992). However, modulation of haematopoiesis was found to occur by ACE through other substrates like substance P or ANGII (Bernstein *et al*., 2011; Lin *et al*., 2011). Most importantly, with respect to therapeutic intervention, AcSDKP has been shown to prevent the proliferation of fibroblasts in the myocardium, aorta and the kidney in models of injury (Liao *et al*., 2010; Lin *et al*., 2008; Peng *et al*., 2001). In male mice spermatozoa, ACE regulates the GPI-anchored protein TEX101, whose removal is essential for fertility and may provide a novel target for male contraceptive medicine (Fujihara et al., 2013). *In vitro* ACE caters to a large array of substrates including the breakdown of substance P (Skidgel *et al*., 1984), hydrolysis of gonadotrophin releasing hormone (GnRH) (Jaspard *et al*., 1993), neurotensin (Matsas *et al*., 1984; Skidgel *et al*., 1984), enkephalins (Deddish *et al*., 1997) and Aβ (Hu *et al*., 2001) to name a few. It is important to note that these latter substrates have not been validated convincingly *in vivo*.

1.4.1 ACE General Properties.

ACE is a zinc-dependent peptidase that requires specific post-transcriptional modifications and chloride in order to remain functionally active. The precise amino acids required for

chloride binding were identified and the functional concentration determined (Rushworth *et al*., 2008; Shapiro and Riordan, 1983; Tzakos *et al*., 2003; Yates *et al*., 2014). ACE is heavily glycosylated and the glycosylation pattern differs depending on the tissue in which ACE is expressed (Baudin *et al*., 1997). As with most eukaryotic proteins, glycosylation is required for correct intracellular folding and formation of the mature enzyme (Anthony *et al*., 2010; Baudin *et al*., 1997). It is important for ACE's thermal stability and may play a role in dimerization and possibly effect inhibitor or substrate accessibility (Kost *et al*., 2003; Margraf-Schönfeld *et al*., 2011; O'Neill *et al*., 2008). The large amount of glycan heterogeneity as well as the quantity (reported up to 22 % of the total enzyme mass) still proves an obstacle towards the crystallization of intact full-length ACE (Baudin *et al*., 1997; Deddish *et al*., 1994; Ripka *et al*., 1993; Yu *et al*., 1997). The problem of glycosylation was overcome with the use of glycosidase inhibitors and the removal of glycosylation sites, by site directed mutagenesis, to yield crystal structures of minimally glycosylated truncated ACE (Anthony *et al*., 2010; Gordon *et al*., 2003; Natesh *et al*., 2003).

The gene encoding ACE (*Ace*) is 21 kb long, with 26 exons (Figure 1.4 A), on the long arm of chromosome 17 at locus q23 and is found behind a promoter region regulated by glucocorticoid response element (Hubert *et al*., 1991). Through cloning of the *Ace* gene it was discovered that ACE consists of two homologous domains (the N-domain and C-domain) each containing a zinc binding motif HEXXH (Soubrier *et al*., 1988) (Figure 1.4 A). This zinc binding motif typifies ACE as a member of the gluzincin family of the MA clan of zinc metallopeptidases, whose catalytic mechanism is dependent on the binding of divalent cations (Rawlings *et al*., 2010), these family properties have been well reviewed in Spyroulias *et al*., 2004 and in Turner and Hooper, 2002. A common polymorphism found within the *Ace* gene occurs as a 287 bp insertion/deletion within intron 16 (Rigat *et al*., 1990). Individuals homozygous for the deletion (D/D) mutation generally present with higher serum ACE activity than those homozygous for the insertion (I/I) (Rigat *et al*., 1992, 1990).

There are two isoforms of ACE, somatic ACE (sACE) and testis ACE (tACE) (Figure 1.4). sACE is expressed across a variety of tissue types: in large quantities within vascular endothelium (Ng and Vane, 1968, 1967), lung , renal epithelium (Cushman and Cheung, 1971a, 1971b), fatty tissue (Böttcher *et al*., 2006), ciliated intestinal epithelium (Bruneval *et al*., 1986; Wildhaber *et al*., 2005), monocytes, immune-activated dendritic cells (Friedland *et al*., 1978; Lin *et al*., 2011), and in the brain (Defendini *et al*., 1983; McKinley *et al*., 2003). The testis isoform arises as a result of a tissue specific promoter found within intron 12 of the *Ace* gene (Figure 1.4 A). It is specific to male germ cells and its expression is regulated by cAMP response element (Howard *et al*., 1990; Langford *et al*., 1991). The somatic form of ACE is expressed, in its maturity, as a large 1 277-amino acid protein with two homologous catalytic domains (Bernstein *et al*., 1989; Soubrier *et al*., 1988; Wei *et al*., 1991) separated by a short linker region. Both isoforms are targeted to the cell membrane by N-terminal signal peptides (29 residues in sACE and 31-residues in tACE) (Ehlers *et al*., 1989) and, being type I integral membrane proteins, contain membrane-anchoring hydrophobic regions as well as juxtamembrane stalk and ectodomains. ACE contains a short cytoplasmic tail with numerous Ser and Thr residues which allows for signalling capabilities (Hubert *et al*., 1991; Kohlstedt *et al*., 2004; Soubrier *et al*., 1988). Differing from sACE, tACE has limited tissue expression and is identical to the C-domain of sACE, barring the first 36 residues (Ehlers *et al*., 1989; El-Dorry *et al*., 1982). Both isoforms are proteolytically-shed from the cell membrane near the

transmembrane region by a yet unidentified ACE sheddase (Ehlers *et al*., 1996). Shedding of the high expressing sACE in vasculature and lung tissue promotes the formation of soluble ACE which forms part of the circulating RAAS (Ehlers *et al*., 1996; Woodman *et al*., 2000) (Figure 1.4).

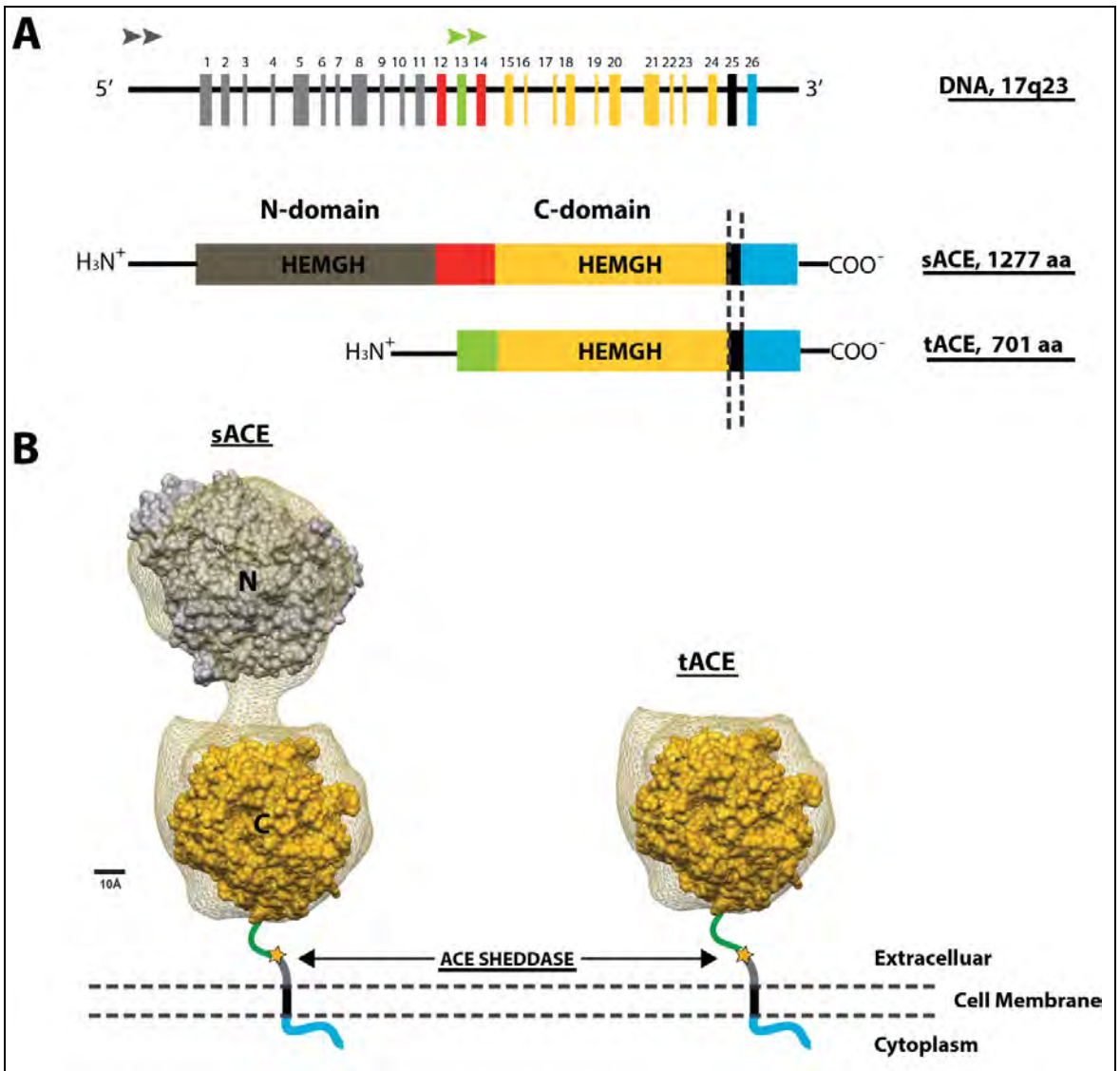

Figure 1.4 **The two isoforms of ACE**. **A)** A schematic representation of the *Ace* gene, with its 26 exons, and corresponding protein regions below, sACE 1277 amino acids long and the shorter tACE of only 701 amino acids. The grey exons represent the N-domain of sACE, and the sACE promoter position is indicated by grey arrows. The red exons beginning at exon 12 indicate those that encode for the linker region. The green arrows and corresponding exon indicate the site of the tACE promoter that transcribes the C-domain (yellow). Exon 13 is seen as an intron and spliced out in the transcription of sACE. **B)** A model based on the crystal structures of the individual N- and C-domains of ACE in the sACE format (Chen *et al.,* 2010) on the left and tACE on the right. The diagram depicts the proteins attached to the cell membrane and emphasises the overlap between tACE and the C-domain. Indicated by the star is the cleavage site of the ACE sheddase responsible for the formation of the circulating sACE.

1.4.2 The two domains of ACE.

1.4.2.1 **Structural similarities.**

The N- and C-domains of ACE can function independently of one another as they are individually able to hydrolyse substrates if the other catalytic site is inactivated (Wei *et al*., 1992). Structurally, there are only minor differences between the two domains (89 % structural homology) (Figure 1.5) (Corradi *et al*., 2006). Both domains can be divided in to two sub-domains, between which lies a central cleft (Corradi *et al*., 2006; Natesh *et al*., 2003). This cleft contains the zinc bearing active site on helix α15, it has been suggested that substrate access to this buried active site occurs through hinge mediated opening (Anthony *et al*., 2010). Both domains have globular elliptical quaternary structures composed largely of α-helices but contain several flexible loops and 6 β-sheets (Corradi *et al*., 2006). There are three α-helices that form an N-terminal lid-like region, which are positioned over the active site cleft. This region is thought to play a role in substrate specificity and active site access as it has higher B factors suggesting some flexibility. The lid regions on the N- and C-domains are associated with glycosylation sites shown to be important for the stability of the lid region and increased thermostability (Anthony *et al*., 2010; Watermeyer *et al*., 2006).

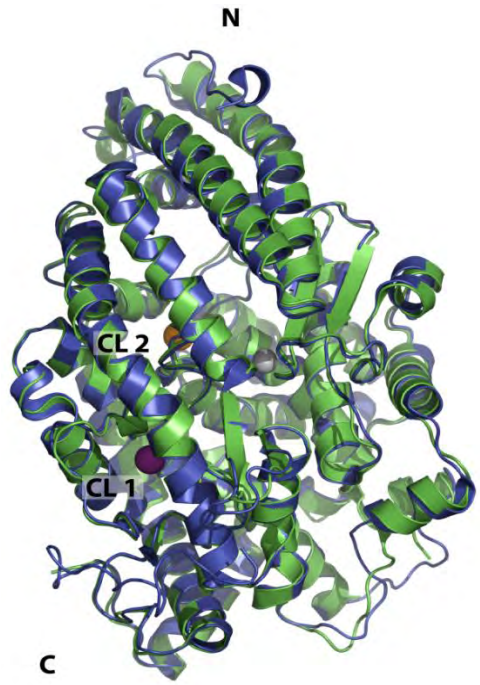

Figure 1.5 **Overall homology of the N- and C-domain topology.** An alignment of the N (sky blue) and the C-domain (tv green) PDB files 2C6F and 1086 respectively, indicating the degree of similarity and positioning of the tertiary and quaternary structures of the two domains. The two zinc ions of each domain (grey,) overlap exactly and the two chloride ions in orange and purple bound within their respective pockets in the C-domain are represented. The deep central cleft can be observed diagonally from top left (N-terminals) to the C-terminals of the molecules, in line with the zinc ion, resulting in two sub-domains. This image was generated using PyMOL software (v 0.99, DeLano Scientific).

There is no current crystal structure of sACE, only a low resolution electron microscopy structure, which gives some positioning information of the two domains (Chen *et al*., 2010). However, insight into the structure function mechanisms of both domains has been determined separately. Kinetic studies suggest interactions between the two domains alter both the binding and hydrolysis of substrates and inhibitors. The theory of interaction or cooperativity between the two domains postulates that the binding of substrates or inhibitors in one domain induces a conformational change in the other. Wherein, if the sum of the catalytic activity of one domain is less or greater than that of sACE, the cooperative effect is either negative or positive, respectively. Thus, sACE is said to display mostly negative cooperativity between the two domains towards substrates and inhibitors alike (Andújar-

Sánchez *et al*., 2004; Binevski *et al*., 2003; Rice *et al*., 2004; Skirgello *et al*., 2005). The one domain of sACE may also occlude substrate or inhibitor access to the other inducing a synergistic regulatory effect on each other (Skirgello *et al*., 2005; Sturrock *et al*., 1997; Woodman *et al*., 2005). Furthermore the proximity of the N-domain to the C, has been implicated as a modulator of sACE shedding, adding another level of regulation to substrate hydrolysis and control (Woodman *et al*., 2005). Resolution of the sACE crystal structure would help explain and expand how the two domains of ACE regulate one another.

1.4.2.2 **The C-domain.**

In vitro the hydrolysis of ANGI by the C-domain is approximately 3 times more efficient than the N-domain (Georgiadis *et al*., 2003; Wei *et al*., 1991). The development of ACE transgenic mice expressing single ACE isoforms, inactivated N- or C-catalytic sites or tissue-specific ACE has greatly increased our understanding of ACE's function *in vivo* (Bernstein *et al*., 2011). Confirmation of ACE's role in blood pressure came from ACE knockout mice that were hypotensive (Esther *et al*., 1996; Kim *et al*., 1995). Aside from being hypotensive, these mice had additional defects including anaemia, decreased renal function and fertility as well as severe physical abnormalities. The lack of fertility is attributed to the deletion of tACE, which is responsible for sperm motility within the oviduct and impaired binding to the zonae pellucidae (Hagaman *et al*., 1998; Krege *et al*., 1995). Thus, fertility is vitally dependent on tACE's hydrolytic activity on an unknown substrate (Fuchs *et al*., 2005). Recently, more sophisticated and elegant mouse studies have further elucidated the functions of the N- and C-domains (Bernstein *et al*., 2011). These studies were performed on mice whose individual N- or C-domains had been inactivated through mutation of the zinc binding motif leaving only one functioning domain (Fuchs *et al*., 2008, 2004; Xiao *et al*., 2004). Mice whose N-domains were inactivated had no changes in blood pressure, renal function or hemocrit levels (Fuchs *et al*., 2004); however, C-domain inactivation resulted in a compensatory increase of renin expression and a concomitant increase in ANGI levels (Fuchs *et al*., 2008). These mice also lacked response on stimulation with ANGI. Together these results implicate C-domain principally in the conversion of ANGI to ANGII, however, both domains hydrolysed BK with similar efficiency (Fuchs *et al*., 2008).

1.4.2.3 **The N-domain.**

The N-domain of ACE catalyses a far more varied repertoire of substrates and is thought to be responsible for ACE's endopeptidase activity (Ehlers and Riordan, 1991; Jaspard *et al*., 1993; Wei *et al*., 1991). In addition, it has a regulatory function on the shedding of sACE (Woodman *et al*, 2000). In sACE shedding is reduced in comparison to tACE and it is thought that the orientation and physical presence of the N-domain (within sACE) sterically hinders the sheddases access to the stalk region (Woodman *et al*., 2000). Thus, the N-domain could be important in regulating the amount of circulating ACE. An active, N-domain of two different molecular weights (65 and 90 kDa) derived from sACE was discovered in ileal fluid (Deddish *et al*., 1994). Since this discovery, it has arisen in urine of hypertensive patients (Casarini *et al*., 2001) and in spontaneously hypertensive rat models, with the 90 kDa variant thought to be a marker for hypertension (Bueno *et al*., 2004; Marques *et al*., 2003; Ronchi *et al*., 2005). The presence of the individual N-domain in isolation suggests an important physiological role *in vivo*. An abundance of N-domain may breakdown N-specific substrates, potentially altering

physiology. *In vivo* studies on mice with inactivated N-domain, however, indicated that it has little prominence within the RAAS as blood pressure was not affected, but Ac-SDKP levels increased by 6-fold (Junot *et al*. 2001; Fuchs *et al*. 2004;). Furthermore, in normal volunteers who were given ACE inhibitors , AcSDKP levels increased 5fold on acute administration and was generally elevated on continuous administration (Azizi *et al*., 2001, 1996). *In vitro* the binding for AcSDKP is equivalent across both domains of ACE, yet the N-domain has proven approximately 40 times better at its catalysis than the C-domain (Rousseau *et al*., 1995). The N-domain has also been found to have an immune function, as macrophages derived from N-domain knockout mice had increased Tumor necrosis factor α (TNFα) compared to the C-domain knockouts and wild type mice (Shen *et al*., 2012). In conclusion, physiologically, the N-domain appears primarily responsible for ACE's immune function and the hydrolysis of Ac-SDKP, and the C-domain is primarily responsible for maintaining the RAAS function.

1.4.3 ACE signalling.

ACE inhibitors (ACEi) function on the premise of lowered ANGII and increased cardio protective BK levels (Hornig *et al*., 1997). BK increases endothelial production of autacoids of the likes of NO, endothelium-derived hyperpolarizing factor (vasodilator) and numerous prostacyclins (Danser *et al*., 2000). ACEi have been shown to have additional effects outside of this inhibitory mechanism. Aside from prolonging the half-life of BK, ACEi also potentiate its vasodilatory responses through enhanced binding to the bradykinin-2 receptor (B_2R) (Marcic *et al*., 1999). For example, the response to increased BK on ACE inhibition in porcine vasculature was observed within seconds of ACEi treatment. Although the half-life of BK in this tissue is approximately 10 minutes, mere increase in peptide could not account for the observed vasoactive response (Erdös *et al*., 1999). These and similar findings prompted research on the effects of ACE outside of its catalytic function. Indeed ACEi were shown to prevent the desensitization and membrane-mediated sequestration of previously activated B_2Rs (Benzing *et al*., 1999). This implied an associative crosstalk between sACE and the B_2R. Confirmatory experiments were performed on cells that lack endogenous expression of ACE or B_2R (Minshall *et al*., 1997). Here, only cells transfected with both sACE and the B_2R elicited an enhanced BK binding response, whereas cells maintaining sACE or B_2R only did not (Minshall *et al*., 1997). The potentiation response occurs through a maintained affinity of B_2R towards BK, and a reduction in B_2R desensitization and internalization as a result of ACE inhibition (Erdös *et al*., 1999).

1.4.3.1 **ACE's receptor-like function**

ACE has a receptor-like composition, with a short cytoplasmic tail that contains a number of serine residues. Of these Ser1253, Ser1263 and Ser1270 occur within the recognition motifs of protein kinase C (PKC), protein kinase A (PKA) and Casein Kinase 2 (CK2), respectively. ACE's alternate, receptor-like function was proposed based on signalling mediated via phosphorylation of Ser1270 residue by CK2 in response to ACEi binding (Kohlstedt *et al*., 2002) (Figure 1.6). Inhibition of CK2 lead to a significant reduction of the phosphorylation of this site, suggesting that CK2 was specific to Ser1270 (Kohlstedt *et al*., 2002). The phosphorylation of Ser1270 appears crucial in maintaining sACE within the cell membrane as basal shedding levels were significantly increased in human umbilical vein endothelial cells (HUVEC) transfected with a non-phosphorylated mutant of sACE (Ser1270 converted to an Ala)

(Kohlstedt *et al*., 2002). As a cell's actin cytoskeleton is thought to influence ectodomain shedding, immunoprecipitation experiments were performed on β-actin and the non-muscle myosin heavy chain IIA (MYH9) that associated, in a basally phosphorylated state, with the Ser1270 of sACE. The CK2 phosphorylation is not only specific to sACE but also to MYH9. Subsequent inhibition of CK2 attenuated ACE and MYH9 phosphorylation, disrupted their association, and enhanced ACE shedding (Kohlstedt *et al*., 2002). These experiments suggest a functional interaction between phosphorylation of the sACE's cytoplasmic tail and cell cytoskeletal proteins. Thus, phosphorylation of sACE by CK2 could modulate ACE shedding, stabilising anchorage to the cytoskeleton.

1.4.3.1.1 The signalling pathway

Protein-Protein associations with ACE extend towards receptors of the RAAS, binding to ITGB1 integrins (Clarke *et al*., 2012) and homozygous dimerization with itself (Kost *et al*., 2003, 1998). The binding of ACEi is said to induce sACE dimerization, which corresponds in time to the point of greatest Ser1270 phosphorylation. Thus, ACE dimerization is thought to initiate the ACE signalling cascade, via CK2-mediated phosphorylation of Ser1270 (Kohlstedt *et al*., 2006a). In porcine aortic endothelial cells, the absolute requirement for sACE signalling is the presence of a catalytically active C-domain. However, dimerization has been indicated to be dependent on the level of glycosylation of ACE (Kost *et al*., 1998). As ACE is heavily glycosylated the type and extent of glycosylation are dependent on the source of the enzyme (Ehlers et al., 1992; Hooper and Turner, 2000; Ripka et al., 1993; Ryan et al., 1993). Thus, one would expect different tissues to have different signalling effects if dimerization was indeed a determinant of sACE signalling. In support of the latter, the pathway seems to have cell or species specific functionality. Human sACE in porcine cells had a small signalling response to BK and no response to ANGI, yet murine sACE in CHO cells produced a significant signalling event towards ANGI, ANGII and BK (Kohlstedt *et al*., 2005; Sun *et al*., 2010). Furthermore, the N-domain in murine sACE was capable of inducing signal, albeit subdued in comparison to the C-domain (Sun *et al*., 2010).

1.4.3.1.2 Activation of JNK and AP-1 and downstream effects

The resultant downstream effect of sACE Ser1270 phosphorylation is the activation of c-Jun NH_2terminal kinase (JNK). JNK is an effector of the mitogen-activated protein kinase (MAPK) signalling pathway. Indeed MAPK kinase (MAPKK) 7 was found to associate with phosphorylated Ser1270-sACE-CK2 immunoprecipitations. The JNK pathway can be activated by numerous stimuli, being a well-known stress response pathway especially in AD and dementia (Borsello and Forloni, 2007; Hashimoto *et al*., 2003; Morishima *et al*., 2001; Wei, 2002; Yoon *et al*., 2012). JNK can be activated by cytokines and environmental stressors to mediate different cellular processes including, inflammation, differentiation, proliferation and apoptosis (Bogoyevitch and Kobe, 2006). ACE signalling directs JNK activation, and induces downstream c-jun phosphorylation and translocation into the nucleus where it homodimerises to form the transcription factor apoprotein-1 (AP-1) (Kohlstedt *et al*., 2004) (Figure 1.6). AP-1 is a known transcription factor of the *Ace* gene and of the pro-inflammatory cyclooxygenase-2 (COX-2) (Figure 1.6). One would anticipate upregulation of ACE and COX-2 to be detrimental to the treatment of cardiovascular disease. However, COX-2 inhibitors have proven a great risk to the development of atherosclerosis as they induce an increase in

platelet aggregation despite being anti-inflammatory. Overall, induction of the ACE signalling pathway by either inhibitor or substrate has both negative and positive implications theoretically in AD.

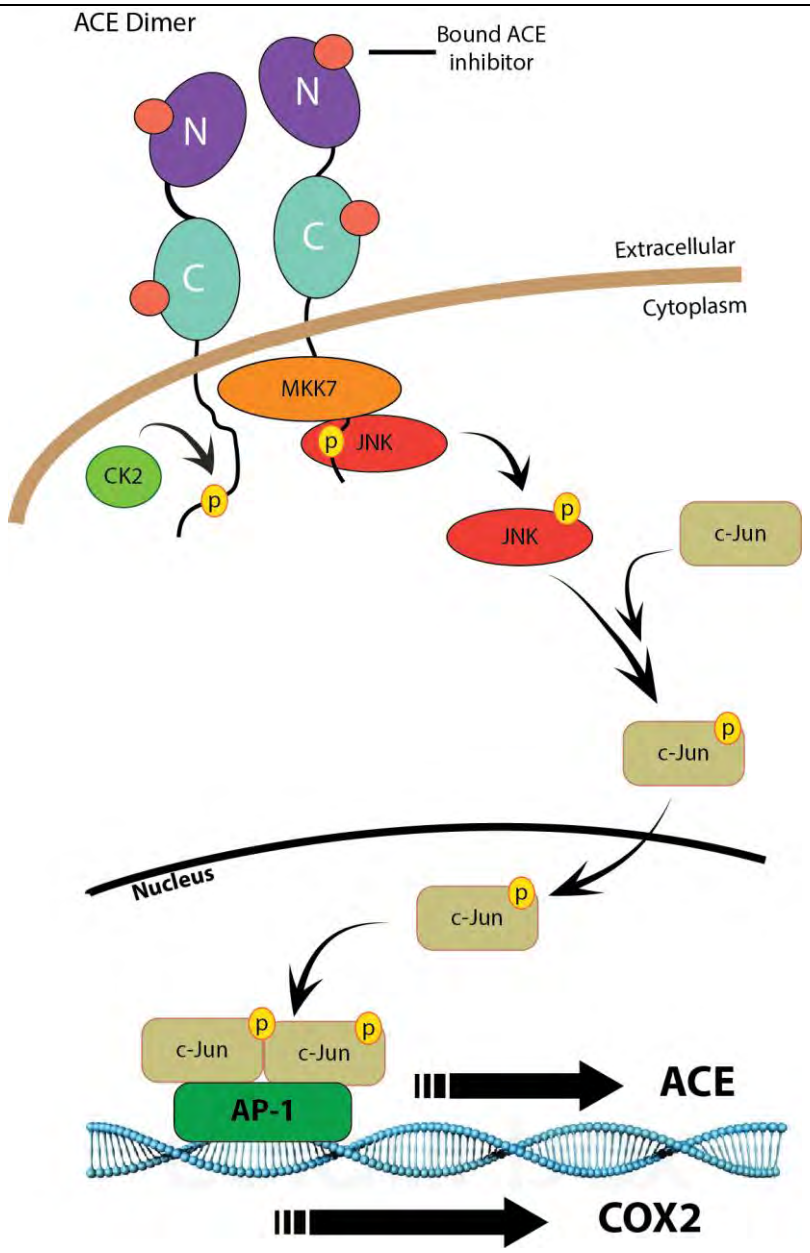

Figure 1.6 **ACE inhibitors and substrates increase ACE expression through ACE signalling.** The ACE signal response is generated by inhibitor binding and molecular dimerization. On binding of the inhibitor phosphorylation of serine ^{1270}, found in a highly conserved 13-amino acid sequence, occurs by a casein kinase 2 (CK2) which stabilises ACE in the plasma membrane. Mutations of Ser ^{1270} or inhibition of CK2 promotes cleavage and secretion of ACE (Kohlstedt *et al*., 2002). Other molecules are associated with the phosphorylation of Ser ^{1270} of ACE, the Mitogen-activated protein kinase kinase 7 (MKK7) and c-Jun N-Terminal Kinase (JNK) are both activated by a putative phosphorylation cascade initiated by the Ser ^{1270} residue. The JNK pathway activates the transcription factor c-Jun causing it to translocate and accumulate in the nucleus where it forms a homodimer that associates with activator protein-1 (AP-1) and binds to the cAMP responsive element sequence of the ACE promoter (Flemming *et al*. 2005, Eyries *et al*. 2002; Kohlstedt 2001, 2003, 2004). This results in the transcription (thick black arrows) of COX-2 and ACE

1.4.3.1 **Insulin sensitivity and ACE signalling implications in AD.**

Hypertension and diabetes often present as comorbidities, a patient with one disease is at high risk of developing the other. As previously mentioned, AD has been termed a type-3 diabetes and the link between AD and type-2 diabetes mellitus (T2DM) is well established being associated with major risk factors such as inadequate brain glucose metabolism and insulin signalling (Akter *et al*., 2011; Yang and Song, 2013). ACE signalling was examined in pre-adipocytes to help describe the improved insulin sensitivity that ACE inhibition provokes (Böttcher *et al*., 2006). Analysis of differential gene expression, in cells expressing sACE or a signalling mutant, indicated that adiponectin was upregulated in the pre-adipocytes (Böttcher *et al*., 2006). Adiponectin is responsible for the promotion of fatty acid oxidation (reducing ROS), lowering glucose production and promoting glucose uptake (for a review associated with dementia see J. Song *et al*. 2014). ACE's signalling pathway regulated cellular retinol-binding protein (CRB1) which could affect gene regulation via peroxisome proliferator-activated receptors (PPAR) (Kohlstedt *et al*., 2009). Indeed, ACEi restoration of adiponectin was thwarted by inhibition of either JNK or PPARγ antagonism. Furthermore, in the *ob/ob* obese mouse model of diabetes ACEi restored adiponectin levels and potentiated the effects of the PPAR-agonist rosiglitazone (Kohlstedt *et al*., 2009). These experiments were further validated in patients with coronary artery disease (Kohlstedt *et al*., 2009). PPARs bind to target DNA response elements as heterodimers with retinoid-X receptor causing gene transcription as well as trans-repression of proinflammatory genes (Chen *et al*., 2012). This trans-repression interferes with the activities of other transcription factors of the likes of nuclear factor-κB (NF-κB) and AP-1 families (Schnegg *et al*., 2012). Although ACE inhibitors have not been tested as PPARγ receptor agonists, telmisartan is a partial agonist of PPARγ that leads to a decrease in ACE activity and an overall reduction of oxidative stress via $p22^{phox}$ inhibition (Takai *et al*., 2007). In AD patients PPARγ expression was shown to be elevated (de la Monte and Wands, 2006) most likely in a protective manner as it had promising neuroprotective effects (Combs *et al*., 2000). PPARγ activation of insulin-sensitizing thiazolidinedione (TZD) drugs, used to treat T2DM, slow onset and development of Alzheimer's and promote cell survival (Rodriguez-Rivera *et al*., 2011; Zolezzi and Inestrosa, 2013)

Another molecular switch related to AD, blood pressure and diabetes, is adenosine monophosphate-activated protein kinase (AMPK). AMPK also mediates adiponectin expression, which stimulates Glucose transporter type 4 ($GLUT_4$) translocation and glucose uptake. Adiponectin binding to its receptors further perpetuates increased insulin sensitivity (Yamauchi *et al*., 2001) and improved vascular function (Fésüs *et al*., 2007; Gustafsson *et al*., 2010) by activating not only AMPK (Iwabu *et al*., 2010) but p38/JNK MAPK (Miyazaki *et al*., 2005) and PPARα (Qiao *et al*., 2011). PPARα has recently been shown to be responsible for the activity of ADAM 10, the α- secretase (Chen *et al*., 2012). In a study on *ex vivo* human peripheral monocytes/macrophages, increased expression of ACE has been shown to reduce their activation and pro-inflammatory cytokine production response (Kohlstedt *et al*., 2011); a response similar to that of non-steroidal anti-inflammatory drug (NSAID) treatment against Aβ-induced macrophage activation (Combs *et al*., 2000).

This, ACE signalling mediated mechanism is induced by lipids from adipocyte-conditioned media and resulted in a 4-fold increase in ACE expression. This was dependent on the presence of ACE and not its activity, as inhibition had no effect, yet gene-silencing ACE did. Mechanistically, the phosphorylation of AMPK was responsible for this increase in ACE expression. Moreover, in AMPKα1(-/-) mice, ACE expression was reduced in spleen derived-monocytes compared to wild-type littermates (Kohlstedt *et al*., 2011). The same group determined later in endothelial cells that ACE expression is down regulated in response to shear stress along the same AMPK pathway that T2DM stimulates (Kohlstedt *et al*., 2013). The activation of AMPKα2 subunit results in subsequent phosphorylation of the pro-cell-survival site (Ser15) on p53. This p53 activation induced a post-transcriptional up-regulation of miR-143/145 which decreased ACE expression (Kohlstedt *et al*., 2013). Taken together, from the upregulation of adiponectin and PPARs to the immune-modulating functions ACE may have, independent of its activity, ACE has a broad range of avenues through which its inhibition may influences outcomes in AD.

1.5 The Brain Renin Angiotensin-Aldosterone System.

There is increasing evidence that vascular disorders, like hypertension and atherosclerosis, are the primary cause of AD (Bell and Zlokovic, 2009; de la Torre and Mussivand, 1993; George-Carey *et al*., 2012). Hypertensive patients are prone to the development of strokes, white matter lesions, silent infarcts, myocardial infarction and cardiovascular diseases (de Leeuw *et al*., 2002). Hypertension is often the introduction to conditions like diabetes mellitus, obesity and hypercholesterolemia (Kivipelto and Solomon, 2006; Launer, 2009; Ruitenberg *et al*., 2001). Vascular diseases lead to dysfunctions of the BBB (Zlokovic, 2004), resulting in brain ischemia, and oxidative stress all of which can result in Aβ accumulation, synaptic loss, neurofibrillary tangles and ultimately AD (Farkas and Luiten, 2001; Hooijmans and Kiliaan, 2008; Launer *et al*., 2000). Thus, there is support towards the notion that vascular disorders like hypertension induce chronic degeneration in AD.

One of the systems responsible for blood pressure maintenance is the RAAS, a fundamental, conserved system that controls the cardiovascular system, renal function and fluid homeostasis (Fournier *et al*., 2012). Over activity of any of its components is generally associated with hypertension, renal disease and metabolic syndrome. The RAAS was initially described as a simple system whose rate-limiting factor was the conversion of angiotensinogen by renin into the inactive ANGI, which was subsequently converted to the vasoactive ANGII by ACE. It was thought that ACE was solely responsible for the formation of ANGII and that ANGII was the only active principle of the RAAS (Skrbic and Igic, 2009). We now know that there are many branches that stem from the classical RAAS axis. The classical axis consists of angiotensinogen, renin, ANGI, ACE, ANGII and the effector of blood pressure AT_1R, which induces aldosterone secretion and triggers sodium reuptake (Figure 1.7). The extended RAAS encompasses the seemingly antagonistic arms of the classic RAAS. Aside from the peripheral RAAS there exists an independent brain RAAS (BRAAS) that extends its role beyond the classical fluid and blood pressure homeostasis into areas such as sexual behaviour, cerebroprotection, diabetes, psychological disorders and many neurodegenerative diseases including AD (Phillips and De Oliveira, 2008; Saavedra *et al*., 2011; Wright and Harding, 1997). The BRAAS, which, apart from the circumventricular regions which have no BBB, is a separate

system from the peripheral RAAS and contains all the components of the RAAS, the central classic axis as well as the branching axis (McKinley *et al*., 2003) (Figure 1.7). There appear to be two axes of the RAAS, the classic axis and the so-called good axis, which includes peptides ANGIII, ANGIV and ANG(1-7). As all the effects of BRAAS peptides are mediated by receptors, it is from this point of view that it will be described.

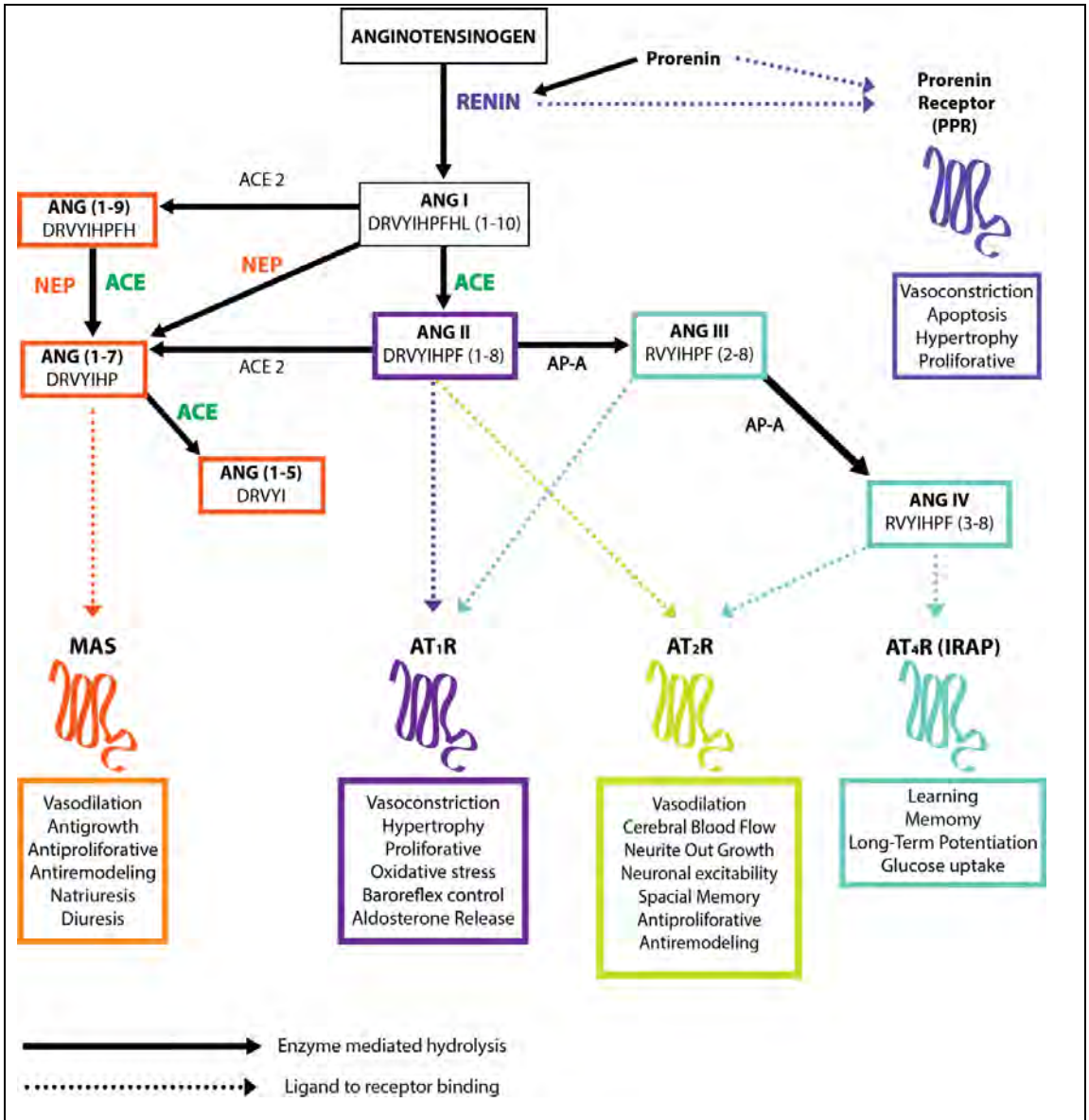

Figure 1.7 **An overview of the brain renin angiotensin-aldosterone system**. The BRAAS appears to be upregulated along the classical axis of angiotensinogen, ANGI, ANGII and activation of the AT_1R and AT_2Rs in AD patients. ACE inhibition is one means to reduce the amount of the AT_1R ligand, ANGII, which is broken down by aminopeptidase A (AP-A), and promote the axis of good via Mas and AT_4R activation instead.

Within the CNS, ACE is found at high levels in the choroid plexus, which may be the source of ACE in cerebrospinal fluid, subfornical organ, basal ganglia, substantia nigra and pituitary (Chai *et al*., 1987). Moderate expression of ACE occurs in the amygdala and in all cortical nuclei. In the cerebellum, dense labelling of ACE was observed in the Purkinje cell layer (Chai *et al*.,

1987). ACE has also been found within the cortical perivasculature, speculated to be a result of interstitial drainage (J S Miners *et al*., 2008). In the BRAAS the formation of ANGII is crucial as it has neurotransmitter-like functions (Ferguson and Washburn, 1998; Johns, 2005; Phillips, 1987) and angiotensinogen is secreted from astrocytes and to help maintains the BBB (Yanai *et al*., 2000). Renin is formed from pro-renin and is responsible for the conversion of angiotensinogen to ANGI. Pro-renin levels in the brain are comparable to levels seen in the heart and are greater than the levels seen in the kidney, liver and pancreas (Nguyen *et al*., 2002). Pro-renin has receptor functions which induce signals much like that of the AT_1R (see below) (Nguyen and Contrepas, 2008). Thus, it is important as most components of the RAAS system cannot cross the blood brain barrier (McKinley *et al*., 2003). In hypertension, which disrupts the BBB, peripheral ANGII mediates a feed-forward mechanism, promoting further BBB permeability and further ANGII access to brain regions which control blood pressure (Biancardi *et al*., 2014). The entire BRAAS, when upregulated, as it has been determined in AD, has both cognitive and pathological implications.

1.5.1 The angiotensin II type 2 receptor (AT_2R).

ANGII is a substrate for numerous enzymes that liberate alternative bioactive substrates within the RAAS. ANGII, the product of ACE hydrolysis, and ANG III, which is formed from aminopeptidase A activity on ANGII, are agonists of the AT_1R and AT_2R subtypes. AT_2Rs are less prominent compared to AT_1R expression in the brain; however, they are upregulated under pathological conditions (Zhu *et al*., 2000). AT_2Rs are found in the thalamus, hypothalamus, and specific brainstem nuclei, as well as in areas of motor and behaviour control (Sokol *et al*., 2004). Hippocampal administration of ANG II induces amnesia, an effect completely reversible by antagonists of the AT_2R, without affecting locomotion, exploratory behaviour or anxiety (Kerr *et al*., 2005). AT_2R stimulation promotes optic nerve and cell differentiation and both axonal and neuronal regeneration in the brain, and is linked to foetal brain development (Li *et al*., 2007; Mogi *et al*., 2006).

1.5.2 The angiotensin II type 1 receptor (AT_1R).

AT_1R is a G-protein coupled receptor which signals via phospholipase-C and calcium (de Gasparo *et al*., 2000; Dinh *et al*., 2001) and is found throughout the brain (Wright and Harding, 2013). There are two subtypes, designated $AT_{1A}R$ and $AT_{1B}R$, with the $AT_{1A}R$ being primarily responsible for BRAAS functions. It regulates the transcription of genes and expression of proteins which are involved in cellular proliferation and growth in many tissues (de Gasparo *et al*., 2000). It is also the major stress receptor; stress induces ANGII increases which bind to $AT_{1A}Rs$ and promotes increased expression and release of norepinephrine via corticotrophin-releasing hormone synthesis and subsequent adrenocorticotrophin release from the anterior pituitary (Gard, 2002; Saavedra *et al*., 2011). Stress is well documented as an etiologic factor in AD (Rothman *et al*., 2012) and contributes significantly to hypertension via the upregulation of the classic RAAS axis. This axial upregulation increases sympathetic nervous system activity via increased ANGII and amyloidogenesis (N. Li *et al*., 2010; S. Li *et al*., 2010; Savaskan *et al*., 2001). AT_1R receptor blockers (ARB) confirmed these findings as a number of studies concluded that ARBs, like olmersartan, candesartan, valsartan, losartan and telmisartan, improved memory and cognitive processing (Mechaeil *et al*., 2011; Ongali *et al*., 2014; Takeda *et al*., 2009; Tota *et al*., 2009; Wang *et al*., 2007). This occurs presumably by blocking the

action of ANGII, reducing blood pressure, stress responses and Aβ accumulation. Blocking the AT_1R receptor subtype appears to prevent delay and/or reverse the memory deficits and damage associated with AD.

1.5.3 The angiotensin II type 4 receptor (AT_4R).

The beneficial effects of ARBs are mediated by their antagonistic effect on ANGII binding to receptors, and as there is an increase in ANGII, provides more substrate for the formation of beneficial substrates of the branching RAAS axis. For instance the angiotensin IV (ANGIV) peptide is produced from consecutive hydrolysis of ANGIII by AP-A and binds with high affinity and selectivity to the AT_4R (Bernier *et al*., 1998; Wright and Harding, 2008) and low affinity to AT_1R and AT_2R (Bennett and Snyder, 1976). AT_4R actions appear to be modulated antagonistically by insulin-regulated membrane aminopeptidase (IRAP), leading some researchers to believe that the AT_4R was indeed IRAP (Albiston *et al*., 2003; Chai *et al*., 2004). AT_4R ligands block IRAP activity as all IRAP substrates are increased specifically, oxytocin, vasopressin and somatostatin, all of which have beneficial effects on cognition and facilitate learning and memory (Lew *et al*., 2003). Importantly it also regulates $GLUT_4$ receptor vesicular trafficking to the cell surface, tying in to diabetes, it regulates glucose uptake through this mechanism (Fernando *et al*., 2008). ANGIV analogues also upregulate dopamine and acetylcholine levels, further increasing the learning and memory response (Braszko, 2004; Gard, 2008). Furthermore, chronic administration of ANGIV to ApoE-/- mice evoked a marked vasoprotective effect that appeared to be mediated by improved NO via AT_4 and/or AT_2R receptors (Vinh *et al*., 2008). ANGIV improves memory recall of passive avoidance tasks in dose dependent manner (Wright *et al*., 1993).

1.5.4 The Mas receptor.

The only other derivative of ANGI is ANG(1-9), which is the precursor for an important product within the BRAAS namely ANG(1-7). The hydrolytic product of ANG(1-9) by NEP or ACE, is ANG(1-7) which binds to the Mas receptor and forms part of the good axis of the BRAAS (Santos *et al*., 2003; Xu *et al*., 2011). The Mas receptor signalling counteracts inflammation, fibrosis and increases insulin sensitisation as well as glucose uptake which are often promoted by the actions of ANGII on AT_1R or AT_2R (Da Silveira *et al*., 2013; Passos-Silva *et al*., 2013; Simões E Silva *et al*., 2013). ACE2, removes the C-terminal Leu residue from ANGI to form ANG(1-9) (Donoghue *et al*., 2000) or the Phe from ANGII to form ANG(1-7) directly (Ferrario and Chappell, 2004). The ACE homologue, ACE2, also forms part of the extended good RAAS axis (Figure 1.7) (Ferrario, 2011; Tipnis *et al*., 2000). ACE2 is also a metallocarboxypeptidase that has been shown to convert Aβ(1-43) to Aβ(1-42) which can then be better cleaved by other Aβ-degrading enzymes like ACE (Liu *et al*., 2014). Interestingly dysfunction and/or dysregulation of IDE and NEP are also implicated in the pathogenesis of vascular disease. Both IDE and NEP are responsible for the hydrolysis of natriuretic peptides, importantly inactivating the vasodilator-atrial natriuretic peptide, which also regulate cardio-renal homeostasis (Potter, 2011; Volpe *et al*., 2014). NEP is also intimate within the RAAS, hydrolysing the bioactive components BK, ANGI and ANG(1-9) (Figure 1.7). Recently ANG(1-7) levels were found to correlate protectively against tau hyperphosphorylation, and ANG(1-7) decreased with progression of AD (Jiang *et al*., 2015). ANG(1-7) also facilitates LTP (Hellner *et al*., 2005), which correlates with the local of the Mas receptor, found in areas important to cognition and

memory, including the hippocampus and piriform cortices (Freund *et al*., 2012). Several excellent reviews on the BRAAS and its receptor-subtypes with relevance to AD have been published over the last two decades (de Gasparo *et al*., 2000; Kehoe and Passmore, 2012; Phillips and Sumners, 1998; Wright and Harding, 2004; Wright *et al*., 2013).

1.6 The ACE and AD debate.

Considering the multifaceted role of the BRAAS in AD and the pivotal role of ACE in the RAS, it is important to addreass the debate around ACE as a potential therapeutic target for AD. As previously mentioned the inhibition of ACE has far-reaching consequences (see section 1.4.3.1) and in the context of AD, these mechanisms have not been investigated. Moreover, biochemically the involvement of ACE in AD remains unclear, as there are several lines of conflicting evidence.

ACE was first linked to AD when various polymorphisms (Katzov *et al*., 2004) of the ACE gene led to variations in ACE expression and activity and increased susceptibility to AD in certain populations (see the accumulative database on all ACE polymorphisms and their association with AD: http://www.alzgene.org/geneoverview.asp?geneID=125) (Bertram *et al*., 2007). The insertion mutations (lower serum ACE levels) in ACE's intron 16 are related to development of AD and the deletions (higher serum ACE levels) to protective functions against AD (Kehoe *et al*., 2003, 1999; Lehmann *et al*., 2005). These genetic findings indicating a role for ACE in AD were bolstered in 2001 by Hu *et al.* who discovered that ACE inhibited Aβ aggregation and polymerisation *in vitro*.

Over a decade on, a lot of uncertainty still exists between evidence generated in cell based, *in vitro* assays and *in vivo* studies of ACE and AD. Cell based models prove that ACE does indeed cleave and clear both soluble and plaque forming versions of the Aβ peptide and that ACEi prevents this (Hemming and Selkoe, 2005; Hu *et al*., 2001; Oba *et al*., 2005). Furthermore, in SH-SY5Y neuronal cells oligomeric species of Aβ induced ACE expression (Ashby *et al*., 2009). In these *in vitro* studies, ACE upregulation could be interpreted as a homeostatic mechanism towards elevated levels of Aβ and cautions against ACE inhibition. However, the more recent studies on human neural tissue and cerebral amyloid angiopathy mouse models (*in vivo*) indicate that ACE may not have a physiological role in the clearance of Aβ peptides (Eckman *et al*., 2006; J S Miners *et al*., 2008). Evidence against ACE, as a metallopeptidase that catabolically maintains Aβ's steady state, is that there is no change in Aβ plaque or level of soluble peptides, when ACEi are applied via direct intracerebroventricular (icv) injection to AD-mouse models (Eckman *et al*., 2006; Hemming *et al*., 2007; J S Miners *et al*., 2008). Furthermore, prolonged chronic treatment with captopril (a centrally active ACEi) in two human APP transgenic AD mice models, saw no increase in Aβ levels (Hemming *et al*., 2007). On further investigation, however, failure of captopril to affect Aβ hydrolysis was thought to occur due to a lack of inhibition of brain ACE activity while renal and arterial ACE inhibition was effective (Hemming *et al*., 2007). Perindopril, another centrally active ACEi, delivered intracerebrally prevented cognitive impairment in a mouse AD model compared to other centrally active ACEi which did not (Dong *et al*., 2011). Here, perindopril did not effect Aβ levels but reduced ACE activity in PS2APP mice, suppressing microglia and astrocyte activation and overall reducing oxidative stress (Dong *et al*., 2011). In a different model of AD, which

contains a double human APP mutation producing more Aβ, captopril administration resulted in a definite increase in Aβ deposition, specifically Aβ(1-42) (Zou *et al*., 2007). A most convincing study by Bernstein *et al*., which used ACE overexpression in myelomonocytes of APP(SWE)/PS1(ΔE9) mice demonstrated the protective effect of ACE against cognitive decline. This effect is most likely linked to an enhanced immune response, possibly activated by ACE (Bernstein *et al*., 2014).

In post mortem studies there is a direct link between Aβ levels and an increase in ACE activity in the brain, specifically parietal cortex, caudate nucleus, cerebral cortex and hippocampal regions (Arriagada *et al*., 1992; Barnes *et al*., 1991; Savaskan *et al*., 2001). ACE protein levels were shown to increase concomitantly with severity of disease - attributed to Braak tangle stage (Ashby *et al*., 2009). In some AD patients cerebrocortical ACE activity is increased and serum activity decreased although this could be a phenomenon of genetics (Rigat *et al*., 1990). On this, there is a disparity between ACE activity and expression levels, independent of genetics, in AD patients, where CSF ACE activity is raised but expression is low in comparison to brain ACE activity and protein expression (Ashby *et al*., 2009; Zubenko *et al*., 1985). A possible cause to this disparity, could be that PTMs like glycosylation influence ACE activity or inhibition profile (Kost *et al*., 1998). However, it is most likely that tissue and space compartmentalisation are to blame for the variations in activity, as microenvironments affect ACE activity (Grinshtein *et al*., 2001). In contrast to their mouse findings Miners, *et al*, found in immunohistochemical studies that ACE expression and activity was increased in post-mortem studies of AD and directly correlated to parenchymal Aβ load. This study also revealed ACE within neurons and cortical blood vessels but the AD patients also had severe CAA, and consequently ACE was most abundant within the perivascular drainage routes (J S Miners *et al*., 2008).

In general, it appears that, there is significant evidence to state that not only is the BRAAS upregulated in AD, but ACE is too. From the upregulation of ACE and subsequently the RAAS, the precise mechanism through which ACE may affect AD pathology remains unknown. There are three potential avenues through which ACE could exert influence, through the excessive formation of ANGII and its hypertensive ramifications, through ACE's apparent immunomodulatory function, or ACE's involvement is limited to the hydrolysis of Aβ.

1.6.1 Questions surrounding domain selectivity and Aβ.

The debate around ACE and AD continues in *in vivo*/cell based studies on Aβ cleavage. Since 2001, ACE was proven *in vitro* to reduce aggregation and cytotoxicity of a variety of Aβ species (Hemming and Selkoe, 2005; Hu *et al*., 2001; Oba *et al*., 2005; Zou *et al*., 2009). Although no in-depth kinetics exists on ACE- Aβ hydrolysis, it is grouped amongst the metalloproteases, like NEP and IDE, responsible for the reduction and clearance of Aβ. Over the years, however, conflicting results have appeared from a number of studies (Table 1.1). Since there seems to be opposing thoughts as to which domain of ACE is primarily responsible for Aβ breakdown along with an apparent lack of cleavage site specificity. Hemming and Selkoe (2005), carried out active site mutations in both the N-and C-domain individually and as a double sACE mutant, inactivating the respective domains, yet maintaining sACE's overall structure. Using these mutants, they then tested the amount of Aβ cleavage. They suggest that the truncated form of the C-domain results in downregulation of its function. As previously mentioned this is

a plausible situation as there is evidence of inter-domain cooperativity in sACE (Binevski *et al*., 2003). This study further stated that the C-domain may not function in Aβ recognition and cleavage *in vitro* if it is not part of the full-length enzyme (Hemming and Selkoe, 2005). The results of their experiments indicate that both the C- and the N-domain of ACE play a role in the cleavage of the Aβ-peptide (Hemming and Selkoe, 2005). Echoing Hemming and Selkoe, only using human and mouse forms of the enzyme (active site knockouts), Sun *et al*., (2008) found no difference between the two domains of murine ACE in the rate of hydrolysis, nor domain specificity to the Aβ peptide (Sun *et al*., 2008). This was the first study looking at how mouse models of ACE-Aβ hydrolysis in AD may be compromised, as the amyloid that mice produce is not pathogenic and has an alternate sequence to human Aβ.

In a study with His-tagged, truncated, individual domains of ACE, Oba *et al*., (2005) determined that the N-domain generated a much larger inhibition of Aβ(1-40) aggregation and cytotoxicity than the C-domain (Oba *et al*., 2005). They suggest that the N-domain is the primary active site for Aβ cleavage. Toropygin *et al*.,(2008) provided important data on the cleavage sites of the isomerized Aβ peptide using Bovine N- and C- truncated proteins. Like Oba *et al*., (2005), the N-domain was found to cleave the Aβ substrate and the C-domain did not. Similarly Zou *et al*.,(2009) found that the N-domain was responsible for the conversion of Aβ(1-42) to Aβ(1-40) (Zou *et al*., 2009). Zou and colleagues have proposed that Aβ(1-40) had protective effects over Aβ(1-42) and that the severity of AD lay in the ratio of Aβ(1-42)/ Aβ(1-40) (Zou *et al*., 2003). However, they found that the C-domain and sACE also cleaved the Aβ(1-42) peptide, butat alternate sites (Zou *et al*., 2009).

Overall, the different cell types, experimental methodology and variants of ACE used across these studies (Table 1.1) come to no consensus as to which domain of ACE indeed hydrolyses Aβ preferentially. Furthermore, studies on truncated domains lose some physiological holding as in sACE domain selectivity is often altered due to cooperativity, and, as suggested by Hemming and Selkoe (2005), tethering to a cell membrane. Without any definitive kinetic data, or further mechanistic insight into ACE- Aβ hydrolysis this avenue around ACE's exact role in AD pathology remains unclear.

Table 1.1 ***In vitro* studies of ACE hydrolysis of Aβ.**

Author	Cleavage site	Aβ Peptide used	ACE variant used	Selectivity
Hu *et al.* 2001	Asp7-Ser8	**1-40**	Purified human sACE	*NA*
Oba *et al.* 2005	Asp7-Ser8 (same group)	**1-40**	Recombinant truncated His tagged human sACE and Ndom, Cdom	N-domain
Hemming and Selkoe. 2005	Asp7-Ser8 (assumed)	**1-40, 1-42 expressing cell lines**	Membrane bound sACE and sACE N/C KO's	Non-selective
Zou *et al.* 2007	Val40-Ile41	**1-42**	Human Kidney sACE	Non-selective
Toropygin *et al.* 2008	Arg5-His6	**1-16, 1-16isoAsp7**	Recombinant bovine ACE truncated domains	N-domain
Sun *et al.* 2008	Leu34-Met35, Lys28-Gly29, Ser26-Asn27, Glu22-Asp23, Phe20-Ala21	**Human and mouse 1-40**	Recombinant human sACE	Non selective
	His13-His14, Glu11-Val12	**Human and mouse 4-15**	Recombinant mouse: sACE, Ndom, Cdom, sACE N/C KO's and wtmACE	
Zou *et al.* 2009	**N-domain:** Val40-Ile41 **C-domain:** Gly33-Leu34, Val24-Gly25, Ala21-Glu	**1-42**	Recombinant truncated sACE, Ndom, Cdom, sACE N/C KO's	Ndom
Kumar *et al.* 2012	Asp7-Ser8, Ser8-Gly9	**1-40 and Phospho-Ser8(1-40)**	Recombinant human sACE	*NA*

KO, refers to active site mutaions disrupting zinc binding and inactivating one specific active site.
NA: not applicable, the study was not concerned with selectivity used sACE.

1.6.2 The roles of ANGII in AD.

There are many negative effects of an upregulated or dysregulated ANGII-mediated BRAAS, as in hypertension, which have severe cognitive implications for AD (see section 1.5 and 1.6). Icv ANGII infusion has been shown to interfere with rabbit operative tasks (Melo and Graeff, 1975) as well as in rat and mice acquisition training, where it blocked memory recall conditioned responses 1-2 days later (Lee *et al*., 1995; Morgan and Routtenberg, 1977). Similarly, icv ANGII infusions in rats impaired memory retention in trained immobilization stress, maze or passive avoidance tasks (Raghavendra *et al*., 1999). This effect appeared to be dose dependent and was blocked by ACEi and/or AT_1R antagonists but not by AT_2R antagonists (DeNoble *et al*., 1991). This suggests that AT_1R mediates these ANGII memory defects. However, it may be that ANGII inhibits memory due to its anticholinergic effects (Barnes *et al*., 1990), independent of its AT_1R action (Shepherd *et al*., 1996).

In contrast, ANGII has been found to improve cognition and recall in some studies. It was suggested that low ANGII dosage induces memory inhibitory effects and higher doses facilitate learning (Braszko *et al*., 1988, 1987). Furthermore microinjection of ANGII into the hippocampus has been shown to facilitate active avoidance learning in rats (Belcheva *et al*., 2000). Object recognition, avoidance response conditioning and locomotive behaviour all appear bettered by ANGII infusion. These effects are motor and anxiety driven (Braszko *et al*., 1995). It appears that the anxiety driven effects occur via AT_1R and AT_2R stimulation but the motor coordination ANGII effect occurs exclusively via AT_1R (Braszko *et al*., 2003, 1998). These studies have one shortcoming in that they did not use ANGII analogues incapable of hydrolysis. Thus, many of these beneficial effects could be due to the upregulation of its hydrolytic products ANGIII, ANGIV and ANG(1-7) acting through the Mas and AT_4R.

Other detrimental aspects of ANGII include the promotion of neurovascular coupling impairment mediated by NADPH oxidase ROS production via AT_1R (Bloch *et al*., 2015). ANGII also down regulates ACE2 expression, as mentioned ACE2 hydrolyses Aβ and is responsible for production of MAS-axis BRAAS components (Koka *et al*., 2008). Over production of ANGII promotes the secretion of fibrotic factors from the extracellular matrix, including fibronectin and transforming growth factor β (TGFβ-1) and its receptors associated with fibrotic disease (Crawford *et al*., 1994; Gao *et al*., 2009). All of these factors are elevated in AD and result in impaired perivascular drainage and accumulation of Aβ along these routes (Lesné *et al*., 2003; Wyss-Coray *et al*., 1997). ANGII also upregulates RAGE-receptors via AT1R stimulation (Ihara *et al*., 2007) and possibly upregulates transcytotic influx of circulating Aβ. In AD mouse models ANGII induces increased production of Aβ via upregulation of BACE-1 via AT_1R signalling. This occurs via AT_1R upregulation of NFκβ, AP-1, and cAMP response element binding protein (CREB), which bind to the BACE1 promoter (Bourne *et al*., 2007; Roßner *et al*., 2006). Most of these transcription factors are also regulated by ANGII through the activation of glycogen synthase kinase-3 (GSK-3β), by increasing its Tyr216 phosphorylation (Agarwal *et al*., 2013). This kinase was discovered and studied for its role in insulin-mediated glycogen metabolism and its dysregulation is renowned for increasing tau pathology by hyper-phosphorylation (Godemann *et al*., 1999; Israel *et al*., 2012). Phosphorylation of GSK-3β at Ser9 induces deactivation, which is mediated through PI3-Akt signalling pathway, regulated by ANGII though AT_1R as well as TGFβ-1 (Agarwal *et al*., 2013; Hughes *et al*., 1993; Rylatt *et al*., 1980).

1.6.2.1 **The pros and cons of ACE inhibition in AD.**

Inhibition of the BRAAS has been suggested as a therapeutic avenue for the treatment of various neurodegenerative diseases including AD (Kehoe and Passmore, 2012; Kehoe and Wilcock, 2007; Savaskan, 2005; Wright and Harding, 2010). The benefits or risk posed by ACE inhibition in patients with AD remains a controversial topic (Kalra *et al*., 2015; Khachaturian *et al*., 2006; T Ohrui *et al*., 2004; Takashi Ohrui *et al*., 2004; Sink *et al*., 2009). There is a scarcity of clinical evidence on the benefits of ACE inhibitors in AD (Louis *et al*., 1999; T Ohrui *et al*., 2004; Sudilovsky *et al*., 1993; Weiner *et al*., 1992). In small observational studies, ACEi have proven to slow the rate of cognitive decline in patients with mild cognitive impairment (MCI) (Ashby *et al*., 2009; Hajjar *et al*., 2008; Rozzini *et al*., 2006) including peripherally acting ACEi (Qiu *et al*., 2013).

ACEi do not fit so comfortably within the collective grouping of a class. This term, class, is based on biological function not on structural or chemical basis (Morice *et al*., 1987). Subgrouping ACEi into inhibitors with brain penetrating abilities was also somewhat limited, as there are conflicting reports on the central acting abilities of some ACEi (Cushman *et al*., 1982; Gohlke *et al*., 1989; Sakaguchi *et al*., 1987; Tan *et al*., 2005). However distinctions between ACEi chemical properties does appear significant, dicarboxyl-containing ACEi like enalapril and lisinopril are associated with a 73-83 % reduced risk of developing MCI in hypertensives (Solfrizzi *et al*., 2011).

The cognitive enhancing effects of ACEi are inherently linked to reduced blood pressure and inflammatory responses, and all the AT_1R mediated effects of ANGII mentioned above. Other substrates are elevated on ACE inactivation like substance P which increases NEP expression and BK which activates IDE, both being proteases of Aβ (Kehoe and Wilcock, 2007). There are also, non-ANGII related benefits to ACE inhibition based on all the downstream signalling events that may occur most notably the upregulation of PPARs by a potential increase in adiponectin. PPARγ decreases oxidative stress and reverses ANGII induced fibrotic effects (Hao *et al*., 2008) and is a known regulator of Aβ production by repressing BACE-1 transcription (Sastre *et al*., 2003). PPARα increases the anti-amyloidogenic processing of APP by upregulating ADAM 10. Furthermore, peripheral macrophages activation and proinflammatory responses are dampened by an increase in ACE expression which could be induced by the ACE signalling pathway (Kohlstedt *et al*., 2011).

Unfortunately, most of the non-ANGII mediated responses have not been tested in neuronal cell lines. Furthermore, ACE inhibition has one startling drawback, that this would block the hydrolysis of Aβ. Furthermore, the upregulation of BK receptors on ACE inhibition could have dire consequences in AD. Blockade of the B_2R protects against the memory deficits induced by Aβ peptide in mice. The Aβ-induced neuroinflammation in human cell lines and mice can occur through the B_2R and B_1R (Bicca *et al*., 2015). Synaptic antagonism of these receptors reduced microglial activation and the levels of pro-inflammatory proteins like COX-2 and a decrease in JNK and p38 kinases (for a review Bicca *et al*., 2015; Viel and Buck, 2011).

Modern clinical inhibitors for the treatment of hypertension are not domain specific and inhibit both domains of ACE (Cushman *et al*., 1973; Michaud *et al*., 1997; Ondetti *et al*., 1977; Sturrock *et al*., 2012). As these two catalytically active domains of human sACE, despite their

similarity in sequence, display marked differences in substrate specificity and thus are possibly independently responsible for varying functions. This has led to side effects associated with ACEi usage, mostly related to the potentiation of the BK response (Hecker *et al*. 1994; Hecker *et al*. 1997; Erdös *et al*. 1999). Within the context of AD, it is important to understand both the domain specificity of the Aβ hydrolysis and which downstream effects Aβ hydrolysis may trigger through ACE. For without clear molecular mechanistic information definitively implicating ACE activity as either beneficial or detrimental, the therapeutic implications of ACEi in AD are ambiguous.

1.7 Research Questions.

1.7.1 Hypothesis statement.

The ACE substrate Aβ's domain selectivity is driven by the presence of unique N- and C-domain active site residues as well as the structural arrangement and cooperative effects that are found in sACE**.** Furthermore, upregulation of ACE protein expression may be augmented through the binding and hydrolysis of Aβ.

1.7.2 Aims and objectives.

The aim of this work is to further elucidate the structure-function and signalling relationship of ACE with the Aβ substrate through the development of a comparative enzyme kinetic assessment system. This includes the kinetic assessment of residues which contribute to Aβ processing. Furthermore, to determine any larger synergistic effects that the two domains may induce towards Aβ substrates as well as mammalian cell signalling effects of Aβ mediated by ACE.

1.7.2.1 **The objectives of the current studies are as follows:**

1. To investigate the cleavage specificity of Aβ peptides by the N- and C-domain catalytic sites of ACE across numerous ACE truncated and full-length variants.
2. To kinetically assess the effect that active site residues contribute to domain-selective hydrolysis of Aβ using active site C-domain mutants with unique residues converted to their corresponding N-domain counterparts.
3. To investigate any cooperative and selective effects that the sACE domain conformation may have on various N-terminal peptides of Aβ.
4. To determine if Aβ affects ACE protein expression through the ACE signalling cascade.

2 CHAPTER

Characterisation of Aβ cleavage by ACE variants.

2.1 Introduction and aims

Cardiovascular insult has been proven clinically, epidemiologically and pathologically to associate with AD and cognition. However, with regard to the implication of ACE with AD, one might say that it may be a result of happenstance and perhaps circumstantial evidence through the years (See Chapter 1 section 1.6 for more associations of ACE with AD). In 2001, Hu *et al* provided the first concrete mechanistic link between ACE and AD. Although clearly an irrefutable association, the cleavage of Aβ by ACE proved in the last decade to be more complicated than it appeared.

In the study by Hu *et al.*, *in vitro* purified sACE cleaved synthetic Aβ(1-40) at the Asp7-Ser8 bond followed by further degradation (Hu *et al*., 2001). The resulting product, a 33-residue peptide, had reduced aggregation, deposition and cytotoxicity profiles (Hu *et al*., 2001). This was followed by efforts to characterise which domain of ACE was responsible for this cleavage, as it is well known that the two domains of ACE have varying substrate specificities (Araujo *et al*., 2000; Bernstein *et al*., 2013, 2011; Deddish *et al*., 1998, 1997; Fuchs *et al*., 2008; Jaspard *et al*., 1993; Rice *et al*., 2004; Rousseau *et al*., 1995; Shen *et al*., 2012; Tzakos *et al*., 2003; Zou *et al*., 2009). Oba *et al*., used soluble His-tagged constructs of sACE and the N- and C-domains to show that the catalytic activity of sACE and Ndom, but not Cdom, caused reduced Aβ aggregation and PC12h cell cytotoxicity (Oba *et al*., 2005). Characterisation of the cleavage of the Aβ(1-40) revealed that the major product, generated by sACE and the N-domain was the Aβ(8-40) peptide (Oba *et al*., 2005). They also determined that Aβ(1-7) underwent further degradation by the N-domain after initial cleavage at the Asp7-Ser8 site (Oba *et al*., 2005). The N-selectivity of cleavage was corroborated through the investigation of synthetic Aβ(1-16) peptide and its modified Asp7 isomer (Aβ(1-16)-L-iso-Asp7), cleaved between residues Arg5 and His6 by the N-domain (Toropygin *et al*., 2008). However, the C-domain of ACE failed to hydrolyse either peptide variant (Toropygin *et al*., 2008).

Later the truncated N-domain was again shown to be selective towards Aβ(1-42), only cleaving in an exopeptidase fashion, converting the more toxic Aβ(1-42) to the Aβ(1-40) peptide (Zou *et al*., 2009, 2003). The specificity of the N-domain cleavage after Val40 was confirmed using domain inactivated mutants and western blotting, indicating that the N-domain controlled this protective effects of this ratio (Zou *et al*., 2009). The truncated C-domain also hydrolysed the Aβ(1-42) peptide, at residues, Ala21, Val24, Lys28 and Gly33 however (Zou *et al*., 2009, 2007). Thus, one cannot refute that the results from this study also implicate the C-domain in the cleavage and hydrolysis of Aβ. The authors proposed that the observed cleavage pattern was due to the use of full-length wild type human sACE with the

transmembrane region attached; as opposed to the seminal plasma secreted sACE and soluble recombinant constructs used by Hu *et al* and Oba *et al*, respectively.

In contrast, Hemming and Selkoe implicated both the C and the N-domain of ACE in the hydrolysis of Aβ(1-40) and Aβ(1-42) (Hemming and Selkoe, 2005). The ACE constructs used in this instance were discrete domain knockout mutants, wherein the N-or C-domain in sACE had been catalytically inactivated. Here the N- and C-domains as well as wild type sACE decreased cell-derived Aβ levels equally and the effects were abrogated on treatment with captopril.

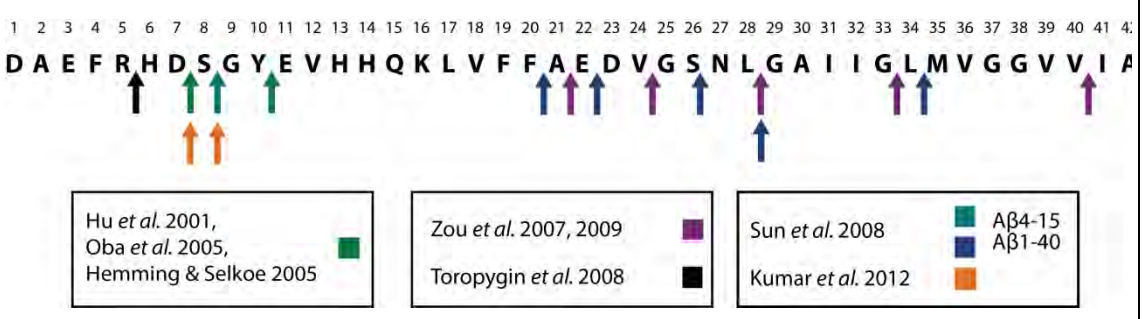

Figure 2.1 **Cleavage specificity towards Aβ**. Diagram illustrating the multiple cleavage sites of various ACE constructs throughout literature over the last decade and a half. The colour coded author-cleavage site key is on the right hand side of the Aβ(1-42) amino acid sequence.

In a study on the species specificity of sACE cleavage of Aβ, using human and mouse forms of the enzyme and substrate, Sun *et al* (2008) confirmed that ACE hydrolysed the N-terminal region of Aβ in both species despite differences in the N-terminal region of the peptide. They determined that murine ACE hydrolysed the human Aβ(4-15) peptide at positions Glu11-Val12 and His13-His14 and that human Aβ was a better substrate of murine ACE. These cleavage sites were consistent across both wild type murine ACE, N- and C-domain active site knockout variants. They then interrogated the human Aβ(1-40) with human ACE and confirmed Zou *et al*'s Lys28-Gly29 cleavage but also identified sites after residues Leu34, Ser26, Glu22 and Phe20. They concluded that there was no difference between the two domains of murine ACE in the rate of hydrolysis, nor domain specificity to the Aβ(1-15) peptide (Sun *et al*. 2008).

The disparate number of cleavage sites of ACE towards Aβ (Figure 2.1) once again reiterates how little we know mechanistically about the substrate specificity of this enzyme and its two domains. With such a large amount of varying cleavage site data throughout the literature, it is very important to qualify which species of both enzyme and peptide one uses; as well as establish cleavage sites specific to experimental models, in order to perform any further enzymatic characterisation.

The Aβ(1-42) peptide is notoriously difficult to work with because of its insolubility and subsequent ability to form fibrils. The Aβ(1-42) has what is known as the central hydrophobic cluster (CHC) (Aviles *et al*., 2006). Residues 17 to 21 (LVFFA) form the core of the CHC and are said to be important in aggregation since the peptide gains some solubility upon substitution

of any two residues (Hilbich *et al*., 1992). This CHC segment of the Aβ(1-42) also appears to form part of the β-sheet core of mature fibrils (Morimoto *et al*., 2004; Williams *et al*., 2004). .

There are numerous reasons why the N-terminus of Aβ is indeed important and relevant to study (see Chapter 1 section 1.2.2). It contains residues which form the zinc chelating group of Aβ, which include Asp7, His6, Glu11, His13 and His14 (Zirah *et al*., 2006). The Aβ(1-16) peptide itself contains the His6, Glu11, His13 and His14 residues which are key to the formation of inter-amyloid zinc binding, creating greater stability and peptide rigidity (Minicozzi *et al*., 2008). As any ACE assay requires Zn^{2+}, we thought it prudent to derive a shorter peptide with greater flexibility that retains the Zn^{2+} chelating ability without the inter-molecular stacking that occurs in the Aβ(1-16). Hence, the design and use of Aβ(2-11) peptide, which has increased flexibility, maintains some Zn^{2+} coordination and less defined secondary structure, making it more susceptible to proteolysis. To determine kinetics and the selectivity of the individual domains of ACE one needs a more malleable substrate. The Aβ(2-11) and Aβ(1-16), would hence allow for the study of the physiologically significant N-terminal region of Aβ, which as mentioned above is prime "cleavage ground" for ACE.

The lack of consensus and explanation throughout the literature on the subject of domain selectivity and lack of specific cleavage towards Aβ, prompts the further characterisation of molecular mechanism that occurs with different ACE constructs in Aβ cleavage.

Aims and Objectives:

The overall aim of this chapter is to investigate the cleavage of Aβ peptides by the N- and C-domain catalytic sites of ACE**.**

The objectives used to achieve this aim include:

1) To express and purify all ACE variants used in this study.
2) To investigate the mode of hydrolysis, and domain specificity of Aβ(2-11) cleavage by the N- and C-domains of ACE using HPLC.
3) To design fluorogenic Aβ substrates that mimic larger Aβ cleavage sites of ACE
4) To determine the primary cleavage sites of various Aβ peptides using mass spectrometry
5) Determine the crystal structure of various Aβ peptides bound to the N-domain.
6) To characterise the cleavage site preference of ACE in the hydrolysis of Aβ peptides using truncated and full-length ACE constructs.

2.2 Methods:

2.2.1 Enzyme constructs

All construct DNA was prepped in DH5α *E.coli* and DNA extracted as in appendix section 7.2. All upscale preparations for transfection of construct DNA, barring CC-sACE, was performed using the Plasmid Midi kit (QIAGEN, USA).

2.2.1.1 Soluble Truncated Constructs

2.2.1.1.1 Wild type C-domain (Cdom)

The wild type tACE construct used throughout this thesis is the fully N-glycosylated tACEΔ36NJ mutant. This lacks the transmembrane region, truncated after residue S625, as well as the unique 36 amino acid N-terminus (Yu *et al*., 1997). This construct is identical to the C-domain of sACE and will be referred to as Cdom (Figure 2.2)

2.2.1.1.2 Wild type N-domain (Ndom)

A soluble form of the N-domain, consisting of amino acids 1 to 629 (Ndom629D)of somatic ACE, in vector pECE was a kind gift from Dr S. Danilov (University of Illinois, Chicago) (Balyasnikova *et al*., 2003; Corradi *et al*., 2006). Ndom629D comprises of a signal sequence of 36 residues (not present in the mature enzyme), targeting the protein for secretion, followed by the first 629 residues of sACE. A soluble form of Ndom629D was created in our lab (Redelinghuys, 2006) and is identical to the N-domain of human somatic ACE and will be referred to as Ndom (Figure 2.2).

2.2.1.2 Full-length Constructs:

2.2.1.2.1 CC-sACE

CC-sACE was constructed in our group as previously described (Woodman *et al*., 2005) via an elaborate cloning strategy. Essentially, CC-sACE consists of two C-domains joined by the sACE inter-domain linker region; it also contains the juxtamembrane stalk, transmembrane (TM), and cytoplasmic regions (Figure 2.2)

2.2.1.2.2 Membrane bound sACE Constructs

2.2.1.2.2.1 Wild type sACE

The wild type human sACE genetic sequence encodes the entire ACE coding region including the signal sequence, N- and C-terminal catalytic domains, the TM region and the cytoplasmic tail (Figure 2.2). This construct, pcDNAsACETM, was created by Kerry Gordon (Gordon, 2011).

2.2.1.2.2.2 Domain inactivated sACE constructs: C-sACE and N-sACE

The full-length domain knock outs of sACE, both in pECE, were a kind gift from Vincent Dive and were constructed by Wei *et al*., 1991., through site directed mutagenesis (Taylor *et al*., 1985). For the construction of N-sACE, the His361 (CAT) and His365 (CAT) residues were

converted to Lys (AAG and AAA respectively). Similarly, C-sACE was generated by mutating sites His959 (CAC) and His963 (CAC) to Lys (AAA and AAG respectively).

Both constructs have the complete signal, TM and stalk regions corresponding to full-length sACE (Figure 2.2). Each construct was sent for sequencing to confirm the integrity and identity of the mutants. This was performed by capillary sequencing and was conducted at the Central Analytical Facility (CAF) (Stellenbosch University, South Africa) using internal sACE sequencing primers (Appendix A1).

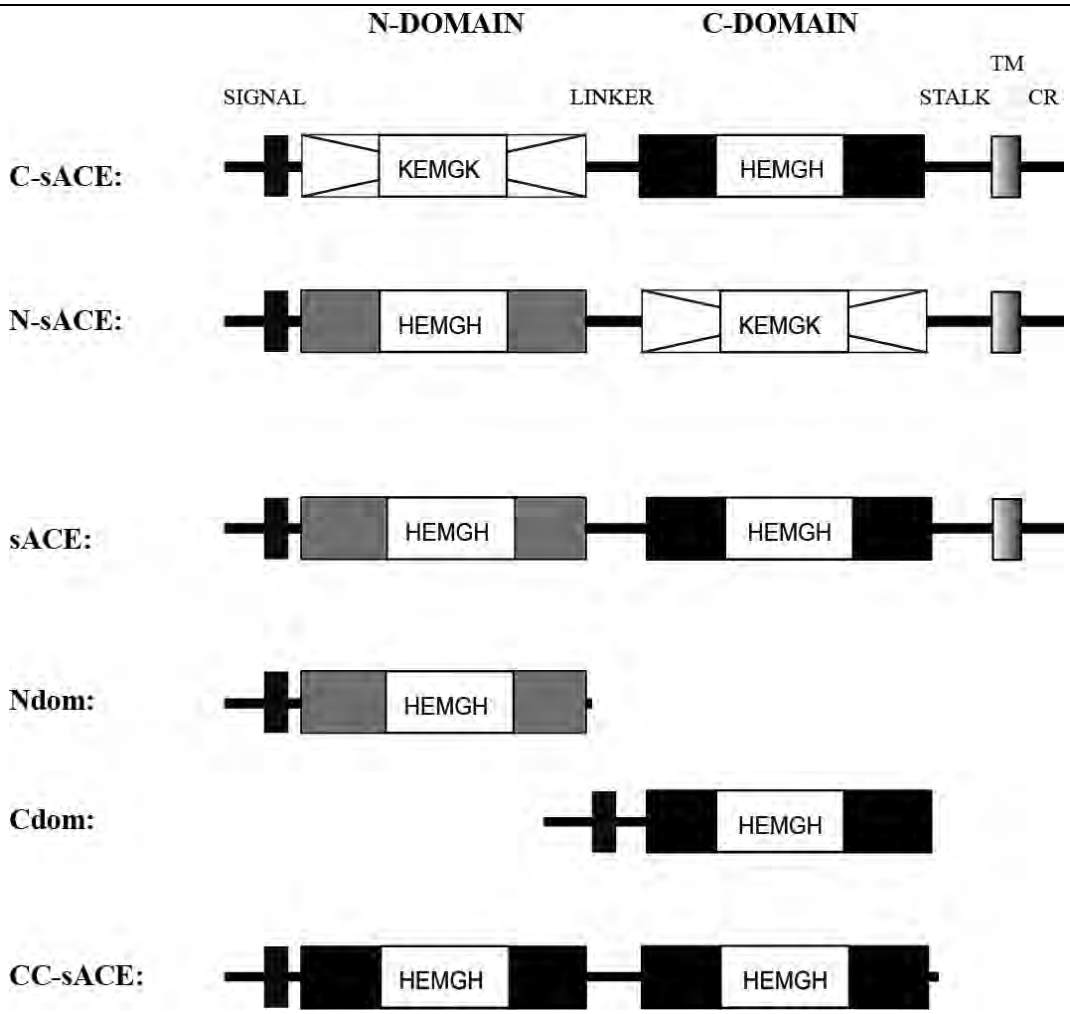

Figure 2.2 **Schematic of ACE constructs used**. The wild-type ACE (sACE) contains a signal peptide (left black box), the two homologous ectodomains (the N-domain in grey and the C-domain in black) with the indicated active site residues necessary for the coordination of Zn. Also indicated is the stalk region just prior to the transmembrane domain (right shaded box) and finally the cytoplasmic region (CR) at the C terminus. The truncated Ndom contains the signal peptide and the N domain. The truncated Cdom is essentially the same as the C-domain in wild type sACE only it lacks the transmembrane region and has the added signal peptide. The domain inactivated mutants are identical to sACE except for the mutation of the catalytic His residues to Lys (white boxes) in the N-domain (N-sACE) and C-domain (C-sACE). The CC-sACE construct is a fusion construct, via the linker region, of a C-domain to the N-terminal C domain (two black domains).

2.2.2 Protein expression and purification

The CHO-K1 (Chinese hamster ovary (CHO)) mammalian cell line was used as a model system for expression of all ACE variants. CHO-K1 cells were cultured at 37°C, 5 % CO_2 and 80 % relative humidity levels in various flasks and dishes. All tissue culture flasks and dishes were supplied by Nunc Ltd.

2.2.2.1 **Mammalian cell expression of ACE enzymes**

Prior to transfection, CHO-K1 cells were grown to 60-80 % confluency in 10 cm dishes. Transfection of the ACE constructs was performed according to manufacturers' instructions using the calcium phosphate Profection® Mammalian Transfection System (Promega Corp.). This entailed application of fresh serum growth medium, 3-4 hours prior to transfection, to the 60 % confluent cells. Actual transfection of the cells required 15-20 ug of pcDNA construct DNA to be precipitated via drop-wise addition to $CaCl_2$. This DNA precipitation mix was incubated for 30 min at room temperature before once again being added to the 10 cm dish of cultured cells in a drop wise fashion. These cells were incubated for 4 hours, following which they underwent glycerol-shock for 2 min to facilitate the uptake of DNA. The cells were then washed and normal growth medium was added for 24 hours post transfection. After this, they were grown to confluency in growth medium containing 0.8mg/ml geneticin G418 (Sigma-Aldrich Co.) to select for positive clones. Cells were grown in the presence of selective medium and showed clear negative control plates (no vector DNA added) with G418 resistant colonies observed in the transfected plates. Colonies were picked, seeded into 12 well plates, grown to confluency and assayed for ACE activity using benzyloxycarbonyl-Phe-L-His-Leu (Z-FHL) assay (see section 2.2.3.1). The highest expressing clones were then reseeded into T-75 cm^2 flasks and grown to confluency.

2.2.2.2 **Selection of high expressing cells lines**

Fluorescence-activated cell sorting (FACS) is a specialized form of flow cytometry used to sort heterogeneous mixtures of cells based on their cell wall protein profiles. It provides a means to physically separate cells more heavily labelled with fluorescent ACE specific antibody, from those which have fewer labels and hence lower ACE expression. This technique was applied to all sACE TM constructs to aid in the selection of high expressing transfected CHO clones.

For FACS analysis, transfected and control untransfected cells were lifted from confluent T-75 cm^2 flasks and washed twice in phosphate-buffered saline (PBS). The cells were then labelled via 1 hour incubation with 10 µg/ml mouse antibody 5C5, which is a monoclonal antibody specific to the N-domain of ACE. Extensive washing in PBS was performed to remove any unbound primary antibody. A secondary antibody was then added to the cells and allowed to incubate for an hour in the dark, which was followed again by extensive washing. This secondary antibody is a chicken anti-mouse IgG antibody coupled to a modified fluorescein isothiocyanate (FITC) Alexa Fluor® 488 (abcam®).

FACS was performed, on the labelled cells in PBS suspension, at the Flow Cytometry Core Facility (Department of Immunology, UCT, South Africa). The machine used was a FACS VantageTM SE cytometer (BD Biosciences, USA). Cells were gated according to highest fluorescence directly into growth medium supplemented with 100 U/ml penicillin and

100 µg/ml streptomycin. The sorted cells were grown to confluency in T-75 cm^2 flasks under selective medium and assayed for ACE activity. Thus, high expressing sACE TM construct cell lines were generated; stocks were made and were subsequently flash frozen in liquid nitrogen.

2.2.2.3 Isolation of secreted ACE protein from growth media

Standard practice of ACE purification within our group is as such: clonal cell lines of CHO-K1 cells overexpressing soluble forms of ACE were grown in T175 cm flasks with growth medium. Once confluent, the medium was replaced with minimal medium (50 % DMEM, 50 % Ham's F12, 20mM HEPES, 2 % FCS (heat-inactivated for a further 15min at 70°C)) and harvested every 48-72 hours until ACE protein over expression becomes compromised by the cells survival response (routinely until harvest 7 or 8). Harvested media is pooled and, if not immediately required, stored at -20°.

Affinity chromatography was used to purify all constructs. The non-selective ACE inhibitor Lisinopril has been coupled, via its P1' Lys group and linker, to sepharose beads creating an ACE specific affinity column (Ehlers *et al*., 1991). This allows for a convenient one step affinity chromatography purification (Bull *et al*., 1985; El-Dorry *et al*., 1982) of ACE from harvested media. Columns were equilibrated in wash Buffer (20 mM HEPES, pH 7.5, 0.5 M NaCl), prior to loading harvested media, for approximately 30 minutes. The media was then loaded on and passed over the column, at a flow rate maximum of 0.5 ml/ min. The column is subsequently washed overnight with the same wash Buffer to remove any impurities and non-specific protein binding.

All ACE constructs were eluted on addition of elution buffer (50 mM borate buffer pH 9.5) in 1.5 ml fractions. These fractions were assayed for ACE activity (section 2.2.3.1). Those with the highest activity readings were pooled and dialysed overnight, through SnakeSkin® pleated dialysis tubing (Pierce Biotechnology Ltd) at 4°C, in 2 L of dialysis solution [5 mM HEPES, pH 7.5, 0.1 mM PMSF (in ethanol)]. A second 6 hour dialysis was then performed in fresh dialysis buffer. Post dialysis, protein concentrations were calculated using the BIORAD Bradford reagent (BioRad Laboratories Inc.) in the Bradford assay (Bradford, 1976) as per manufacturer's instruction. Proteins were concentrated down using 30 kDa Amicon Ultra-15 centrifugal filters (Merck Millipore) and buffer exchanged into 50 mM HEPES (pH 7.5). Activity of the purified ACE protein was assayed (section 2.2.3.1) and the integrity, size and purity were analysed on a 10 % polyacrylamide sodium dodecylsulphate gel following electrophoresis (SDS-PAGE) (Laemmli, 1970). Finally, aliquots of protein were stored at 4 and -20°C.

2.2.2.4 Isolation of transmembrane protein from cell lysis:

A modified purification procedure was developed to increase the amount of protein generated for all TM constructs. Natural secretase induced secretion into the cell growth medium was not sufficient, despite FACS selection of high expressing clones. Cells, expressing high levels of TM sACE, were grown to confluency in six T-150 cm^2 flasks and lysed in 5ml triton lysis buffer (0.05 M HEPES, 0.5 M NaCl, 1% triton X-100, 1 mM PMSF) containing Protease Inhibitor Cocktail (Set III, Calbiochem, USA - 0.2 mM AEBSF, 0.16 M Aprotinin,

0.01 mM Bestatin, 3 µM E-64, 4 µM Leupeptin and 2 µM Pepstatin A). Flasks were left to incubate at 0°C for 30 minutes before the whole-cell lysates were scraped from the flasks, pooled, centrifuged at 10000 x *g* for 5 minutes and the supernatant extracted.

In total, approximately 30 ml of cell lysate was extracted. This was subsequently diluted 1:2 into Wash Buffer and syringe filtered through a 0.8 µm filter, to ensure no cell debris remained prior to loading the affinity column. The lysates were kept on ice at all times and sample aliquots were tested for ACE activity, at each step, to ensure that no loss of protein occurs prior to purification. Purification of all TM sACE constructs was carried out using the same ACE specific lisinopril affinity column chromatography process as previously mentioned (Section 2.2.2) (Ehlers *et al*., 1991).

Columns were equilibrated in wash buffer, for approximately 30 minutes, prior to loading harvested and cleaned lysate. The lysate was, loaded on and passed over the column at a flow rate maximum of 0.5 ml/min. The column was then washed with approximately 200 ml of the same wash buffer to remove any impurities and non-specific protein binding. Elution procedure occurs as above (section 2.2.2.3). However, a slightly longer elution step was required if multiple TM constructs are to be purified in one sitting to ensure the column is clean. This was performed to avoid cross contamination of separate constructs.

2.2.3 Synthetic ACE substrates

2.2.3.1 **Z-FHL ASSAY**

ACE activity can be measured by assaying the fluorescent adduct of the cleaved product His-Leu (HL), from either ZFHL or hippuryl-L-histidyl-L-leucine (HHL) synthetic substrate. This assay was developed by Friedland and Silverstein (1977) and adapted according to Schwager *et al*. (2006). The generation of HL from ZFHL (Bachem, Ltd) was assayed in 96-well plates with 30 µl of 1mM ZFHL in phosphate buffer (100 mM $KHPO_4/KH_2PO_4$ (pH 8.3), 300 mM NaCl, 10 µM $ZnSO_4$) and 6 µl of medium or 3 µl of cell lysate (1 in 10 dilution is usually appropriate). Samples were incubated at 37°C for 15 (C-and N-domain mutants) or 20 minutes (sACE and sACE mutants). The endogenous fluorescence of the sample and assay constituents was accounted for by the inclusion of a blank zero time (BZT).

The reaction is stopped via addition of 125 µl of 0.4 M NaOH. The cleavage product HL is converted to a fluorescent adduct on addition of 10 µl of o-phthalaldehyde (24 mg/ml) whilst shaking, in the dark, at room temperature for 10 minutes. This reaction is stopped on addition of 30 µl of 3 M HCl. The resulting fluorescence was measured on a Cary Eclipse fluorescence spectrophotometer (Varian Inc.) at 360 nm excitation wavelength and 485 nm emission wavelength. The fluorescence readings, conducted in triplicate for each sample, were converted to ACE activity (mU) with the use of an HL standard curve (see appendix 7.5.1). ACE activity (Unit) is defined as the amount of nmols of HL produced per ml of sample, per minute (nmols/ml/min).

2.2.3.2 **HL Standard Curve**

For the conversion of fluorescent intensity units to nmols of HL product liberated from a ZFHL or HHL reaction, a HL standard curve is required. Construction of this curve was carried out as described in (Schwager *et al*., 2006). Briefly, a 5 mM stock of HL (Sigma-Aldrich Co.) dissolved in water was made. A 0.5 mM working stock of this was made up in phosphate buffer. A dilution series of this 0.5mM working stock was performed in phosphate buffer in a 96-well plate in 30 µl aliquots. From this step onwards, the HL fluorescence assay commenced (see section 2.2.3.1) with the addition of 0.4 M NaOH. Linear regression analysis was used to correlate the change in fluorescence to the nmols of HL product formed (see appendix 7.5.1)

2.2.4 HPLC

HPLC of the Aβ(2-11) substrate was performed using a C18 Jupiter column. To determine progress curves for the hydrolysis of Aβ(2-11), 2 nM Ndom and 200nM Cdom (100-fold excess) were incubated with 44 µM Aβ(2-11) in IX HEPES assay buffer (50 mM HEPES buffer, 300 mM NaCl, 10 µM $ZnSO_4$) for varying periods of time at 37°C. Reactions were stopped on addition of 50 µl 1.25 % trifluoroacetic acid (TFA). The final reaction volume was 250 µl. Samples were separated by HPLC over a gradient of 4 % to 40 % ACN (in 0.1 % TFA). Absorbance was read at λ = 225nm which is the determined absorbance maximum for Aβ(2-11).

The hydrolysis of Aβ(1-16) was assessed via HPLC chromatography. Reactions had final volumes of 50 µl and were performed at 37ºC in IX HEPES assay Buffer. The reactions were stopped with the addition of 10 µl of 0.25% TFA. The comparison of cleavage site specificity across ACE subtypes, for both 15 minute and 24 hour incubations, were performed with enzymes concentrations determined under kinetic assay conditions (See Chapter 4). Samples were analysed on the Agilent 1260 Infinity HPLC at a multiple wavelengths simultaneously, however λ=214 nm was adequate for detection of product peaks. The total reaction (60 µl) was cleared of contaminants on a spin column (GHP Nanosep® MF Centrifugal Device 0.45 µm pore size) prior to being run on the column. Mixtures were separated on a Poroshell 120 EC-18 column with a 2.7 micron pore size over an isocratic gradient of 40% ACN in 0.1% TFA.

All sample runs, per peptide, were compared to those with buffer only and substrate only.

2.2.5 Mass Spectrometry analysis of Aβ peptides

2.2.5.1 **Sample clean up procedure**

Fractions corresponding to product and substrate peaks on the HPLC chromatograms were collected, dried down and resuspended in 20 µl of a 60 % ACN, 0.1 %TFA solution prior to MALDI-TOF analysis. Whole peptide reactants not collected from HPLC fractions were cleaned over a C18- Zip Tip's (Millipore™) as per manufacturer's instructions.

2.2.5.2 **Mass Spectrometry**

The Mass spectrometry was analysed at the Centre for Proteomic and Genomic Research (CPGR, Cape Town, South Africa). The collected peptides were spotted onto a 10 mg/ml α-cyano-4-hydroxycinmanic acid matrix (Fluka, USA) in 80% ACN, 0.2% TFA for a final

concentration of 5mg/ml matrix in 40% ACN, 0.1% TFA, and 10 mM $NH_4H_2PO_4$. Mass spectrometry was performed with a 4800 MALDI TOF/TOF (Applied Biosytems) with all spectra recorded in positive reflector mode. Spectra were generated with 400 laser shots/spectrum at a laser intensity of 3800 (arbitrary units) with a grid voltage of 16kV.

2.2.6 X-ray Crystallography

Crystallization of the Ndom with various Aβ peptides was performed by collaborators Prof K. Ravi Acharya and Dr G Masuyer (Department of Biology and Biochemistry, University of Bath, Bath, United Kingdom). Crystals were generated through co-crystallization with 1 µl of 2.5 mM peptide mixture (5-10 mg/ml in 50 mm HEPES, pH 7.5, 0.1 mm PMSF). The peptides Aβ(1-16) (Sigma, SCP0052), Aβ(10-16) (Sigma, SCP0031), Aβ(4-10) (GenScript, RP20173), Aβ(35-42) (GenScript RP20145), and Aβ(4-10)Y were used. Crystals were grown in an equal volume of reservoir solution consisting of 30 % PEG550 MME/PEG20000, 100 mM Tris/Bicine, pH 8.5, and 0.06 M divalent cations (Molecular Dimensions) and suspended above the well as a hanging drop. Crystals of better quality were obtained after 2-3 cycles of macro-seeding.

Prof K. Ravi Acharya and Dr G Masuyer also performed all diffraction studies and solved the Ndom- Aβ structures. X-ray diffraction data were collected on station IO3 at the Diamond Light Source (Oxon, UK). Crystals were kept at constant temperature (100 K) under the liquid nitrogen jet during data collection. Images were collected using a PILATUS-6M detector (Dectris, Switzerland). Raw data images were processed and scaled with MOSFLM (Leslie and Powell, 2007), and SCALA using the CCP4 suite 6.5 (CCP4, 1994). Initial phases for structure solution were obtained using the molecular replacement routines of the PHASER program (McCoy *et al*., 2007). The atomic coordinates of N-domain (PDB code 3NXQ (Anthony *et al*., 2010) were used as a search model for structure determination. The resultant models were refined using REFMAC5 (Murshudov *et al*., 1997). Manual adjustments of the model were carried out using COOT (Emsley *et al*., 2010).

Water molecules were added at positions where $F_o–F_c$ Fourier difference electron density peaks exceeded 3σ, and potential hydrogen bonds could be made. Validation was conducted with the aid of the program MOLPROBITY (Chen *et al*., 2010). Crystallographic data statistics are summarized in Table 2.4. All figures were drawn with PyMOL (Schrödinger, LLC, New York). Hydrogen bonds were verified with the program LigPlot$^+$ (Laskowski and Swindells, 2011).

2.3 Results:

2.3.1 Protein purification of ACE constructs

The human sACE, C-sACE, N-sACE, Ndom, Cdom and CC-sACE variants (Figure 2.2) were expressed in mammalian CHO cells and then purified using lisinopril-sepharose affinity chromatography. The sACE, C-sACE and N sACE constructs are expressed as membrane-bound proteins and undergo poor ectodomain shedding (Kost *et al*., 2003; Pang *et al*., 2001; Woodman *et al*., 2006, 2000). Hence, these constructs were purified directly from cell lysates of stably transfected cell lines. CC-sACE is also membrane bound, but is shed much more efficiently than the other TM constructs and thus was purified from the culture medium. All ACE variants were purified to apparent homogeneity as assessed by SDS-PAGE (Figure 2.3). The sACE proteins migrated at approximately 170 kDa, while the recombinant glycosylated Ndom and Cdom migrated with an apparent molecular mass of 100 kDa and 90 kDa, respectively. It is known that CC-sACE is less stable than other sACE constructs, as can be seen by a small band at approximately the same size as Cdom (Woodman *et al*., 2006).

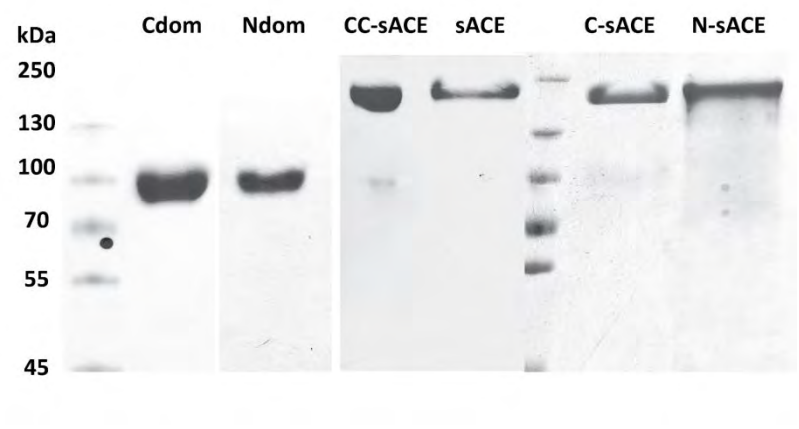

Figure 2.3 **Purified ACE constructs**. The affinity-purified preparations of recombinant human ACE (approximately 10 µg of protein each) were analysed by SDS-PAGE as described in the Materials and methods section. Molecular-mass markers (kDa) are indicated mid gel.

2.3.2 The hydrolysis of Aβ(2-11)by Ndom and Cdom

2.3.2.1 **Analysis of product peaks over time:**

The Ndom was employed to determine what concentration of enzyme was necessary to produce sufficient product for further kinetic analysis. On incubation of Aβ(2-11) with increasing amounts of Ndom, two product peaks were formed: P22 and P10 at retention times 22 and 10 minutes, respectively (Figure 2.4). It is likely that P22 is the primary product as with higher concentrations of Ndom substrate P22 is further converted to P10 (Figure 2.4 F). Sufficient P22 product was measured after 15 minute incubation with 2 nM Ndom. To investigate the hydrolysis of Aβ(2-11) by Ndom and Cdom, a time course of Aβ(2-11) incubated with Ndom and Cdom was carried out; and the relative increase of product and decrease of substrate was compared (Figure 2.5). Notably, 2 nM Ndom produced a substantial (13 % of total substrate injected) amount of product (P22), with a peak area of 146 917, after 5min incubation while zero product was generated by the Cdom at a concentration of 100 nM.

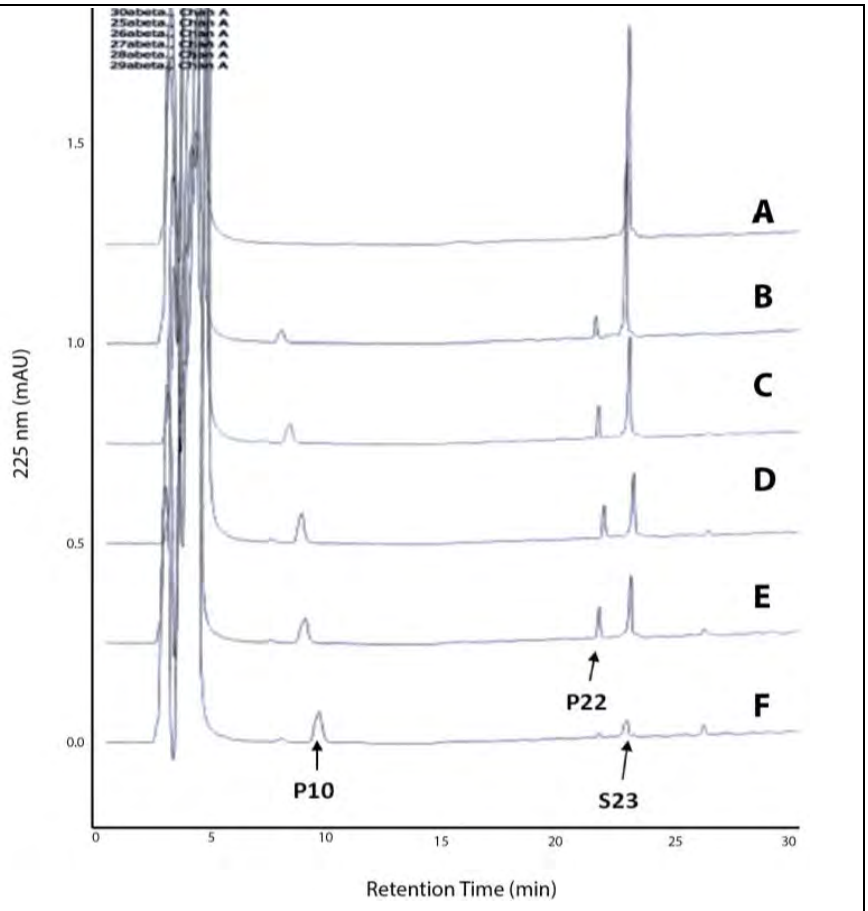

Figure 2.4 **Sequential break down of Aβ(2-11) by Ndom**. Overlaid HPLC traces of 44µM Aβ(2-11) digested with N-domain for 15 minutes at 37°C to determine concentration of enzyme required to generate a product peak (P22) within 10% hydrolysis of substrate (S23). **A**) Substrate Aβ(2-11); incubated with **B**) 2 nM Ndom; **C**) 10 nM Ndom; **D**) 22 nM Ndom; **E**) 28 nM Ndom; **F)** 100 nM Ndom.

With 2nM of Ndom, complete hydrolysis of Aβ(2-11) was achieved in 3 hours; however Cdom (125 nM) required 20 hours of incubation. These data show that the Ndom is far more efficient at Aβ(2-11) hydrolysis than the Cdom and provided a basis for continuing with the Aβ peptide cleavage site analysis. Kinetic analysis of the ACE variants hydrolysis of different Aβ peptides is presented in the following Chapters 3 and 4.

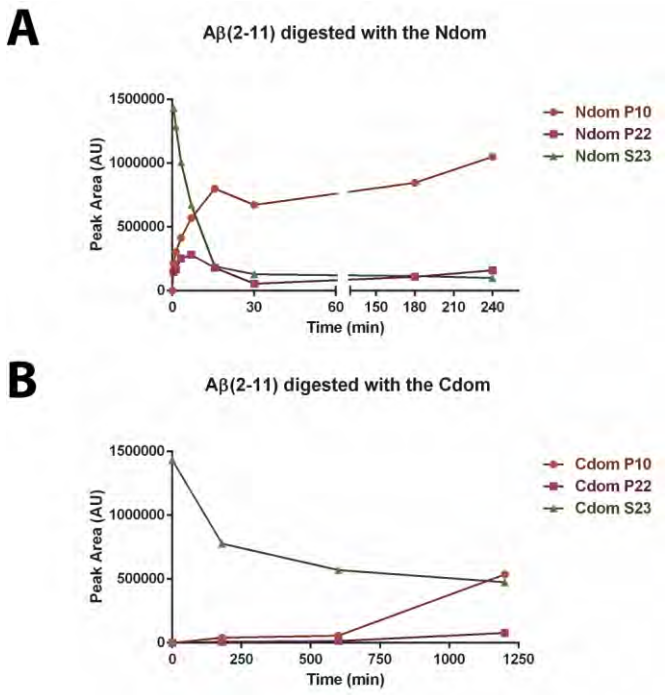

Figure 2.5 **Digestion of Aβ(2-11) by the N and C-domain**. The integrated peak area of Aβ(2-11) substrate (S23) digested with: **A)**The Ndom construct and **B)** The Cdom construct over time. The Aβ(2-11) proving a better substrate for the Ndom as seen by the rapid formation of product peaks P22 and P10

2.3.3 ACE cleavage-site analysis of Aβ peptides

2.3.3.1 **N-terminal peptide Aβ(2-11).**

The N-domain cleavage site on Aβ(2-11) was ascertained using HPLC of the cleavage products (Figure 2.4) followed by MALDI-TOF mass spectrometry. The results indicated that the primary cleavage site (P22) under substrate saturating conditions, was between residues Asp7 and Ser8, evident from the corresponding *m/z* fragment detected (Table 2.). This was confirmed by MS/MS analysis of the product Aβ(2-7). Thus, ACE has an endopeptidase action on this peptide. The P10 peak did not reveal any peptides with a signal above the matrix background. It is hence most likely that P10 consists of much smaller peptide degradation products.

2.3.3.2 **Design of small fluorescence resonance energy transfer (FRET) Aβ(4-10) mimics of Aβ(2-11).**

Based on the Aβ(2-11) cleavage site, fluorogenic versions of the amyloid beta peptide were designed, namely: Aβ(4-10)Q with an N-terminal, o-aminobenzoic acid (Abz) donor group and a C-terminal, ethylenediamine 2, 4-dinitrophenyl (EDDnp); and with an alternative 3-nitrotyrosine quenching group, Aβ(4-10)Y. These fluorogenic substrates are described in the following chapters, where they were used to further characterise the cleavage of Aβ by the Ndom and Cdom catalytic sites (Chapter 3 and 4).

Table 2.1 **Primary cleavage sites of Aβ(2-11) and Aβ(1-16)**. The MALDI-TOF analysis of Aβ(2-11) and Aβ(1-16) digested with 2 nM Ndom for 15min. The substrate and cleavage sites corresponds toS23 and P22 for Aβ(2-11) and S5.6 and P5.8 for Aβ(1-16) respectively.

Amyloid Peptide	Peptide Residues	Calculated *m/z*	Observed *m/z*
Aβ(2-11) Substrate	Ac-AEFRHDSGYE-NH_2	**1252.53**	1251.55
Product	Ac-AEFRHD	**816.37**	816.38
Aβ(1-16) Substrate	H-DAEFRHDSGYEVHHQK-OH	**1954.88**	1954.88
Product	H-DAEFRHDSGYEVHH	**1698.73**	1698.58

2.3.3.3 **Physiological Aβ(1-16) peptide**

Cleavage of the Aβ(1-16) peptide was investigated using the truncated Ndom variant. The HPLC chromatogram of the hydrolysis of Aβ(1-16) by the Ndom indicated a product peak (P5.8) that eluted slightly later than the substrate (S5.6) (Figure 2.5 B). This shift suggests a slight increase in hydrophobicity of the product peptide. Substrate and product peaks were collected and subjected to mass analysis (Table 2.) which indicated the loss of the last two residues of Aβ(1-16) consistent with a slight loss of hydrophilicity. Thus, ACE functions as a dicarboxypeptidase towards this substrate, cleaving between residues His14–Gln15 and liberating Aβ(1-14) as the P5.8 primary product (Figure 2.6). This product had an observed mass corresponding to Aβ(1-14) (Table 2.). Although Aβ(1-16), like Aβ(2-11), is comprised of the N-terminal region of Aβ(1-42), they have different cleavage sites.

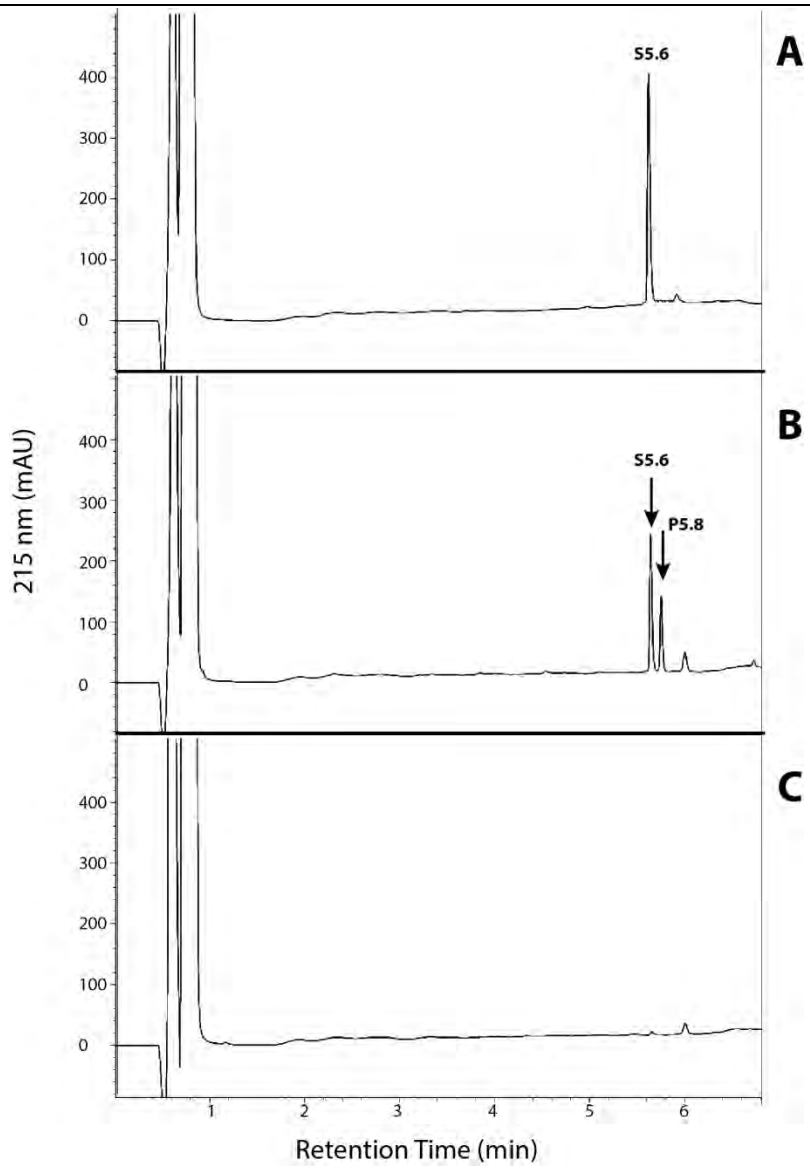

Figure 2.6 **Ndom hydrolysis of Aβ(1-16)**. The HPLC chromatogram of **A)** The substrate Aβ(1-16), incubated for 30 minutes without enzyme. **B)** Aβ(1-16) incubated with 1 nM Ndom for 30 minutes, the substrate peak is indicated as S5.6, and the product peak is indicated as P5.8. **C)** The chromatogram of the buffer constituents used in the enzyme reaction.

2.3.3.4 Cleavage site specificity of the various forms of ACE

To determine the bond at which the β-amyloid peptides were cleaved by the different ACE variants, each substrate was incubated under the stated assay conditions (see Chapter 3 and 4) and the resultant peptide products were purified and analysed by MALDI–TOF MS. The FRET peptides constructed from Aβ(2-11) (Table 2.), Aβ(4-10)Q and Aβ(4-10)Y, yielded a product with a *m/z* (Table 2.2) corresponding to the N-terminal Abz-FRHD, on digestion with Ndom, N-sACE, C-sACE and sACE. Thus, both FRET Aβ(4-10) peptides were endoproteolytically cleaved at the Asp7-Ser8 bond in the same fashion as the non-FRET parent peptide Aβ(2-11) (Table 2.2). The Cdom and CC-sACE cleavage sites were not analysed, as hydrolysis of the Aβ peptides by these ACE variants under assay conditions was negligible. All four constructs cleaved these short synthetic peptides at the same position with no apparent difference in specific cleavage preference between the Ndom and Cdom. Hydrolysis of Aβ(1-16) by all the ACE variants except Cdom yielded peptides with *m/z* ratio corresponding to the N-terminal peptide Aβ(1-14) (Table 2.2). This indicates that Aβ(1-16) undergoes dicarboxypeptidase cleavage at the His14-Gln15 bond by all five ACE variants and there is no apparent difference in cleavage site selectivity between the two functioning domains of ACE under these conditions.

Table 2.2 **Observed $[M+H]^+$ ions of the peptide products generated by endoproteinase and exoproteinase action of the various ACE constructs on the Aβ(1-16), Aβ(4-10)Q and Aβ(4-10)Y substrates.**

Amyloid Peptide	Peptide Residues	Calculated *m/z*	Observed *m/z*					
			Ndom	N-sACE	sACE	C-sACE	CC-sACE	Cdom
Aβ(1-16) Substrate	H-DAEFRHDSGYEVHHQK-OH	**1954.88**	1954.82	1954.82	1954.82	1954.83	1954.80	1954.83
Product	H-DAEFRHDSGYEVHH	**1698.73**	1698.58	1698.68	1698.76	1698.67	1698.66	
Aβ(4-10)Q Substrate	Abz-FRHDSG(Q)-EDDnp	**1191.49**	1191.49	1191.44	1191.45	1191.37	*nd*	*nd*
Product	Abz-FRHD	**693.31**	693.30	693.31	693.30	693.31		
Aβ(4-10)Y Substrate	Abz-FRHDSG(Y)-3NO2	**1064.43**	1064.37	1064.43	1064.39	1064.39	*nd*	*nd*
Product	Abz-FRHD	**694.32**	694.26	694.29	693.28	694.29		

To determine if the Aβ(1-16) is further degraded over time by all forms of ACE, 36.5 µM of Aβ(1-16) was incubated for 24 hours under assay conditions described in Chapter 4 section 4.2.5.1. The reaction products were separated by HPLC and analysed via MALDI-TOF (Table 2.3). Interestingly, the mass of the initial cleavage intermediate, Aβ(1-14), was present across all ACE constructs except for N-sACE. However, the Aβ(1-12) peptide was only generated by the sACE mutants (expected *m/z* of 1325.54). The corresponding C-terminal peptide Aβ(12-16) was detected in both Cdom and Ndom digests as well as in sACE and C-sACE, but not N-sACE or CC-sACE. Presumably, the Aβ(1-12) product is hydrolysed faster by the Cdom, Ndom and wild type sACE. Overall, there appears to be no absolute domain preference towards any specific cleavage site, similar to the hydrolysis for 15 minutes. The Aβ(1-7) cleavage site is also found across constructs barring N-sACE and CC-sACE. These results indicate that the hydrolysis of Aβ(1-16) by both domains of ACE is not limited or specific, and that under certain conditions the C-domain does hydrolyse Aβ peptides.

Table 2.3 **The cleavage product $[M+H]^+$ ions generated by of the various ACE constructs on the Aβ(1-16) substrate over a 24 hour period.**

Amyloid Peptide	Peptide Residues	Calculated m/z	Observed m/z					
24 hour digestion with:			Ndom	N-sACE	sACE	C-sACE	CC-sACE	Cdom
Aβ(1-16)	H-DAEFRHDSGYEVHHQK-OH	**1954.88**	1954.75	1954.75	1954.80	1954.79	1954.81	1954.82
N-terminal products:								
Aβ(1-14)	H-DAEFRHDSGYEVHH	**1698.73**	1698.68		1698.65	1698.68	1698.64	1698.66
Aβ(1-12)	H-DAEFRHDSGYEV	**1424.61**	1424.53	1424.52	1424.54	1424.57	1424.55	1424.57
Aβ(1-11)	H-DAEFRHDSGYE	**1325.54**		1324.50		1325.52	1325.49	
Aβ(1-7)	H-DAEFRHD	**889.38**	889.33		889.35	889.36		889.38
Aβ(1-6)	H-DAEFRH	**774.35**				774.36		
Aβ(1-5)	H-DAEFR	**637.29**	637.30	637.27	637.29	637.30	637.29	637.28
C-terminal products:								
Aβ(2-16)	AEFRHDSGYEVHHQK-OH	**1839.85**						1839.80
Aβ(4-16)	FRHDSGYEVHHQK-OH	**1639.77**	1639.73					
Aβ(12-16)	VHHQK-OH	**648.36**	648.30		648.31	648.30		648.36

2.3.4 Crystal Structures of Ndom in Complex with Aβ Peptides

In order to better understand the molecular interactions that occur between Aβ and ACE, considering the variation in cleavage position both in this study and in literature, crystallization experiments were planned. The peptides chosen for crystallography were based on cleavage sites derived from this study as well as from the literature, with focus on the N-terminal region of the full length Aβ(1-42). Furthermore our lab in collaboration with Prof K. Ravi Acharya and Dr G Masuyer (Department of Biology and Biochemistry, University of Bath, Bath, United Kingdom) have had success in the crystalisation of larger products like ANGII (Masuyer *et al*., 2012). Ndom was pepared as in section 2.2.2 in this labroratory and sent to our collaborators Prof K. Ravi Acharya and Dr G Masuyer for crystallisation, diffraction studies and resolution of the structures in this thesis.

Crystallisation trials were performed initially on the full length Aβ(1-42) and while co-crystals with Aβ(1-42) could not be obtained, trials with shorter Aβ fragments, namely Aβ(4-10), Aβ(10-16), Aβ(1-16), Aβ(35-42) and Aβ(4-10)Y, were successful. These fragments we specifically chosen as mentioned, based on ACE cleavage sites found along Aβ(1-42). These crystals have generated high-resolution (1.5-1.9Å) structural data of the latter co-crystal complexes (Table 2.4).

Overall, the structure of Ndom did not show any major conformational change upon peptide binding (Figure 2.7 A). The previously observed hinge motion of the N-terminal helices (Anthony *et al*., 2010), was slightly more pronounced in some of the molecules. This resulted in a larger asymmetric unit (a=73, b=102, c=114 Å; α=85, β=86, γ=81°) of four Ndom chains, still in space group *P1*, for the Aβ(4-10), Aβ(10-16), Aβ(1-16) complexes (Table 2.4). The structures with Aβ(35-42) and Aβ(4-10)Y were in the same crystallographic cell as previously reported for Ndom comprising of 2 chains per asymmetric unit in *P1* (a=73, b=77, c=83 Å; α=89, β=64, γ=75°) (Table 2.4). The degree of movement however, appeared limited. This lack

of movement could not be correlated to the size of the substrates or bound peptides, but visible disorder in the N-terminal region of the Ndom did occur and is highlighted by higher B-factors (Table 2.4) (Figure 2.7 A).

In each of the structures, electron density was clearly observed in the S' side of the Ndom catalytic pocket for what correspond to a dipeptide. Electron density maps for the side chains of sites P1' and P2' of the peptides were interpreted as the products of the prolonged reactions of Aβ cleavage by Ndom (Figure 2.7 C). The carboxy-dipeptide residues of Aβ(35-42) and Aβ(4-10)Y were visible, Ile41-Ala42 and Gly9-nitroTyr10 respectively. Both Aβ(4-10) and Aβ(1-16) presented the Asp7-Ser8 residues.

The structure of Ndom with Aβ(10-16) was unique in offering two alternative dipeptides, each present in two of the chains forming the asymmetric unit, and corresponding to Glu11-Val12 and Gln15-Lys16. Coincidentally, the Aβ(10-16) structure also showed unusual ion coordination in proximity to the binding site. In presence of Glu11-Val12 a cation is octahedrally coordinated by Glu262, Asn263 and Asp354 of Ndom along with three water molecules, while the same residues are involved in cationic interaction with only two water molecules when Gln15-Lys16 is bound (Figure 2.10). The ion coordination was carefully analysed in each case using the CMM validation server (Zheng *et al*., 2014) and interpreted as calcium and sodium ions, respectively. Both are present in the crystallisation conditions but are unlikely to have any physiological role and have not been observed in any of the other N-ACE crystal structures.

Table 2.4 **Crystallographic statistics of the Ndom structures in complex with Aβ fragments.**

	Ndom complexed with:				
	Aβ(4-10)	**Aβ(10-16)**	**Aβ(1-16)**	**Aβ(35-42)**	**Aβ(4-10)Y**
Resolution (Å)	1.9	1.8	1.8	1.55	1.65
Visible peptide	D7-S8	E11-V12 / Q15-K16	D7-S8	I41-A42	G9-(NT)
Space group	*P1*				
Cell dimensions (Å; a, b, c);	73, 102, 114;	73, 102, 114;	73, 102, 114;	73, 77, 83;	73, 76, 83;
angle (°; α,β,γ)	85, 86, 81	85, 86, 82	85, 86, 81	89, 64, 75	89, 64, 76
Molecule/AU	4	4	4	2	2
Total/Unique reflections	384,870/293,455	929,478/291,734	461,830/281,258	324,307/200,050	520,452/172,512
Completeness (%)	93 (84)[a]	97 (95.7)[a]	94 (82)[a]	88 (56)[a]	92 (64)[a]
R_{merge} [a, b]	7.1 (43.8)	12.0 (76.3)	6.1 (46.0)	4.2 (44.4)	8.1 (70.6)
R_{pim} [a, c]	7.1 (43.8)	7.9 (49.7)	6.0 (45.9)	4.2 (44.4)	5.4 (49.8)
I/σ(I) [a]	5.8 (1.4)	5.3 (1.4)	6.8 (1.4)	7.5 (1.4)	6.4 (1.3)
CC(1/2)	0.996 (0.816)	0.993 (0.325)	0.998 (0.635)	0.993 (0.565)	0.995 (0.318)
R_{cryst} [d]	18.5	19.7	18	15.8	20.8
R_{free} [e]	22.4	22.9	21	18.1	24.1
Rmsd in bond lengths (Å)	0.016	0.012	0.011	0.014	0.011
Rmsd in bond angles (°)	1.34	1.4	1.34	1.4	1.33
B- factor statistics (Å²)					
Protein all atoms	27.4/24.8/22.2/23.1	29.3/26.3/24.3/27.0	26.5/23.3/21.2/23.4	33.0/37.8	27.9/31.0
Protein main chain atoms	26.4/23.7/21.1/22.3	28.4/25.2/23.4/26.2	25.2/22.1/20.0/22.3	30.8/35.4	26.7/29.9
Protein side chain atoms	28.4/25.8/23.2/23.9	30.2/27.3/25.2/27.9	27.7/24.6/22.4/24.5	35.2/40.1	29.1/31.1
Peptide atoms	26.0/23.5/24.6/23.3	27.5/23.5/21.9/28.1	27.4/27.3/23.5/26.3	28.4/28.9	41.7/44.6
Solvent atoms	29.7	31	30.9	44.8	35.3
Zn^{2+} / Cl^- ions	16.7/16.2	19.2/19.7 (Na^+ 33.5/Ca^{2+} 35.2)	17.5/16.7	25.5/26.9	19.9/21.5
Glycosylated/ carbohydrate atoms	48.6	54.1	47.7	67.3	58.9
Ramachandran statistics (Molprobity)					
Favored	98%	98%	98%	98%	98%
Outliers	0.20%	0.20%	0.20%	0.20%	0.20%
PDB code	**5am8**	**5am9**	**5ama**	**5amb**	**5amc**

[a] Values in parentheses refer to the highest resolution shell.

[b] $R_{merge} = \Sigma\Sigma_i |I_h - I_{hi}| / \Sigma\Sigma_i I_h$, where I_h is the mean intensity for reflection h.

[c] $R_{pim} = \Sigma_h (1/n_h - 1) \Sigma_l |I_{hl} - (I_h)| / \Sigma_h \Sigma_l (I_h)$

[d] $R_{cryst} = \Sigma||F_o| - |F_c|| / \Sigma |F_o|$, where F_o and F_c are measured and calculated structure factors, respectively.

[e] $R_{free} = \Sigma||F_o| - |F_c| / \Sigma |F_o|$, calculated from 5% of the reflections selected randomly and omitted during refinement.

2.3.4.1 Mode of Peptide Binding in N-domain S' pockets

The crystal structures of Ndom in complex with the Aβ fragments present a common mechanism of peptide binding within the S' catalytic pocket (Figure 2.7 B). The Ndom essentially recognises the main chain of the peptides through seven hydrogen bonds. The P1' position interacts with the main chain of Ala332, and the side chains of Glu362, His491 and His331. The S2' pocket is composed of Gln259, Lys489 and Tyr498 whose polar side chains anchor the carboxy-terminal end of the peptide. Furthermore, a network of water molecules was also observed in all structures that further mediates interaction of the peptides' main chain with residues Ala332, Glu362, Tyr501 and Lys489 of Ndom (Figure 2.8). The N-terminal groups of the peptides are closely tied up to the zinc ion via two coordinating water molecules. Additional and more specific contacts were observed with peptides Asp7-Ser8

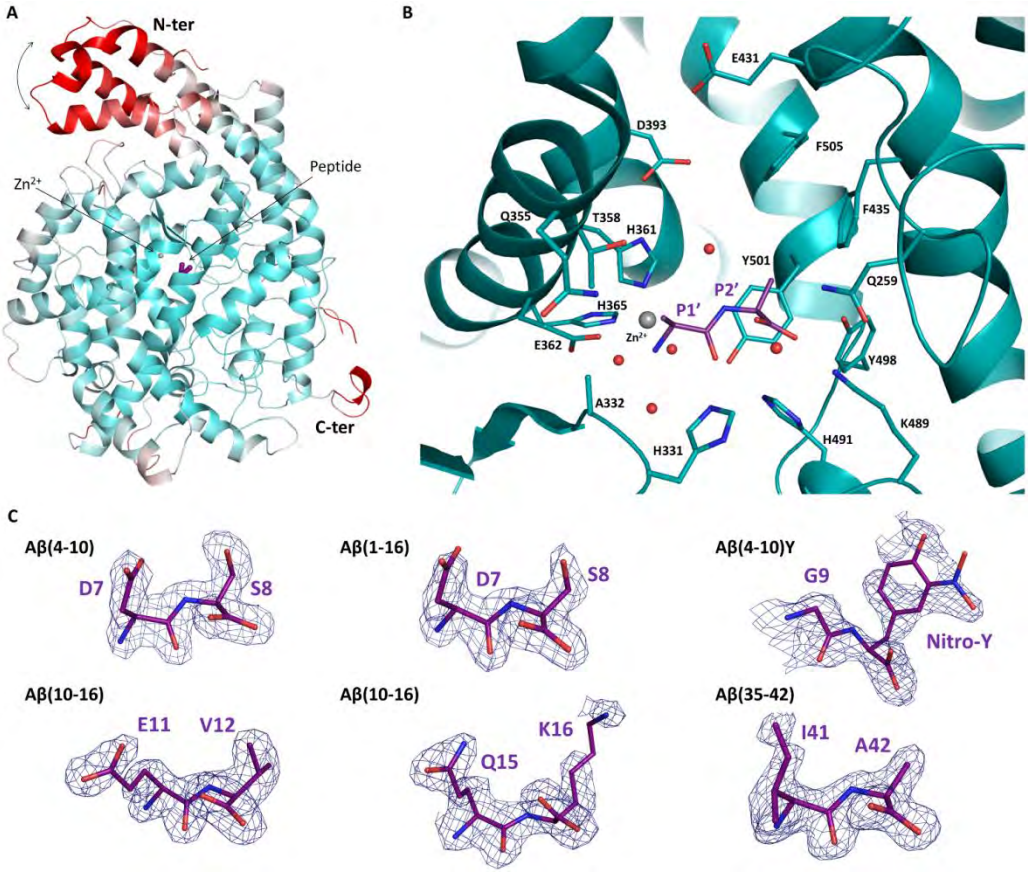

Figure 2.7 **General properties of the five Aβ peptides crystallised within the Ndom.** Overall structure of Ndom coloured in a B-factor spectrum (white=low; red=high) to highlight the hinge region of the N-terminal domain 'capping' the catalytic channel. The bound dipeptide is shown in purple, the catalytic zinc ion as a grey sphere. **B)** Close up view of the catalytic site of the N-domain in complex with a bound dipeptide. The dipeptide, modelled as Ala-Ala, reflects the common mechanism of binding observed in all complex structures with Aβ fragments. The dipeptide is shown in purple and the N-domain residues involved in binding are represented as sticks. The spheres represent the zinc ion (in grey) and water molecules (in red). **C)** Portions of the Fourier electron density map at the site of the bound peptides. The picture was generated using REFMAC5 (Murshudov *et al.*, 1997) and correspond to the difference weighted 2mFo-DFc density map, contoured at 1.0σ level, in which the peptide atoms were omitted.

where the side chain of Thr358 makes a hydrogen bond with the acidic group of Asp7, and a water-mediated bond exist between Gln259 and the Ser8 side chain (Figure 2.8). Interestingly the two alternative peptides seen within the structure of Aβ(10-16) show similar contacts at the P1' position with the longer side chain of Glu11 or Gln15 able to make direct contact with Ala332 and two water mediated interactions with Gln355 (Figure 2.8). The side chain of residues at P2' may be held in position by the surrounding hydrophobic residues Phe435, Tyr501 and Phe505. Additionally, the Lys16 ε-amino group is within distance (5.5Å) of a potential cation-π interaction with Phe435. In the case of Aβ(4-10)Y, the larger nitrotyrosine fits well within the S2' pocket. The additional nitro group is within hydrogen-bond distance of Gln259 and the hydroxyl group can make water mediated interactions further down the catalytic channel with residues Asp393 and Glu431. Electron density was observed to be weaker in both molecules of the asymmetric unit for the nitrotyrosine, which may be indicative of some flexibility (Figure 2.7 C).

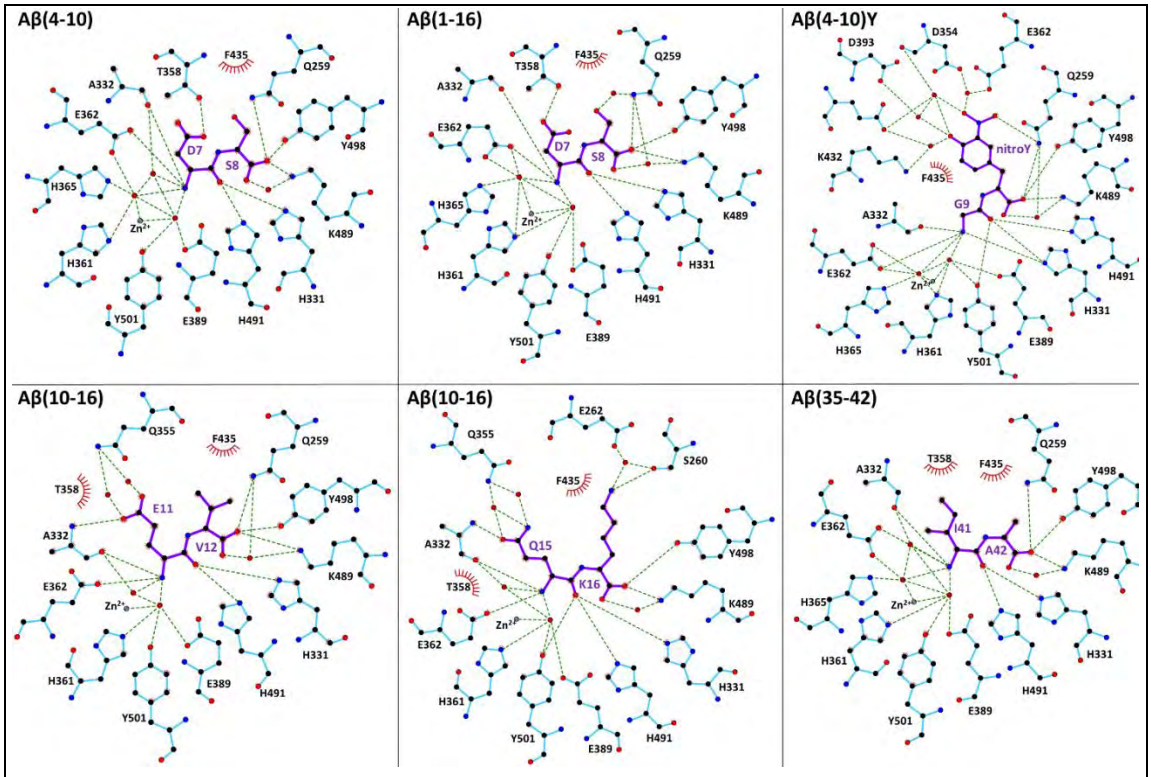

Figure 2.8 **Mechanism of Aβ fragment binding to the N-domain**. Schematics of peptide binding to the N-domain. Interactions were calculated with LigPlot^{+} (Laskowski and Swindells, 2011). The two alternative peptides for Aβ(10-16) are included with Glu11-Val12 and Glu15-Lys16 observed in chains A, D and B, C respectively.

2.4 Discussion:

The hallmark of AD is the accumulation of Aβ within the brain. This peptide is constitutively shed and produced via proteolysis of its precursor APP (see Chapter 1). It is comprised of 39-43 residues and is renowned for its N- and C-terminal heterogeneity and toxicity. Thus, subtle disturbances in metabolism of APP can have severe pathophysiological consequences. The production of Aβ by different proteolytic enzymes has been well characterised. However, the molecular basis for the hydrolysis of Aβ by ACE is less clear. In this chapter, we investigated the mode of binding and hydrolysis of Aβ peptides to ACE, through crystallography and MS, in the hope to better understand the role of ACE in AD.

ACE's primary catalytic function is as an exopeptidase, known to remove the last two amino acids from the C-termini of its substrates. However, ACE also functions as an endopeptidase towards some substrates like substance P (cleaved at Phe8-Gly9 and Gly9-Leu10) (Yokosawa *et al*., 1983), gonadotropin-releasing hormone (GnRH) (Ehlers and Riordan, 1991; Skidgel and Erdös, 1985) and, of course, Aβ (Hu *et al*., 2001). It is worthwhile noting that C-terminal amidated peptides, like substance P and GnRH, inhibit the exopeptidase ability of ACE (Skidgel *et al*., 1984). The Aβ(2-11) peptide was endoproteolytically cleaved which was not surprising considering it has an amidated C-terminus. The Aβ(2-11) cleavage at the Asp7-Ser8 bond is consistent with previous studies where varying forms of both full-length cellular and truncated synthetic Aβ were used (Hemming and Selkoe, 2005; Hu *et al*., 2001; Kumar *et al*., 2012; Oba *et al*., 2005) (Table 2.) (Figure 2.1).

The amidated form of Aβ(1-16), on the other hand did not produce any proteolytic product even after prolonged incubation with the Ndom (data not shown). The free acid version, however, was effectively cleaved in ACE's traditional exopeptidase fashion. (Table 2.2) Subsequent degradation of the Aβ peptide after the initial cleavage was more rapid with Aβ(2-11) than Aβ(1-16), presumably due to the secondary structure of the Aβ(1-16) and indicative of structure dependent cleavage specificity. If incubation with the different ACE variants is prolonged, Aβ(1-16) is further broken down from the primary Aβ(1-14) intermediate to other fragments, including Aβ(1-7) (Table 2.3 and Table 2.4). NEP hydrolyses the N-terminal region of Aβ(1-42) between residues Gly9-Tyr10 and Gly37-Gly38, liberating the primary intermediate Aβ(10–37) (Iwata *et al*., 2000). This then undergoes subsequent degradation in a similar fashion to ACE cleavage of Aβ(2-11) and Aβ(1-16) found in this study and of Aβ(1-42) found in other studies.

The production of the Aβ(10-37) intermediate by NEP seems to constitute a rate-limiting step in the enzyme's Aβ(1-42) catabolism (Iwata *et al*., 2000). NEP thus removes the N-terminal and C-terminal regions of Aβ(1-42) before further breakdown. It is conceivable that this removal of the N-terminal region destabilizes the molecule as a whole due to the removal of the metal coordinating His-rich Aβ(1-10) region (Curtain *et al*., 2001; Istrate *et al*., 2012). ACE appears to perform a similar function. The endoproteolytic degradation of the N-terminal region of Aβ(1-42) and the removal of the final Aβ(41-42) residues, found in this study and others (Zou *et al*., 2009, 2007), removes Aβ's metal stacking ability and greatly reduces Aβ's aggregation potential. This is exemplified in the progression of the Aβ(2-11) hydrolysis by the Ndom and Cdom construct over time (Figure 2.5). The Aβ(2-11) peptide is cleaved efficiently by the truncated Ndom over time. The truncated Cdom, in contrast, cleaved the Aβ(2-11) very

inefficiently. These data support the evidence that the single C domain has a very small role, if any, to play in the cleavage of the Aβ peptide (Oba *et al*., 2005; Toropygin *et al*., 2008; Zou *et al*., 2009). In terms of domain selectivity, the Aβ peptides appear N-selective. As AD is a chronic illness, one should not discount the fact that the C-domain does cleave Aβ, confirmed by studies done on full-length ACE (Hemming and Selkoe 2005; Sun *et al*. 2008; Zou *et al*. 2009;), for it may only take a very long time to do this. However, the physiological relevance of such slow hydrolysis is questionable. The selectivity towards Aβ(1-16) was much the same as that of Aβ(2-11) for after 24 hours of incubation multiple degradation products were found from all C-domain constructs (C-sACE, CC-sACE and Cdom), both exo- and endoproteolytically. (Table 2.4)

For the first time, we have confirmed the exopeptidase cleavage of Aβ by ACE using X-ray crystallography (Figure 2.7). High-resolution structures of six Aβ peptides in complex with the truncated N-domain were solved by our collaborator Professor Ravi Acharya. In each of the structures presented here, a dipeptide, representing different cleavage sites, was observed occupying the active site of Ndom. In congruence with Zou *et al*. 2007, the crystal structure indicated that the Aβ(35-42) was cleaved between Ile41-Ala42 (Figure 2.9 and Figure 2.10 B). Crystallisation experiments of Aβ(4-10) and Aβ(1-16) with Ndom yielded structures with the Asp-Ser dipeptide bound in the active site, suggestive of cleavage at the His6-Asp7 bond (Figure 2.7 C). This was contrary to results found under kinetic assay conditions wherein the Asp7-Ser8 bond in Aβ(4-10) is hydrolysed within 5 minutes (Figure 2.9). However, the alternate cleavage, of both Aβ(4-10)and Aβ(1-16), is likely due to the longer incubations under slightly different conditions required for the formation of crystals. Supporting this, Aβ(1-16) hydrolysis at His6-Asp7 was seen after 24 hour incubation with C-sACE, though no N-domain constructs generated this hydrolysis product (Table 2.3). MS analysis of the peptides generated by digestion of Aβ(1-16) with Ndom showed that it undergoes extensive degradation. This finding was supported by the crystal structures of Ndom in complex with Asp7-Ser8, Glu11-Val12 and Gln15-Lys16 alluding to multiple cleavage of the Aβ(1-16) peptide (Figure 2.9). Presumably, based on the MS analysis, primary cleavage occurs between residues His14 and Gln15 emphasized by the Ndom-Gln15-Lys16 crystal of Aβ(10-16) (Figure 2.10C). The presence of the Ndom-Glu11-Val12 crystal could be indicative of secondary exopeptidase action removing His13-His14. This peptide correlates well with the cleavage sites found after prolonged incubation of Aβ(1-16) with all constructs, both N and C-domain forms (Table 2.3). Presumably, the next exopeptidase digestion step, on what would now be left of the Aβ(10-16), was found in the Glu11-Val12-Ndom crystal complex (Figure 2.10 D). This presented a cleavage site, between Tyr10-Glu11, found in the study by Sun *et al*. 2008 who used the Aβ(4-15) as a substrate, yet was not seen in this study (Figure 2.9).

Fluorogenic ACE substrates are frequently used to investigate substrate and inhibitor mechanisms (Araujo *et al*., 2000; Jullien *et al*., 2006; Skirgello *et al*., 2005). The substrates Aβ(4-10)Q and Aβ(4-10)Y used in this thesis were intended for exactly this purpose as well as to facilitate kinetic analyses with the different ACE variants. Under kinetic assay conditions both fluorogenic peptides (Aβ(4-10)Q and Aβ(4-10)Y) were endoproteolytically cleaved at the previously identified Asp7-Ser8 bond (Hemming and Selkoe, 2005; Hu *et al*., 2001; Kumar *et al*., 2012; Oba *et al*., 2005). Again, the cleavage site was consistent across all ACE variants.

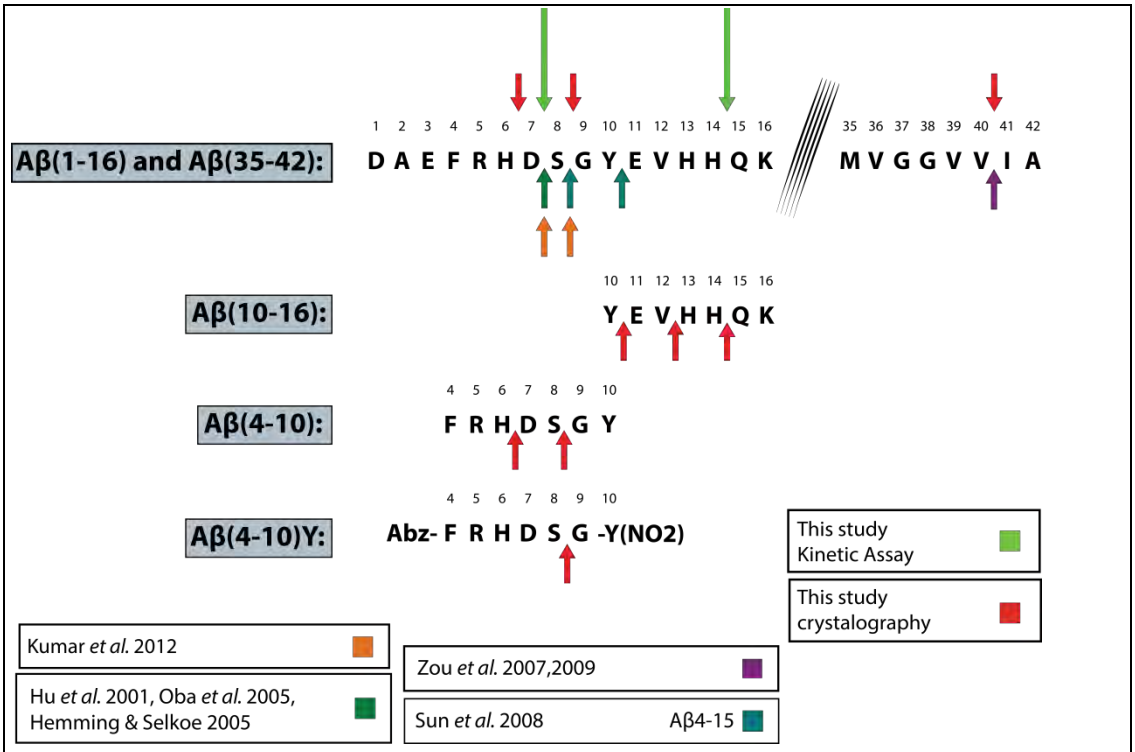

Figure 2.9 **Diagram of the five peptides crystalized with cleavage sites.** Indicated are the cleavage sites found in the literature, kinetic studies in this thesis and those based on the dipeptides found in the Ndom co-crystallisation.

The crystal structure of the Ndom-Aβ(4-10)Y complex found that the Gly9-nitroTyr10 residues were occupying the S1' and S2' pockets of the Ndom, respectively (Figure 2.8 and Figure 2.10A). In agreement with this result, previous studies on ACE FRET substrates, indicated that a large C-terminal EDDnp group usually occupies the S2' pocket and cleavage occurs one residue away from this acceptor group (Araujo *et al*., 2000). In contrast to the crystal results, MS analysis of products after 30 minutes of ACE digestion revealed that cleavage was consistently three residues from the EDDnp and nitrotyrosine groups (Table 2.2). Combined, these results provide evidence that the fluorogenic peptide may undergo endoproteolytic or classical exoproteolytic activity depending on the experimental conditions used for a single substrate.

Both MS and crystal structure data demonstrate ACE's ability to cleave peptides of diverse length and composition. The high-resolution structures of the Aβ dipeptides in complex with Ndom present a common mode of binding in the active site. This principally targets the C-terminal P2' position of the substrate to the S2' pocket and recognises the main chain of the P1' peptide. It is a mechanism reminiscent of Cdom binding to ANGII and the bradykinin potentiating peptide b (BPPb) (Masuyer *et al*., 2012). The residues involved in the binding of Aβ within the S' pockets are conserved in both ACE domains. The apparent Ndom selectivity for Aβ could be conferred through interactions upstream of the catalytic channel above position S2 (Anthony *et al*., 2010; Masuyer *et al*., 2012). Additionally, Ndom should be able to accommodate larger substrates through movement of its flexible lid region of N-terminal helices. This is evident from the level of disorder of the hinge region in the crystal structures.

Although the chloride ion is expected to play a role in substrate binding in domains (Yates *et al*., 2014), the structures presented did not provide any further evidence of this.

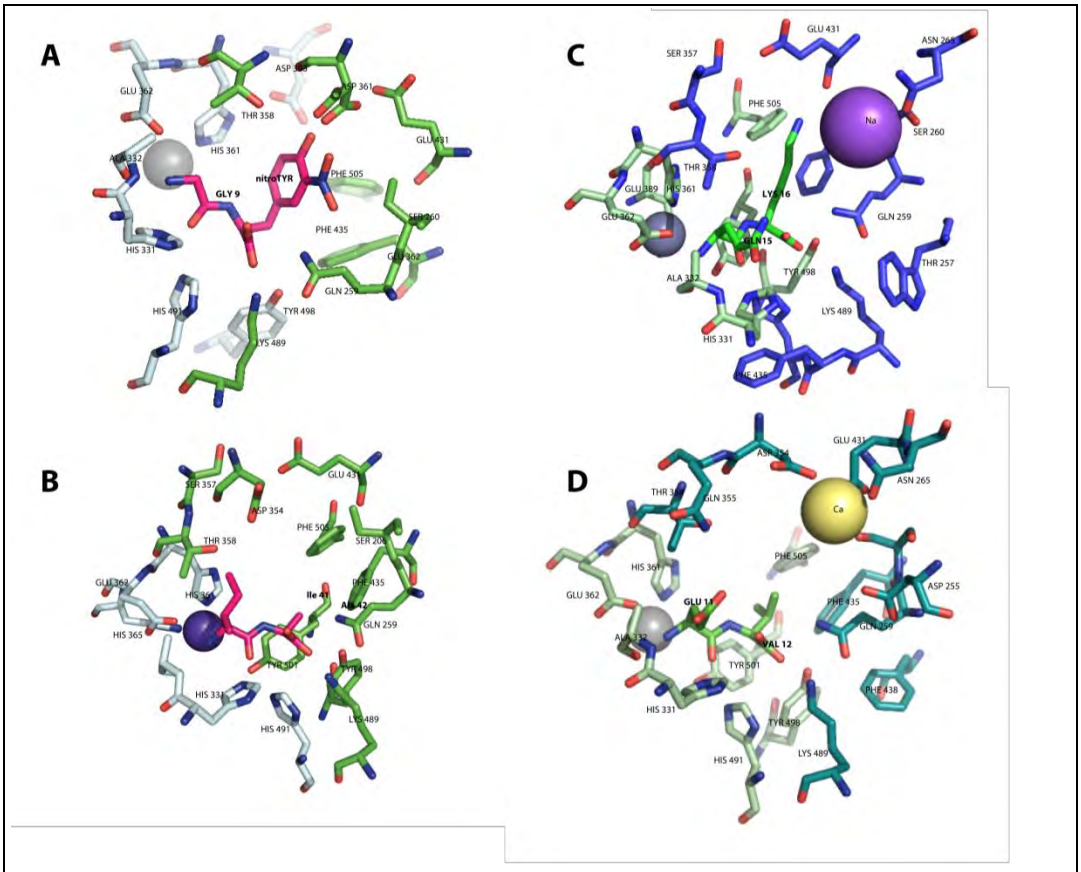

Figure 2.10 **Ndom S1' and S2' residues within 5 Å of the Aβ dipeptides**. **A)** The cleavage products Gly9-nitroTyr10 (hot pink sticks) of the Aβ(4-10)Y peptide, the pale cyan residues make up the S1' pocket and the green residues the S2' pocket with the zinc ion in grey. **B)** The Aβ(35-42) short peptides cleavage product Ile41-Ala42 in hot pink, zinc in purple and the S1' and S2'residues in pale cyan and green respectively. **C)** The putatively initial cleavage product, Gln15-Lys16 (TV-green), of the Aβ(10-16) peptide. The pale green residues indicate the active site residues of the S1' pocket, and the blue residues of the S2' pocket with a large purple Na^{2+} ion deeper in the S2' pocket and the catalytic zinc in grey. **D)** The second cleavage product crystallised of Aβ(10-16), Glu11-Val12 (in TV green), coordinated to the S1' active site residues in pale green and the S2' residues in cyan. Again bound deeper in the S2' pocket is the pale yellow Ca^{2+} ion and in grey the catalytic zinc sphere. These images were generated using PyMOL software (v 0.99, DeLano Scientific).

Additional interactions, despite the common mode of binding described above, exist as evident from the five high-resolution structures. There are two groups of residues, from the different fragments, which coordinate well with the S1' subsite. The first is distinguished by peptides with P1' longer polar side chains (Aβ-Asp7, Glu11 and Gln15) which make hydrogen bonds with Ala332 or Thr358 of Ndom. The second includes small hydrophobic residues, such as Ile41, at the P1' position of the substrate, however such residues have also been shown to be cleaved effectively by both domains of ACE (Araujo *et al*., 2000). The unique residues of the S2' pocket offer strong hydrophobic interactions for the P2' position, as seen with Val12, Ala42 and the nitroTyr group of Aβ(4-10)Y (Figure 2.10 A). Furthermore, longer polar side

chain may also be stabilised by electrostatic interactions (e.g. Lys16) deeper into the pocket (Figure 2.10 C). Due to the size and possibly the affinity that the N-terminal region of Aβ has for zinc, the two different domains of ACE may adjust accordingly to accommodate the peptide. The Aβ peptides in all the crystal structures presented only occupy the S1' and S2' subsites and, thus, one is unable to comment on the molecular basis of their interaction with the non-prime subsites of the enzyme.

Within controlled and set conditions this study has established conserved primary intermediate products across four different N-terminal variants of the Aβ(1-42) and multiple forms of ACE. Thus, this has established a basis for molecular understanding of the cleavage of Aβ by ACE, which will be elaborated on in the following chapters.

3 CHAPTER

What residues are responsible for the lack of activity in the C-domain?

3.1 Introduction and Aims

The findings in the previous chapter and in the literature, that the N-domain catalytic site of ACE selectively hydrolyses Aβ peptides, provide a rationale to investigate the basis for this domain-selectivity. With the increase of three-dimensional structures of ACE in complex with domain-specific inhibitors, key active-site residues responsible for domain selectivity have been identified (Corradi *et al*., 2007; Douglas *et al*., 2014; Georgiadis *et al*., 2003; Kröger *et al*., 2009; Natesh *et al*., 2003). Characterising and substituting the unique C-domain active site residues for the corresponding N-domain active site residues may indicate which residues in the C-domain are impeding the hydrolysis of Aβ and facilitating cleavage by the N-domain.

Previous studies performed in our lab as well as by others have taken advantage of the differences in homology between the N- and C-domains to develop better inhibitors of ACE. These differences combined with the multitude of crystal structures, in both bound and unbound states, can pinpoint structurally specific interactions between the enzyme and ligand. The benchmark for N- and C-domain selective inhibitors is set with the two phosphinic peptide analogues RXP407 and RXPA380, respectively. They are currently the most potent C- and N-selective inhibitors; with 3 orders of magnitude more potent inhibition for the C- and N-domains, respectively (Dive *et al*., 1999; Georgiadis *et al*., 2004). These inhibitors are fantastic tools, used to tease out residues within the active sites, which play decisive roles in their substrate specificity.

There are only two residues (Phe391 and Glu403 (tACE numbering)) within the S2 pocket of the C-domain that likely contribute to the selectivity of C-domain inhibitors. These residues have been implicated due to their hydrophobic interactions with the P2 Phe of RXPA380 seen in the co-crystalized structure with the C-domain (Corradi *et al*., 2007; Natesh *et al*., 2003). In contrast, the RXP407 co-crystal structure with the N-domain shows salt-bridge interactions between the S2 Arg381 to the small acidic P2 residue(Anthony *et al*., 2010). In addition, the N-domain contains Tyr369, which is substituted by Phe391 in the C-domain, to which RXPA380's phenyl P2 group may concede to steric hindrance within the N-domain as a result.

Mutagenic studies revealed that the Phe391 residue of the C-domain played a more important role in selectivity than Glu403 (Kröger *et al*., 2009). Furthermore, Phe391 was found to have more of a hydrophobic interaction with the C-selective ketomethylene compounds kAW and kAF, both P2' derivatives of the tripeptide ACE inhibitor keto-ACE (Watermeyer *et al*., 2008). Keto-ACE (Bz-Phe-Gly-Pro), was the first ACE inhibitor to exhibit C-domain selectivity, by 26-34-fold, towards a large array of substrates (Almquist *et al*., 1980; Deddish *et al*., 1998). The C-domain specificity of keto-ACE was further improved via the substitution of the P2' group with larger hydrophobic residues to generate kAF and kAW (Nchinda *et al*., 2006). The derivatives

implicate the C-selectivity of S2-Phe391, S1-Val518 and S2'-Glu376 and Val380 via further hydrophobic interactions (Watermeyer *et al*., 2010).

These hydrophobic interactions are lost in the N-domain where the Phe391 (S2), Val518 (P1), Glu376 (S2') and Val380 (S2') residues are replaced by more polar Tyr369, Thr496, Asp435 and Thr358 residues, respectively (Watermeyer *et al*., 2010).

The C-domain S2' subsite is physically larger than that of the N-domain. This is due to the presence of Ser357 and Thr358 on the border between S1' and S2' sites which occlude the pocket. Furthermore, the N-domain contains the E431 residue which is replaced in the C-domain with a much shorter Asp453 adding to the smaller size of the N-domain S' pockets. Overall, the difference in charge, size and hydrophobicity of this subsite is mainly responsible for the selectivity of the C-domain. This is exemplified in RXPA380 and Lisinopril-Trp where the P2' Trp drives the C-domain selectivity (Georgiadis *et al*., 2004; Corradi *et al*., 2007). Interestingly, further potential substituted residues Thr282, Val379, Glu403, Asp453, and Ser516 did not individually contribute favourably to the binding of these inhibitors.

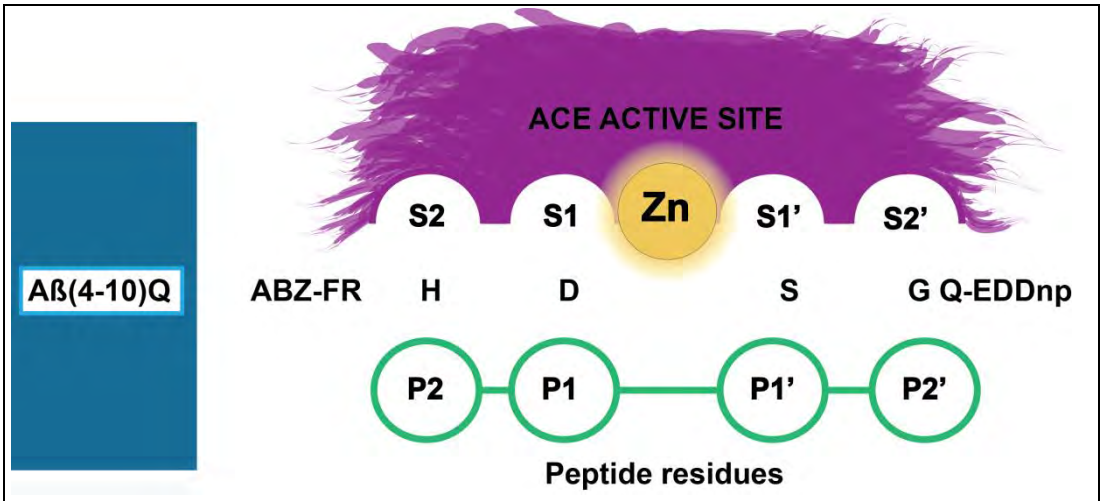

Figure 3.1 **Schechter and Berger representation of subsites and putative binding sites of the Aβ(4-10)Q peptide within the ACE active site**. The active site subsites are indicated by S2, S1 on the N-terminus of the scissile bond and S1' and S2' subsites on the C-terminus. The corresponding peptide residues positions are indicated in green from P2, P1, P1' and P2' accordingly

Determinants of N-domain selectivity, however, also implicate the S2' pocket which contains the largest amount of unique amino acids. The implication is largely based on the results from the removal of the C-terminal amide of RXP407 (P2' position). There is a massive loss in N-selectivity, despite a lack of proximity of RXP407, in the crystal structure to any unique residues in the S2' pocket (Dive *et al*., 1999). Secondly, the residues in the S2 and S1´ subsites are distant from RXP407 in the crystal structure (Anthony *et al*., 2010).

Previous literature reports implicate both the S2 and S2´ subsites in N-selective binding and processing. Based on the site of cleavage of Aβ(2 11), Aβ(4 10), Aβ(4 10)Q and Aβ(4 10)Y (see Chapter 2), the peptides in this study correlate well theoretically to inhibitor studies in that their amino acid properties, in the bound cleavage positions, may determine thier selectivity (Figure 3.1). Thus, screening was performed on a set of S2' pocket mutants. The particular

mutants screened were chosen for their great shift in domain selectivity from C-domain to N-domain (Kröger, 2009; Kröger *et al*., 2009; Watermeyer *et al*., 2008).

Aims and Objectives:

The major aim of this chapter is to identify the determinants for N-domain vs. C-domain selective hydrolysis of Aβ peptides using mutagenesis and a kinetic approach. .

Objectives designed to achieve this aim were:

1) To develop optimum conditions for the kinetic analysis of Aβ(4-10)Q hydrolysis
2) To express and purify wild type and active site substitution mutant ACE constructs.
3) To determine the kinetic constants of the hydrolysis of the Aβ(4-10)Q FRET peptide by the N-domain, C-domain and C-domain active site substitution mutants
4) To investigate the selectivity of, the FRET peptide, Aβ(4-10)Y and the effect of the capping groups on substrate selectivity.

3.2 Methods:

3.2.1 Enzyme constructs

3.2.1.1 **C-domain constructs**

3.2.1.1.1 Wild type C-domain (Cdom)

The wild type tACE construct used is the fully N-glycosylated tACEΔ36NJ mutant. Refer to Chapter 2 section 2.2.1.1.1 for more detail

3.2.1.1.2 C-domain Active Site Substitution Mutants

Here, key active site C-domain residues were converted to their corresponding N-domain counterparts. All substitution mutants were previously generated in our lab (Kröger, 2009). Briefly, a pcDNAtACEΔ36NJ template was used to mutate various residues in the S2' region. This region was sub-cloned from the pcDNA-tACEΔ36NJ construct into the cloning vector pGEM11-Zf(+). This generated a convenient shuttle vector, pGEM-S2', from which subsequent site directed mutagenesis reactions were performed to generate the substitution mutants of interest. Positive clones were identified by restriction endonuclease digestion. These newly mutated fragments were then cloned back into pcDNAtACEΔ36NJ to create V379S, V380T, E378D, D453E, T282S and the VV/ST double mutant (containing both V379S and V380T mutations) (Table 3.1).

Table 3.1 **Summary of the C-domain active site substitution mutants and corresponding N-domain substitution mutants used in this study.**

Pocket	Mutant	Cdom residues mutated to corresponding N-domain residues (sACE C-domain numbering)	N-domain residue
S2'	**E376D**	Glu 376 (952)	Asp 354
	D453E	Asp 453	Glu 431
	T282S	Thr 282 (859)	Ser 260
	V379S	Val 379 (955)	Ser 357
	V380T	Val 380 (956)	Thr 358
	VV/ST	Val 379, Val 380	Ser 357, Thr 358
	TEVD/SDTE	T282, E376, V380, D453	S260, D354, T358, E431
	TEVVD/SDSTE	T282, E376, V379, V380, D453	S260, D354,S357, T358, E431
	S2'F	T282, E376, V379, V380, D453, F391	S260, D354,S357, T358, E431, Y369
		Ndom residues mutated to corresponding C-domain residues	**C-domain residue**
S2'	**Ndom: T358V**	Thr 358	Val 380(956)
	Ndom: S357V	Ser 357	Val 379 (955)

The complete substitution of the C-domain S2' pocket with N-domain residues, was performed in a similar fashion. They were created by sequential mutagenesis of the, already mutated, template pGEMS2' constructs. Three multiple mutants were used in this study namely: TEVD (T282S, E376D, V380T and D453E), TEVVD (containing the V379S mutation in addition to the TEVD substitutions) and S2'F (which contains the F391Y mutation in addition to those in the TEVVD construct). The mutants used in this study were selected because of the large differences displayed in inhibitor binding studies compared to the N-domain (Kröger, 2009).

3.2.1.2 **N-domain constructs**

3.2.1.2.1 Wild type N-domain (Ndom)

A soluble form of the N-domain (Ndom) (see Chapter 2 section 2.2.1.1.2). This construct is essentially the N-domain of human somatic ACE

3.2.1.2.2 N-domain active site substitution mutants

Those C-domain active site mutants that gave the most dramatic change in selectivity towards Aβ were investigated in a reciprocal manner. Here, the N-domain active site residues are converted to their corresponding C-domain residues. The two mutants investigated (S357V and T358V) were created via site directed mutagenesis (by R.G Douglas) of the shuttle vector pBS-D629. Once the mutants were screened and sequence integrity checked, each successfully mutated template was doubly digested with EcoRI and XbaI. Each mutant was then cloned via the same compatible restriction sites into the mammalian expression vector pcDNA3.1(+).

3.2.2 Protein expression and purification

The CHO-K1 mammalian cell line was used as the model system for transfection and expression of all enzymes as described in Chapter 2 section 2.2.2

3.2.3 Mammalian cell expression of ACE enzymes

See Chapter 2 section 2.2.2.1

3.2.4 Isolation of secreted C-domain derivatives of sACE

Purification of soluble constructs via affinity chromatography was performed as described in Chapter 2 section 2.2.2.3. Activity of the purified ACE protein was assayed (See Chapter 2 section 2.2.3.1)and the integrity, size and purity were analysed on a 10% SDS-PAGE (Laemmli, 1970) (Figure 3.3.).

3.2.5 Isolation of secreted N-domain derivatives of sACE

For N-domain constructs, 0.8M NaCl was added to the cell culture medium to increase binding to the column, otherwise all harvested medium was processed and stored as described Chapter 2 section 2.2.2.3

3.2.6 Active site titrations

The kinetic characterization of enzymes requires an accurate quantification of the amount of enzyme present in any reaction. Methods often used to quantify amount of enzyme rely solely on the amount of protein present; whilst this is often useful, this is not an indication of how much active enzyme is actually present. Over time, even in correct storage conditions, degradation and or protein instability can lead to a loss of active enzyme (Knight, 1995). As with most enzyme inhibitors conditions can be manipulated so that the inhibitor appears to be a tight binding inhibitor (Morrison, 1982, 1969). It is best not to assume and rather to use a

well-characterised inhibitor with known K_i's, such as lisinopril to single domain ACE. ACE active site concentrations have successfully been determined by assessment of remaining enzyme activity (Ehlers *et al*., 1991). This remaining activity is determined through analysis of the 1:1 stoichiometric binding of inhibitor to enzyme molecule, across an inhibitor concentration range (Binevski *et al*., 2003; Rice *et al*., 2004; Skirgello *et al*., 2005).

Using a modified ZFHL assay (see section 2.2.3.1), active ACE concentrations were determined according to the above mentioned principle. A serial dilution of the tight binding lisinopril was incubated with an appropriate amount of enzyme (enough to have a fluorescent emmision reading of 200 after 15 minutes at zero inhibitor concentration) in AST-phosphate buffer (100 mM $KHPO_4/KH_2PO_4$ pH 8.3, 300 mM NaCl, 10 µM $ZnSO_4$, 1 mg/ml albumin). This reaction was incubated for 15 minutes in the dark at room temperature. Of each enzyme-inhibitor reaction complex, 20 µl aliquots were plated in triplicate into a 96-well plate. To this substrate (2 mM ZFHL in AST-phosphate buffer) was as added and incubated at 37°C for 15 minutes. The reaction was then stopped with 125 µl of 0.4 N NaOH. The free HL dipeptides were then derivatised and fluorescence read as previously described (see section 2.2.3). The equimolar (S:I) inhibitor concentration required to achieve no enzyme activity (0%) is indicative of the amount of active site present in the final reaction (Figure 3.2). This can then be correlated back to determine the active enzyme concentration in one's stock

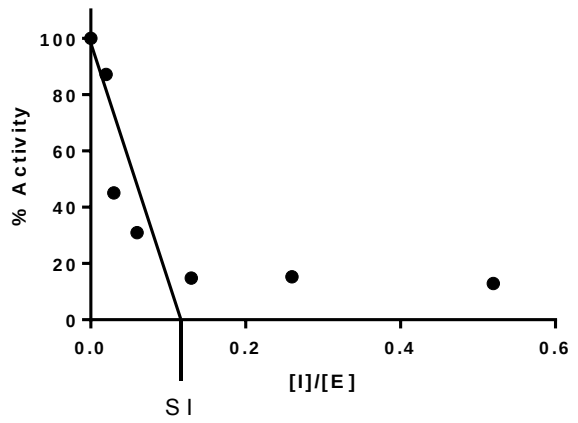

Figure 3.2 **Representative active site titration curve**. Graph of the percentage activity remaining after enzyme-inhibitor incubation against the ratio of lisinopril concentration over Enzyme concentration ([I]/[E]). The equimolar point, SI, is indicated on the x-axis. The initial enzyme concentration is determined from specific activity determinations.

.

3.2.7 Fluorescent resonance-energy transfer (FRET) assay

Fluorescence resonance energy transfer peptide assays make use of intermolecular proximity of two groups; namely an N-terminal, o-aminobenzoic acid (Abz) donor group and a C-terminal, ethylenediamine 2, 4-dinitrophenyl (EDDnp) acceptor group. When the substrate of interest is intact, the two molecules do not emit a signal as the donor (Abz) signal is quenched by the acceptor (EDDnp) group. On proteolytic cleavage, however, the free Abz groups are no longer in close proximity to the quenchers and emit a measurable fluorescence. These assays have been utilized for years as a high-throughput means to quantify enzyme activity, ACE included (Araujo *et al*., 2000, 1999; Dive *et al*., 1999; Wang *et al*., 1993).

3.2.7.1 **Standard Curve**

A simplified molecule of product only, a free donor Abz group coupled to a Gly, Abz-Gly (Bachem Ltd.), was used to quantify the product yielded. A standard curve was set up with Abz-Gly to correlate fluorescence intensity to amount of free donor group. A serial dilution of a 2 µM stock of Abz-Gly was carried out in HEPES buffer (50 mM HEPES (pH 7.5), 100 mM NaCl, 10 µM ZnSO4, 10 µM ZnCl), to a final concentration range of 0-600 pmols. Aliquots of 300 µl volumes of this range were pipetted, in triplicate, into a 96-well plate. The fluorescence intensities were then determined using excitation and emission wavelengths at 320 nm and 420 nm respectively in a Cary Eclipse spectrofluorimeter (Varian Inc.). A linear regression analysis was performed on the subsequent fluorescent output and a standard curve generated (v 4.01, GraphPad Prism4®) (Figure 7.1).

3.2.7.2 **The inner filter effect and the Correction Curve**

The principle of the FRET peptide assay is based on the proximity of the donor group (in this study Abz) to the acceptor (EDDnp and 3-nitrotyrosine [(Y)3NO_2]) used in this study). In a confined volume, however, the increasing concentrations of substrate (necessary for a kinetic curve) proceed to quench any signal generated by means of acceptor group substrate inhibition. Simply put, there is no space between the uncleaved substrate and Abz-product molecules, resulting in fluorescent quenching and an overall decrease in the signal at higher concentrations. This effect is known as the inner filter effect (IFE) (Liu *et al*., 1999). This effect is problematic in the accurate characterization and determination of enzyme kinetic parameters. IFE can be overcome by means of correction through empirical method.

Liu *et al*. 1999, developed a simple 96-well plate assay to empirically correct for IFE. Briefly, a baseline of fluorescence of a concentration range of 0-45 µM of Abz-FRKG-E(DDnp) at a volume of 296 µl in HEPES assay buffer was measured as above mentioned (Section 3.2.7.1). To this, 4 µl of 38 µM Abz-Gly was added (final concentration of 0.5 µM), mixed thoroughly and reread as above. The change in fluorescence with increasing substrate concentration was compared to zero substrate concentration to determine a ratio. This generated a non-linear equation, fit to the substrate concentration range known as a correction curve (Figure 3.4). The values of each substrate concentration were then used to correct all further kinetic experiments. As all donor groups in this study were Abz, and both acceptor groups have similar mechanism and structure this correction is applicable to all.

3.2.8 Kinetic analysis of amyloid FRET peptides

3.2.8.1 **Aβ(4-10)Q**

Hydrolysis of the fluorogenic peptide Abz FRHDSG(Q)-EDDnp (Aβ(410)Q), a kind gift from A. Carmona, Universidade Federal de São Paulo) by ACE was performed in HEPES buffer (50 mM HEPES (pH 7.5), 100 mM NaCl, 10 µM ZnSO4 buffer) with 150 µl enzyme (at a concentration within 10% hydrolysis) and equal volume of substrate ranging from 0 to 35 µM. The assay is a modified form of the continuous assay (Araujo *et al*., 2000) where the assay is set up, on ice, in triplicate in a 96 well plate. The baseline fluorescence was taken at time zero and then incubated at 37ºC and fluorescence read at a 45 min time point on a Cary Eclipse spectrofluorimeter (Varian Inc.) at λex= 320 nm and λem= 420 nm. Again, kinetic constants were calculated using the Michaelis-Menten method with GraphPad Prism software (v 4.01, GraphPad Prism®). The detected fluorescence was converted to pmol product formed through the slope of a calibration curve of Abz-Gly. A correction curve was also applied to correct the data for the inner filter effect (Liu *et al*., 1999)

3.2.8.2 **Aβ(4-10)Y**

An alternate fluorogenic peptide, Abz-FRHDSG-(Y)3NO_2 (BIOPEP ™South Africa) (Aβ(4-10)Y) was assayed as above in 96 well plates. The only exception being that the samples were read at a 5 min time point on a Cary Eclipse spectrofluorimeter (Varian Inc.) with λ_{ex}= 320 nm and λ_{em}= 420 nm. Kinetic constants, inner filter effect and standard curves were calculated as above.

3.2.9 Peptide integrity and cleavage site analysis

3.2.9.1 **Mass spectrometry**

The Mass spectrometry was analysed at the Centre for Proteomic and Genomic Research (CPGR, Cape Town, South Africa). As further elaborated in Chapter 2 section 2.2.5

3.3 Results:

3.3.1 Protein expression and Purification:

The constructs of human recombinant Ndom, Cdom and active site mutants (Table 3.1) were expressed in mammalian cells and then purified. All constructs are soluble and secreted into the cell medium. The constructs were purified from conditioned medium by affinity chromatography on a lisinopril-sepharose affinity resin as previously described in (Ehlers *et al*. 1996). All preparations were purified to apparent homogeneity as assessed by SDS-PAGE (Figure 3.3). Recombinant Ndom and N-domain mutants T358V and S357V migrated as a single band with an apparent molecular mass of 90 kDa. The Cdom and single and multiple S2' mutants (T282S, E376D V380T, V379S, D453E, VV/ST, TEVD, TEVVD and S2'F) migrated with an apparent molecular mass of 80 kDa (Figure 3.3).

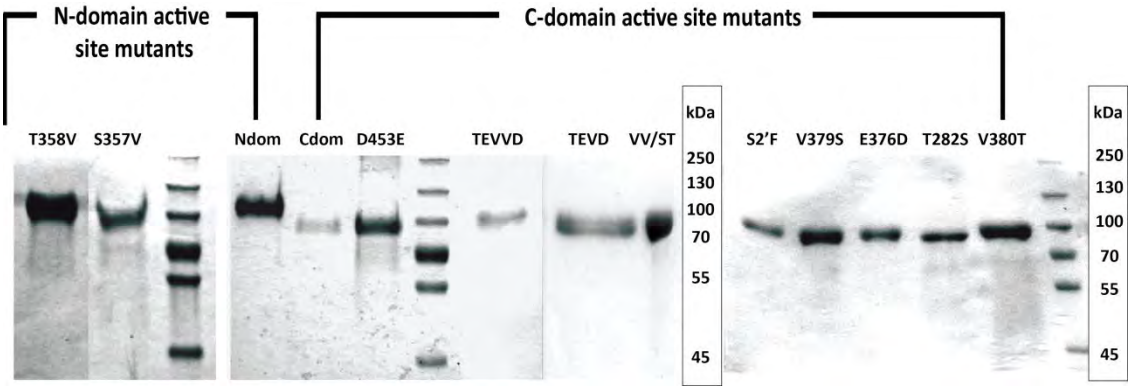

Figure 3.3 **Representative SDS-PAGE gels of approximately 10 µg of all the constructs used.** From left to right: Indicated are the N-domain active site residues converted to their corresponding C-domain residues next to the N-domain or D629 construct. Followed by the C-domain and the indicated active site substitution mutations. The mass ladders are as indicated on the far right and in the centre of the gels.

3.3.2 Correction Curve for the Inner Filter Effect

The incubation of increasing concentrations of substrate with a fixed concentration of the free donor results in a non-linear decrease in fluorescence intensity. This result is in congruence with the theory of the inner filter effect. The correction values were determined as described (in section 3.2.7.2). From these values a polynomial trend line can be derived which allows for the correction of substrate quenching from concentrations ranging from 0 to 50 μM (Figure 3.4).

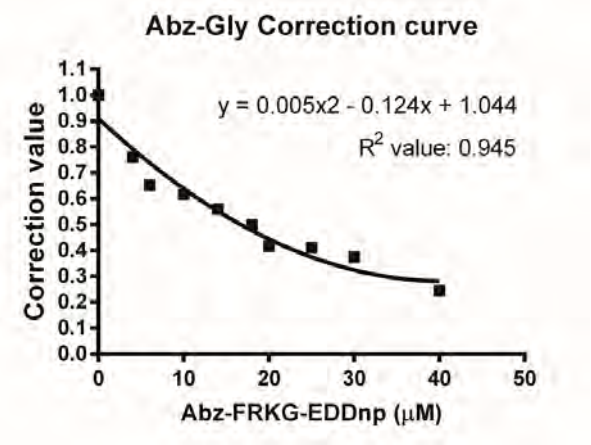

Figure 3.4 **Correction curve and derived polynomial equation, used to determine the necessary adjustments for the correction of the inner filter effect.**

3.3.3 Kinetics of the hydrolysis of the fluorogenic Aβ(4-10)Q peptide.

In order to assess the N-domain selectivity towards Aβ cleavage, the contribution of unique residues in the C- and N-domain active sites were interrogated. Specifically a panel of C-domain S2' substitution mutants were characterised using the FRET peptide Aβ(4-10)Q .

The Aβ(4-10)Q peptide was hydrolysed very slowly (k_{cat} 0.220 ± 0.020 s^{-1}) yet selectively by the Ndom, as the Cdom did not produce measurable levels of activity, even after prolonged incubation times (Table 3.2). Mutation of the C-domain's S2' pocket residues E376D, D453E, T282S did little to improve the catalysis or affinity (Table 3.2 and Figure 3.5 A). However, the conversion of the C-domain V379 to the N-domain Ser residue induced a 7-fold increase in catalytic efficiency (k_{cat}/K_m 1.580 ± 0.01 x 10^5 $M^{-1}.s^{-1}$) compared to that of the Ndom and was the most efficient construct screened. The substitution of the adjacent Val380 for a Thr residue led to an increase in Aβ(4-10)Q hydrolysis, but the catalytic efficiency (k_{cat}/K_m 0.065 ± 0.04 x 10^5 $M^{-1}.s^{-1}$) was still 3-fold less than the Ndom. Surprisingly, for the double valine mutant the overall efficiency (k_{cat}/K_m 0.007 ± 0.001 x 10^5 $M^{-1}.s^{-1}$) dropped 9-fold below that of the individual V380T mutant.

Subsequent sequential conversion of more C-domain to N-domain residues in the S2' active site did little to improve the efficiency of the Cdom (Figure 3.5 A). This is evident since the TEVD mutant, which contains all but the V379S mutation, only has a catalytic efficiency of 0.003 ± 0.0002x 10^5 $M^{-1}.s^{-1}$, while TEVVD containing both valine substitutions has a k_{cat}/K_m of 0.009 ± 0.001 x 10^5 $M^{-1}.s^{-1}$. These are 80 and 26-fold lower than that of the Ndom, respectively. The complete S2' C-domain substitution (TEVVD) and the S2 F391Y mutation (S2'F) had an efficiency equal to the Ndom. However, the turnover rate was 3-fold lower than the Ndom (k_{cat} 0.163 ± 0.008 s^{-1} and k_{cat} 0.220 ± 0.020 s^{-1}, respectively), their efficiencies are only equal as the K_m of the S2'F mutant also increased 3-fold (7.62 ± 1.07 μM) (Figure 3.5 B). The affinity of the other multiple mutants are all similar (TEVVD K_m 24.22 ± 4.15 μM; TEVD K_m 17.54 ± 4.18 μM) to the Ndom; yet their turnover rates are abysmal (Figure 3.5 B and C). The same holds for the two Val residues whose increase in efficiency is largely related to the increase in catalytic rate and not a change in affinity towards Aβ(4-10)Q. Most notable, is the dramatic increase in the k_{cat} of V379S (1.462 ± 0.084 s^{-1}), being 3-fold higher than the Ndom, yet its K_m is only half the Ndom's.

Table 3.2 **Aβ(4-10)Q (Abz-FRHDSG(Q)-EDDnp) kinetic parameters. Determined by the hydrolysis of different active site substitution mutations of the N and C-domain of ACE.**

Enzyme	k_{cat}/K_M ($M^{-1}.s^{-1}$)(x10^5)	k_{cat} (s^{-1})	K_M (μM)
Ndom: T358V	0.240 ± 0.003	0.528 ± 0.061	22.06 ± 2.86
Ndom: S357V	0.138 ± 0.007	0.485 ± 0.015	35.14 ± 2.19
Ndom	0.220 ± 0.020	0.480 ± 0.039	22.24 ± 3.23
S2'F	0.223 ± 0.024	0.163 ± 0.008	7.62 ± 1.07
TEVVD/SDSTE	0.009 ± 0.001	0.020 ± 0.002	24.22 ± 4.15
TEVD/SDTE	0.003 ± 0.000	0.005 ± 0.001	17.54 ± 4.18
VV/ST	0.007 ± 0.001	0.007 ± 0.002	10.44 ± 6.06
V380T	0.065 ± 0.040	0.080 ± 0.007	12.32 ± 0.88
V379S	1.580 ± 0.010	1.462 ± 0.084	9.25 ± 0.49
T282S	nd	nd	nd
D453E	nd	nd	nd
E376D	nd	nd	nd
Cdom	nd	nd	nd

In order to ascertain whether the two valine residues could cause a reciprocal decrease in the activity of the N-domain towards Aβ(4-10)Q, we characterised the N-domain mutants S357V and T358V (N-domain numbering). Overall, there was no drastic change in the mutants' catalytic rates compared to wild type Ndom. The affinity for S357V is just less than 2-fold higher (K_m 35.14 ± 2.19 μM) and its turnover rate (k_{cat} 0.485 ± 0.015 s^{-1}) is equal to the Ndom, which in effect brings down the efficiency making it equal to the Ndom (Figure 3.5). Surprisingly, the T358V mutant was equivalent to the Ndom across all constants k_{cat} (0.528 ± 0.061 s^{-1}) K_m (22.06 ± 2.86 μM).

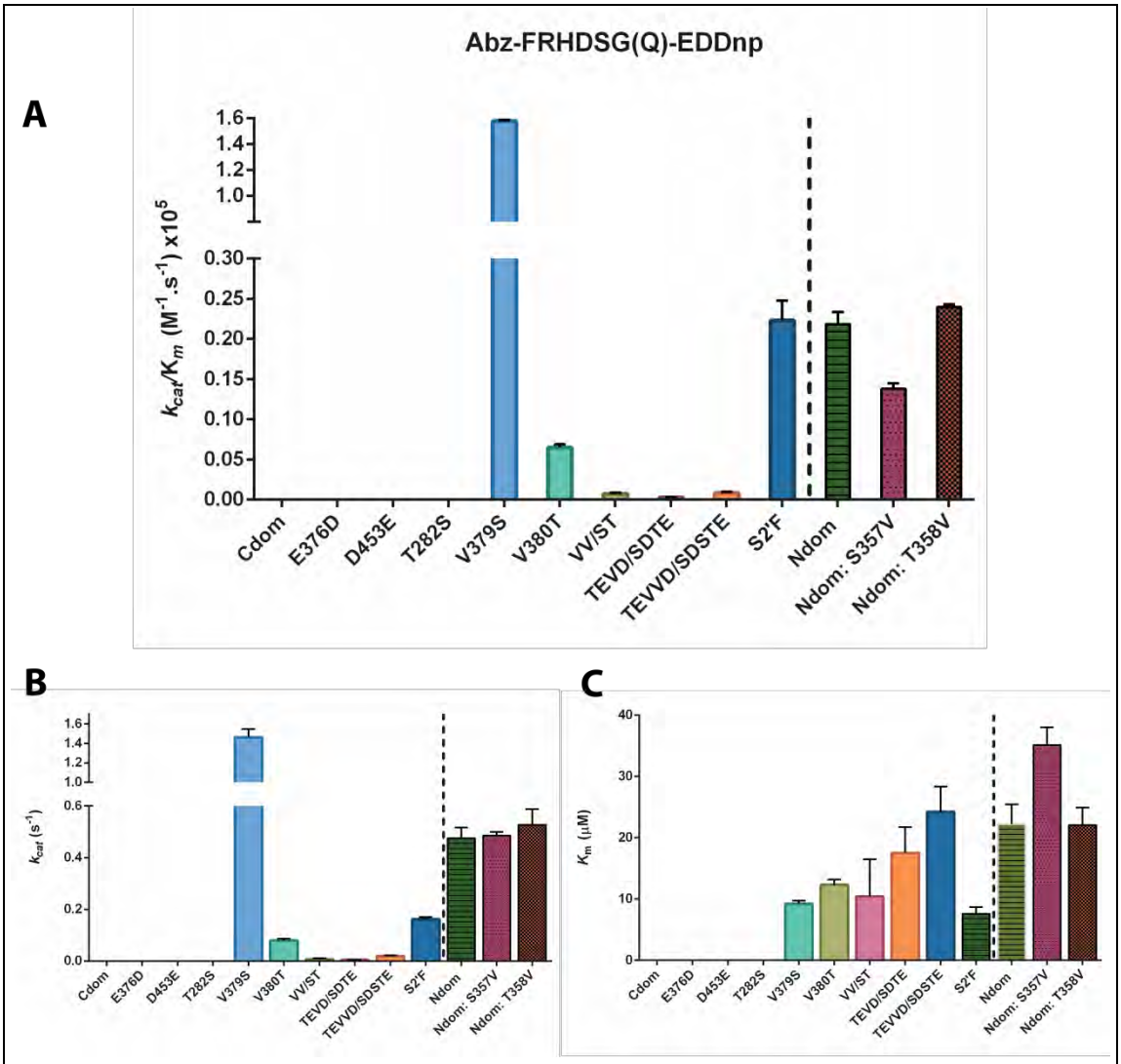

Figure 3.5 **Graphic representation of the kinetic parameters determined for the hydrolysis of the FRET Aβ(4-10)Q (Abz-FRHDSG(Q)-EDDnp). A)** The overall catalytic efficiency ratio of all the mutants screened: k_{cat}/K_M (s^{-1}. M^{-1})(x10^5). **B)** Turnover rate for all the mutants screened represented as k_{cat} (s^{-1}). **C)** The binding affinity of Aβ(410)Q towards each enzyme determined as K_m (μM).

3.3.4 Confirmation of V397S trend and N-domain selectivity of ACE with the use of an alternate FRET peptide Aβ(4-10)Y.

To investigate the role that the large end group EDDnp and the attached Gln, might have on the selectivity of the FRET peptide, we used an alternate FRET peptide Aβ(4-10)Y in the kinetic analysis of Ndom, Cdom and V397S.

This peptide contains the wild type sequence FRHDSGY of the Aβ(4-10). The Tyr residue forms part of the acceptor group, however, the donor remains the same: Abz-FRHDSG-(Y)3NO_2. There is increased catalytic efficiency of Cdom Aβ(4-10)Y compared to Aβ(4-10)Q; however, Aβ(4-10)Y is still N-domain selective. The increased activity of the C-domain is further elaborated on in the following chapter (Chapter 4). Overall Aβ(4-10)Y is a much better substrate than Aβ(4-10)Q (Figure 3.6 A and B) (Table 3.3). This is evident from the k_{cat} values of the Ndom constructs, where the turnover rate of Aβ(4-10)Y substrate was two orders of magnitude faster than that of Aβ(4-10)Q.

It is also quite clear from the turnover rates of V397S that Aβ(4-10)Y is a better substrate as the Aβ(4-10)Y k_{cat} for V397S was 24-fold greater than the Aβ(4-10)Q peptide (Table 3.3). In terms of catalytic efficiency, the V397S mutant still hydrolyses the Aβ(4-10)Y 2-fold better than the Ndom. This increase in efficiency is due to V397S's increased catalytic ability (k_{cat} 36.26 ± 2.75 s^{-1}), the affinity being equivalent to the Ndom and similar to that of Aβ(4-10)Q (Figure 3.6 C). The Cdom gained activity (k_{cat} 6.26 ± 2.75 s^{-1}) with the Aβ(4-10)Y peptide and its efficiency was approximately 6-fold lower than that of the Ndom. Thus, this substrate is still N-domain selective. The general trend of the results remains the same (Figure 3.6).

Table 3.3 **The comparative kinetic parameters of the N-domain, C-domain and V379S mutant to Aβ(4-10)Y.** The Aβ(4-10)Y (Abz-FRHDSG-(Y)3NO_2) substrate is highlighted in green and Aβ(4-10)Q (Abz-FRHDSG(Q)-EDDnp) in yellow.

Substrate	Enzyme	k_{cat}/K_M ($M^{-1}.s^{-1}$)(x10^5)	k_{cat} (s^{-1})	K_M (μM)
Aβ(4-10)Y	**Ndom**	9.22 ± 0.41	21.72 ± 1.19	23.56 ± 0.24
	Cdom	1.67 ± 0.10	6.39 ± 0.71	38.08 ± 3.45
	V379S	16.83 ± 2.08	36.26 ± 2.75	22.72 ± 3.87
Aβ(4-10)Q	**Ndom**	0.220 ± 0.020	0.480 ± 0.039	22.24 ± 3.23
	Cdom	nd	nd	nd
	V379S	1.58 ± 0.01	1.46 ± 0.08	9.25 ± 0.49

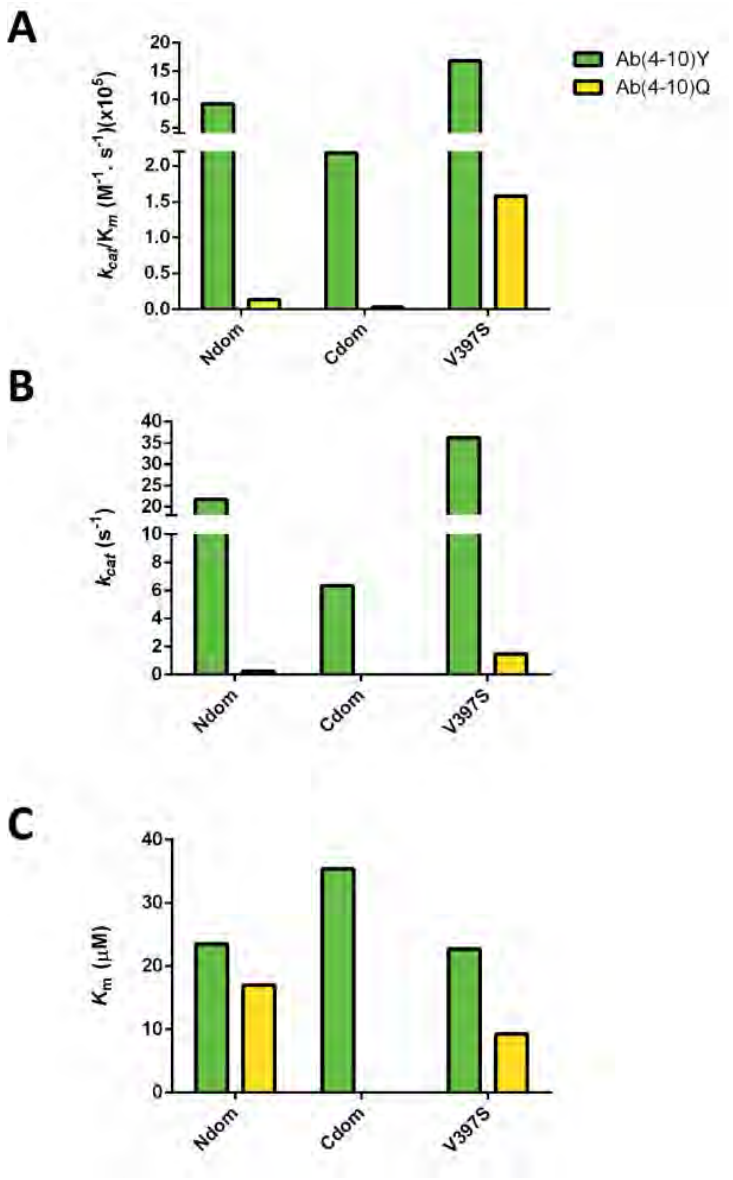

Figure 3.6 **A graphic illustration of the mean kinetic parameters determined for the N-domain, C-domain and V397S C-domain active site mutant on two FRET substrates with different acceptor groups.** Aβ(4-10)Y (Abz-FRHDSG-(Y)3NO_2) kinetic parameters are represented in green and Aβ(4-10)Q (Abz-FRHDSG(Q)-EDDnp) are represented in yellow. A) The mean comparison of the enzymes hydrolytic efficiency represented by: k_{cat}/K_M ($s^{-1}.M^{-1}$)(x10^5). B) The mean turnover rate represented as k_{cat} (s^{-1}). C) The binding affinity of the substrates towards each enzyme, determined by K_m (μM).

3.4 Discussion:

The two domains of ACE are responsible for the enzyme's diverse functions. The substrates of ACE and the resulting products are key to many physiological mechanisms besides blood pressure regulation including haematopoiesis, reproduction, immune response and of course neurological behaviour (Acharya *et al*., 2003; Ferrington *et al*., 2012; Gräff *et al*., 2012; Riordan, 2003). These physiological functions emphasise the importance of determining the exact requirements for domain selectivity and functionality, in order to develop better treatment for complex disease states like AD.

The use of spectrophotometric tools to interrogate ligand–protein interactions is pivotal to many fields of study, structural biology, biotechnology, and drug discovery being but a few examples (Hovius *et al*., 2000). Advances in peptide synthetic chemistry has made the incorporation of non-coded amino acids into polypeptide chains possible (Nilsson *et al*., 2005). FRET peptides are an example of modern spectrophotometric tools for protein analysis, which are useful in that they have high assay sensitivity and allow continual reaction monitoring. This is key in the determination of enzyme kinetics and subsequent mechanistic characterization. This study emphasises, and reiterates the truncated N-domain selectivity of Aβ found in Chapter 2 and the literature using the FRET peptides Aβ(4-10)Q and Aβ(4-10)Y.

The S2' pocket active site mutants were screened to identify which residues were determinants of Aβ selectivity, inducing a switch from the C-domain to N-domain-like activity towards Aβ(4-10)Q. This substrate has an Abz fluorescent group and EDDnp quencher group (attached via the substitution of Tyr10 for Gln10). The donor-acceptor pair have an excellent energy overlap, and a fluorescence quenching which is not affected by pH (De Souza *et al*., 2000). As previously, mentioned (Chapter 2) the large C-terminal EDDnp group usually occupies the S2' pocket, thus cleavage ensues one residue away (Araujo *et al*., 2000). However, under the assays conditions in this study, both fluorogenic peptides were cleaved at Asp7-Ser8 as previously described for the non-FRET Aβ peptides. With regards to the substrate, this cleavage site shifts the large EDDnp group into the P3' position. The greater the hydrophobicity of the P1' residues of a substrate, the less domain-selective it is and the better it is cleaved by both domains (Araujo *et al*., 2000). It is conceivable that the two smaller Ser8 and Gly9 residues occupy the S1' pocket and, as they are rather neutral and hydrophobic, respectively, this would facilitate binding to both N-and C-domain (Figure 3.7). However, the substituted Gln10 residue would then occupy the S2' pocket generating N-selectivity, as interactions with similar large charged residues have previously been shown to drive selectivity (Douglas *et al*., 2014). Electrostatic and chloride mediated interactions with the unique charged residues could then shift the acceptor groups into S3' pocket (Yates *et al*., 2014).

Substitution of Val379 and Val380 with the N-domain Thr and Ser, respectively, induced the most significant gain in activity. This suggests that the two valines in the S2' pocket of the C-domain are largely responsible its lack of enzyme activity on Aβ(4-10)Q. All other unique individual mutations failed to generate N-domain activity towards Aβ(4-10)Q in the C-domain. Of the two mutations, the V380T indicated only a moderate increase in overall catalytic efficiency compared to the Ndom. This moderate effect has been seen before on this mutant with the C-selective Abz-LFK(Dnp)-OH FRET substrate (Kröger, 2009). However, in terms of C-

selective binding to inhibitors such as RXPA380, kAW and kAF, this single residue mutation caused the greatest decrease in affinity. This residue is found on the border of the S2' and S1' pockets in the C-domain and it is unlikely that the slight change in hydrophobicity of this large S1' pocket would affect the affinity towards the P1' Ser8 and Gly9 residues. However, the C-selective inhibitors' P1' residues were much bulkier and the effect of this mutation is thus understandable in their case (see review Acharya *et al*., 2003).

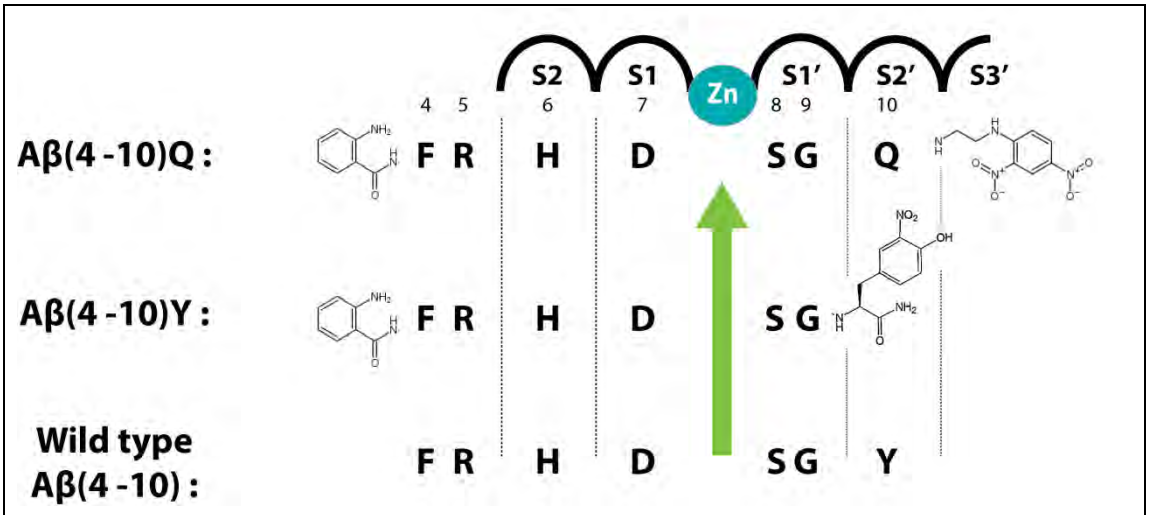

Figure 3.7 **Schechter and Berger representation of subsites and comparison of putative binding sites of the Aβ(4-10)Q, Aβ(4-10)Y and the wild type Aβ(4-10) sequence.** The ACE active site subsites are indicated by S2, S1 on the N-terminus of the scissile bond and S1' and S2' subsites on the C-terminus.

Replacement of Val379 with a serine results in a C-domain gain in affinity and improved catalysis compared to the other S2' substitutions. The presence of the Ser residue in the S2' pocket induces a 3-fold increase in catalytic activity over the Ndom, along with a large 7-fold enhancement in efficiency. The decrease in hydrophobicity of the Cdom S2' pocket induced more favourable interactions towards the large, charged, Gln10 residue of Aβ(4-10)Q. A similar effect was found on this mutant towards N-selective inhibitor RXP407's affinity (Kröger *et al*., 2009). Stabilisation of the S2' interactions overcame any lack of interaction in the other pockets towards Aβ(4-10)Q. However, the presence of the Ser in V379S, is only beneficial if all the residues within the C-domain S2' pocket remain, otherwise possible inhibitory associations and conformations could occur between the residues in S1' and S2' pocket (Watermeyer *et al*., 2008). It is likely that without ligand-mediated stabilising interactions within the S1 and S2 pockets, the presence of more charged residues within the C-domain's S2' pocket disrupt it fundamentally, tipping the balanced charge state as it also contains other conserved hydrophobic residues . Hence introducing more N-domain residues together into the C-domain does not produce an overall enhancement of substrate hydrolysis.

This gain of Aβ(4-10)Q hydrolysing ability by the V379S mutant was substantiated through the hydrolysis of the Aβ(4-10)Y FRET substrate with a wild type P2' nitrotyrosine (assuming the S1' occupancy of Ser8 and Gly9). This peptide was a far better substrate for both domains of ACE and reflected the same trend in selectivity and activation of the C-domain in the V379S mutant. Tyrosine is a mildly hydrophilic residue due to the presence of the hydroxyl group on its hydrophobic aromatic ring. Thus, it would most likely be a non-selective P2' residue as it is

neither, large and hydrophobic, nor highly charged, placing greater emphasis on the substrate interactions with pockets other than the S2'. That said, the addition of the 3-NO_2 group to the benzene ring of Tyr, makes the Y3NO_2 group 10 000-fold more acidic (De Filippis *et al*., 2006). The only possible caveat with this quencher group is that its absorption properties are strongly pH-dependent, unlike the EDDnp group. The Y3NO_2 side chain length, being 30 Å larger than the natural Tyr, and its electron-withdrawing NO_2 group make the hydroxyl group more acidic with a pKa of 6.8 (Sokolovsky *et al*., 1966). Thus, at lower pH the molecule becomes more hydrophobic, and possibly more C-selective, and at neutral to higher pH's more acidic. Our assays were performed at physiological pH and thus this group remains acidic. However, this acidity did not affect Cdom hydrolysis of the Aβ(4-10)Y substrate and, most notably, improved the interaction with the mutant Ser residue. This is possibly due to the electron sharing of the hydroxyl group with the NO_2 group, as they approach the S2' pocket entrance. Interactions with the N-domain would most likely occur between the Ser357 or Thr358 and Glu431 through hydrogen bonding to either hydroxyl or NO_2 group of the molecule. In the C-domain this opening is gated via the two Val379 and Val380 residues and the Glu431 is replaced by Asp453 (Figure 3.8). Thus, the NO_2 or the hydroxyl group could still make hydrogen bonding to the Asp453 residue inducing a gain in C-domain hydrolysis. This interaction would not be possible with the Aβ(4-10)Q as the hydrophobicity of the two valines would repel the large polar Gln10 as well as its bulky charged EDDnp group.

Given that V379S was the only single mutation to induce N-domain-like binding, with better catalysis of Aβ(4-10)Q, and that this was reproducible with another FRET substrate, and one may speculate that this residue is very important for N-domain selectivity towards Aβ. With this in mind, the converse mutation of the N-domain's Ser357 to the corresponding C-domain valine (S357V) reduced the catalytic efficiency of the N-domain 2-fold. Mutation of N-domain's Thr358 to Val380 (T358V) had no effect. Notably, S357V catalysis was comparable to the N-domain but substrate affinity was weakened. The S357V loss of efficiency may be attributed to disruption of the backbone hydrogen bonding at the opening of the S2' pocket caused by the inclusion of a valine residue at this position. Hydrogen bonding occurs via Ser357 to Glu431, its disruption allows the helix 17 of the N-domain, on which the Glu431 residue and other S2' pocket residues exist, to drop and open (Figure 3.8 and Figure 3.9). This could allow for easier access of the Gln10-EDDnp groups, as is seen by the higher K_M and thus weaker affinity. Movement of this helix is thought to occur based on comparison of the similar N-domain bound crystal structure to that of the open ACE2 structure (ACE2 is structurally very similar to the N-domain with 40% homology) (Guy *et al*., 2003; Towler *et al*., 2004).

The more N domain-like the C-domain S2' pocket became the less benefit was conferred from the individual V379S and V380T changes. This is evident from the double VV/ST mutant, for which an additive beneficial effect was expected via the overall reduction of hydrophobicity at the S2' pocket opening. On the contrary, the double mutant had very poor catalytic activity, despite very similar binding to V379S. Similarly, with the TEVD mutant, the binding reverted to N-domain-like affinity, yet the catalysis remained dismal. With the added mutation of V379S, to complete the conversion of the C-domain S2' pocket to that of the N-domain, the K_M surpassed that of the N-domain, reducing the affinity of the interaction but did little to restore enzyme activity.

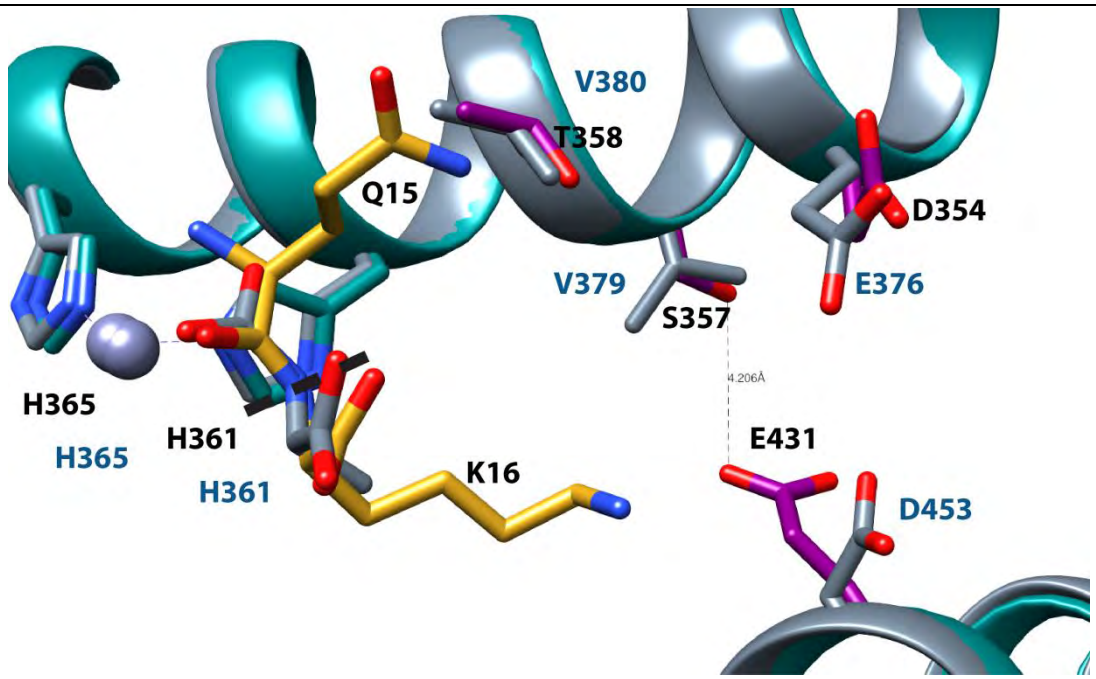

Figure 3.8 **Structural overlay of the Cdom (grey) open structure, with that of the Ndom (cyan) bound to the dipeptide Aβ(10-16) cleavage product.** Indicated is the 4.206 Å bond between the Ndom Ser357 and Glu431 residues creating the S2' gate. The Ndom S2' residues are indicated in purple and the $Zn^{2=}$ coordinating His residues in cyan. All Cdom residues are in grey.

The inhibitor studies and crystal structures (Acharya *et al*., 2003; Anthony *et al*., 2012; Corradi *et al*., 2007, 2006; Kröger *et al*., 2009; Watermeyer *et al*., 2009, 2008) indicate that there should have been an additive effect of these multiple mutants towards a switch in selectivity. It is likely that additional intermolecular electrostatic interactions occurred between the newly introduced amino acid residues within the more rigid C-domain prime pockets, changing the overall conformation of the molecule (Kröger *et al*., 2009).

It is also likely that the affinity of Aβ towards these mutants was stronger on the prime side of the molecule. It is possible that there were little or no interactions in the C-domain non-prime end to the peptide. Thus, it simply does not bind to the non-prime side and positioning for catalysis to occur is weak. This is supported in the complete S2' mutant combined with the S2 pocket F391Y mutation (S2'F). With the S2'F enzyme the affinity of Aβ(4-10)Q improved 3-fold towards this mutant, catalysis was restored and the efficiency equalled the Ndom. The single Phe391 residue appeared essential for the C-selectivity of RXPA380 (Kröger *et al*., 2009) for, once mutated to the Tyr, a 36-fold decrease in K_i resulted. The increased K_M towards Aβ(4-10)Q in the combination mutations (TEVD and TEVVD) could be a reflection of the lack of any S2 interactions and strong S2' affinities, which together produce rather average affinity and a decreased catalytic rate compared to the individual valine mutants.

The His6 residue, of both FRET peptides, in the P2 position forms part of the Aβ peptide's natural Zn^{2+}chelating region (which includes Glu11, His13 and His14) (Zirah *et al*., 2006). The available crystal structures combined with the kinetics determined in this study compared to N-domain inhibitors, allow for speculation as to the interactions driving selectivity from the non-prime side. It is quite possible that the His6 residue interacts with the H388 conserved residue in the S2 pocket as well as with the two Zn^{2+}-coordinating H361 and H365 residues via

stacked π-bonds. An example of such an interaction can be found in the binding mode of the tetrazole residue of the RXP407-based inhibitor 33RE (Douglas *et al*., 2014). These π-stacking interactions could shift the peptide further along into the S' subsites and the cleavage site towards the non-prime side (as found in the kinetic studies), thus placing more emphasis on the S2' pocket's water mediated-hydrogen bonding network and the charged residues, all of which would interact with the charged Gln10 and $Y3NO_2$ groups. When the S2 Phe391 of the C-domain is converted to the N-domain Tyr369, hydrogen bonding could occur to the π-bonded Aβ His6 residue strengthening the affinity. One further observation from the Aβ(1-16) crystal structure with its Gln15 and Lys16 dipeptide is that R381 is outwards facing (Figure 3.9).The R381 residue on the S2 pocket may well swing round, as it does with RXP407 where it forms a salt bridge to the P2 acetylated aspartate residue (Kröger *et al*., 2009). This interaction is lost in the 33RE N-domain crystal structure (Douglas *et al*., 2014) and from the current crystal structures of Aβ fragments this R381 also faces away as in 33RE (PDB number 4BXK) (Figure 3.9).

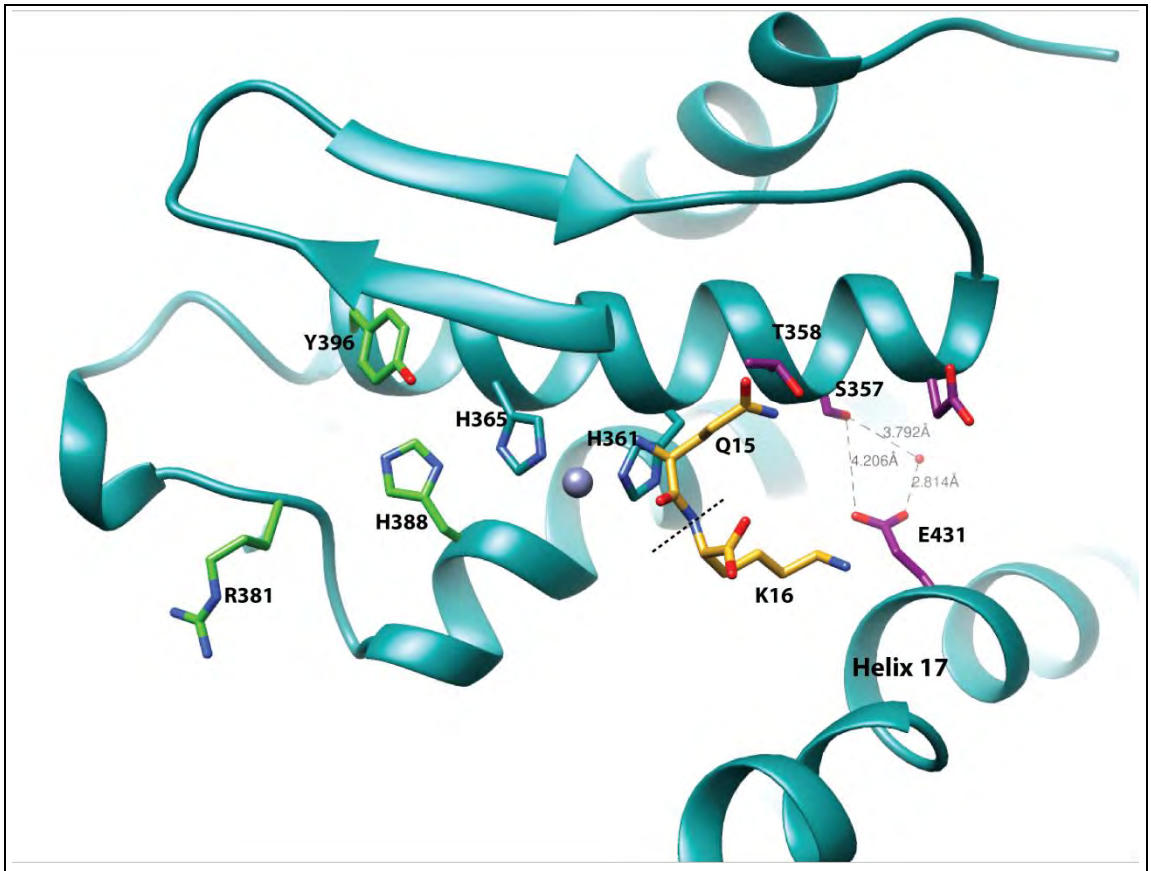

Figure 3.9 **The crystal structure of the Ndom active site (cyan ribbons) with the Aβ Gln15 and Lys16 (gold sticks) dipeptide product bound to the S2' pocket.** The S2' pocket residues are in purple with the Ser357,Glu431 and water mediated gate interactions indicated. Helix 17 is closed as a result. The $Zn^{2+}$is indicated in grey, coordinated to the two cyan H365 and H361. The S2 pocket residues of interest are indicated in green, with the Arg381 turned away from the active site.

This balance of enzyme-inhibitor interactions in the different active site binding pockets is currently being investigated in our lab on the N-selective inhibitor 33RE (Douglas *et al*., 2014) using molecular dynamics. The S2' interactions are identical in both 33RE and RXP407, with the unique N-domain S2' residues quite distant from the inhibitors, indicating direct interactions to conserved residues only, like many of the Aβ-crystals indicated. Mutation of these unique residues did little to reduce RXP407 affinity towards the N-domain (Kröger *et al*., 2009), yet removal of the P2' amide of RXP407 abolished selectivity (Dive *et al*., 1999). Similarly, we did not see a gain in activity towards Aβ(4-10)Q with the complete conversion of unique C-domain S2' residues to their N-domain counterparts. It appears that N-selective substrates require interations to occur through N-domain specific residues and indirectly through a water network. This suggests that the P2 (small acidic reisdues) and P2' (larger charged residues) groups of the substrate synergistically govern N-selectivity, in a similar fashion to that of N-selective inhibitors, like RXP407, where selectivity is driven by less obvious interactions. Also, the amyloid substrates used all appear to have the requirements of an N-domain selective substrate, namely a small acidic P2 residue (His6) and charged P2' group (Douglas *et al*., 2014; Kröger *et al*., 2009; Vazeux *et al*., 2001) like Gln10 and $Y3NO_2$ in the case of Aβ(4-10)Q and Aβ(4-10)Y, respectively.

The lack of C-selectivity towards Aβ is likely dependent on what fragment of the full-length sequence the active site is exposed to at a time. The identification of various Aβ cleavage sites in this study strongly suggests that ACE does not have a preference for specific residues in the P1 and P1' position with regard to Aβ, being targeted to conserved residues only. However, within the N-terminal region of Aβ its large charged groups in the P2' or P3' position combined with acidic P2 groups make it a preference of the N-domain active site. These ligand characteristics, be they substrates or inhibitors, form part of the molecular basis for N-domain specificity. As Aβ appears to fit these requirements, the results in these studies have implications towards the development of domain selective ACEi for the treatment of hypertension and or AD. Specifically these results are in support of the development of C-selective inhibitors that may provide both cognitive and anti-hypertensive beneficial effects.

4 CHAPTER

Kinetic characterisation of the interactions between the two domains of sACE on the hydrolysis of N-terminal Aβ peptides

4.1 Introduction and aims

The most well-known toxic form of the Aβ is 42 residues long, although Aβ also occurs in many truncated variants and in more soluble forms (Kummer and Heneka, 2014) (see Chapter 1 section 1.2.1). These more soluble oligomers and protofibrils are strongly correlated with increased toxicity compared to the more structured fibrils (Mc Donald *et al*., 2010; McLean *et al*., 1999; Tomic *et al*., 2009; Woltjer *et al*., 2009). The Aβ(1-16) amyloid variant is formed via both amyloidogenic and non-amyloidogenic secretion pathways, however it has a controversial role in AD and its toxicity is unclear (see Chapter 1 section 1.2.1.2).

The level of ACE's substrate promiscuity has a lot to do with its physiological two-domain sACE form. There is conflicting evidence regarding N- and C-domain-selectivity of Aβ cleavage by ACE and the enzyme's P1 and P1' preference (see Chapter 2). The general trend of results indicates that the N-domain alone is more effective at Aβ cleavage than the C-domain (Oba *et al*., 2005; Toropygin *et al*., 2008; Zou *et al*., 2009) (See Chapter 3). However, in sACE the C-domain appears to have equivalent selectivity to the N-domain (Hemming and Selkoe, 2005; Sun *et al*., 2008a). To date, the mechanism of interaction between the N- and C-domains of ACE is not fully understood. It is, however, evident that there is a degree of cooperativity between the two domains with certain substrates and inhibitors (Andújar-Sánchez et al., 2007; Binevski et al., 2003; Ehlers et al., 1991; Jaspard et al., 1993; Junot et al., 2001; Wei et al., 1991). Cooperativity refers to the synergistic effect that ligands or substrates have on enzymes where binding to one site influences the binding and catalysis of the other. The N- and C-domains of ACE have been shown to display negative cooperativity in substrate hydrolysis (Binevski *et al*., 2003; Rice *et al*., 2004; Skirgello *et al*., 2005). While this was observed with many synthetic and naturally occurring peptides, not all substrates displayed such an effect (Rice *et al*., 2004).

As established within this thesis, the truncated domains of ACE are N-selective towards both short FRET peptides, Aβ(4-10)Q and Aβ(4-10)Y, supporting the results from the literature on various forms of amyloid (Chapter 1 section 1.6.1). Characterisation of the cleavage site of Aβ(1-16) suggested that the N-domain was selective for this substrate (Chapter 2). This peptide contains the metal binding region of Aβ(1-42) and also undergoes multiple PTMs following aging and AD states, which enhance its aggregation and that of the longer Aβ(1-X) peptides (reviewed in Chapter 1 section 1.2.1.1). This emphasises the need to further evaluate the kinetic analysis of its hydrolysis by ACE. As selectivity occurs within the truncated domains, it is important to understand whether this selectivity is conserved within the two-domain form of ACE.

Aims and Objectives:

The main aim of this chapter is to analyse the soluble species of Aβ, the possibly toxic Aβ(1-16) (Du *et al*., 2011; Kozin *et al*., 2011; Portelius *et al*., 2006; Ramteke *et al*., 2014) and two fluorogenic peptides of the N-terminal region of Aβ to investigate the kinetics of processing, the degree of domain substrate specificity and potential co-operative effect the two domains of ACE have on hydrolysis.

Objectives:

1) To kinetically characterise and assess the truncated N-and C-domains, full-length sACE, and its domain knock-out forms as well as the double C-domain sACE construct towards Aβ(1-16) .
2) To examine and compare, kinetically, the FRET substrates (Aβ(4-10)Q and Aβ(4-10)Y) in terms of hydrolysis by the truncated and full-length ACE variants.

4.2 Methods:

4.2.1 Enzyme constructs

For expression of protein in CHO cells, the relevant genes were cloned into the mammalian expression vectors. For the construction of full-length, human, recombinant sACE constructs see Chapter 2 section 2.2.1.2. This includes the construction of sACE, CC-sACE, N-sACE and C-sACE (Figure 2.2). Briefly, sACE consists of wild type membrane bound human sACE. CC-sACE consists of sACE, in which the N-domain has been substituted for a second C-domain. For the full-length domain knockouts of sACE, both constructs have the complete signal, TM and stalk region corresponding to full-length sACE with their N and C-domain active sites inactivated (C-sACE and N-sACE respectively). For the soluble, truncated, human Cdom and Ndom constructs, see Chapter 2 section 2.2.1.1.

4.2.2 Protein expression and purification

Transfection and expression of all enzymes as described in Chapter 2

4.2.2.1 **Mammalian cell expression of ACE enzymes.**

For the cellular expression of ACE proteins See Chapter 2 section 2.2.2.1

4.2.2.2 **Selection of high expressing cells lines.**

The FACS technique was applied to all sACE TM constructs, barring CC-sACE, which is shed in high amounts and can be purified directly from all growth media, see Chapter 2 section 2.2.2.2.

4.2.2.1 **Isolation of secreted ACE protein from growth media.**

For purification of soluble constructs (Ndom, Cdom and CC-sACE) affinity chromatography was used as described in Chapter 2 section 2.2.2.3.

4.2.2.2 **Isolation of transmembrane protein from cell lysis.**

For the purification of the membrane bound sACE, N-sACE and C-sACE a modified procedure of affinity chromatography (Ehlers *et al*., 1991) was used, as described in Chapter 2 section 2.2.2.4.

4.2.3 Determination of ACE activity

Cell lysate, medium or purified protein was assayed for ACE activity using the synthetic peptide ZFHL see Chapter 2 section 2.2.3.1.

4.2.4 Specific activity/active site titrations

In addition to active site titrations, specific activities were also performed and used to determine enzyme concentration for all kinetics performed in this chapter. This technique was implemented as inhibitor binding to two domain molecules induces cooperativity and one mole of sACE is equivalent to one mole of non-selective inhibitor (Lisinopril) (Andújar-Sánchez *et al*., 2007). Thus, active site titrations in sACE are not ideal, as the total amount of potential Aβ degrading actives sites could not be determined. In order to determine loss of enzymatic activity due to storage, specific activities were calculated immediately after purification. It was assumed that the enzyme, which is eluted off the lisinopril column, must be active in order to bind the ligand. Specific activities were then re-determined prior to kinetic analysis and protein concentrations adjusted accordingly towards two active sites (Rice *et al*., 2004).

4.2.5 Amyloid kinetics

4.2.5.1 **The unmodified Aβ(1-16) substrate.**

The Aβ(1-16) (H-DAEFRHDSGYEVHHQK-OH) (Bachem AG) ACE hydrolysis assays were performed in reaction tubes and transferred to HPLC vials for analysis using the Agilent 1260 Infinity HPLC.

4.2.5.1.1 Determination of Aβ(1-16) kinetic parameters.

4.2.5.1.1.1 HPLC based assay on the unmodified Aβ(1-16).

Enzyme reactions were initiated on the addition of 25 µl enzyme (at a concentration within 10% hydrolysis of substrate of 0.25 nM Ndom, 1 nM N sACE, 2.4 nM sACE, 35 nM C-sACE, 290 nM CC-sACE and 300 nM Cdom) to 25 µl Aβ(1-16) in 1X HEPES buffer, ranging in concentration from 0 to 45 µM. The reaction was incubated for 15 min at 37ºC and stopped with the addition of 10 µl 0.25% TFA. The total reactions (60 µl) were cleared of contaminants on a spin column (GHP Nanosep® MF Centrifugal Device 0.45 µm pore size) prior to loading on the HPLC. All reactions were performed in duplicate and 50 µl injections were used to analyse samples, via HPLC (Agilent technologies), across a gradient of 0.1% TFA and 2% ACN in water to 0.1% TFA, 95% ACN. Importantly the substrates and products eluted at an isocratic step of 40% of the high ACN solution. The initial rates of reactions were generated via plotting the resultant peak product area, and converting it to pmols Aβ(1-14) product formed by means of a calibration curve (see below). This was then used to assess enzyme activity. The kinetic constants, for each enzyme, were calculated using the Michaelis-Menten method using Graph Pad Prism software (v 4.01, GraphPad Prism®).

4.2.5.1.1.2 Calibration Curve of Aβ(1-16).

In quantitative HPLC, the height and peak area are proportional to the concentration of the corresponding specific compound. A calibration curve was set up to convert product peak area to pmols product formed, through the complete hydrolysis of the substrate with the Ndom. Simply put, the curve allows for the determination of the amount of Aβ(1-14) produced from a specific concentration of Aβ(1-16). Initial reaction rates, generated by converting and plotting the resultant product (Aβ(1-14)) peak area, enables the assessment of

enzyme activity (See appendix 7.5.3). For the generation of calibration curves, reaction mixtures were separated on a Poroshell 120 EC-18 column with a 2.7 micron pore size. The reaction consists of 25 µl aliquots of Aβ(1-16) in 1X HEPES buffer, over the concentration range 0 to 40 µM, incubated with 25 µl 1 nM Ndom for 2 hours at 37ºC for complete digestion. The reactions were stopped with the addition of 10 µl of 0.25 % TFA. The total reaction (60 µl) was cleared of contaminants on a spin column (GHP Nanosep® MF Centrifugal Device 0.45 µm pore size) and run on the HPLC (Agilent technologies). Linear regression analysis was used to correlate the change in peak area to pmols of Aβ(1-14) product formed, with GraphPad Prism software (v 4.01, GraphPad Prism®).

4.2.5.2 **Fluorogenic Amyloid Substrates.**

Fluorogenic substrates designed around the established N-terminal Asp7-Ser8 cleavage site of the Aβ(2-11) were used as for a more high-throughput assessment of kinetic characteristics. There are two variations of FRET peptides, the first Aβ(4-10)Q, (Abz-FRHDSG(Q)-EDDnp) has an N-terminal o-aminobenzoyl (Abz) donor and a C-terminal ethylenediamine 2, 4-dinitrophenyl (EDDnp) quencher group, which is attached to an additional Gln10 substitution residue . The second peptide has a different quencher molecule, a 3-nitrotyrosine, a modification, which occurs in amyloid plaques, to the naturally occurring Tyr10 residue, Aβ(4-10)Y (Abz-FRHDSG-(Y)3NO_2).

4.2.5.2.1 Determination of the Fluorogenic amyloid Substrate kinetic parameters.

4.2.5.2.1.1 Fluorogenic Aβ(4-10)Q Substrate.

Hydrolysis of Abz-FRHDSG(Q)-EDDnp (Aβ(4-10)Q), a kind gift from A. Carmona, Universidade Federal de São Paulo) was performed in 1X HEPES buffer with 150 µl enzyme (at a concentrations of 5 nM Ndom, 30 nM N-sACE, 5 nM sACE, 5 nM C-sACE, 20 nM CC-sACE, 20 nM Cdom, within 10% hydrolysis) and an equal volume of substrate ranging from 0 to 30 µM. The assay is a modified form of the continuous assay (Araujo *et al*., 2000) performed in 96 well plates. Again, kinetic constants were calculated using the Michaelis-Menten method with GraphPad Prism software (v 4.01, GraphPad Prism®). The detected fluorescence was converted to pmol product via a Abz-Gly standard curve and data was corrected for IFE (Liu *et al*., 1999). Also see Chapter 3 section 3.2.7.

4.2.5.2.1.2 Flourogenic Aβ(4-10)Y Substrate.

An alternate fluorogenic peptide, Abz-FRHDSG(Y)3NO_2 (BIOPEP ™South Africa) (Aβ(4-10)Y) being more physiological apart from its Abz-group, was assayed, as above, in 96 well plates. They had a final volume of 200 µl (final enzyme concentrations, within 10% hydrolysis of 1 nM Ndom, 0.6 nM N-sACE, 0.2 nM sACE, 1.3 nM C-sACE, 0.3 nM CC-sACE and 4.2 nM Cdom once more within 10 % hydrolysis). The samples were read at a 5 min time point on a Cary Eclipse spectrofluorimeter (Varian Inc.) at excitation wavelength of 320 nm and emission wavelength of 420 nm. Kinetic constants, IFE and standard curves were calculated as above. Also, see Chapter 3 section 3.2.7.

4.2.6 Peptide integrity and cleavage site analysis

4.2.6.1 **Mass Spectrometry**

The Mass spectrometry was performed at the Centre for Proteomic and Genomic Research (CPGR, Cape Town, South Africa), as further elaborated in Chapter 2

4.2.7 Statistical Analysis

Statistical analysis of the data was determined by Student's t-test. Differences with $p < 0.05$ were considered statistically significant.

4.3 Results:

4.3.1 Kinetics of hydrolysis β-amyloid peptides by ACE

Kinetic constants were determined for the hydrolysis of various Aβ peptides by the two separate domains of ACE (Ndom and Cdom) and full-length sACE variants in order to further delineate domain selectivity and probe cooperative effects of the two domains. The human sACE, C-sACE, N-sACE, Ndom, Cdom and CC-sACE variants were purified to apparent homogeneity as assessed by SDS-PAGE (Chapter 2 Figure 2.3). For all average Michaelis-Menten curves see section 7.6.

4.3.1.1 **The Aβ(1-16) substrate:**

The Aβ(1-16) peptide was cleaved most efficiently by the truncated Ndom (k_{cat}/K_m 17.70 x 10^5 $M^{-1}.s^{-1}$), but was not hydrolysed by the truncated Cdom even after prolonged incubation times (Figure 4.1.1 A) (Table 4.1). A similar trend was found with the full-length sACE constructs. The sACE with a catalytically inactive N-domain (C-sACE) was approximately 18-fold less efficient than N-sACE. The efficiencies of N-sACE and wild type sACE, however, are comparable with k_{cat}/K_m's of 3.21 ± 0.22 and 2.36 ± 0.03 x 10^5 $M^{-1}.s^{-1}$, respectively. The varying catalytic efficiencies between N-sACE and C-sACE are due to an 16-fold difference in k_{cat} as the K_m's for sACE, N-sACE and C-sACE are almost equivalent (Figure 4.1.1 B and C respectively).

It is important to note that the k_{cat}/K_m for N-sACE and sACE was approximately 6-fold lower ($p < 0.05$) than that of the truncated N-domain (Ndom) (Figure 4.1.1 A). This is attributed to the relatively low affinity (K_m 22.85 ± 0.21 μM) and the high catalytic activity (k_{cat} 39.30 ± 1.99.s^{-1}) of the Ndom (Figure 4.1.1 C and B respectively) (Table 4.1). The CC-sACE construct was investigated to see if there was any structural or physical effect on the C-domain of sACE through the presence of another protein other than the N-domain. Similarly to the Cdom, CC-sACE processed Aβ(1-16) poorly compared to C-sACE. Although CC-sACE did process Aβ (1-16), the rate was too slow to generate accurate kinetic constants (Table 4.1).

Table 4.1 **Kinetic parameters of Aβ(1-16) (H-DAEFRHDSGYEVHHQK-OH) hydrolysis by different ACE variants/molecules**. Turnover rates were normalised to activity per unit active site for enzymes containing two functional domains (sACE and CC-sACE). (Error is represented as standard error of the mean (± SEM)

Enzyme	k_{cat}/K_M ($\mu M^{-1}.sec^{-1}$)	k_{cat} (sec^{-1})	K_M (μM)	V_{max}	R^2
Ndom	17.70 ± 0.70	39.30 ± 1.99	22.85 ± 0.21	0.49 ± 0.02	0.9566
N-sACE	3.21 ± 0.22	11.03 ± 1.62	34.20 ± 5.90	0.55 ± 0.08	0.9230
sACE	2.36 ± 0.03	8.37 ± 1.54	35.63 ± 6.23	1.00 ± 0.19	0.9497
C-sACE	0.17 ± 0.02	0.67 ± 0.08	42.36 ± 9.57	1.15 ± 0.14	0.9355
CC-sACE	ND	ND	ND	ND	ND
C-Dom	ND	ND	ND	ND	ND

*ND, not determined

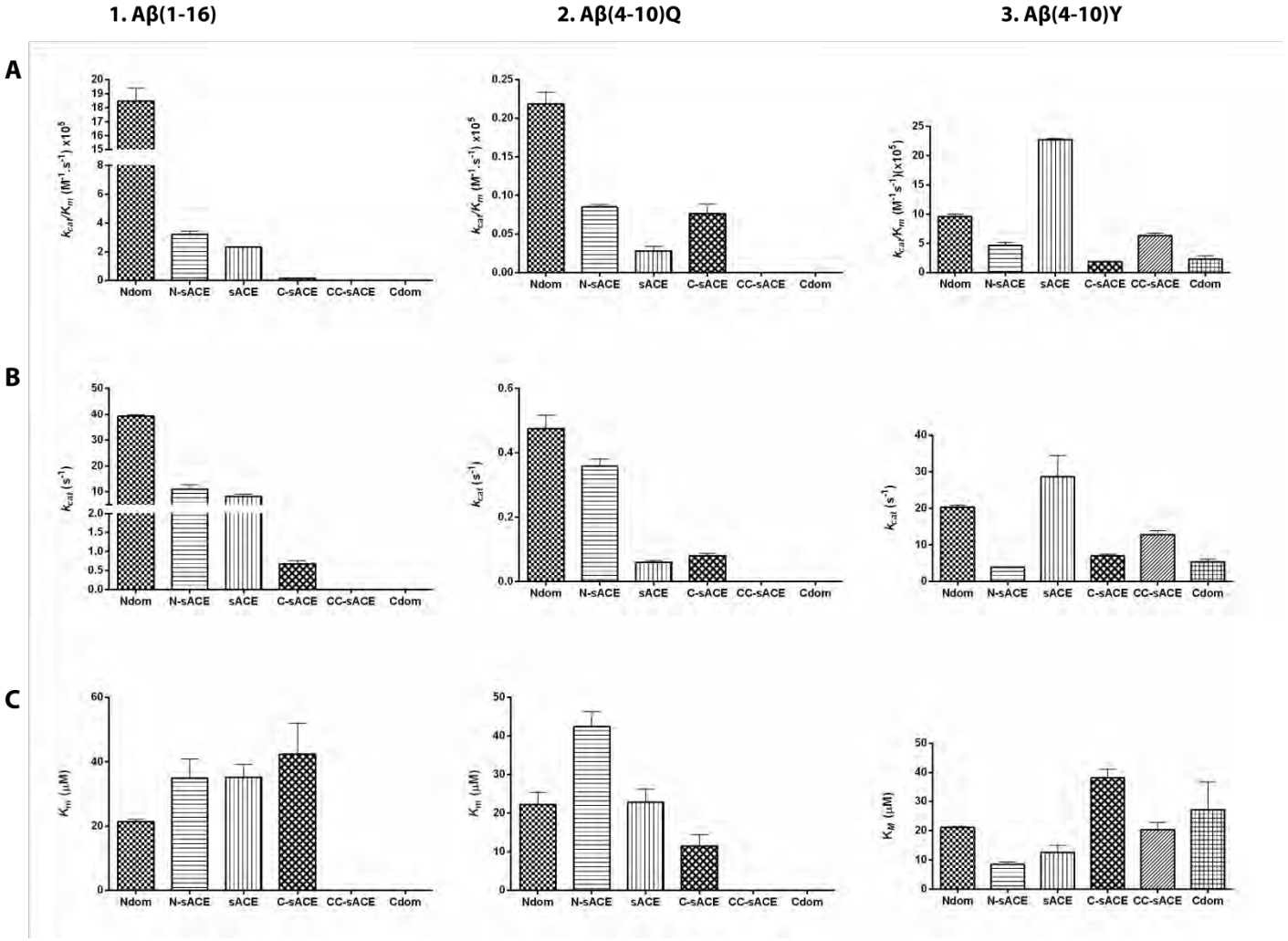

Figure 4.1 **The hydrolysis of 1: Aβ(1-16) 2: Aβ(4-10)Q 3: Aβ(4-10)Y by ACE**. Bar graph diagrams illustrating **A)** The overall catalytic efficiency (kcat/Km), **B)** the turnover rates (kcat)and **C)** the relative affinity (Km) of the Aβ(1-16) hydrolysis by both truncated and full-length constructs of ACE, including wild type sACE.

4.3.1.2 **The FRET Aβ(4-10) Substrates:**

Following Aβ(1-16), I examined theability of different ACE constructs to hydrolyse the fluorogenic Aβ(4-10) peptides with different quencher groups.

4.3.1.2.1 The Aβ(4-10)Q substrate.

The Aβ(4-10)Q peptide was hydrolysed very inefficiently by both Ndom and N-sACE (k_{cat}/K_m 0.22 x 10^5 and 0.09 x 10^5 $M^{-1}.s^{-1}$, respectively) (Figure 4.1.2 A) (Table 4.2). However, the trend of the full-length and truncated ACE constructs was similar to the physiological Aβ(1-16), being more selective for the truncated Ndom.

Compared to N-sACE, Ndom's greater selectivity for the Aβ(4-10)Q peptide was due to a tighter affinity alone (Figure 4.1.2 C), as the catalytic rate of N-sACE (0.36 ± 0.02 s^{-1}) was roughly equal to the Ndom (0.48 ± 0.04 s^{-1}) (Figure 4.1.2 B). By comparison, the C-sACE has very poor catalytic ability (k_{cat} 0.08 ±0.01.s^{-1}) and tight affinity, with K_m half that of the Ndom (Figure 4.1.2 B and C), creating an equivalent efficiency to N-sACE.

The efficiency of sACE was very poor compared to Ndom, due to its approximately 8-fold lower k_{cat}; its affinity was equal to the Ndom (22.90 ± 3.45.s^{-1}). Overall, the efficiency of sACE was 3-fold lower in comparison to the mutants with only a functional C- or N-terminal active site. This is indicative of a synergistic effect between the two active domains. The two domain CC-sACE cleaved Aβ(4-10)Q very slowly and accurate kinetic constants could not be calculated (Table 4.2).

Table 4.2 **Aβ(4-10)Q (Abz-AβFRHDSG(Q)-EDDnp) kinetic parameters by hydrolysis of different ACE variants/molecules.** Error is represented as standard error of the mean (± SEM).

Enzyme	k_{cat}/K_M (s^{-1}. M^{-1})(x10^5)	k_{cat} (s^{-1})	K_M (μM)	V_{max}	R^2
Ndom	0.22 ± 0.02	0.48 ± 0.04	22.20 ± 3.23	0.28 ± 0.02	0.9500
N-sACE	0.09 ± 0.01	0.36 ± 0.02	42.43 ± 3.92	3.230 ± 0.20	0.9797
sACE	0.03 ± 0.01	0.06 ± 0.01	22.90 ± 3.45	0.09 ± 0.01	0.9002
C-sACE	0.08 ± 0.01	0.08 ± 0.01	11.50 ± 3.03	0.12 ± 0.01	0.9181
CC-sACE	ND	ND	ND	ND	ND
Cdom	ND	ND	ND	ND	ND

*ND, not determined

4.3.1.2.2 The Aβ(4-10)Y substrate.

The more physiological fluorogenic peptide, Aβ(4-10)Y, was a far better substrate than Aβ(4-10)Q. When comparing the truncated constructs, Aβ(4-10)Y was more N-domain-specific. It was cleaved with half the catalytic efficiency of Aβ(1-16) by Ndom (9.2 vs. 13.0 x 10^5 $M^{-1}.s^{-1}$) yet there was a gain of function with Cdom (Figure 4.1.3 A) (Table 4.3).

Contrary to the results of Aβ(1-16), sACE hydrolysed Aβ(4-10)Y more efficiently than Ndom, this difference is due to the larger K_m value of the Ndom, as their catalytic rates are equivalent (Figure 4.1.3). Most surprisingly, the catalytic efficiency of sACE towards Aβ(4-10)Y was equivalent to the Ndom Aβ(1-16) catalytic efficiency. Notably, there was a general gain in C-domain activity with Aβ(4-10)Y. This is evident in the comparable efficiencies between, Cdom and C-sACE, and, N-sACE and CC-sACE (Figure 4.1.3 A) (Table 4.3). The C-sACE K_m is, however, 2-fold larger than its active N-domain counterpart (Figure 4.1.3 C) accounting for C-sACE's lower catalytic efficiency (Figure 4.1.3 B).

Interestingly, the CC-sACE construct cleaved the Aβ(4-10)Y with a higher k_{cat}/K_m than N-sACE, but a lower efficiency than the truncated Ndom. The overall turnover rate for CC-sACE was double that of the Cdom and much greater than C-sACE for Aβ(4-10)Y.

Table 4.3 . **Aβ(4-10)Y (Abz-FRHDSG-(Y)3NO_2) kinetic parameters on hydrolysis with different ACE variants/molecules.** Error is represented as standard error of the mean (± SEM).

Enzyme	k_{cat}/K_M (s^{-1}. M^{-1})(x10^5)	k_{cat} (s^{-1})	K_M (μM)	V_{max}	R^2
Ndom	9.22 ± 0.41	21.72 ± 1.19	23.56 ± 0.24	4.62 ± 0.14	0.9662
N-sACE	3.88 ± 0.11	4.45 ± 0.45	11.52 ± 1.49	0.44 ± 0.01	0.9413
sACE	17.35 ± 1.48	24.30 ± 3.55	13.15 ± 2.66	0.90 ± 0.18	0.9798
C-sACE	1.67 ± 0.10	6.39 ± 0.71	38.08 ± 3.45	1.57 ± 0.09	0.9826
CC-sACE	5.51 ± 1.21	9.92 ± 0.58	18.67 ± 3.06	0.90 ± 0.08	0.9462
Cdom	2.18 ± 0.70	6.33 ± 1.81	35.38 ± 19.65	4.45 ± 0.63	0.9065

4.4 Discussion:

In order to understand the potential differences between the two domains of ACE and their synergy in full-length sACE we have investigated the metabolism of the Aβ peptide by single and double domain ACE forms. Previous studies have noted potential discrepancies in kinetic data and a lack of substrate specificity based on different sources and forms of ACE (Marcic *et al*., 2000; Rice *et al*., 2004). Thus, all of the constructs were purified from one cell line of CHO cells and assay conditions were as physiological as possible for the assessment of Aβ. With regard to this, the cleavage of Aβ under kinetic assay conditions was examined extensively in chapter 2 and the Aβ(1-16) peptide was cleaved at the penultimate His14-Gln15 bond by all the ACE constructs, typical of ACE's exopeptidase action. The fluorogenic ACE substrates, Aβ(4 10)Q and Aβ(4 10)Y, were both endoproteolytically cleaved at the anticipated Asp7-Ser8 bond. Again, the cleavage site was consistent across all ACE variants (Chapter 2). Thus, it is unlikely that any differences, across ACE variants, in selectivity and cooperativity would be attributed to variations of cleavage specificity of these peptides within this assay.

The only kinetic constants, available for ACE and Aβ, in the literature were characterised using an ELISA assay, which is not the most reliable and accurate technique (Zou *et al*. 2007). Furthermore, only sACE was used and there was no deeper investigation into selectivity or cooperativity. Comparatively, the Aβ(1-16) is a better substrate of ACE than Aβ(1-42) with a faster catalytic rate. The soluble Ndom had a much higher catalytic turnover for Aβ(1-16) than either sACE or N-sACE. Furthermore Aβ(1-16) was a better Ndom substrate than the smaller Aβ(4-10) substrates (Figure 4.1.1, 4.1.2 and 4.1.3 B).

Interestingly, N-domain selectivity is affected in the full-length form of ACE across all substrates. Thus, sACE with an inactivated C-domain (N-sACE) has lower k_{cat} values for both Aβ(1-16) and Aβ(4-10)Y than the truncated Ndom. This decrease in turnover rate substantially reduces the N-domain selectivity of the full-length knockouts. For example, the k_{cat} for Aβ(4-10)Y is similar for the N- and C- sACE constructs (Figure 4.1.3 B), even though the K_m of the C-sACE is greater than that of N-sACE (K_m of 38.08 ± 3.45 and 11.52 ± 1.49 μM respectively) (Table 4.3). On the other hand, the truncated Ndom and Cdom have large differences in their k_{cat}'s and similar K_m's and thus are highly N-domain selective. The sACE form appears to improve the interaction of the Aβ(4-10)Y within the N-domain of N-sACE and slow the turnover rate. The opposite is true for Aβ(4-10)Q.

Despite a general decrease in selectivity of N-sACE compared to the Ndom, our results indicate amyloid is far more N-domain selective in the current optimal C-domain conditions (higher NaCl concentrations, which are critical to C-domain activity). The two active sites within human and bovine sACE have been shown to exhibit negative cooperativity with synthetic tripeptide substrates (Binevski *et al*. 2003; Skirgello *et al*. 2005; Woodman *et al*. 2005). In addition, a study using physiological substrates and human ACE enzymes showed a similar result for ANGI and ANG(1-7), but not ANG(1-9) (Rice *et al*. 2004). This implies that different substrates result in varying synergistic effects of the two domains (Rice *et al*. 2004). Similar to other kinetic observations with physiological substrates such as ANG(1-9) and BK, the degree of cooperativity between domains, with regard to Aβ(1-16) and Aβ(4-10)Q and sACE constructs, is considerably less than that observed with synthetic peptides (Jaspard *et al*. 1993; Rice *et al*. 2004).

Given the discrepancy between the magnitude of selectivity of the truncated domains and the sACE forms, there are most certainly cooperative effects taking place with regard to the Aβ substrates analysed. The equivalent affinity, of the truncated and full-length constructs, to Aβ(1-16) and the largely varying turnover rates suggests a close interaction between the two domains (Figure 4.1.2 A and B). Thus, the binding and hydrolysis of their individual active sites appear to be affected by the domain proximity. The cooperative effects of the two domains towards Aβ(1-16), overall, are negative (Figure 4.1.2 B). Due to the C-domains poorer hydrolysis of Aβ we can infer that the C-domain appears to negatively regulate the N-domain in sACE. This is also true for the Aβ(4 10)Q substrate, although to a lesser extent.

There is a large shift in both level of cooperativity and type of cooperativity when comparing the truncated domains to the full-length knockouts. For instance, with Aβ(1-16) the magnitude of the negative cooperativity with the full-length constructs is much smaller than that derived from the truncated domains. However, Aβ(4-10)Q has no shift in cooperativity. The positive effect of the N-domain on Aβ hydrolysis is evident with the C-sACE variant. C-sACE exhibited improved activity when compared to the truncated Cdom for all Aβ substrates, suggesting that the N-domain plays an auxiliary role. This notion is further supported by the poor activity of CC-sACE and its interaction with Aβ(1-16). This confirms that the mere presence of another domain does not improve the C-domain hydrolysis of Aβ peptides and that the interaction is N-C-specific. Our laboratory has previously shown that the presence of the N-domain has regulatory effects on the post-translational shedding of ACE and hydrolysis of substrates ZFHL and (Abz)-LFK(Dnp)-OH (Woodman *et al*. 2005). In contrast to these substrates, sACE CC-domain enzyme possessed a catalytic ability per active site similar to the individual domains, indicating an additive effect between the two C-domains with Aβ(4-10)Y substrate. Taken together, these data suggest that the type of substrate could influence the effects caused by domain interactions.

With this in mind, the cooperativity in the two-domain sACE variants was drastically altered by the presence of Aβ capping groups. The FRET substrates, considering only the truncated domains (Ndom and Cdom), induce a negative cooperative effect on the activity of sACE (Figure 4.1.3 B and to a much smaller extent Figure 4.1.4 B). On examination of the N-sACE and C-sACE constructs, a positive form of cooperativity is now found towards the Aβ(4-10)Y peptide. The binding and hydrolysis of the two catalytic sites is thus affected by both the structural arrangement of the two domains as well as the substrate-binding site interactions. The different cooperative effects of Aβ(4-10)Q and Aβ(4-10)Y could be ascribed to their distinct quencher groups. Specifically, the Aβ(4-10)Y contains a nitrotyrosine, instead of the Gln-EDDnp group, and the linker to the quencher also differs, resulting in cooperativity contrary to what was observed with FRET Aβ(4-10)Q and Aβ(1-16).

Oba *et al*. (2005) discovered that the larger Aβ(1-40) substrate did not out-compete smaller substrates like HHL within the truncated C-domain. They advocated that the C-domain was not conducive to the binding of large Aβ peptides, as Aβ did not inhibit the C-domain. This observation is supported by the architecture of the central cavity found in the tACE crystal structure and the chloride-dependent substrate interactions (Natesh *et al*. 2003; Yates *et al*. 2013). The Oba *et al*. (2005) study was performed on recombinant truncated domains only, resulting in a large N-domain preference for Aβ hydrolysis. This is supported by the results on truncated domains found in this study. The full-length C-sACE, however, gains activity towards

both the longer Aβ(1-16) and the shorter FRET substrates. This suggests that physiologically the role of the C-domain in Aβ cleavage cannot be excluded. Based on the results of this study and the synergistic effect that the C-domain exerts on the N-domain, it is likely to be important *in vivo*.

Smaller Aβ molecules, like Aβ(1-16), may have better access to the C-domain. Indeed, the C-domain of sACE most certainly has some Aβ affinity, as is evident in the Aβ(1-16) and the FRET Aβ(4-10)Q and Aβ(4-10)Y peptides. One might speculate that the structure of the C-domain in sACE may be more open due to the physical, and specific, presence of the N-domain. The N-domain, possibly, stretches out the flexible lid of helices α1-α3 in the C-domain, giving it more efficient substrate access (Corradi *et al*. 2006). Fluorogenic peptides may not necessarily be the best at indicating selectivity. This is so as the addition of, or derivativisation with, artificial groups may bias domain specificity due to their size, charge and the additional amino acids required to attach them (Araujo *et al*. 2000; Narawane *et al*. 2014). It is also possible for these groups to stabilise an interaction that would not necessarily take place (Narawane *et al*. 2014). Nevertheless, it is interesting to note the shifting selectivity within the FRET systems themselves, particularly towards Aβ(4-10)Y, as it contains a naturally occurring nitrotyrosine (Kummer *et al*., 2011; Radi, 2004). This modification may make targeting and proteolysis by the C-domain of ACE easier, especially since the Abz groups are shared between FRET peptides implicating the final residue position as crucial. Thus, extrapolating in theory, C-domain hydrolysis of peptides bearing this PTM could enhance the plaque clearing abilities of sACE within the human brain with its induced positive cooperativity.

In this study, we have assessed the domain selectivity and cooperativity of Aβ peptide hydrolysis. This further emphasises the dynamic roles of the two domains of sACE in substrate processing. This dynamism is not conserved across all ACE substrates, but rather appears dependent on the nature of the substrate itself. Together these data could assist in providing a perspective towards the relative domain orientation in sACE, with regard to substrate and inhibitor binding as well as kinetic cooperativity. Resolution of the sACE crystal structure combined with the already existing EM structure (Chen *et al*., 2010) will undoubtedly assist in providing further mechanistic insight into these observations. These considerations are important for the future design of N- and C-domain selective ACE inhibitors especially in consideration of hypertensive AD patients.

5 CHAPTER

The effects of the Aβ substrate on ACE signalling.

5.1 Introduction and Aims

ACE is a membrane bound molecule and has a short cytoplasmic domain, a transmembrane region and a large ectodomain - all of which are necessary components of receptors. Receptors can make use of phosphorylation to propagate negative and positive feedback to stimuli. It is thus intuitive that the one tyrosine and five serine residues, found in ACE's cytoplasmic tail, could act as potential phosphorylation sites for cell signal transduction. These observations prompted the investigation of the potential signalling mechanism of ACE (Kohlstedt *et al*., 2004). Kohlstedt *et al*., found that upon inhibitor binding, dimerization of membrane bound sACE and CK2 mediated phosphorylation of Ser1270 occurred. This phosphorylation, a result of an ACE outside-in signal response, was found to induce recruitment and activation of the JNK through the MKK7 pathway, which ultimately results in AP-1 mediated transcription of the *Ace* gene (Kohlstedt *et al*., 2006a, 2006b, 2004, 2002) (see Chapter 1.4.3). Aside from inhibitors, interactions of ACE substrates ANGI, BK, AcSDKP and the product ANGII were shown to trigger sACE signalling along the same pathway (Sun *et al*., 2010).

During the pathogenesis of AD, accumulation of Aβ in the ECM and blood vessels in the brain, combined with ACE's ability to degrade Aβ, may induce ACE signalling. The expression of ACE was upregulated in post-mortem studies on the brains of AD patients, specifically the temporal cortex which is a region severely affected in AD (Barnes *et al*., 1991). More recently, an elegant and comprehensive study on ACE10/10 mice by Bernstein *et al.,* indicated that AD mice over-expressing ACE within monocytes had decreased plaque and inflammatory burden. In addition to this, they also regained their cognitive abilities (Bernstein *et al*., 2014). Chronic ACE inhibition in transgenic mice models of AD has been shown to induce enhanced deposition of Aβ (Hemming *et al*., 2007). These results, along with ACE's ability to hydrolyse Aβ, suggest an important and possibly protective role of ACE activity in the diseased brain. The specific role of ACE inhibition on amyloid, however, is still somewhat controversial as some studies found no effect of ACE inhibition on Aβ load (Eckman *et al*., 2006) (See Chapter 1 section 1.6). Nevertheless, an increasing number of studies, some involving mouse and epidemiological work, have indicated that ACE inhibitors improve memory function and have a protective role against the development and progression of AD (Chapter 1 section 1.6).

Another factor which may further increase the amount of ACE present is substrate binding. Sun *et al.,* (2010) reported activation of the mouse ACE signalling cascade upon binding of a number of ACE substrates including ANGI, AcSDKP and BK (Sun *et al*., 2010). ANGII, an important inflammatory mediator in AD, also resulted in elevated JNK activity upon binding to ACE. Importantly, in contrast to mouse sACE and the results from the Sun *et al* study, the

Kohlstedt group reported that while binding to the C-domain of human endothelial sACE induced a signalling response, N-domain binding did not (Kohlstedt *et al*., 2006b; Sun *et al*., 2010). Previous work from our and other laboratories has shown that Aβ is N-domain selective. It is thus important to confirm the selectivity of human sACE signalling towards Aβ in different cellular systems. These are important questions to answer, as there is the concern that N-domain inhibition would prevent its degradation of Aβ. The ACE signalling pathway also cannot directly account for the beneficial effects of ACE inhibitors. Therefore, if Aβ does not induce signalling, other mechanisms are likely to influence ACE expression and may thus have an effect on the role that ACE inhibitors play in AD.

Phosphorylation is one of the most commonly occurring PTM of proteins and peptides. They arise via protein kinase transfer of phosphate groups, which induce conformational changes, affecting the activity and function of the target. Phosphorylation is crucial to regulation of a broad range of cell functions from cell-cycle, metabolism, cell differentiation and neurotransmission, to name a few (Hunter, 2000). While some phosphorylation is perpetual, other residues are only transiently phosphorylated. This transience is essential to the rate of signal transduction of any pathway. Thus, phosphoprotein abundance is generally very low, being between 1-2 % of total whole cell protein levels. Techniques commonly employed to interrogate levels of phosphorylation include radiometric and flourometeric kinase assays (Johnson and Hunter, 2005); phospho-specific antibody based straightforward techniques like Western blotting; immunoprecipitation and immunofluorescence microscopy (Delom and Chevet, 2006; Johnson and Hunter, 2005; Sefton and Shenolikar, 2001). Technically the detection of phosphorylation levels still remains challenging as most of the classic methods are not without limitation (Arnott *et al*., 2003).

Mass spectrometry has consequently developed into a robust and extremely sensitive method for the characterization of protein phosphorylation sites (Sickmann and Meyer, 2001). It has become the method of choice for the analysis of protein phosphorylation as a result (Delom and Chevet, 2006; Hunter, 2000; Piersma *et al*., 2015; Sickmann and Meyer, 2001). In order to study the signalling mediated by Aβ, high-resolution and accurate mass (HR/AM) analysis on the Q-Exactive mass spectrometer can be used to quantify possible Ser1270 phosphorylation of ACE. This instrument has a unique configuration in that it consists of a quadrupole mass filter as the front-end (for precursor ion mass selection) attached to an orbitrap mass analyser (Michalski *et al*., 2011). This enables quantitative methods based on HR/AM measurements, including targeted analysis in MS mode (otherwise known as single ion monitoring (SIM)) and in MS/MS mode (parallel reaction monitoring (PRM)) (Gallien *et al*., 2012) as depicted in the work flow (Figure 5.1). The dynamic range limitation of in-line quadrupole trapping devices is overcome by the ability of the quadrupole to select a restricted *m/z* range. This, combined with the MS/MS mode, provides an additional stage of selectivity. Targeted MS of complex mixtures with this machine yields better performance in terms of selectivity, dynamic range, and sensitivity - ideal for detection of low abundance phosphorylated peptides (Gallien *et al*., 2012; Kelstrup *et al*., 2011; Michalski *et al*., 2011).

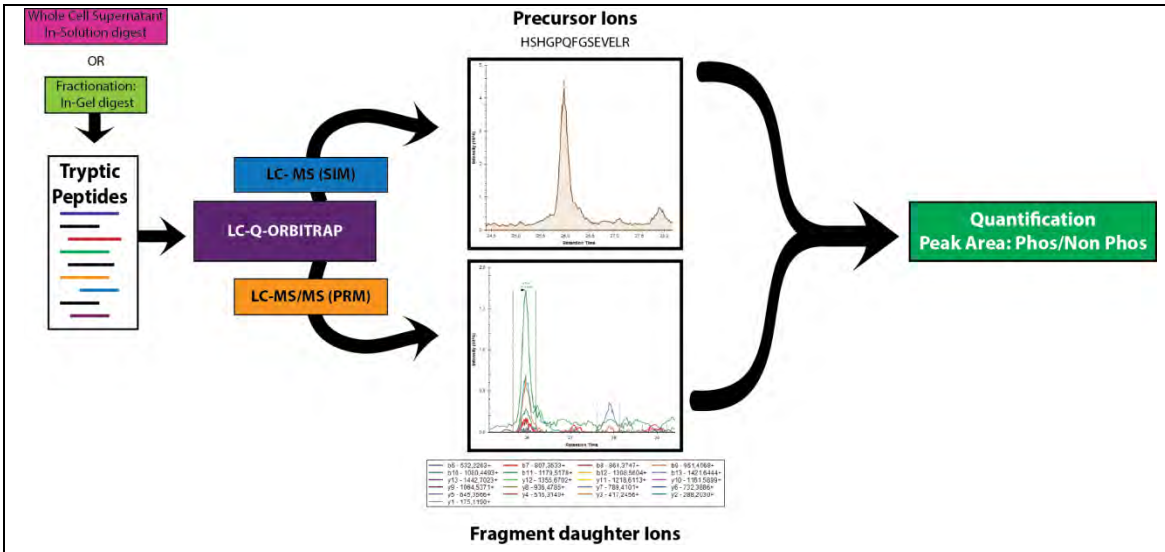

Figure 5.1 **Schematic of Q-Exactive PRM workflow**. For the detection of Ser1270 phosphorylation in complex mixtures two label-free sample preparation techniques will be used, in-solution digest and in-gel digestion. The spectrum of peptides will be separated via high performance liquid chromatography and then selected based on predefined precursor ion masses. Following this parent precursor ions are fragmented into product daughter ions, detected in the Orbitrap, generating simultaneous MS/MS spectra. Simplified diagram based on the study by Gallien *et al*., 2012.

The observation that the BRAAS in general is upregulated in AD and that ACE levels correlate well with Aβ load begs the question, does Aβ induce a signalling response via ACE? There is sufficient evidence throughout the literature and within this study that indicates that Aβ is a substrate for ACE, albeit catalysis is poor in comparison to ANGI for instance. However, the interactions between ACE and Aβ may have ramifications towards the consideration of ACE inhibitors in the treatment of AD and or hypertension.

Aims and Objectives:

The overall objective of this chapter is to investigate whether binding of Aβ and lisinopril to sACE affects ACE phosphorylation and cellular signal transduction. This aim was achieved through the following objectives:

The objectives used to achieve this aim include:

1) To investigate the association of ACE, JNK and pJNK upon treatment with lisinopril, Aβ(1-16) or Aβ(1-42) via immunoprecipitation and Western blotting.
2) To determine if increased ACE expression and JNK phosphorylation occurs after induced signalling.
3) To determine if ACE expression is affected by treatment with lisinopril or Aβ(1-42) and if this induces an increase in Ser1270 phosphorylation using a targeted mass spectrometry approach.

5.2 Methods:

5.2.1 Membrane bound Enzyme constructs.

5.2.1.1 **Wild type sACE.**

See Chapter 2 section 2.2.1.2.2.1

5.2.1.2 **sACE S1270A signalling mutant.**

5.2.1.2.1 Site Directed mutagenesis.

To create a signalling null mutant, conversion of the Ser1270 on the cytoplasmic tail of ACE to an Ala residue, was carried out by Vinasha Ramasamy using polymerase chain reaction (PCR)-based site directed mutagenesis and KAPA HiFi™ DNA polymerase (KapaBiosystems, South Africa) (method adapted from (Andreou, 2013). Briefly, complimentary primers were designed to introduce the Ser1270 to Ala mutation and a *Nar*I site (for screening), into pBSK-sACETM (See appendix 7.2.3.1). Parent DNA was digested overnight with *Dpn*I restriction endonuclease (Fermentas, USA) (see appendix 7.2.1); the digest products were amplified via replication of DH5α competent cells grown under 150mg/ml ampicillin selection. Single colonies were picked and grown) and plasmid DNA extracted (see appendix 7.2.5). Crude DNA from selected colonies was screened with *Nar*I endonuclease digestion (NEB, UK) (see appendix 7.2). DNA integrity and incorporation of the mutation was confirmed through sequencing, using primers flanking the multiple cloning sites as well as internal primers for sACE (see appendix 7.2.3). Sequencing was performed as in Chapter 2 Section 2.2.1. The sACE S1270A gene was then sub-cloned into the mammalian expression vector pcDNA3.1(-) to create pcDNA.S1270A, referred to as S1270A for simplicity from hereon in. DNA was prepared for transfection using the Plasmid Midi Kit (QIAGEN, USA).

5.2.2 Mammalian cell expression of sACE and S1270A enzymes.

The CHO-K1 mammalian cell line was used as the model system for transfection and expression of all enzymes as described in Chapter 2 section 2.2.2. CHO cells are an ideal system to investigate ACE signalling responses, as they do not express ACE, ACE receptors, nor Bradykinin receptors.

For the activity assessment of both cell lysate and growth medium sACE protein, see Chapter 2 section 2.2.3.1

5.2.2.1 **Determination of ACE shedding.**

Cells expressing sACE and S1270A were grown until confluency in 6 well plates in growth medium. Confluent cells were then serum starved and synchronised in minimal medium for 18 hours (Cooper, 2003). Medium was harvested, the cells lysed in triton lysis buffer and assayed (refer to Chapter 2 section 2.2.3.1) for ACE activity. The amount of shedding was calculated as a ratio of the total ACE activity from the medium to the sum of the total ACE activity in the medium and cell lysate.

5.2.2.2 **Substrate or inhibitor treatment of CHO cells.**

For the treatment of CHO cells with Aβ or the non-selective ACE inhibitor Lisinopril, cells were seeded into 6 well plates or 10 cm dishes, depending on the experiment, and grown to 60% confluency in growth medium (See appendix 7.1.1.1). Cell growth and division was synchronised under serum starvation conditions (2 %FCS for 17 hours and then in Opti-MEM (Invitrogen, USA) for 1 hour) prior to performing any experiment (Cooper, 2003). Cells were washed in PBS prior to adding 1 ml (for experiments in 6 well plates) or 5 ml (for experiments in 10 cm dishes) of inhibitor or substrate in Opti-MEM and vehicle in Opti-MEM to the cells. Thereafter, the plates were incubated for the periods detailed in Results section 5.3.

5.2.3 Immunoblotting and Immunoprecipitation.

ACE monoclonal antibodies, 9B9 used for immunoprecipitation and 4G6 for immunodetection, were made by our collaborator (Balyasnikova *et al*., 2005, 2002). All other antibodies were purchased from Cell Signalling Technologies and are specific towards GAPDH, pJNK and JNK. Cells were lysed immediately after removal of substrate, inhibitor or vehicle, in 150-200 µl (for 6 well plates) or 500 µl (for 10 cm dishes) of triton lysate buffer containing the protease cocktail mix and phosphatase inhibitors (PhosSTOP Roche Life Sciences) (see appendix 7.3.1.5). Lysis was performed on ice, for 20 minutes. All cell lysates were spun down at 14000rpm for 20 minutes at -4°C and the whole cell supernatant extracted for either immediate immunoprecipitation or immunodetection. Where necessary, whole cell supernatant was frozen at -80°C for later Western blot analysis. All samples were electrophoresed in sodium dodecyl sulphate polyacrylamide gel using standard lab protocol (appendix 7.7.1.5).

5.2.3.1 **Immunoblotting.**

For Western blot analysis the wells were scraped and lysed as mentioned above. Samples were normalised to the lowest amount of ACE activity and 25 µl of total cell lysate was then separated by SDS-PAGE (Laemmli, 1970). Following electrophoresis, proteins were transferred from the gel to a Hybond-ECL, nitrocellulose membrane (Amersham, Buckinghamshire, UK) in cold transfer buffer (0.5 M Tris, 1.44% (w/v) glycine, and 0.2% (v/v) methanol) at a constant 300 mA for 1 hour. Membranes were then incubated in blocking buffer (5% (w/v) skim milk, 0.1% (v/v) Tween-20, 0.2 M NaCl, 0.05 M Tris (pH7.4)) for 30 minutes prior to addition of primary antibody, in blocking buffer, which was then incubated overnight at 4°C. Membranes were washed 3 times for 5 minutes with Tris-buffered saline containing 0.1 % (v/v) Tween-20 (TBS-T)(0.1% (v/v) Tween-20, 0.2 M NaCl, 0.05 M Tris (pH7.4)) prior to 4 hour incubation with relevant secondary antibody (1/2000 dilution in blocking buffer). For the detection of ACE, a 1/250 dilution of primary rat 46G antibody specific to the linear epitope of the N-domain, was used (Balyasnikova *et al*., 2005, 2003). To detect GAPDH, pJNK and JNK, specific primary antibodies were diluted 1/1000 in blocking buffer. The membrane was then washed with TBS-T 3 times for 5 minutes to remove any residual unbound antibody. Detection was carried out using the Clarity™ Western ECL Substrate (BioRad, (Hercules, CA, USA)) as per manufacturer's instructions. Resulting chemiluminescence was visualized on a G:Box iChemi™ chemiluminescence imager (Syngene, Cambridge, UK) and signal quantification determined using ImageJ software (http://rsbweb.nih.gov/ij).

5.2.3.2 **Immunoprecipitation.**

Cells were lysed as above (see section 5.2.3) and immunoprecipitations were performed with Protein-G+ Agarose beads (Merck Millipore, Germany) on whole cell lysate supernatant. All samples were precleared with 10–30 µl of 50% bead slurry (protein G coupled agarose beads) per 200 µl cell lysate prior to immunoprecipitation. Proteins were precipitated from 200 µl whole cell lysates (1 mg/ml) with 1/100 dilution of their respective primary antibodies (as detailed under *Results* section 5.3.) and incubated at 4°C overnight with rotation. Following antibody binding to protein, 10–30 µl of 50% bead slurry was added and the samples incubated at 4°C for 4 hours with rotation. The beads were pelleted by centrifugation at 2000 rpm at 4°C. The supernatant was discarded and the beads washed 5 times with 500 µl of triton lysis buffer. The samples were kept on ice between washes. Antigen and antibody were then eluted from the beads by boiling in 50 µl of Laemmli buffer for 5 minutes. Co-immunoprecipitated proteins were subsequently detected by Western blotting as detailed above (section 5.2.3.2)

5.2.4 Targeted Mass Spectrometry.

All sACE and S1270A expressing cell lines were lysed in RIPA buffer (150 mM NaCl, 50 mM triethylammonium bicarbonate, 1 % SDS, 0.5 % deoxycholate, (pH 8)), containing protease inhibitor and phosphatase inhibitor cocktails, for mass spectrometry analysis.

5.2.4.1 **Protein precipitation.**

For the total protein precipitation, 400 µl whole cell lysate supernatant, was mixed vigorously with 400 µl of methanol and 300 µl of chloroform in a glass tube. The mixture was centrifuged in order to precipitate the protein in the interphase between the chloroform and methanol. Excess chloroform was removed (top layer) and the methanol and protein phases were mixed once more with 300 µl extra methanol. This was then centrifuged again at 13 000 rpm for 10 min, the supernatant was discarded and the remaining protein pellet air dried for resuspention in the appropriate buffer.

5.2.4.2 **In-solution Tryptic Digestion.**

For in-solution trypsin digestion 50 µg of total protein was reduced with 1 mM DTT for 1 hour with agitation and then alkylated in 5.5 mM IAA for 1 hour in the dark. Proteins were pre-digested with Lysyl Endopeptidase LysC (Waco, Neuss, Germany) at room temperature for 3 hours and diluted 4 times with ammonium bicarbonate (ABC) before adding sequencing grade modified trypsin (Promega, Madison, USA) (1:100 w/w). Proteolysis was carried out at 25°C for 18 hours with agitation at 30 rpm. This digestion was stopped by the addition of TFA (Sigma Aldrich, St Louis, USA).

5.2.4.3 **In Gel Tryptic Digestion.**

Proteins from cell lysates normalised to total protein were separated by SDS-PAGE (see appendix section 7.7.1.5) and visualized using Coomassie staining. Bands in the size region of sACE were excised, cut into 1 mm pieces and destained with 200 mM NH_4CO_3: acetonitrile (ACN) (50:50) until clear. The gel slices were dehydrated with 100 % ACN and dried on a

Savant SpeedyVac (ThermoScientific, USA). Slices were further reduced with 10 mM dithiothreitol (DTT) (Sigma, USA) in 25 mM NH_4CO_3 for 30 minutes at room temperature in the dark. Any excess DTT was removed and the gel slices dehydrated once again. Cysteine protection by carbamidomethylation with 55 mM iodoacetamide (IAA) (Sigma, USA) in 25 mM NH_4CO_3 was performed for 30 minutes at room temperature in the dark. The gel slices were finally dehydrated and washed with 25 mM NH_4CO_3. Digestion of these slices was performed with sequencing-grade modified trypsin (Promega, Madison, 162 USA) at a concentration of trypsin: estimated protein of 1:100 (w/w) overnight at 37°C.

5.2.4.4 **Sample Desalting.**

Desalting of digested peptides was performed over homemade C18 (Empore Octadecyl C18 solid-phase extraction disk (Supelco)) stage tips (Rappsilber *et al*., 2003) They were activated and equilibrated with 3 rinses of 80% ACN followed by 3 washes with 2 % ACN, both buffers contained 0.1 % Formic acid (Sigma Aldrich, St 179 Louis, USA). Peptides were loaded onto the C18 disk and centrifuged. Desalting was performed with 3 washes of 2 % ACN in 0.1 % formic acid and desalted peptides were eluted with 3 rounds of 100 µL of 60 % ACN in 0.1% formic acid. All desalting steps were carried out using 5min centrifugation intervals of 3000 rpm. Solvent was evaporated by vacuum centrifugation at room temperature and peptides were resuspended in 2 % ACN, 0.1 % formic acid at 250 ng/µl.

5.2.4.5 **MS of potential Lisinopril induced phosphorylation of Ser1270.**

5.2.4.5.1 High performance liquid chromatography.

Liquid chromatographic (LC) separation of, duplicate, in-gel extracted samples was performed using an Proxeon Easy n-LC II (Proxeon Biosystems, Odense, Denmark) system. Coupled to the Easy n-LC II, were two columns, the first was a home packed precolumn (100 µm ID X 20 mm) connected to the second, an analytical column of Luna 5 µm C18 100 Å-beads (75 µm X 500 mm) (phenomenex 04A-5452). In the initial mobile phase of 5 % ACN and 0.1 % formic acid, 1 µl (50 ng/µl) of resuspended ACE peptides were loaded onto the column. Peptides were eluted over a gradient of 5 % ACN to 50 % ACN for 35 minutes, with a 5 minute isocratic of 50 % ACN, then up to 90 % ACN over 35 minutes and back down to starting conditions over 5 minutes. The flow rate was held constant at 450 ml/min.

5.2.4.5.2 TSQ-Vantage™ triple quadrupole mass spectrometer parameters.

Mass spectra were acquired in positive mode on the Thermo TSQ-Vantage (Thermo Fisher, San Jose, CA, USA). Protein dilutions to 50 ng were applied to the EASY LC system. Transfer capillary temperature was set to 250 °C with a sheath gas pressure of 10. The ESI spray voltage was 1 kV and current discharge was set at 4. A 90 minute unscheduled multiple reaction monitoring (MRM) assay was conducted on the in-gel digested samples. 185 transitions were monitored (see appendix 7.8.2), with predicted collision energies based on the default skyline equation. Chrom filter peak width and declustering voltage were not used. Collision gas pressure was set to 1 mTorr. The Q1 and Q3 peak widths were set to 0.7 full width at half maximum (FWHM) and the calibration tuned, S-Lens value was used for all transitions. A Cycle time of 5 seconds was used, which translates to 27 milliseconds per transition, not accounting

for quadrupole switching delay. A product ion signal threshold trigger of 1 was used for all transitions.

5.2.4.6 **MS of potential Aβ induced phosphorylation of Ser1270.**

5.2.4.6.1 Ultra High Performance Liquid Chromatography.

Prior to mass spectrometry, re-suspended lyophilized samples were diluted to 50 ng/µl using HPLC grade water containing 0.1 % (v/v) formic acid. Nanoflow high performance liquid chromatography (ultra-LC) was carried out in-line on a Dionex UltiMate® 3500 RSnano UPLC system (Thermo Fisher, San Jose, CA, USA) using a reverse phase precolumn trap (100 µm×5 cm; 5 µm; 100Å; C-18) and analytic column (75 µm×50 cm; 5 µm; 100 Å; C-18). Gradient chromatography was carried out at 23^{o}C with a flow rate of 300 nL/min and peptides were eluted with a 3-80 % gradient of water-acetonitrile from 0-140 minutes. The binary mobile phase system consisted of buffer A, 0.1 % formic acid and water, while buffer B contained 0.1 % formic acid and ACN. The gradient used to elute peptides was 3 % B from 12-68 minutes, then increasing to 80 % B over 5 minutes, remaining isocratic at 80 % for 15 minutes, then a drop from 80 % to 2 % B over 2 minutes following another isocratic step of 2% B for 15 minutes before proceeding to wash conditions. Washes and equilibrations were included at the end of each run; they consisted of an increase of B from 2-50 % over 15 minutes, followed by a 1-minute transition back to starting conditions (1 % B).

5.2.4.6.2 Q-Exactive™ quadrupole-Orbitrap mass spectrometer PRM parameters.

Sample analysis was carried out on a Q-Exactive™ Hybrid Quadrupole-Orbitrap Mass Spectrometer (Thermo Fisher, San Jose, CA, USA). Analysis settings to samples introduced from the in-line ultra-HPLC system were: the resolution was set to 70 000, at a maximum injection time of 250 milliseconds or an automatic gain control (AGC) target value of 5 x 10^6. However, this AGC was set at the maximum so that the injection time is consistent across chromatographic elution for reproducible quantification. The programed target ion masses were selected by the quadrupole during initial scan with an isolation window of 4.0 *m/z*. These targeted peptides were then further subjected to fragmentation via high-energy collision dissociation (HCD). Peptide fragmentation was performed at HCD with a normalized collision energy (NCE) of 25. The abundance threshold for targeted ion selection was 1.7 x 10^4 with a charge exclusion of *z*=1 and z>5 ions.

5.2.5 Statistical analysis.

Data was analysed using built-in statistical software in GraphPad PRISM 4.0 (GraphPad software Inc, USA). Un-paired, nonparametric, student t-tests were used to analyse samples, which are represented as ratios of treated vs. untreated or phosphorylated vs. un-phosphorylated. Results were viewed as statistically significant when $p < 0.05$. Statistically significant data in figures throughout are indicated as follows: * $p < 0.05$; ** $p < 0.01$; *** $p < 0.001$.

5.3 Results:

5.3.1 Mutagenesis and Expression of Phosphorylation Mutant S1270A.

Mutagenesis in sACE of Ser1270 to an alanine (S1270A) was successful as can be seen from the sequence data determined after mutagenesis (Figure 5.2 A). No other spurious mutations were detected and the exchanged amino acid did not induce a frame shift (Figure 5.2 B).

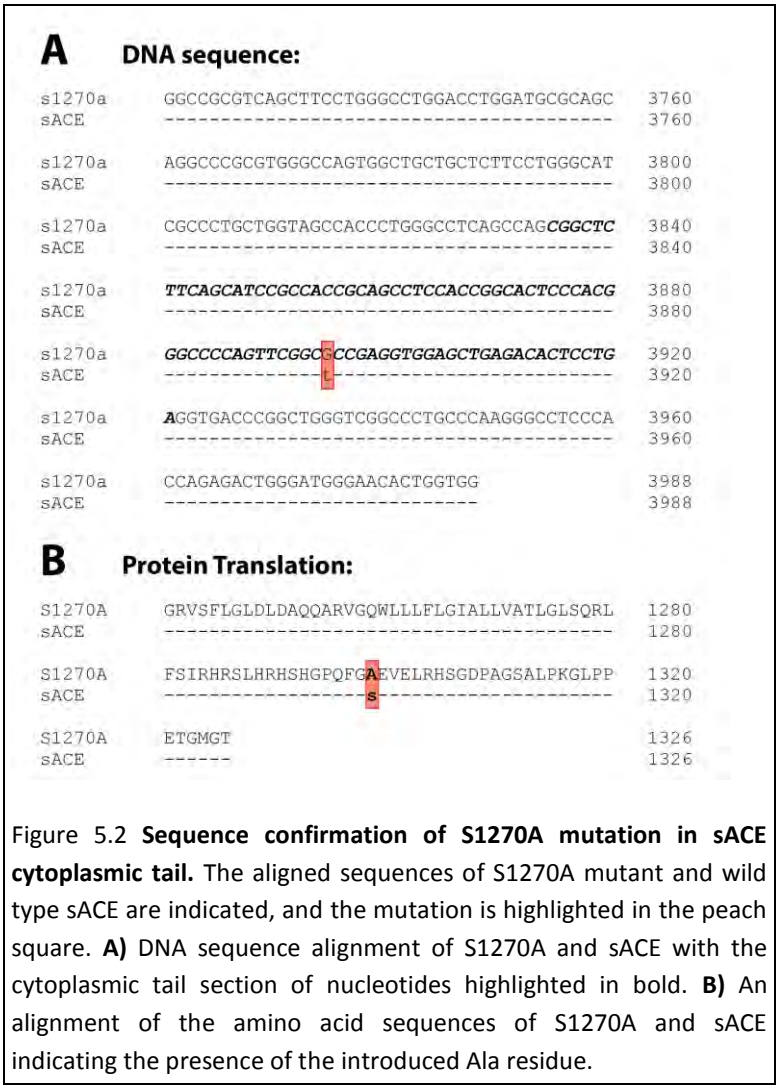

Figure 5.2 **Sequence confirmation of S1270A mutation in sACE cytoplasmic tail.** The aligned sequences of S1270A mutant and wild type sACE are indicated, and the mutation is highlighted in the peach square. **A)** DNA sequence alignment of S1270A and sACE with the cytoplasmic tail section of nucleotides highlighted in bold. **B)** An alignment of the amino acid sequences of S1270A and sACE indicating the presence of the introduced Ala residue.

On comparison of the activity present in the medium to the total activity (lysate and medium combined) a 20-fold increase in S1270A activity was observed (Figure 5.3). As indicated by the literature, the expression of S1270A induced an increase in endogenous shedding of S1270A from the membrane of CHO cells. Thus, phosphorylation of this Ser residue either plays a role in the membrane retention of sACE or the S1270A mutation results in increased affinity for the ACE sheddase.

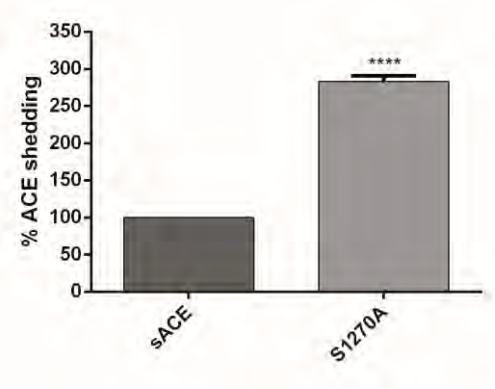

Figure 5.3 **Basal shedding of wild-type sACE and sACE1270A**. Shedding was determined as a percentage of total ACE activity in the growth medium over total activity in the cell lysate and medium. Results are the mean ±SEM of two experiments performed in triplicate with the significance indicated as *** $p < 0.001$

5.3.2 Lisinopril induced sACE signalling response.

5.3.2.1 **Lisinopril induces sACE signalling via Ser1270 phosphorylation.**

Cells expressing sACE were incubated for 0, 5 and 7 minute periods with 200 NM lisinopril. The samples were normalised to total protein and separated via SDS-PAGE. The Coomassie stained bands, corresponding to the size of sACE, were excised and an in-gel tryptic digestion of each sample was performed (as in section 5.2.4.3). The peptide pool was desalted and cleared over a C18 column (as in section 5.2.4.4) so that targeted MS/MS could be performed on the corresponding peptide digest. A targeted method was developed to specifically detect MS1 and subsequent MS2 ions that correspond to the phosphorylated cytoplasmic tail of ACE (H**S**HGPQFG**S**EVELR (870.35 *m/z*), HSHGPQFG**S**EVELR (830.36 *m/z*)) as well as to the non-phosphorylated sequence (HSHGPQFGSEVELR, (790.38 *m/z*)). This method was applied to the samples that were analysed on a Thermo TSQ-Vantage (Thermo Fisher, San Jose, CA, USA) mass spectrometer. The resultant chromatograms of parent to product ion transitions were analysed using Skyline (MacLean *et al*., 2010) and the corresponding peak area data extracted and plotted accordingly (Figure 5.4). The levels of phosphorylation of Ser1270 increased with exposure to lisinopril. The maximum increase with 7 minutes treatment was 8-fold greater than that with 0 minutes (Figure 5.4). Comparison of the parent peptide masses (total product ion sum) to that of the specific product ion y6 (**S**EVELR with a single *m/z* of 812,36), which corresponds to the shortest peptide that contains the S1270 residue, gave a similar trend increasing 2-fold with 7 minutes treatment (Figure 5.4). It should be noted that the quantification of the specific product ion could not be deduced due to low signal (See appendix section 7.8.2 for representative chromatograms for the phosphorylated and non-phosphorylated peptides from this experiment).

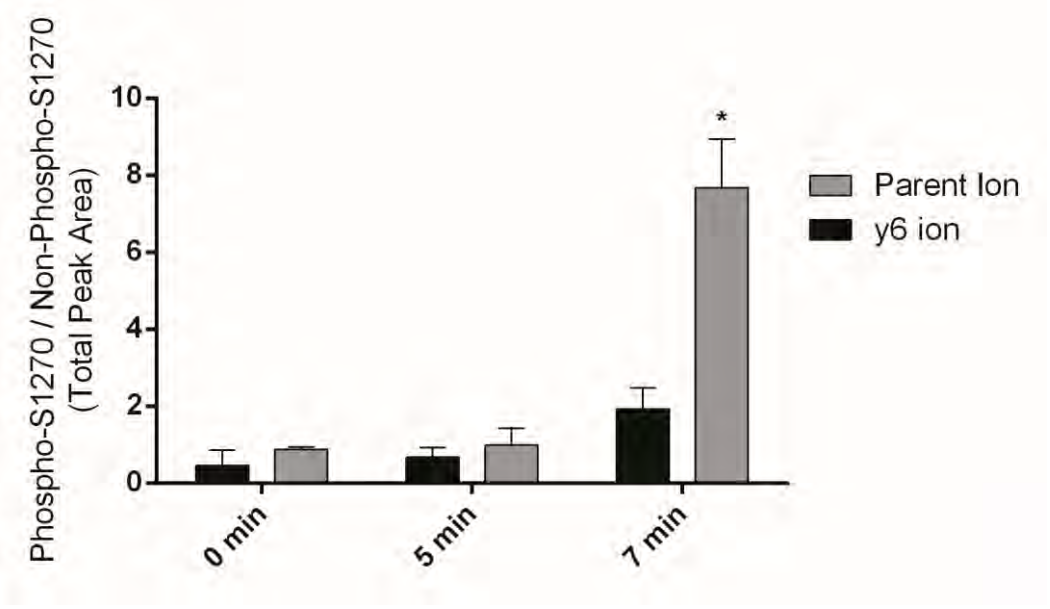

Figure 5.4 **MS analysis on the TSQ-Vantage of Ser1270 phosphorylation on Lisinopril treatment.** Comparison of parent ion (HSHGPQFGSEVELR) and y6 (SEVELR) ion, normalized to total ion count, of phosphorylated Ser1270 over non-phosphorylated. Parent ion ratios of phosphorylated over non-phosphorylated cytoplasmic tail over different incubation periods of lisinopril (LIS) To account for peptide extraction differences across samples, the peak areas for all parent peptides were normalized to total pool of potential Ser1270 phosphorylation site peak areas prior to comparison.

5.3.2.2 **Co-immunoprecipitation of ACE and pJNK.**

To investigate if the ACE outside-in signalling cascade does occur with treatment of sACE with 200 nM lisinopril, co-immunoprecipitations were performed with antibodies against sACE, JNK and pJNK. The cell lysates were normalised to the samples with lowest total protein concentrations prior to immunoprecipitation. The signal-induced associations were detected using Western blotting against sACE and pJNK (Figure 5.5). It is evident that there is activation of JNK through an increase in the amount of sACE co-immunoprecipitated with the activated pJNK in comparison to JNK. Furthermore, activated pJNK co-immunoprecipitated with sACE suggesting that an association with sACE at the cytoplasmic domain. Overall, the signal intensity of sACE-corresponding bands was detected in the proportions expected from the induced signal cascade (Figure 5.5). Phosphorylated JNK was thereby enriched in lisinopril treated cells from 6 well plates.

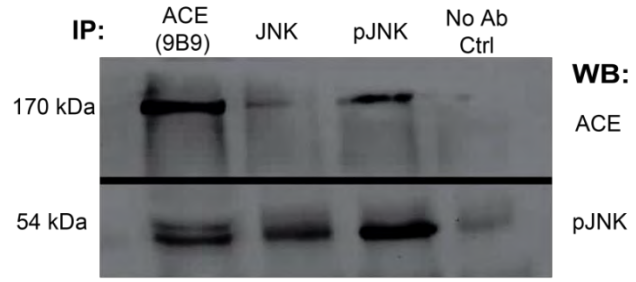

Figure 5.5 **Co-Immunoprecipitation of sACE, JNK and pJNK after treatment with lisinopril.** A representative Western blot (WB) of the immunoprecipitation of sACE expressing CHO cell lysis after a 7 minute treatment with lisinopril The bands corresponding to the correct size of sACE were found at 170 kDa and bands indicating pJNK were found at 54 kDa on detection with sACE and pJNK specific antibodies respectively. The antibodies used in the immunoprecipitation (IP) are found above the lanes corresponding to their elution products.

5.3.2.3 **Determination of the effect of Aβ(1-16) on ACE signal transduction.**

Due to the relatively low dose toxicity of Aβ and in an attempt to keep levels physiological, sACE-expressing cells were treated with a relatively high to low concentration range of Aβ(1-16) and vehicle control for 7 minutes. To determine if any dose effect takes place, samples were immunoprecipitated using an antibody specific to JNK and Western blotting was employed to probe for total JNK and induced pJNK levels. Overall no dose effect was observed, the induction of JNK phosphorylation on treatment occurred at 50 nM Aβ(1-16) as all other concentrations, up to 6 µM, did not induce an increase in the ratio of pJNK/JNK above that of the control to any statistical significance (Figure 5.6).

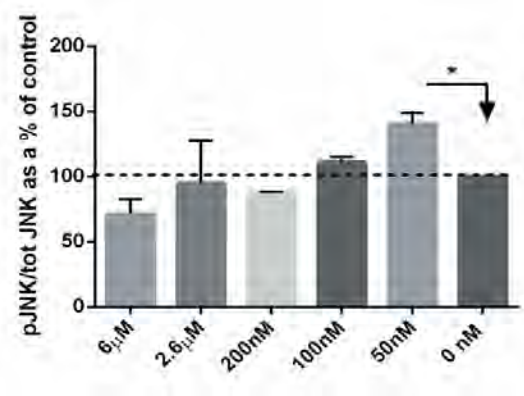

Figure 5.6 **The pJNK response to increased dosage of Aβ(1-16).** Immunoprecipitations, after treatment with various concentrations of Aβ(1-16) for 7 min, with JNK specific antibody. Results were determined by Western blotting with both pJNK and JNK. Data is representative of ±SEM of two experiments in duplicate and significance is indicated by* $p < 0.05$.

5.3.3 Determination of Lisinopril and Aβ(1-16) induced up-regulation of sACE expression.

To determine if sACE expression increases after the initial signal burst of 7 minutes on treatment with either lisinopril or Aβ(1-16), cell lysate of samples was normalised to total protein content prior to analysis using Western blotting. As this study uses only one cell line, CHO cells, densitometry of sACE expression was normalised to the expression of an internal housekeeping protein GAPDH. The results from 8, 12 and 24 hour incubations, with both Aβ(1-16) (Figure 5.7 A) and lisinopril (Figure 5.7 B), yielded no significant increase in sACE expression barring 8 hours post lisinopril treatment. This time point generated the only significant increase above vehicle control levels (Figure 5.7 B). Neither lisinopril nor Aβ(1-16) appear to upregulate ACE expression post initial 7 minute treatment.

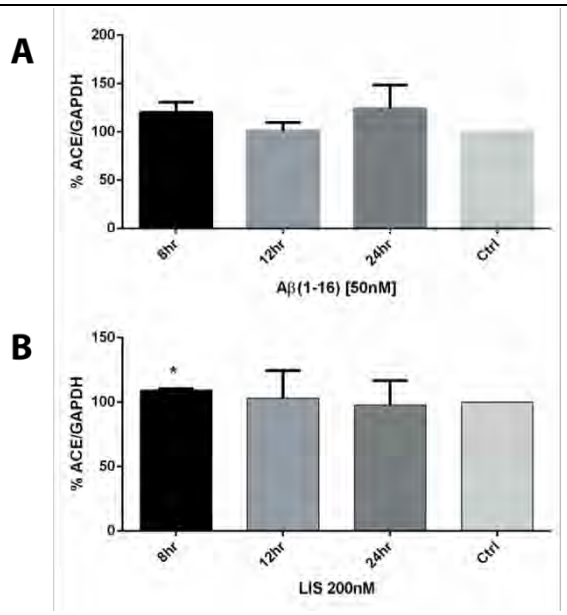

Figure 5.7 **Induced expression of ACE, post treatment, by Aβ(1-16) and lisinopril.** Densitrometery of Western blots performed in duplicate of **A)** CHO cells treated with 50 nM Aβ(1-16) over 7 minutes; and **B)** CHO cells treated with 200 nM of lisinopril for 7 minutes. Controls represent cells treated with the corresponding vehicles for 7 min. Data is representative of ±SEM of duplicates. The significance is indicated by* $p < 0.05$

5.3.4 Aβ(1-42) Induction of ACE signalling

5.3.4.1 **Incubation with Aβ(1-42) induces the association of pJNK with sACE.**

Previously, we indicated that ACE hydrolyses Aβ's N-terminal region as well as the C-terminus removing the last two amino acids of the full-length Aβ(1-42) peptide. In order to determine if treatment with Aβ(1-42) induces the outside-in ACE signal cascade, immunoprecipitations were performed against sACE and JNK. The co-immunoprecipitates were then probed for sACE and pJNK levels through Western blotting analysis. As observed with Aβ(1-16), pJNK signals were enriched by their association with sACE (Figure 5.8), suggesting that Aβ(1-42) does induce an ACE signal response.

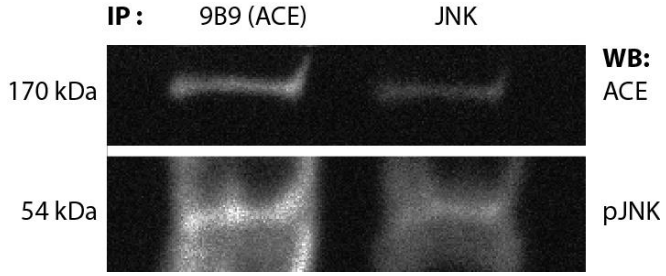

Figure 5.8 **Aβ(1-42) induced association of pJNK and JNK with sACE.** Co-immunoprecipitation of pJNK with sACE and JNK after treatment for 7 minutes with Aβ(1-42)

5.3.4.2 **Immuno-quantitation of Aβ(1-42) and Lisinopril Induction of ACE Signalling.**

In order to assess if the full-length Aβ(1-42) induces the same association with sACE and activation of JNK, that lisinopril and Aβ(1-16) stimulate, immunoprecipitations with sACE specific monoclonal antibody 9B9 were performed on cells expressing either sACE or S1270A. Interestingly, sACE levels were 2-fold higher on treatment of Aβ(1-42) compared to the lisinopril treated cells (Figure 5.9 A and B). Furthermore, treatment with both lisinopril and Aβ(1-42) yielded significant increases in sACE expression (0.5- and 2.5-fold, respectively) over their vehicle controls and the S1270A mutant, after treatment for 7 minutes (Figure 5.9 A and B). Similarly, both lisinopril and Aβ(1-42) induced significant JNK activation over S1270A and that of their respective controls (Figure 5.9 C). Despite having a greater sACE precipitation, the amount of activated JNK (pJNK) after treatment with Aβ(1-42) was 1.5-fold lower than that of the lisinopril treated precipitants (Figure 5.9 C and D). This suggests that Aβ(1-42)-induced signal through sACE may be weaker than that of the signal induced by lisinopril. It should be noted however, that the beads used to bind 9B9 and perform the precipitations underwent some degradation and the pJNK bands were fairly smeared as a result. These co-immunoprecipitants were performed in duplicate, however, and the analysis by Western blot in triplicate lending greater power to the densitometry despite smearing.

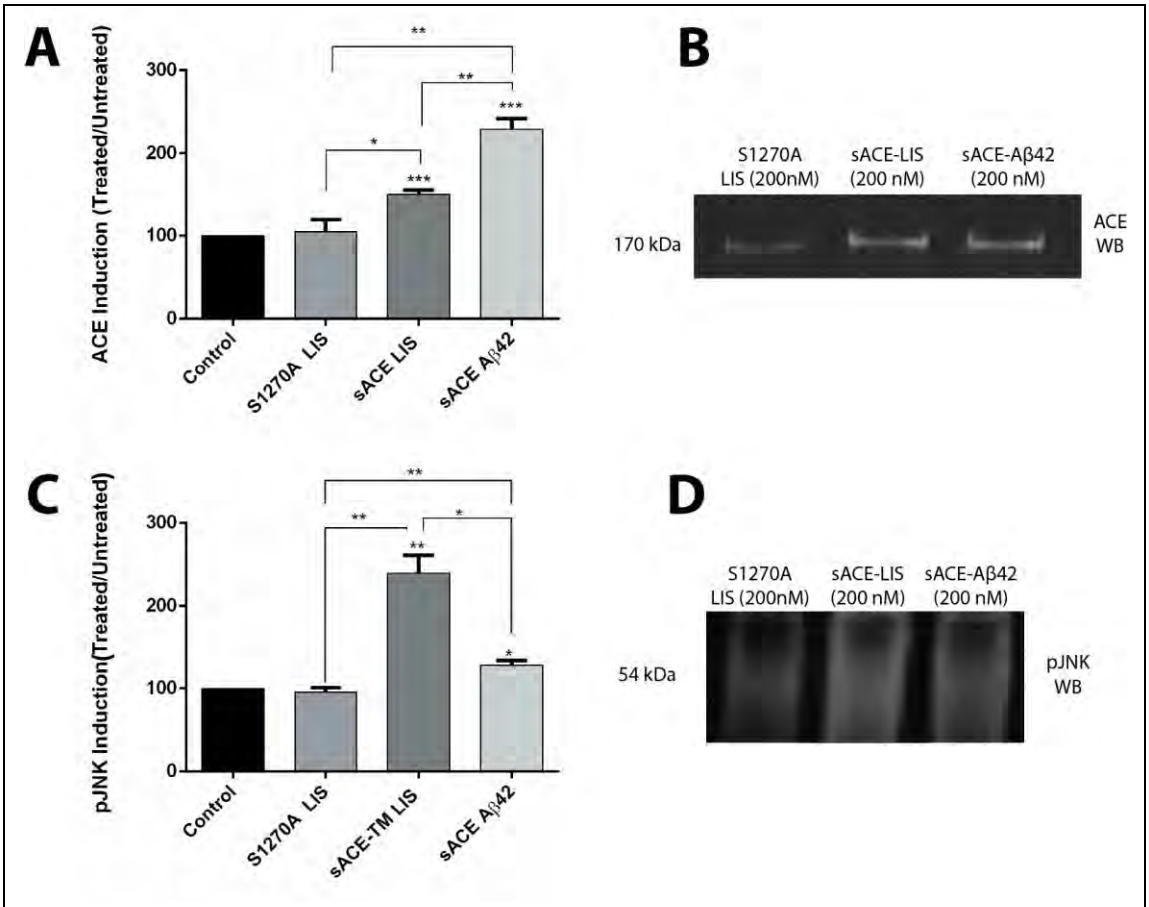

Figure 5.9 **Co-immunoprecipitation of pJNK with sACE on treatment with lisinopril and Aβ(1-42).** Lysates from cells expressing sACE and S1270A were immunoprecipitated with 9B9 after exposed to 200 nM lisinopril and 200 nM Aβ(1-42) and their corresponding vehicle controls for 7 minutes. **A)** Densitrometry analysis of ACE expression as a % of treated over untreated. **B)** Representative Western blot of sACE on the treated immunopreciptants. **C)** Densitrometry results on pJNK, as a percentage of treated over untreated samples. **D)** Representative Western blot on the co-immunoprecipitation of pJNK with sACE on treated cells. Data is representative of ±SEM of two immunoprecipitation experiments per sample blotted n=3 each. The significance is indicated by * $p < 0.05$; ** $p < 0.01$; *** $p < 0.001$.

5.3.4.3 **Aβ(1-42) induced up-regulation of sACE expression and activation.**

To investigate if the initial signal induction of 7 minutes produces an increase in sACE expression Western blot analysis was performed on cell lysate sACE. Cells were treated with either Aβ(1-42) or vehicle for 7 minutes, followed by extensive washing with PBS and medium exchange, before being left to grow for 24-48 hours. No change in either activity or expression of sACE was seen 24 hours post Aβ(1-42) treatment (Figure 5.10) However, the sACE activity increased by 20 % after 48 hours compared to the control (Figure 5.10 B) with a concomitant increase of 50 % in expression of sACE 48 hours post Aβ(1-42) (Figure 5.10 C).

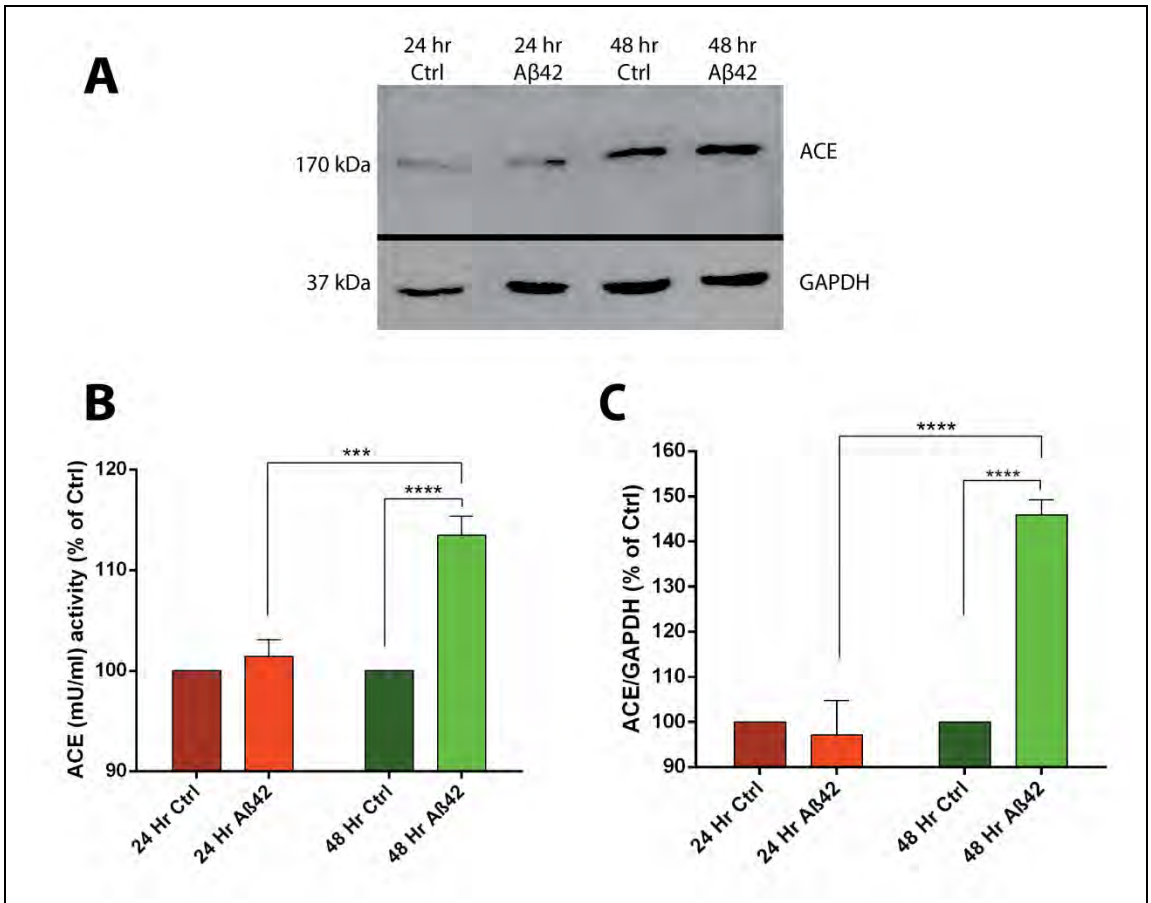

Figure 5.10 **Increased expression and activity of sACE post Aβ(1-42) treatment.** Cells were treated with 200nM Aβ(1-42) for 7 minutes before extensive washing and changing of medium, then incubated for 24-48 hours before lysing. **A)** A representative Western blot of sACE and GAPDH, **B)** Cell lysate sACE activity as a percentage of vehicle treated samples and **C)** Densitrometry of the Western blot analysis of both 24 hour and 48 hour time lapses post treatment. The data represent the ±SEM of 4 experiments performed in duplicate.

5.3.4.4 **MS-Quantification of Ser1270 phosphorylation on treatment with Aβ(1-42).**

A direct indication of sACE's ability to induce a signal cascade requires analysis of phosphorylation of the signalling-specific Ser1270 site. In a series of PRM-MS experiments we attempted to optimise the detection of the modified variants of sACE's cytoplasmic tail (Figure 5.11) from in-solution tryptic digests of whole cell lysate. As the peptide of interest is already present in low amounts, we targeted all possible modifications of it including the other serine phosphorylation site and all histidine oxidation. Histidine oxidation modifications may occur due to sample processing steps prior to MS (Bridgewater *et al*., 2007). It was apparent that the peptides with modified histidines gave the highest signal, and thus, accepted the most charge (with signal intensity three orders of magnitude greater) (Figure 7.12) by comparison to the unmodified when scanning for $M+H^{++}$ masses. The phosphorylation of Ser1270 also appears to consistently induce a shift in retention time from 26 to 25.7 minutes (see appendix 7.8.2.2). This can be seen in the optimisation experiments with lisinopril at a resolution of 17 000 on the nano-LC column (Figure 7.12). However, when the samples were run on the ultra-LC with only one set of targets at a higher resolution, 70 000 on the Q-Exactive, these low abundant masses could not outcompete other peptides for charge and thus the signal for the phosphorylated Ser1270 was too low to quantify.

As a result, separation of whole cell supernatant was required in an attempt to enrich for the low abundance phos-Ser1270 sACE peptide. Cell lysate proteins were resolved using SDS-PAGE separation and an in-gel digestion was carried out on bands that had a similar mobility to sACE. For Aβ(1-42) treated samples good replicates of the unmodified peptide (HSHGPQFGSEVELR) were detected with very good transitions (intensity well discernable from the background) at 70 000 resolution (Figure 5.12 A). However, the Ser1270 phosphorylated peptide (HSHGPQFG**S**EVELR) had very low signal and did not have very good transitions (very few ions had intensity above background) (Figure 5.12 B). These data indicate that further enrichment is required to enable accurate quantification since this signal is not as strongly induced as it is for lisinopril.

Group 1	Group 3
Ser1263 and Ser1270 Phosphorylation modifications	His 1264 Oxidation and Phospho modifications
HSHGPQFGSEVELR	HSHGPQFGSEVELR
HSHGPQFGSEVELR	HSHGPQFGSEVELR
HSHGPQFGSEVELR	HSHGPQFGSEVELR
HSHGPQFGSEVELR	HSHGPQFGSEVELR
Group 2	**Group 4**
His 1262 Oxidation and Phospho modifications	His 1262 and 1264 Oxidation and Phospho modifications
HSHGPQFGSEVELR	HSHGPQFGSEVELR
HSHGPQFGSEVELR	HSHGPQFGSEVELR
HSHGPQFGSEVELR	HSHGPQFGSEVELR
HSHGPQFGSEVELR	HSHGPQFGSEVELR

Figure 5.11 **Initial target groups for PRM of sACE Ser1270 phosphorylation.** The Ser1270 residue is highlighted and underlined in red, the other Ser1263 is highlighted in bold. The different combinations of His oxidation modifications that were accounted for are highlighted in blue (His1262) and green (His1264)

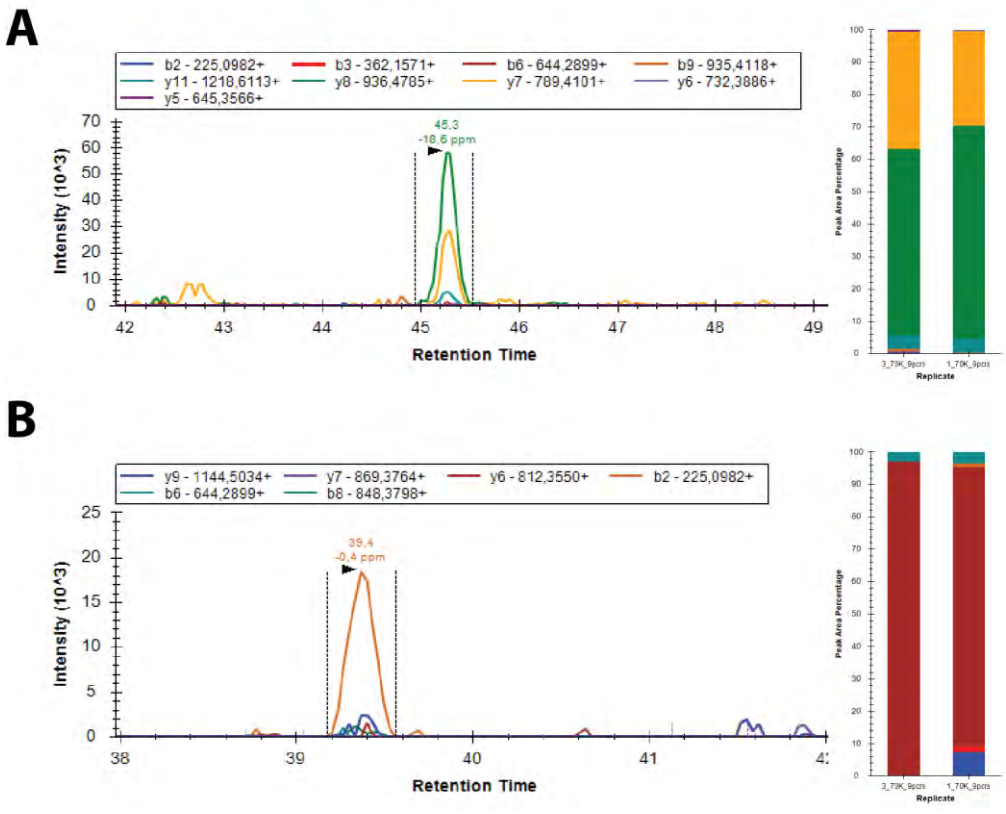

Figure 5.12 **Mass spectra chromatograms from Aβ(1-42) 7 minute treatment of sACE expressing cells**. **A)** Representative chromatogram of the unmodified HSHGPQFGSEVELR, peptide with y and b product ion keys indicated. **B)** A representative chromatogram indicating the poor signal of the Ser1270 phosphorylated HSHGPQFG**S**EVELR peptide with the highest signal generated by the b2 ion. The replicate, transition ion, bar graphs are indicated to the right of both chromatograms.

5.4 Discussion:

The dysregulation of the RAAS leads to very complex detrimental signalling processes, a number of them overlapping with aberrant signalling that occurs in AD. ACE has been shown to induce a signalling cascade, via phosphorylation of its Ser1270, in a receptor-like mechanism upon binding to inhibitors, hydrolysis products and substrates (Barauna *et al*., 2011; Guimarães *et al*., 2011; Kohlstedt *et al*., 2013, 2011, 2006a, 2006b, 2005, 2004, 2002; Sun *et al*., 2008b, 2010). The general up-regulation of the RAAS in AD may be a direct result of Aβ binding to and hydrolysis by ACE as ACE has been shown to behave like a receptor towards inhibitor binding, substrate binding and shear stress - all of which affect ACE transcription (Barauna *et al*., 2011; Kohlstedt *et al*., 2013, 2006a; Sun *et al*., 2010). Higher ACE levels lead to more ANGII production and possibly more inflammation. However, ACE also hydrolyses the pathological Aβ peptide and thus may be beneficial with regard to AD as discussed previously.

In an attempt to provide more quantitative data on the degree of phosphorylation of Ser1270 and the ACE signalling response upon treatment with lisinopril and Aβ, we carried out MS analysis on two different mass spectrometers. The TSQ-Vantage could detect the parent ions corresponding to the cytoplasmic tail of sACE that contains the phosphorylated Ser1270 (pSer1270), after lisinopril treatment, although detection was poor compared to its unmodified form. No absolute quantification could thus be generated on the amount of pSer1270 induced by lisinopril. Relative quantification was however possible on analysis of the pool of parent ions and comparisons were made between treated and untreated as well as to the level of phosphorylation in an analysis comparable to Western blotting (Figure 5.4). Moreover, the involvement of the pSer1270 was confirmed, as the trend of the phosphorylation of Ser1270 on the y6 ion and the significant increase in was reassuringly similar to that of the parent pSer1270 levels. It was not identical, however, in that this ion could not always be detected on all the samples from the TSQ-Vantage mass spectrometer. The level of Ser1270 phosphorylation increased 1.5-fold at 7 minutes (Figure 5.4) exposure to lisinopril. This is similar to the 1.3-fold increase that ramipril had in human endothelial cells (Kohlstedt *et al*., 2004). This is further confirmation that lisinopril induces phosphorylation on the Ser1270 residue of sACE.

Lisinopril, a non-selective inhibitor of ACE, induced the ACE signalling cascade triggered by pSer1270 as indicated by the immunoprecipitation of ACE, association of pJNK (Figure 5.5) and *vice versa*. Similarly, Aβ(1-16) associated with pJNK and levels were increased in an inverse dose-dependent manner, with the low concentration of 50 nM inducing a significant increase in pJNK/total JNK compared to controls. However, no significant up-regulation of sACE occurred post 7 minute exposure to Aβ(1-16), unlike lisinopril, which induced a small but significant increase in sACE expression after 8 hours. Aβ(1-42) however, caused a significant increase in ACE levels and activity 48 hours post treatment (Figure 5.10). This result was interesting in that it appears the activation of pJNK by Aβ(1-42) via ACE signalling was muted in comparison to lisinopril (Figure 5.9), thus the levels of ACE upregulation were anticipated to be lower or undetectable. This muted signal is not unprecedented, as Aβ is an N-domain selective substrate, and these N-selective substrates have been shown to have a weaker signal induction through mouse ACE in CHO cells (Sun *et al*., 2010). Human sACE N-domain did not induce a signalling response in porcine endothelial cell models while the C-domain did

(Kohlstedt *et al*., 2006a). This may be a cell specific interaction as the cell line transfected with sACE in this study is the same cell line used in the mouse ACE study where the N-domain had some signalling function.

As Aβ(1-42) induced such a marked change in ACE expression and activity, an attempt was made to quantify the level of pSer1270, possibly induced by Aβ(1-42), to investigate if ACE expression is directly linked to the up regulation of pJNK. Since the MS results from the lisinopril treatment indicated poor detection of the phosphorylated target peptides and it was apparent from the immunoprecipitation experiments (Figure 5.9) that Aβ(1-42) signalling is weaker through ACE, HR/AM spectrometry was employed to interrogate pSer1270. The characterisation of signal induction is a challenging analytical task, as phosphorylated peptides are low in abundance and phosphorylation is typically stoichiometric. Despite the historical prominence of triple quadrupole mass spectrometers (like the TSQ) in targeted analyses (Stergachis *et al*., 2011), the Q-Exactive was used to overcome the aforementioned challenges. The Q-Exactive combined with ultra-LC provided HR/AM for better sensitivity and higher resolution. The use of HCD in the Q-Exactive orbitrap provides greater and more extensive fragmentation from its higher energy of collisions, generating deeper scans and more informative data, compared to the collision induced dissociation (CID) of the TSQ machine (Olsen *et al*., 2007). CID is not appropriate for phosphorylation analysis due to the low energy of collision causing phosphate losses off of the peptide backbone (Palumbo and Reid, 2008). The ideal fragmentation type would be ETD (electron transfer dissociation) (McAlister *et al*., 2008) which was unavailable. HCD of the Q-Exactive however, is more appropriate for phosphoproteomic analysis as the higher fragmentation energy produces fewer phosphorylation site rearrangements making specific phosphorylation site detection accurate (Kelstrup *et al*., 2011).

Optimisation on the Q-Exactive was performed with lisinopril as a positive control. Groups of various histidine modification and phosphorylation target combinations (Figure 5.11) were probed at their corresponding resolutions. The higher the resolution settings, the less targets and multiplexing capabilities the Q-Exactive has; however the pSer1270-carrying parent peptide generated a far better signal than on the TSQ-Vantage. Whole-cell lysate tryptic digests increase the chance that two ions of a similar mass and retention will compete for charge and those in abundance will always win. The low abundance of the pSer1270-containing peptides and the parent peptide make quantification difficult without prior fractionation or enriching. Hence, final analysis on Aβ(1-42) treated samples that were fractionated via gel filtration, had good transitions (y and b ions) for the unmodified peptide HSHGPQFGSEVELR but poor transitions for the pSer1270 HSHGPQFG**S**EVELR variants (Figure 5.12) - even when considering the phosphate loss. It is possible that gel fractionation and tryptic digestion caused further depletion of the already low abundant peptide as peptide extraction can be a variable process.

The approach used in this study was hypothesis driven, initiating the experiments through the theoretical knowledge that the cytoplasmic tail of ACE is phosphorylated, without prior MS-detection of this specific peptide. As we have successfully detected the peptide of interest in this manner but have been unable to quantify it accurately, a different approach is necessary - that of evidence based discovery with subsequent PRM analysis. Simply put this is a data-independent strategy (Masselon *et al*., 2000), detecting the peptide of interest within the

cellular peptide milieu, before targeting it for more accurate quantification. This would overcome many issues; from the low abundance of the pSer1270 peptide to the multiple modifications which limit pure PRM. Futhermore, where simple statistically significant increases and decreases of one molecule or phosphorylation site do not determine absolute biological significance, an evidence based discovery approach would provide better biological significance to the ACE signalling cascade.

Aβ(1-42) affects ACE, inducing sACE expression and the activation of the ACE outside-in signalling, however, this still requires pSer1270-specific accurate quantification. Especially as the Aβ(1-42) response appears to be weaker than inhibitor-based signalling and there could be other more effective ways, apart from ACE signalling, in which Aβ upregulates ACE expression. An upregulation of RAAS aggravates hypoxic and cell metabolism disturbances which upregulate, and may also be triggered by, Aβ (Auerbach and Vinters, 2006; Bell and Zlokovic, 2009; Bloch *et al*., 2015; Iadecola, 2004). This then induces large cytoplasmic rearrangements with subsequent microtubule hyperphosphorylation, neurofibrillary tangles and finally cell death (Mattson, 2004). ACE signalling is intrinsically linked to shedding and cytoskeletal alterations. This is borne out by the increase in shedding observed on mutation of the signal-inducing Ser1270 to an Ala (Figure 5.3) (Kohlstedt *et al*., 2002). CK2 modulates ACE retention in vasculature and the activity of CK2 is 3-8-fold higher in the brain than the peripheral nervous system and non-neural tissues (Blanquet, 2000; Kohlstedt *et al*., 2002). CK2 is activated to phosphorylate ACE and induce the ACE signalling cascade (Figure 5.13). In neuronal cell lines it is activated by the brain-derived neurotrophic factor (BDNF) and neurotrophin-4 (NT-4) (Blanquet, 2000, 1998). Both these factors are involved in synaptoplastic protective mechanisms against stress induced by metabolic dysregulation as in hyperglycaemia, Aβ or ischemia (Inoue *et al*., 2014; Klumpp *et al*., 2004). During metabolic stress, BDNF has been shown in septal neurons to enhance bone morphogenetic protein-7 (BMP7)-induced Smad phosphorylation and nuclear translocation to prevent apoptosis in a CK2-dependent manner (Hilgard *et al*., 2004). Although the cell line used in this study is not neuronal, CK2 is not only upregulated in neuronal tissue but in other human, rat and mouse tissue, in response to a number of stressors.

The expression of ACE may initially be mediated by Aβ-induced metabolic stress in AD brain tissue since CK2 levels are low in late AD. Furthermore, it appears that neurotrophin-induced activation of CK2 is dependent on PKC-induced intracellular calcium (Blanquet, 1998) with ANG II regulating PKC via AT_1R receptor and calcium signalling through ACE (Chan and Chan, 2013; Murasawa *et al*., 1998; Villard, 1998). In addition, many of the neurotrophic factor receptors are cholinergic, thus up-regulation of ACE may have a modulating function as ANGII inhibits acetylcholine release (Barnes *et al*., 1990; Blanquet, 2000; Savaskan *et al*., 2001). Thus, positive feedback loops of ACE expression and activity could be a protective mechanism, being induced by either dysregulation or, Aβ-induced, hypoxic and metabolic disturbances in cells.

Aβ could also affect ACE expression via AMPK. AMPK is a cellular metabolic sensor in many ways and responds to levels of insulin and glucose, both of which are affected by the RAAS and AD (Cai *et al*., 2012; Greco *et al*., 2011; Kohlstedt *et al*., 2013, 2011; Mairet-Coello and Polleux, 2014; Thornton *et al*., 2011). This enzyme down-regulates ACE expression in the endothelium upon stimulation by shear stress and activates p53 via phosphorylation of Ser15.

This promotes cell survival, as opposed to p53's usual apoptotic role, by post-transcriptionally upregulating miR143/145 and reducing ACE expression (Kohlstedt *et al*., 2013, 2011) (Figure 5.13). As Aβ in AD induces severe cellular dysfunction which in many ways is related to AMPK dysregulation (Cai *et al*., 2012), it is possible that this induces ACE transcription and expression disturbances which lead to greater ACE and consequential RAAS upregulation.

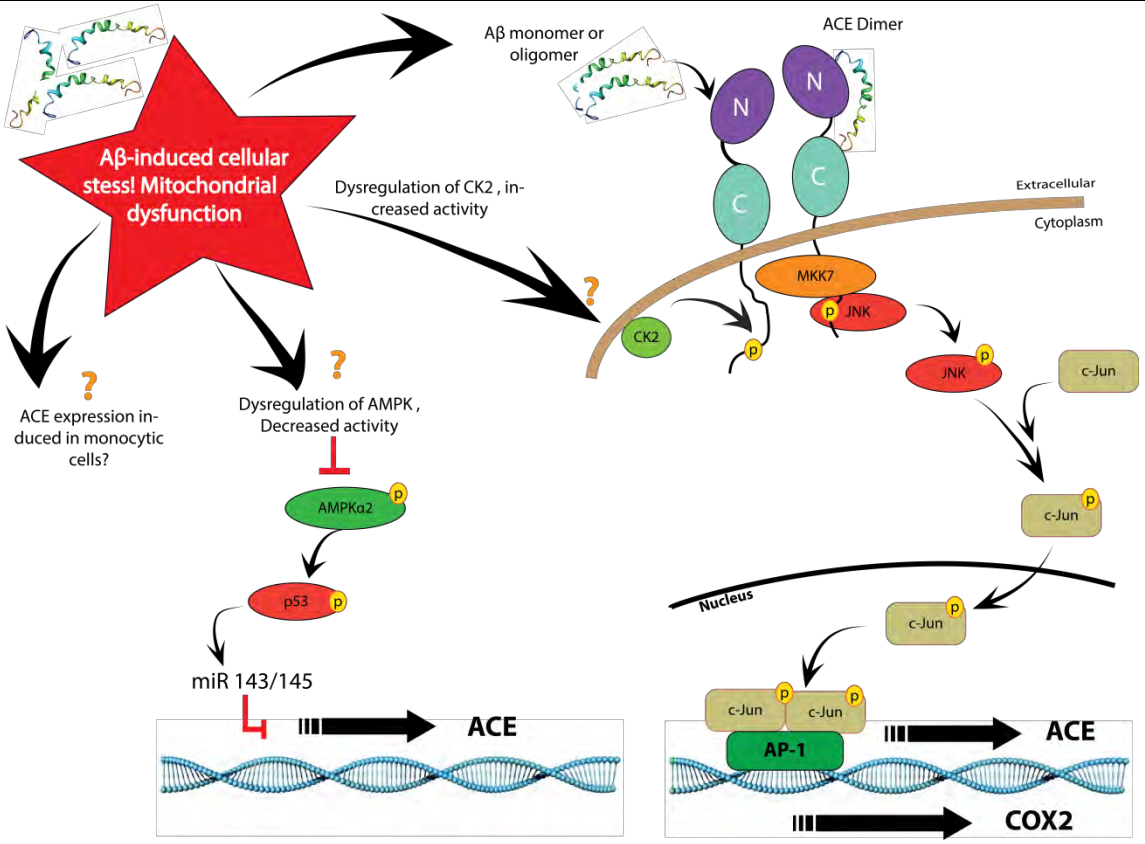

Figure 5.13 **Possible mechanisms for Aβ-induced upregulation of ACE expression.** ACE expression can be activated via the outside-in signalling response as with ACE inhibitors and other substrates. Alternatively dysregulation of CK2 (becoming over activated), or AMPK (via a reduction of activity) could induce increased up-regulation of ACE expression in neuronal tissue. Whether Monocytes alter their expression of ACE in response to inflammatory or stress indications has yet to be tested. This poses another possible means by which increased ACE expression may form part of a protective response to AD pathology.

Overall, the inhibition of ACE appears to have cell-mediated interactions that could prove either beneficial or detrimental. In the absence of a complete understanding of ACE inhibitor and amyloid-mediated signalling, C-selective inhibitors that do not cross the BBB could confer added benefits in the treatment of hypertension. It is plausible that treatment with these inhibitors would not only maintain the natural up-regulation of ACE in the brain to reduce the Aβ burden, but also maintain the possible ACE inhibitor-induced up-regulation via ACE signalling in peripheral monocytes. ANGII production would be slowed and the overall inflammatory distress it causes lowered, this would help maintain the BBB, and slow the transport of Aβ into the brain via RAGE (induced by ANGII) (Ihara *et al*., 2007).

As hypertension and glucose regulation are strongly interlinked and affect one another via signalling mechanisms, reducing high BP has added benefits towards cell metabolism

(Kohlstedt *et al*., 2009; McFarlane *et al*., 2003). A peripheral C-selective ACE inhibitor would allow for the lowering of blood pressure and its related increase in ROS induced by multiple ANGII mechanisms (See Chapter 1 section 1.4.3.1 and section 1.6.2). Less ANGII improves cell energy metabolism and reduces insulin desensitization (Fogari *et al*., 1998; Marrero *et al*., 2004; Olivares-Reyes *et al*., 2009; Ongali *et al*., 2014). These responses would, in-turn, remedy cytoskeletal derangements through GSK-3β (Agarwal *et al*., 2013) and lower cell death induced by Aβ accumulation (Zhu *et al*., 2011). Further investigation around ACE signalling would be helpful in assessing any further effects that ACE inhibitors have, be they detrimental or beneficial.

6 CONCLUSIONS AND FUTURE DIRECTIONS

In the light of the debate surrounding the role of ACE in Alzheimer's and, more specifically, the clearance of the plaque-forming Aβ peptide, this study investigated the molecular and kinetic mechanisms of Aβ hydrolysis by ACE. The domain selectivity of amyloid cleavage was interrogated by kinetic and mass spectrometry approaches and a comparative model system, using the physiological Aβ(1-16) as well as two FRET peptides derived from the metal binding N-terminal region of Aβ(1-42), was developed. Furthermore, ACE mediated signalling responses to Aβ and the ACE inhibitor lisinopril were investigated using immunoprecipitation and HR/AM MS.

In Chapter 2 the preference for ACE to cleave different Aβ peptides at specific peptide bonds was examined. The successful expression and purification of six full-length and truncated ACE variants (Ndom, N-sACE, sACE, C-sACE, CC-sACE and Cdom) and several active site mutants, combined with consistent primary cleavage intermediates that they generated, provided a robust model system for analysis. This is important, as throughout the literature there is variation in the types of construct and source of ACE used to assess the domain-selectivity of Aβ. Furthermore, there has been a lack of Aβ cleavage site specificity and little explanation of enzyme-Aβ interactions at a molecular level (see Chapter 2 section 2.1). The model system used in this study enables the determination of: domain selectivity, the specific differences within the individual domains that may drive selectivity, what cooperative interactions occur affecting selectivity, and the rates of hydrolysis of the N-terminal region of Aβ(1-42). In order to further understand the mechanism of Aβ hydrolysis, a number of Aβ peptides were crystallised with the Ndom and high-resolution structures were solved.

ACE's adaptability towards various substrates is exemplified in its endoproteolytic and exoproteolytic activity towards peptides derived from the N-terminus of full-length Aβ(1-42). The cleavage site and domain specificity of Aβ(2-11) by the N- and C-domains of ACE was successfully determined using HPLC. The Aβ(2-11) was endoproteolytically cleaved at the Asp7-Ser8 bond as previously described (Hemming and Selkoe, 2005; Hu *et al*., 2001; Kumar *et al*., 2012; Oba *et al*., 2005). This knowledge enabled the development of shorter fluorogenic FRET-Aβ substrates, Aβ(4-10)Q and Aβ(4-10)Y, which harbour cleavage sites of the larger Aβ peptides. These FRET peptides maintained the Asp7-Ser8 cleavage site under kinetic assay conditions. The physiological Aβ(1-16) underwent dicarboxypeptidase cleavage by all variants of ACE, generating an Aβ(1-14) primary intermediate, again, under kinetic assay conditions. This cleavage site has not been documented before but was consistently found using the different truncated and full-length ACE variants. The kinetic trend of Aβ(1-16) domain selectivity was similar to that of the shorter zinc binding Aβ(2-11). Overall, based on the

hydrolysis progress curves, the N-domain variant hydrolysed the Aβ peptides more efficiently than the other ACE forms. However, there was no difference in cleavage site specificity between N- and C-domains. Notably, truncated C-domain hydrolysis of Aβ does occur, but it is likely that it is not physiologically significant.

To examine the interactions of Aβ peptides with the ACE obligatory binding site, six high-resolution crystal structures of N-domain in complex with fragments of five Aβ peptides (Aβ(4-10), Aβ(4-10)Y, Aβ(1-16), Aβ(10-16) and Aβ(35-42)) were solved. The crystal structures provided further evidence of ACE's endopeptidase activity. However, as crystallisation conditions require long incubations with a large amount of substrate, it is likely that these cleavage products are the result of both primary and secondary cleavage. Thus, for Aβ(10-16) and Aβ(1-16) the crystal structures indicated a cleavage site between residues His14 and Gln15; however, the Aβ- Asp7-Ser8 dipeptide was crystalized from more than one substrate. This presence of the Aβ- Asp7-Ser8 dipeptide was surprising as it was the major cleavage site found under kinetic assay conditions and it indicates cleavage at His6-Asp7 and Ser8-Gly9. These variances are likely attributed to different experimental conditions but, corroborate previous findings regarding ACE's ability to accommodate a variety of P1 and P1' residues.

A general mode of binding to the Aβ binding to the Ndom was proposed from the six crystal structures. Interestingly, the general dipeptide S' binding mechanism appears to be conserved, as it is similar to that of the Cdom binding of ANGII and BPPb (Masuyer *et al*., 2012). Furthermore, any overlapping interactions occur mostly with conserved residues. N-domain selectivity based on these structures may occur through a number of additional interactions with residues unique to the N-domain. More specifically, the larger polar chains of Aβ form hydrogen bonds with Thr389 and, through a network of water mediated interactions, the unique residues of the S2' pocket. Furthermore, there were direct hydrophobic interactions between N-specific S2' residues and the Aβ -Val12, Ala42 and nitroTyr10.

Besides direct interactions, there are other mechanisms by which either domain of ACE may better hydrolyse Aβ and affect selectivity. The Aβ(1-42) is one of the largest substrates known to be hydrolysed by both ACE and NEP. ACE and NEP were thought to be structurally similar since they share common substrates and ACE inhibitors inhibit NEP to some degree (Kukkola *et al*., 1995). Thus, as NEP and IDE have hinge bending mechanisms, allowing for a larger variety of substrates to access their active sites, it is conceivable that ACE functions in this way too (Holland *et al*., 1995; Malito *et al*., 2008). Based on crystallographic structures, the large Aβ substrate might have difficulty in accessing the small active site pockets. There is also an N-terminal lid on the C domain which consists of three charged α helices that may further restrict the access of large substrates (Natesh *et al*., 2003). The C-domain has high homology to two other metallopeptidases neurolysin and thermolysin (Natesh *et al*., 2003; Roychaudhuri *et al*., 2012). Thermolysin has an open conformation if a substrate is not present, and undergoes a five degree rotation of its two ends towards each other in its closed conformation (Hausrath and Matthews, 2002). Such a mechanism was previously proposed for the C-domain of ACE with six hinge regions identified (Watermeyer *et al*., 2006). Furthermore, ACE2, a close homolog of ACE (40% homology), is known to undergo hinging about the active site cleft (Towler *et al*., 2004). ACE2 has been crystallized in both the open and closed conformations (PDB ID: 2R42 and 2R4L, respectively) (Towler *et al*., 2004). This

hinging of ACE2 was inhibitor-dependent and could be extrapolated towards substrates as it brings residues important to catalysis into position for optimal enzyme activity. The N-domain, which is structurally homologous to the ACE2 closed crystal structure, is likely to undergo a large amount of movement and hinging about its catalytic subdomains (Guy *et al*., 2003). As the N- and C-domains share a high degree of structural homology, it is likely that they share this potential hinging ability. Thus, the hinging mechanism may allow either domain to interact with a large substrate like Aβ-peptide or conformational changes may be activated allowing access, prior to substrate binding, by chloride on which C-domain catalysis is highly dependent (Wei *et al*.,1991; 1992).

In this study, the Aβ dipeptide crystals did not induce major conformational shifts in the structure of the Ndom (Figure 2.7 A). However, hinging motion of the Ndom lid helices (Anthony *et al*., 2010), was observed in some of the molecules, evident from the higher b-factors found in these regions. With this in mind, this study sought to determine which unique N-domain active site residues might induce Aβ-hydrolysis within the truncated C-domain. As the S' subsite has been implicated as a determinant of N-selectivity towards substrates and inhibitors alike (Araujo *et al*., 2000; Dive *et al*., 1999; Michaud *et al*., 1999), and contains a large number of domain-specific active site residues, its role in Aβ selectivity was interrogated.

In this study the FRET peptides Aβ(4-10)Q and Aβ(4-10)Y showed clear N-domain selectivity. Interestingly, the kinetic assay cleavage site results positioned the Gln10 residue within the S2' pocket, and the EDDnp quencher in the S3' pocket. This positioning could drive the N-selectivity of Aβ(4-10)Q as the Aβ(4-10)Y peptide has a nitrotyrosine in this same position and, although still N-selective, had moderate C-domain activity. The increased C-domain selectivity of Aβ(4-10)Y is likely to be the result of the conserved S2' hydrophobic interactions indicated by the crystal structure.

The two active site residues within the C-domain that generated the greatest increase in Aβ hydrolysis once mutated, were also determinants of C-selective inhibition (RXPA380, kAW and kAF) (Kröger *et al*., 2009; Watermeyer *et al*., 2010, 2008). The V380 and V379 residues are found on the border of the S2' and S1' pockets in the C-domain. Thus, it is unlikely that a slight change in hydrophobicity of this large S1' pocket would affect the affinity towards the P1' Ser8 and Gly9 residues that theoretically occupy it jointly. Considering this, most of the effects caused by these mutants are probably due to increased polar S2' interactions with the hydrophilic Gln10 and $Y3NO_2$ groups of Aβ(4-10)Q and Aβ(4-10)Y, respectively. The most significant increase in activity was derived from V379S Cdom mutant, which had a similar K_M to the V380T mutant, but a much higher k_{cat} towards Aβ(4-10)Q. Furthermore, its catalytic rate far exceeded that of the Ndom towards Aβ(4-10)Q. This mutants selectivity was not specific to the large EDDnp quencher of Aβ(4-10)Q, as similar trends were found towards Aβ(4-10)Y. To understand this better, the corresponding N-domain mutant S357V was analysed. Here there was a loss in substrate affinity but equivalent catalysis to the Ndom. Overall the efficiency of S357V was reduced, indicating that this residue does play a significant role in the selectivity of Aβ(4-10)Q. Theoretically, the position of the Ser357 residue forms a hydrogen bond mediated tightening of the S2' interactions by bringing helix 17, on which the residues are positioned, into closer contact with the substrate. This interaction helps drive overall N-domain conformational selectivity. Further combinations of N- to C-domain active

site mutations within Ndom could be examined with the two FRET substrates to further elucidate possible unique interactions in the Ndom that make Aβ so selective.

As physiological ACE does not occur abundantly as truncated N- and C-domains, it is important to establish whether the catalytic sites in full-length sACE display similar selectivity. As current clinical ACE inhibitors inhibit both domains of ACE, maintaining Aβ-hydrolytic function may be of significance towards patients at risk of AD. Furthermore, understanding how the Aβ substrate interacts with the full-length sACE, compared to the truncated domains, could better predict how ACE inhibitors may induce beneficial or non-beneficial effects. Four additional ACE constructs were employed to determine absolute selectivity and any co-operative interactions that may occur between the two domains of ACE in Aβ(1-16), and FRET Aβ hydrolysis.

Interestingly, the magnitude of N-domain selectivity is reduced in the full-length form of ACE across all substrates. This is due to an overall decrease in catalytic rate with little influence from substrate affinity. The cooperative effects, like many ACE substrates (Binevski *et al*. 2003; Skirgello *et al*. 2005; Woodman *et al*. 2005), were negative towards the physiological Aβ(1-16) and the Aβ(4-10)Q. Surprisingly the Aβ(4-10)Y generated a large positive cooperative effect. This positive cooperativity between the two domains was maintained when comparing sACE to either truncated or full-length N- and C-constructs. Unlike Aβ(4-10)Q where the sum of the full-length constructs indicated only slight negative cooperativity yet remaining large between truncated constructs. This positive domain interaction with Aβ(4-10)Y may be of significance as the nitrotyrosine is a common PTM of the wild type Tyr10 in Aβ plaques. Interestingly ANG(1-7), inversely associated with increasing tau hyperphosphorylation in AD (Jiang *et al*., 2015), has also been shown to have a positive cooperative effect between the two domains of ACE (Rice *et al*., 2004). On catalytic rate alone, the Aβ(1-16) and Aβ(4-10)Q have similar trends, where the truncated Ndom is most selective, and the individual active site knockouts are also N-selective, with a C-domain mediated negative cooperativity in sACE. In both these substrates, the C-sACE construct gained a small amount of activity, indicating an importance to the physical and specific presence of the N-domain. This was corroborated by the domain-substitution mutant where the N-domain of sACE was replaced with a second C-domain that exhibited poor Aβ hydrolysis. The same is true towards the Aβ(4-10)Y substrate; however, unlike the other substrates the C-domain selectivity was increased and measurable.

In Chapter 5, the putative signalling of Aβ via membrane-anchored ACE in CHO cells was examined. Aβ(1-16), Aβ (1-42) and lisinopril elicited JNK association and activation with ACE's cytoplasmic tail. Only Aβ(1-42) however induced a significant (doubling) increase in ACE expression and activity 48 hours post treatment. Targeted mass spectrometry was used to quantify changes in Ser1270 phosphorylation as an indication of ACE signalling. For numerous reasons this proved difficult to do using hypothesis driven conditions. The phosphopeptide of interest could be detected, but the signal was to poor for quantification with the added complication of additional PTMs. Thus, an evidence based discovery approach, where the native pSer1270 containing peptide could be identified and then targeted using PRM, would provide a way forward for absolute quantification of the signalling response. This is otherwise known as a data independent acquisition (DIA) approach, which involves tandem MS scans collected independently of precursor ion information that is then probed through a targeted search for known ACE pSer1270 peptides (Parker *et al*., 2015). This can be performed as a

label-free quantification–based DIA (LFQ-DIA) which has proven to be robust and reproducible technique for the quantification of signalling responses across many samples (Masselon *et al*., 2000; Parker *et al*., 2015). This approach requires added sample preparation, that of phospho-enrichment via titanium dioxide (TiO2) chromatography (Delom and Chevet, 2006). This is a highly efficient method for purification of phosphopeptides and is suited to the characterization of phosphoproteins from both *in vitro* and *in vivo* studies. It is possible to characterise entire signalling pathways using this technique on the Q-Exactive. One would glean a global image of the signalling processes on an MS/MS level, achieved upon ACE inhibition or substrate binding, through data independent full scan analysis (Gallien *et al*., 2012; McAlister *et al*., 2008; Parker *et al*., 2015; Stergachis *et al*., 2011). Identifying entire pathways may aid in explaining benefits of ACE inhibitors beyond their ability to reduce enzyme activity

Despite a general decrease in selectivity of the N-sACE compared to the Ndom, our results indicate amyloid is far more N-domain selective in the current optimal C-domain conditions (higher NaCl concentrations, which are critical to C-domain activity). This decrease in selectivity may have implications to the relevance of domain selective inhibitors towards the treatment of hypertension and AD. Furthermore, it would be of great value to know the precise signalling pathway Aβ utilizes to induce increased ACE expression and whether this is a cell-specific function. It is especially relevant considering the N-domain has Aβ degrading ability and immune-response capabilities forming part of the MHC antigen recognition system in macrophages (Bernstein *et al*., 2014; Shen *et al*., 2011), to see if Aβ-ACE signalling is induced here. Mouse models of AD and ACE over-expression in monocytic cell lines have been shown to reverse AD- pathologies (Bernstein *et al*., 2014). With regard to immune response, *ex vivo* macrophages from fat cells elicit an ACE dependent activation and reduction of pro-inflammatory cytokines in response to lipids (Kohlstedt *et al*., 2011). This response is similar to NSAID treatment against Aβ-induced macrophage activation (Combs *et al*., 2000).

In the absence of a complete physiological understanding of ACE's biochemical effects in AD, a cautionary approach towards ACEi may be warranted. With the treatment of hypertension, current ACE inhibitors block both the N- and the C-domains (Anthony *et al*., 2012). This leads to numerous side effects, like the development of angioedema, due to the accumulation of bradykinin and substance P (Hecker *et al*. 1994; Hecker *et al*. 1997; Erdös *et al*. 1999). This study has added kinetic and structural mechanistic data indicating that the N-domain is selective towards Aβ hydrolysis in all forms of ACE. It provides further rationale for the development of C-domain-selective inhibitors that could be efficacious in the treatment of AD and hypertension while presenting an improved side effect profile (Acharya *et al*., 2003; Georgiadis *et al*., 2003). This thesis paves the way for future *in vivo* studies towards a complete understanding of the functional significance of ACE in an upregulated BRAAS and RAAS and its role in AD.

7 APPENDICES

7.1 Cell Culture

7.1.1.1 **Growth Medium**

50% Dulbecco's Modified Eagle Medium (DMEM) (Sigma, USA), 50% HAMS-F12 (Sigma, USA) supplemented with 10% foetal calf serum (FCS) (Sigma, USA) and 20M HEPES buffer]

7.1.1.2 **Minimal Medium**

50 % DMEM, 50 % Ham's F12, 20mM HEPES, 2 % FCS (heat-inactivated for a further 15min at 70°C

7.1.1.3 **PBS**

137 mM NaCl, 2.7 mM KCl, 10 mM Na_2HPO_4, KH_2PO_4, pH 7.5.

7.2 DNA and Restriction enzyme digests

7.2.1 TENS Mini-Plasmid DNA isolation

Spin 2 ml bacterial overnight culture for 1 min at 6-7000 rpm. Discard supernatant and resuspended pellet in 300 µl TENS solution for less than 10 min. Add 150 µl of cold 3 M NaOAc to the TENS suspension and then vortex and put on ice. Centrifuge for 10 min at 13000 rpm at 4°C which should precipitate all protein. Remove 400 µ of the supernatant and transfer to a new eppindorf. Add 800µl of 100% EthOH incubate at -20 °C for +/- 15 min to precipitate the DNA spin this mixture for 5 min at 4°C at 13000 rpm a clear pellet of DNA should form. Wash the DNA with 70 % ethanol 3 times in 300 µl by reversing the tube in the centrifuge and spinning for 10 min at 13000 rpm. Dry the pellet and resuspended in TE/Rnase buffer 30 µl

.

7.2.1.1 **TENS (500 mL)**

5 ml	1M Tris pH8.0
12.5 ml	20% SDS
5 ml	10N NaOH
1 ml	0.5M EDTA

Make up the volume to 500 ml with MilliQ H_20.

7.2.2 Restriction digests

100-300ng DNA

1X Restriction Enzyme Buffer

1U Restriction Enzyme

Made up to 20 µl with nuclease water

Standard digests from 1-2 hours at 37°C

7.2.3 Site directed mutagenesis (SDM)

7.2.3.1 **SDM primers**

The signalling Ser1270A knock out mutation was created using the following primers, Figure 7.1, with the aid of WATCUT (http://watcut.uwaterloo.ca/watcut, designed by Michael Palmer, University of Waterloo, Canada.) to create pBSK.S1270A. Primers were synthesised by Inqaba Biotechnical Industries (South Africa).

Fwd: 5′- CAGTTCGGC**G**CCGAGGTGGAGCTGGAGCTGAGACACTC-3′

Rev: 5′-GAGTGTCTCAGCTCCACCTCGGC**G**CCGAACTG -3′

Figure 7.1 **S1270A signalling mutant primers.** Both forward and reverse primers are indicated as well as the introduced *Nar*I sight, which is underlined.

7.2.3.2 **PCR parameters for SDM**

Initial Denaturation: 95 ºC	2 min
Denaturation: 98 ºC	20 sec
Annealing: Tm of primers for	15 sec

20 cycles of Denaturation and annealing

Extension: 72 ºC	30 sec/kb
Final Extension: 72 ºC	1 - 5 min

7.2.4 Internal sACE primers

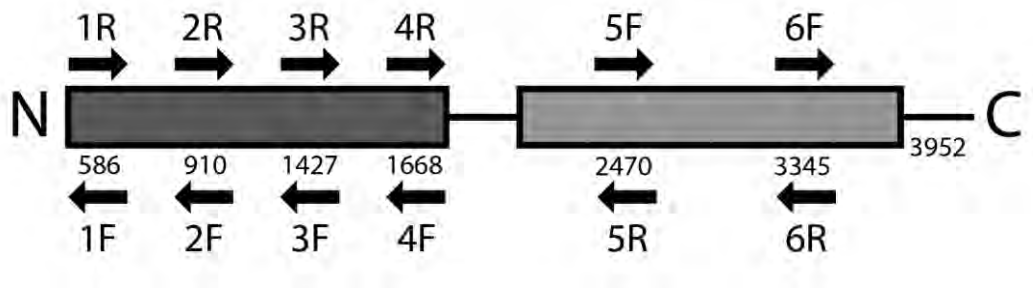

Figure 7.2 **Internal sequencing primers.** These primers are used routinely in our group to confirm the integrity of constructs after any site directed mutagenesis reactions have been performed.

7.2.5 *E.coli* growth and transformation

7.2.5.1 **Luria-Broth (LB)**

Bacterial culture medium used to propagate and, if necessary select for transformed DH5α *E.coli*

10 g Tryptone

5 g Yeast Extract

5 g Sodium Chloride

Made up to 1L of dH_2O prior to autoclaving. Once cooled to sufficient temperature prior to ampicillin is added when necessary.

7.2.5.2 **Luria-Broth Agar**

Bacterial agar used to select single colonies of transformed or untransformed DH5α *E.coli*

10 g Tryptone

5 g Yeast Extract

5 g Sodium Chloride

12 g Agar

Made up to 1L of dH_2O prior to autoclaving.

Once cooled to sufficient temp ampicillin is added when necessary.

7.2.5.3 **DH5α Strain**

This strain has endogenous *dam* and *dcm* methylation, ideal for screening DNA mutated via site directed mutagenesis, with the methylation sensitive restriction enzyme *Dpn*I.

Genotype: F– Φ80lacZΔM15 Δ(lacZYA-argF) U169 recA1 endA1 hsdR17 (rK–, mK+) phoA supE44 λ– thi-1 gyrA96 relA1 Supplied by Promega (Madison, WI, USA).

7.2.5.4 **Calcium chloride competent cell preparation**

Competent cells were prepared in accordance with (Sambrook *et al*., 1989). A single DH5α colony from a plate streaking, was inoculated into 5 ml of LB and grown O/N whilst shaking at 37°C. Of this, 1 ml was used as an inoculum into 100 ml of LB, grown whilst shaking at 37°C until logarithmic growth phase occurs at an $O.D_{600}$ of 0.5-0.6. Cells were pelleted at 5000 rpm for 10 minutes at 4°C,the supernatant discarded and the pellet resuspended in 100 ml of cold 100 mM $MgCl_2$ followed by incubation for 20-30min on ice. The cells are then pelleted once more for 10 minutes at 5000 rpm at 4°C, and resuspended in cold 100 mM $CaCl_2$ in 15 % glycerol solution. Aliquots of 200 µl cell suspension were then frozen at -80°C for later use.

7.2.5.5 **Transformation of competent cells**

For the transformation of DH5α *E.*coli cell approximately 50-100 ng of DNA was added to 100 µl of competent DH5α cells and incubated on ice for 20 minutes. The cells were heat shocked at 37°C for 5 minutes followed by 1 minute incubation on ice. The cells were then incubated in 450 µl of LB for 1 hour at 37°C for plasmid replication. The transformants are then plated onto selective LB agar plates containing 150 mg/ml ampicillin and incubated O/N at 37°C. Positive clones are picked and screened accordingly.

7.3 Protein Expression and Purification

7.3.1 Buffers

7.3.1.1 **Wash Buffer**

20 mM HEPES, pH 7.5, 0.5 M NaCl

7.3.1.2 **Elution buffer**

50 mM borate buffer pH 9.5

7.3.1.3 **Dialysis solution**

5 mM HEPES, pH 7.5, 0.1 mM PMSF (in ethanol)

7.3.1.4 **1X triton lysis buffer**

0.05 M HEPES, 0.5 M NaCl, 1% triton X-100, 1 mM PMSF

7.3.1.5 **Protease Inhibitor Cocktail**

Set III, Calbiochem, USA, 0.2 mM AEBSF, 0.16 M Aprotinin, 0.01 mM Bestatin, 3 µM E-64, 4 µM Leupeptin and 2 µM Pepstatin A

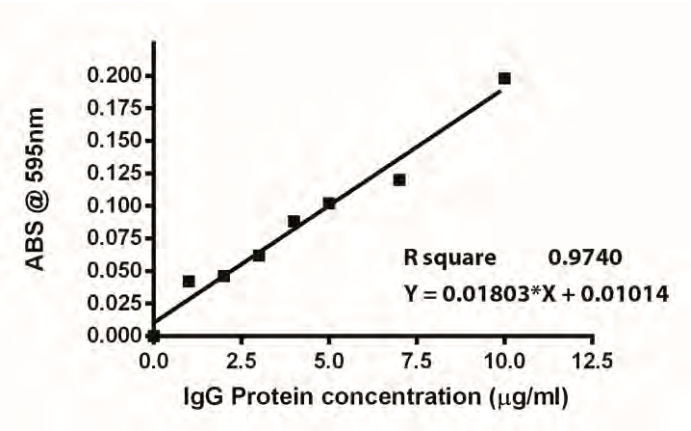

Figure 7.3 **Representative Bradford standard curve. IgG was used as a standard measure for ACE concentrations.**

7.3.2 Bradford Protein Concentration Determination

Protein concentration of full-length sACE was determined using the IgG curve and for single domain ACE (Ndom and tACE), the albumin curve was used. The curves were determined by linear regression analysis using GraphPad Prism 4.0 software.

7.4 Assay Constituents

7.4.1 Substrates and working stock preparations.

Table 7.1 **Sequence and manufacturer of all amyloid peptides used.**

Aβ peptides	Amino Acid Sequence	Manufacturer
Aβ(2-11)	Ac-AEFRHDSGYE-NH_2	A. K. Carmona
Aβ(4-10)	H-FRHDSGY-OH	China Peptides
Aβ(4-10)Q	Abz-FRHDSG(Q)-EDDnp	A. K. Carmona
Aβ(4-10)Y	Abz-FRHDSG -Y(3NO2)-OH	Biopep™
Aβ(1-16)Bach	H-DEAEFRHDSGYEVHHQK-OH	*© Bachem A G*
***Aβ(1-42)**	H-DAEFRHDSGYEVHHQKLVFFAEDVGSNKGAIIGLMVGGVVIA-OH	rPeptide™

7.4.1.1 **Aβ(2-11)**

Dissolved in 100 % DMSO, to form a 4.31 mM Stock solution. This was then diluted in 1XHEPES Buffer to a final DMSO concentration of 1% prior to performing any assay. This peptide had an absorbance maximum of 0.6 at 225nm.

7.4.1.2 **Aβ(4-10)**

Received 20 µl of 20 mM stock, in water thus, a simple dilution to a 200 µM working stock was made.

7.4.1.3 **Aβ(4-10)Q**

A stock of 289 µl of 4.31 mM was made in DMSO. This was then diluted out into 1XHEPES buffer to a working stock concentration of 88 µM.

7.4.1.4 **Aβ(4-10)Y**

A 10.5 mM stock was made in 500 µl in DMSO. For the assays a working stock of 100 µM was made up in 1XHEPES buffer.

7.4.1.5 **Aβ(1-16)**

1mg of Aβ(1-16) was dissolved into 51.2 µl of DMSO to a final concentration of 10 mM. Aliquots of 6.75 µl of this stock was then frozen at -80°C until required. To make working stocks 1XHEPES buffer was added to a final concentration of 500 µM.

7.4.1.6 **Aβ(1-42)**

1mg of Aβ(1-42) was dissolved into 88.8 µl of DMSO to a final concentration of 2.5 mM. The stock was then sonicated for 5 min, aliquots of 8 µl of this stock was then frozen at -80°C until required.

7.4.2 Buffers

7.4.2.1 **phosphate buffer**

100 mM $KHPO_4/KH_2PO_4$ (pH 8.3), 300 mM NaCl, 10 µM $ZnSO_4$

7.4.2.2 **IX HEPES assay Buffer**

50 mM HEPES buffer, 300 mM NaCl, 10 µM $ZnSO_4$

7.4.2.3 **AST-assay Buffer**

100 mM KHPO4/KH2PO4 pH 8.3, 300 mM NaCl, 10 µM ZnSO4, 1 mg/ml albumin

7.5 Standard Curves

7.5.1 HL Standard Curve

An HL product standard curve was generated to determine ACE activity using the synthetic ZPHL or HHL substrates.

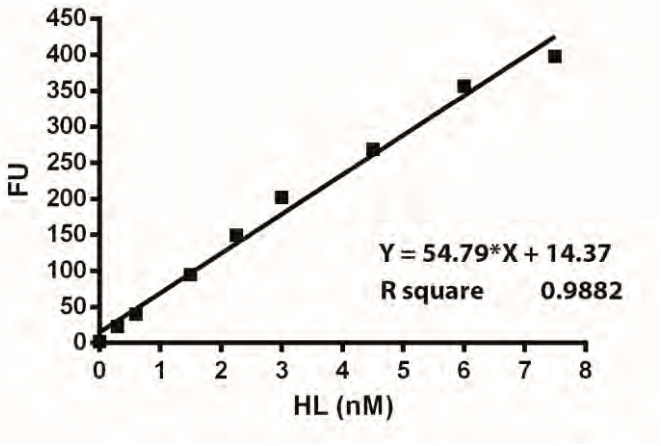

Figure 7.4 **HL standard curve for the determination of ACE activity towards the substrates HHL and ZFHL**

ACE activity is measured in mU defined as:

$$mU\ ACE = \frac{(FU) \times (\mu l\ of\ total\ reaction\ vol) \times (sample\ dilution\ factor)}{(Slope\ of\ HL\ std\ curve) \times (reaction\ time) \times (volume\ of\ sample\ assayed)}$$

7.5.2 Abz-Gly Standard Curve

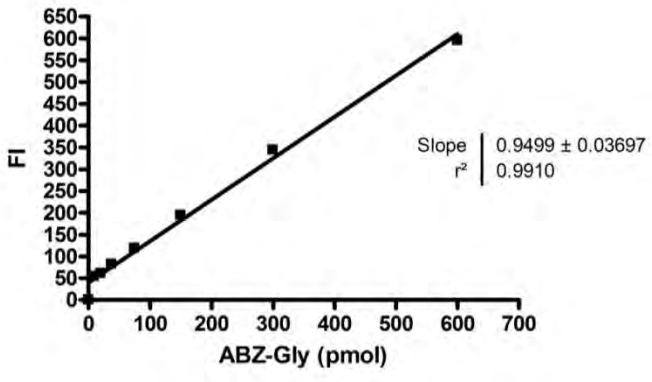

Figure 7.5 **A standard curve for the determination of product formed for all FRET substrates**

An Abz-product formation standard curve was generated for the determination of ACE activity on the two FRET substrates Aβ(4-10)Q and Aβ(4-10)Y.

7.5.3 Calibration curve of Aβ(1-14)

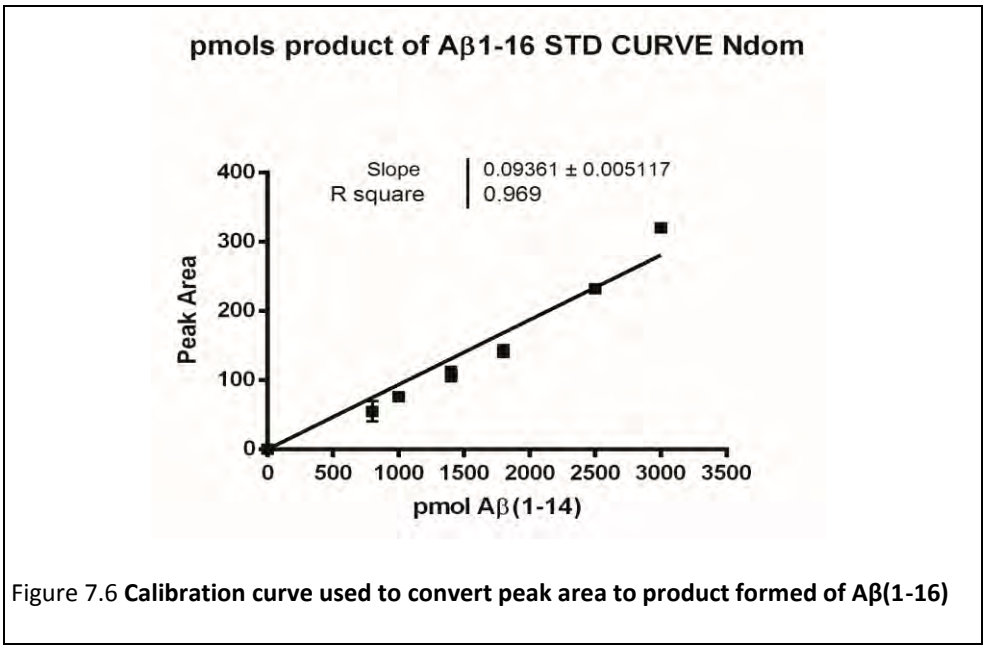

Figure 7.6 **Calibration curve used to convert peak area to product formed of Aβ(1-16)**

7.6 Cooperativity Kinetics Curves.

The Michaelis-Menten curves for the determination of all cooperative kinetics determined in Chapter 4.

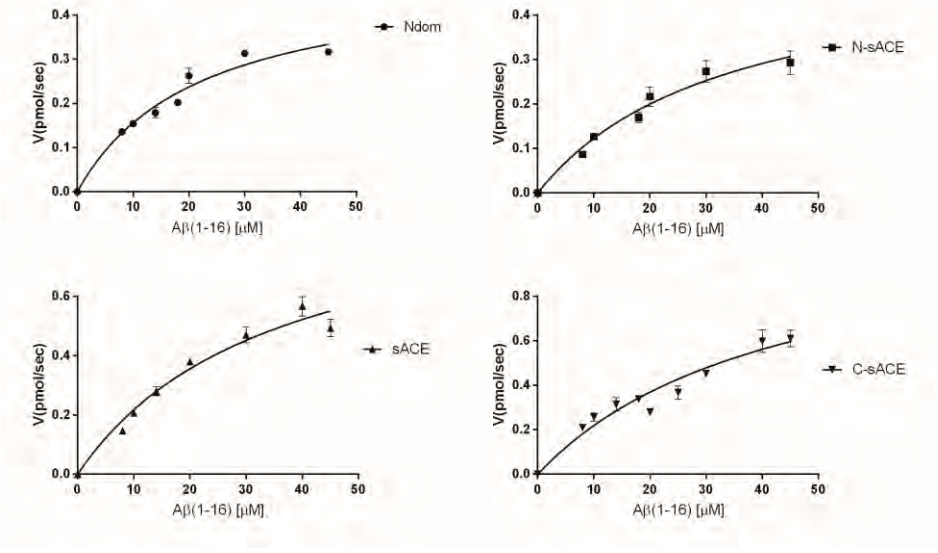

Figure 7.7 **Aβ(1-16) Michaelis-Menten curves for the determination of kinetic constants.**

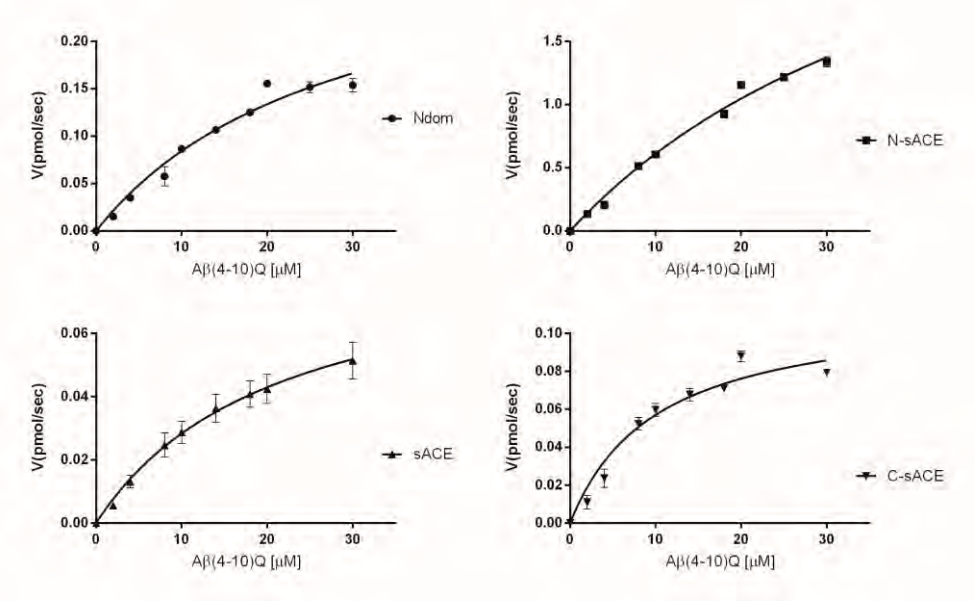

Figure 7.8 **Aβ(4-10)Q Michaelis-Menten curves for the determination of kinetic constants.**

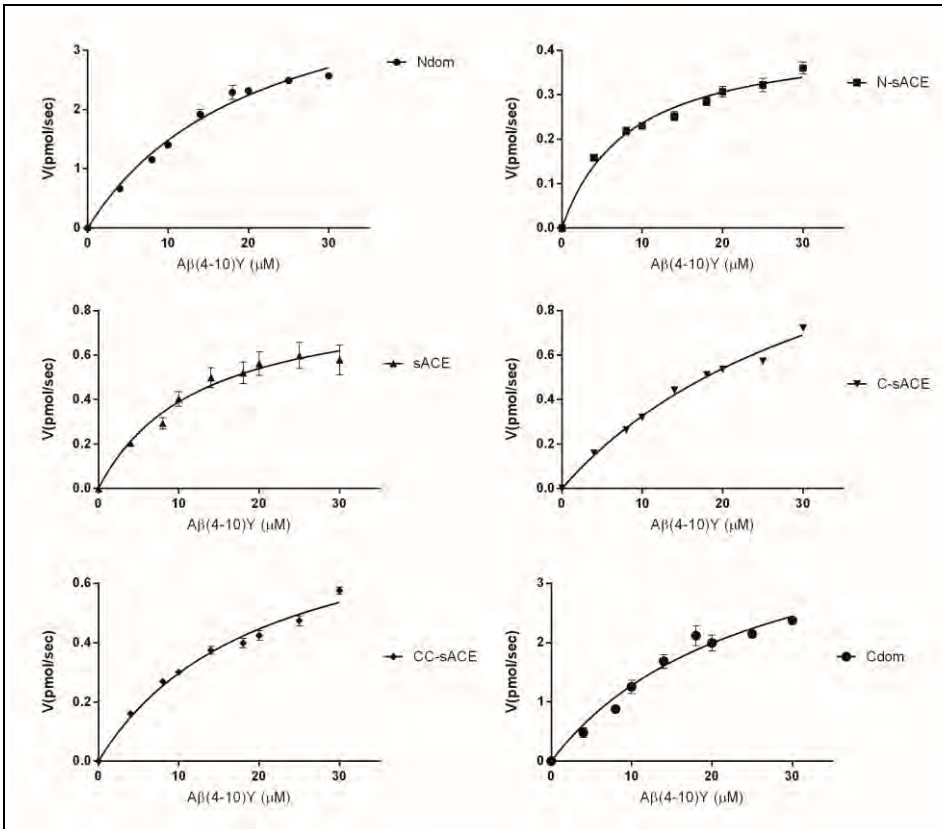

Figure 7.9 **Aβ(4-10)Y Michaelis-Menten curves for the determination of kinetic constants.**

7.7 Western blotting.

7.7.1.1 **Transfer Buffer**

20 mM Tris, 150 mM glycine, 20 % methanol

7.7.1.2 **Blocking buffer**

5% (w/v) skim milk, 0.1% (v/v) Tween-20, 0.2 M NaCl, 0.05 M Tris (pH7.4)

7.7.1.3 **TBS-T**

0.1% (v/v) Tween-20, 0.2 M NaCl, 0.05 M Tris (pH7.4)

7.7.1.4 **Laemmli Buffer**

20 % glycerol, 6 % SDS, 125mM Tris, 5 %β-mercaptoethanol, Bromophenol blue, pH 6.8

7.7.1.5 **SDS-PAGE Running conditions**

Protein detection of cell lysate or immunoprecipitation required that samples be mixed with laemmli buffer (20 % glycerol, 6 % SDS, 125mM Tris, 5 %β-mercaptoethanol, Bromophenol blue, pH 6.8) and separated by SDS-PAGE using the Mini PROTEAN^{TM} III system (BIO-RAD,USA). For the resolution of high molecular weight proteins like sACE, 8 % resolving gels (final concentrations of 0.4 %SDS, 1.5 M Tris, pH 8.8) and 3% stacking gels (final concentrations of 0.1 %SDS, 125 mM Tris, pH 6.8) were used.

7.8 Mass spectrometry.

7.8.1 Buffers

7.8.1.1 **RIPA buffer**

150 mM NaCl, 50 mM triethylammonium bicarbonate, 1 % SDS, 0.5 % deoxycholate, (pH 8)

7.8.2 Representative Spectra and transitions

7.8.2.1 **Representative traces from the TSQ-Vantage of lisinopril treatment and induced Ser1270-phosphoyrlation**

Lisinopril 200 nM treatment of sACE expressing CHO cells for 0, 5 and 7 minutes. Targeted mass spectrometry traces of the un-modified HSHGPQFGSEVELR (Figure 7.11) and Ser1270-phosphorylated HSHGPQFG**S**EVELR peptides (Figure 7.10). The transition lists used to perform the targeted analysis are found in (Table 7.2).

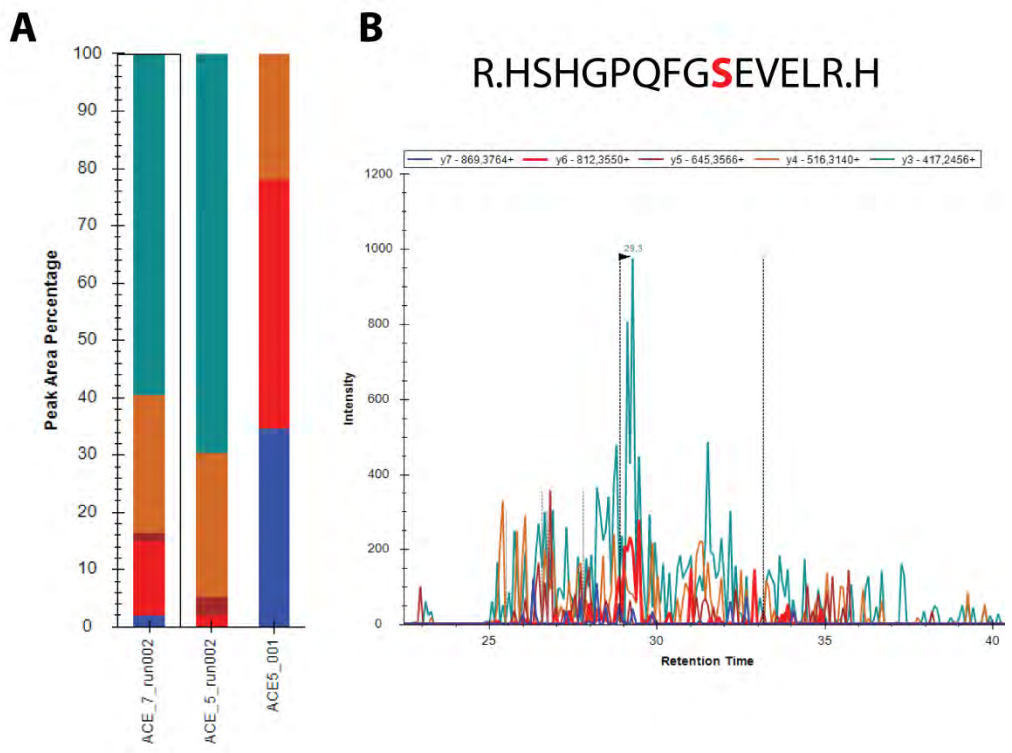

Figure 7.10 **The S1270 phosphorylated peptide, lisinopril 200 nM treatment, traces with poor transitions above background.** The total ion count however correlated to the increase of the y6-daughter ion well.**A)** Replicates peak area percentage bar graph as an indication of ion signal reproducibility or changes. **B)** The chromatogram trace from the TSQ-Vantage.

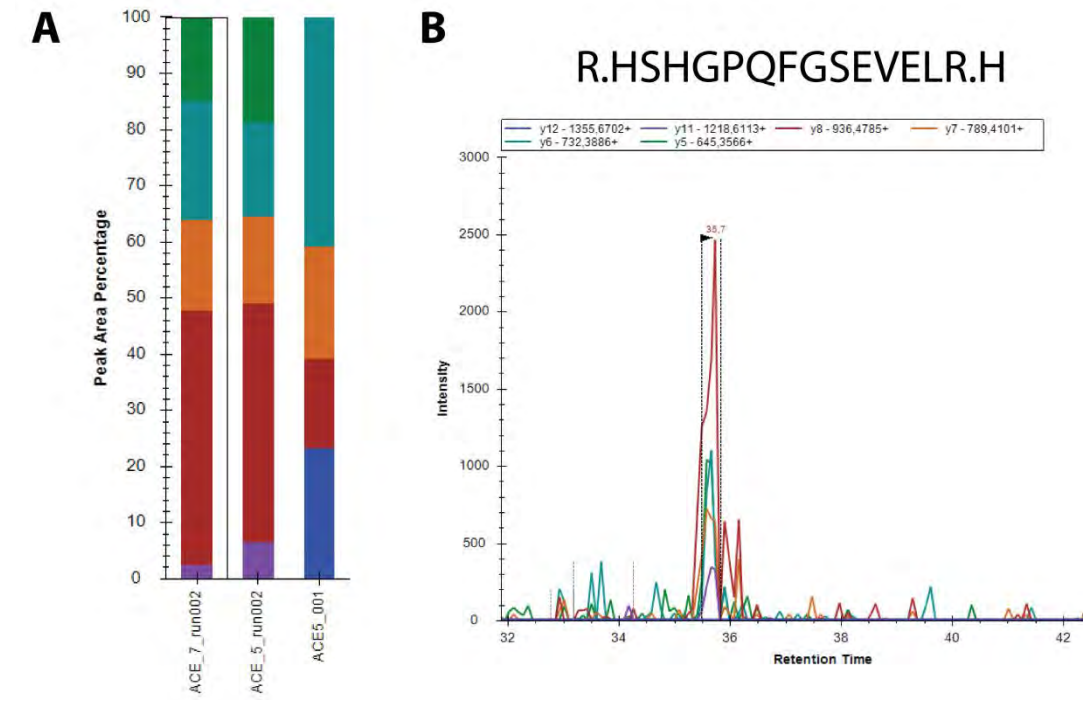

Figure 7.11 **The parent unphosphorylated peptide of lisinopril 200 nM treatment, traces with good transitions above background. A)** Replicates peak area percentage bar graph as an indication of ion signal reproducibility or changes. **B)** The chromatogram trace from the TSQ-Vantage.

Table 7.2 **Transition list and settings used on the TSQ-Vantage.**

Parent ion (m/z)	Product ion (m/z)	Collision Energy	Start time	Stop time	Polarity	Trigger	Reference	corresponding peptide
404.709	466.241	15	0	90	1	1	0	WGVFSGR
404.709	565.309	15	0	90	1	1	0	WGVFSGR
404.709	622.331	15	0	90	1	1	0	WGVFSGR
479.219	405.685	17	0	90	1	1	0	FVEEYDR
479.219	582.252	17	0	90	1	1	0	FVEEYDR
479.219	711.294	17	0	90	1	1	0	FVEEYDR
490.284	554.297	18	0	90	1	1	0	AILQFYPK
490.284	682.356	18	0	90	1	1	0	AILQFYPK
490.284	795.44	18	0	90	1	1	0	AILQFYPK
507.746	399.709	18	0	90	1	1	0	SEGPLPDSGR
507.746	531.252	18	0	90	1	1	0	SEGPLPDSGR
507.746	741.389	18	0	90	1	1	0	SEGPLPDSGR
507.746	798.41	18	0	90	1	1	0	SEGPLPDSGR
518.241	487.251	19	0	90	1	1	0	TQGDFDPGAK
518.241	634.32	19	0	90	1	1	0	TQGDFDPGAK
518.241	806.368	19	0	90	1	1	0	TQGDFDPGAK
527.259	209.126	27	0	90	1	1	0	HSHGPQFGSEVELR
527.259	258.66	27	0	90	1	1	0	HSHGPQFGSEVELR
527.259	323.182	27	0	90	1	1	0	HSHGPQFGSEVELR
527.259	366.698	27	0	90	1	1	0	HSHGPQFGSEVELR
527.259	395.208	27	0	90	1	1	0	HSHGPQFGSEVELR
527.259	417.245	27	0	90	1	1	0	HSHGPQFGSEVELR
527.259	468.743	27	0	90	1	1	0	HSHGPQFGSEVELR
527.259	516.313	27	0	90	1	1	0	HSHGPQFGSEVELR
527.259	532.772	27	0	90	1	1	0	HSHGPQFGSEVELR
527.259	581.298	27	0	90	1	1	0	HSHGPQFGSEVELR
527.259	609.809	27	0	90	1	1	0	HSHGPQFGSEVELR
527.259	645.356	27	0	90	1	1	0	HSHGPQFGSEVELR
527.259	678.338	27	0	90	1	1	0	HSHGPQFGSEVELR
527.259	732.388	27	0	90	1	1	0	HSHGPQFGSEVELR
527.259	789.409	27	0	90	1	1	0	HSHGPQFGSEVELR
527.259	936.478	27	0	90	1	1	0	HSHGPQFGSEVELR
527.259	1064.536	26	0	90	1	1	0	HSHGPQFGSEVELR
527.259	1161.589	25	0	90	1	1	0	HSHGPQFGSEVELR
527.259	1218.611	24	0	90	1	1	0	HSHGPQFGSEVELR
527.259	1355.67	23	0	90	1	1	0	HSHGPQFGSEVELR
553.914	209.126	28	0	90	1	1	0	HSHGPQFGS[Phosphoryl]EVELR
553.914	258.66	28	0	90	1	1	0	HSHGPQFGS[Phosphoryl]EVELR
553.914	323.182	28	0	90	1	1	0	HSHGPQFGS[Phosphoryl]EVELR
553.914	406.681	28	0	90	1	1	0	HSHGPQFGS[Phosphoryl]EVELR
553.914	417.245	28	0	90	1	1	0	HSHGPQFGS[Phosphoryl]EVELR
553.914	435.192	28	0	90	1	1	0	HSHGPQFGS[Phosphoryl]EVELR
553.914	508.726	28	0	90	1	1	0	HSHGPQFGS[Phosphoryl]EVELR
553.914	516.313	28	0	90	1	1	0	HSHGPQFGS[Phosphoryl]EVELR
553.914	572.755	28	0	90	1	1	0	HSHGPQFGS[Phosphoryl]EVELR
553.914	621.281	28	0	90	1	1	0	HSHGPQFGS[Phosphoryl]EVELR
553.914	645.356	28	0	90	1	1	0	HSHGPQFGS[Phosphoryl]EVELR
553.914	649.792	28	0	90	1	1	0	HSHGPQFGS[Phosphoryl]EVELR
553.914	718.322	28	0	90	1	1	0	HSHGPQFGS[Phosphoryl]EVELR
553.914	812.354	28	0	90	1	1	0	HSHGPQFGS[Phosphoryl]EVELR
553.914	869.376	28	0	90	1	1	0	HSHGPQFGS[Phosphoryl]EVELR
553.914	1016.444	28	0	90	1	1	0	HSHGPQFGS[Phosphoryl]EVELR
553.914	1144.503	26	0	90	1	1	0	HSHGPQFGS[Phosphoryl]EVELR
553.914	1241.556	25	0	90	1	1	0	HSHGPQFGS[Phosphoryl]EVELR
553.914	1298.577	25	0	90	1	1	0	HSHGPQFGS[Phosphoryl]EVELR
553.914	1435.636	23	0	90	1	1	0	HSHGPQFGS[Phosphoryl]EVELR
588.822	559.295	21	0	90	1	1	0	YVELINQAAR
588.822	672.379	21	0	90	1	1	0	YVELINQAAR
588.822	914.505	21	0	90	1	1	0	YVELINQAAR
676.815	620.273	23	0	90	1	1	0	LNGYVDAGDSWR
676.815	806.343	23	0	90	1	1	0	LNGYVDAGDSWR
676.815	905.411	23	0	90	1	1	0	LNGYVDAGDSWR
681.817	637.346	23	0	90	1	1	0	YNFDWWYLR
681.817	938.452	23	0	90	1	1	0	YNFDWWYLR
681.817	1085.52	23	0	90	1	1	0	YNFDWWYLR
708.813	753.368	24	0	90	1	1	0	QDGFTDTGAYWR
708.813	868.395	24	0	90	1	1	0	QDGFTDTGAYWR
708.813	969.442	24	0	90	1	1	0	QDGFTDTGAYWR
738.372	610.793	25	0	90	1	1	0	AALPAQELEEYNK
738.372	667.335	25	0	90	1	1	0	AALPAQELEEYNK
738.372	1220.579	25	0	90	1	1	0	AALPAQELEEYNK
762.847	561.314	26	0	90	1	1	0	ENYNQEWWSLR
762.847	747.394	26	0	90	1	1	0	ENYNQEWWSLR
762.847	876.436	26	0	90	1	1	0	ENYNQEWWSLR
766.907	688.337	26	0	90	1	1	0	VSFLGLDLDAQQAR
766.907	916.448	26	0	90	1	1	0	VSFLGLDLDAQQAR
766.907	1086.554	26	0	90	1	1	0	VSFLGLDLDAQQAR
790.384	209.126	30	0	90	1	1	0	HSHGPQFGSEVELR
790.384	258.66	30	0	90	1	1	0	HSHGPQFGSEVELR
790.384	323.182	30	0	90	1	1	0	HSHGPQFGSEVELR
790.384	366.698	30	0	90	1	1	0	HSHGPQFGSEVELR
790.384	395.208	30	0	90	1	1	0	HSHGPQFGSEVELR
790.384	417.245	30	0	90	1	1	0	HSHGPQFGSEVELR
790.384	468.743	30	0	90	1	1	0	HSHGPQFGSEVELR
790.384	516.313	30	0	90	1	1	0	HSHGPQFGSEVELR
790.384	532.772	30	0	90	1	1	0	HSHGPQFGSEVELR
790.384	581.298	30	0	90	1	1	0	HSHGPQFGSEVELR
790.384	609.809	30	0	90	1	1	0	HSHGPQFGSEVELR
790.384	645.356	30	0	90	1	1	0	HSHGPQFGSEVELR
790.384	678.338	30	0	90	1	1	0	HSHGPQFGSEVELR
790.384	732.388	30	0	90	1	1	0	HSHGPQFGSEVELR
790.384	789.409	30	0	90	1	1	0	HSHGPQFGSEVELR

Table 8.2 continued.

Parent ion (m/z)	Product ion (m/z)	Collision Energy	Start time	Stop time	Polarity	Trigger	Reference	corresponding peptide
790.384	936.478	30	0	90	1	1	0	HSHGPQFGSEVELR
790.384	1064.536	30	0	90	1	1	0	HSHGPQFGSEVELR
790.384	1161.589	29	0	90	1	1	0	HSHGPQFGSEVELR
790.384	1218.611	28	0	90	1	1	0	HSHGPQFGSEVELR
790.384	1355.67	27	0	90	1	1	0	HSHGPQFGSEVELR
827.837	195.608	35	0	90	1	1	0	VGQWLLLFLGIALLVATLGLSQR
827.837	252.15	35	0	90	1	1	0	VGQWLLLFLGIALLVATLGLSQR
827.837	280.661	35	0	90	1	1	0	VGQWLLLFLGIALLVATLGLSQR
827.837	337.203	35	0	90	1	1	0	VGQWLLLFLGIALLVATLGLSQR
827.837	387.727	35	0	90	1	1	0	VGQWLLLFLGIALLVATLGLSQR
827.837	390.209	35	0	90	1	1	0	VGQWLLLFLGIALLVATLGLSQR
827.837	423.245	35	0	90	1	1	0	VGQWLLLFLGIALLVATLGLSQR
827.837	472.779	35	0	90	1	1	0	VGQWLLLFLGIALLVATLGLSQR
827.837	503.293	35	0	90	1	1	0	VGQWLLLFLGIALLVATLGLSQR
827.837	529.322	35	0	90	1	1	0	VGQWLLLFLGIALLVATLGLSQR
827.837	560.314	35	0	90	1	1	0	VGQWLLLFLGIALLVATLGLSQR
827.837	585.864	35	0	90	1	1	0	VGQWLLLFLGIALLVATLGLSQR
827.837	621.382	35	0	90	1	1	0	VGQWLLLFLGIALLVATLGLSQR
827.837	673.399	35	0	90	1	1	0	VGQWLLLFLGIALLVATLGLSQR
827.837	677.924	35	0	90	1	1	0	VGQWLLLFLGIALLVATLGLSQR
827.837	706.435	35	0	90	1	1	0	VGQWLLLFLGIALLVATLGLSQR
827.837	762.977	35	0	90	1	1	0	VGQWLLLFLGIALLVATLGLSQR
827.837	774.446	35	0	90	1	1	0	VGQWLLLFLGIALLVATLGLSQR
827.837	836.511	35	0	90	1	1	0	VGQWLLLFLGIALLVATLGLSQR
827.837	845.483	35	0	90	1	1	0	VGQWLLLFLGIALLVATLGLSQR
827.837	893.053	35	0	90	1	1	0	VGQWLLLFLGIALLVATLGLSQR
827.837	944.552	35	0	90	1	1	0	VGQWLLLFLGIALLVATLGLSQR
827.837	949.595	35	0	90	1	1	0	VGQWLLLFLGIALLVATLGLSQR
827.837	1006.137	35	0	90	1	1	0	VGQWLLLFLGIALLVATLGLSQR
827.837	1057.636	35	0	90	1	1	0	VGQWLLLFLGIALLVATLGLSQR
827.837	1099.177	35	0	90	1	1	0	VGQWLLLFLGIALLVATLGLSQR
827.837	1163.206	35	0	90	1	1	0	VGQWLLLFLGIALLVATLGLSQR
827.837	1170.72	35	0	90	1	1	0	VGQWLLLFLGIALLVATLGLSQR
827.837	1241.757	35	0	90	1	1	0	VGQWLLLFLGIALLVATLGLSQR
827.837	1354.841	35	0	90	1	1	0	VGQWLLLFLGIALLVATLGLSQR
827.837	1411.863	35	0	90	1	1	0	VGQWLLLFLGIALLVATLGLSQR
830.367	209.126	32	0	90	1	1	0	HSHGPQFGS[Phosphoryl]EVELR
830.367	258.66	32	0	90	1	1	0	HSHGPQFGS[Phosphoryl]EVELR
830.367	323.182	32	0	90	1	1	0	HSHGPQFGS[Phosphoryl]EVELR
830.367	406.681	32	0	90	1	1	0	HSHGPQFGS[Phosphoryl]EVELR
830.367	417.245	32	0	90	1	1	0	HSHGPQFGS[Phosphoryl]EVELR
830.367	435.192	32	0	90	1	1	0	HSHGPQFGS[Phosphoryl]EVELR
830.367	508.726	32	0	90	1	1	0	HSHGPQFGS[Phosphoryl]EVELR
830.367	516.313	32	0	90	1	1	0	HSHGPQFGS[Phosphoryl]EVELR
830.367	572.755	32	0	90	1	1	0	HSHGPQFGS[Phosphoryl]EVELR
830.367	621.281	32	0	90	1	1	0	HSHGPQFGS[Phosphoryl]EVELR
830.367	645.356	32	0	90	1	1	0	HSHGPQFGS[Phosphoryl]EVELR
830.367	649.792	32	0	90	1	1	0	HSHGPQFGS[Phosphoryl]EVELR
830.367	718.322	32	0	90	1	1	0	HSHGPQFGS[Phosphoryl]EVELR
830.367	812.354	32	0	90	1	1	0	HSHGPQFGS[Phosphoryl]EVELR
830.367	869.376	32	0	90	1	1	0	HSHGPQFGS[Phosphoryl]EVELR
830.367	1016.444	31	0	90	1	1	0	HSHGPQFGS[Phosphoryl]EVELR
830.367	1144.503	30	0	90	1	1	0	HSHGPQFGS[Phosphoryl]EVELR
830.367	1241.556	29	0	90	1	1	0	HSHGPQFGS[Phosphoryl]EVELR
830.367	1298.577	29	0	90	1	1	0	HSHGPQFGS[Phosphoryl]EVELR
830.367	1435.636	27	0	90	1	1	0	HSHGPQFGS[Phosphoryl]EVELR
862.962	604.284	29	0	90	1	1	0	IAFLPFGYLVDQWR
862.962	640.825	29	0	90	1	1	0	IAFLPFGYLVDQWR
862.962	1280.642	29	0	90	1	1	0	IAFLPFGYLVDQWR
877.967	489.257	29	0	90	1	1	0	IAFIPFSYLVDQWR
877.967	604.284	29	0	90	1	1	0	IAFIPFSYLVDQWR
877.967	1310.653	29	0	90	1	1	0	IAFIPFSYLVDQWR
1241.251	195.608	35	0	90	1	1	0	VGQWLLLFLGIALLVATLGLSQR
1241.251	252.15	35	0	90	1	1	0	VGQWLLLFLGIALLVATLGLSQR
1241.251	280.661	35	0	90	1	1	0	VGQWLLLFLGIALLVATLGLSQR
1241.251	337.203	35	0	90	1	1	0	VGQWLLLFLGIALLVATLGLSQR
1241.251	387.727	35	0	90	1	1	0	VGQWLLLFLGIALLVATLGLSQR
1241.251	390.209	35	0	90	1	1	0	VGQWLLLFLGIALLVATLGLSQR
1241.251	423.245	35	0	90	1	1	0	VGQWLLLFLGIALLVATLGLSQR
1241.251	472.779	35	0	90	1	1	0	VGQWLLLFLGIALLVATLGLSQR
1241.251	503.293	35	0	90	1	1	0	VGQWLLLFLGIALLVATLGLSQR
1241.251	529.322	35	0	90	1	1	0	VGQWLLLFLGIALLVATLGLSQR
1241.251	560.314	35	0	90	1	1	0	VGQWLLLFLGIALLVATLGLSQR
1241.251	585.864	35	0	90	1	1	0	VGQWLLLFLGIALLVATLGLSQR
1241.251	621.382	35	0	90	1	1	0	VGQWLLLFLGIALLVATLGLSQR
1241.251	673.399	35	0	90	1	1	0	VGQWLLLFLGIALLVATLGLSQR
1241.251	677.924	35	0	90	1	1	0	VGQWLLLFLGIALLVATLGLSQR
1241.251	706.435	35	0	90	1	1	0	VGQWLLLFLGIALLVATLGLSQR
1241.251	762.977	35	0	90	1	1	0	VGQWLLLFLGIALLVATLGLSQR
1241.251	774.446	35	0	90	1	1	0	VGQWLLLFLGIALLVATLGLSQR
1241.251	836.511	35	0	90	1	1	0	VGQWLLLFLGIALLVATLGLSQR
1241.251	845.483	35	0	90	1	1	0	VGQWLLLFLGIALLVATLGLSQR
1241.251	893.053	35	0	90	1	1	0	VGQWLLLFLGIALLVATLGLSQR
1241.251	944.552	35	0	90	1	1	0	VGQWLLLFLGIALLVATLGLSQR
1241.251	949.595	35	0	90	1	1	0	VGQWLLLFLGIALLVATLGLSQR
1241.251	1006.137	35	0	90	1	1	0	VGQWLLLFLGIALLVATLGLSQR
1241.251	1057.636	35	0	90	1	1	0	VGQWLLLFLGIALLVATLGLSQR
1241.251	1099.177	35	0	90	1	1	0	VGQWLLLFLGIALLVATLGLSQR
1241.251	1163.206	35	0	90	1	1	0	VGQWLLLFLGIALLVATLGLSQR
1241.251	1170.72	35	0	90	1	1	0	VGQWLLLFLGIALLVATLGLSQR
1241.251	1241.757	35	0	90	1	1	0	VGQWLLLFLGIALLVATLGLSQR
1241.251	1354.841	35	0	90	1	1	0	VGQWLLLFLGIALLVATLGLSQR
1241.251	1411.863	35	0	90	1	1	0	VGQWLLLFLGIALLVATLGLSQR

7.8.2.2 **Representative traces from the Q-Exactive of lisinopril treatment and induced Ser1270-phosphoyrlation**

Using the shorter Easy column, optimisation targeted runs determined the best charge state for to reach the highest signal were doubly charged. The S1270-phosphorylation was detected here at 7 min treatment with lisinopril, and there appeared to be a retention time delay with the presence of the phosphor-Ser1270.

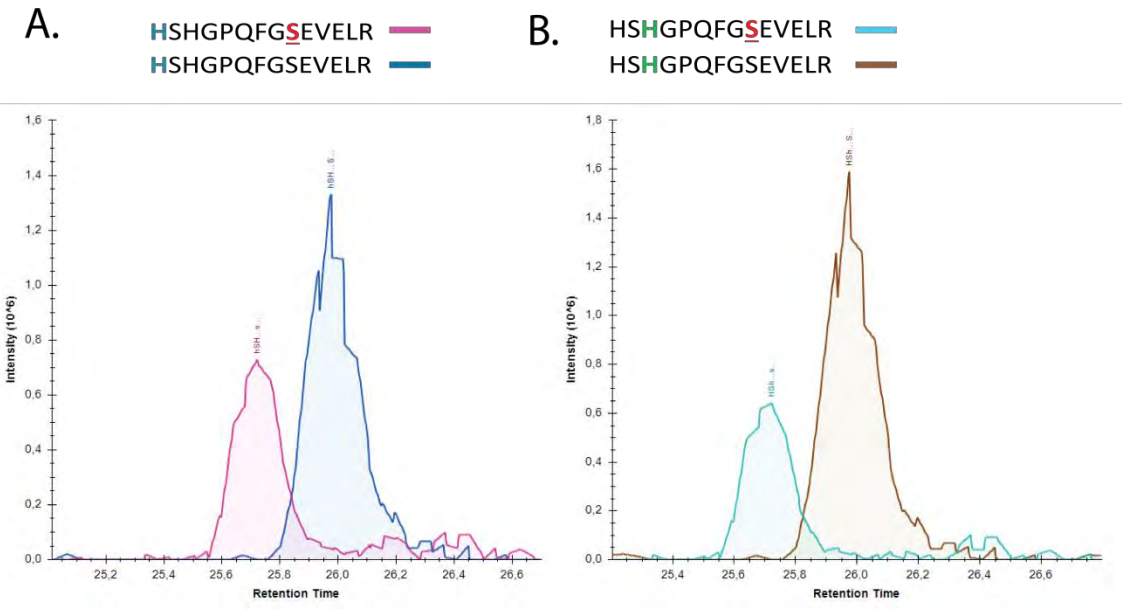

Figure 7.12 **Total ion peaks from targeted optimisation on the Q-Exactive, indicating the retention shift on phosphorylation of Ser1270 in ACE's cytoplasmic tail. A)** Group 2, histidine and phosphor Ser1270 combination traces, with a peak shift from 25.7 min (phosphor-S1270) to 26.2 min (parent with one histidine oxidation). **B)** Group 3, histidine and pSer1270 combination traces, with the same time shift found in group 2. Note the much larger signal intensity of these histidine oxidation modification peptides.

8 REFERNCES

Abbott, N.J., 2004. Evidence for bulk flow of brain interstitial fluid: Significance for physiology and pathology. Neurochem. Int. doi:10.1016/j.neuint.2003.11.006

Abdul-Hay, S.O., Kang, D., McBride, M., Li, L., Zhao, J., Leissring, M.A., 2011. Deletion of Insulin-degrading enzyme elicits Antipodal, age-dependent effects on glucose and insulin tolerance. PLoS One 6, e20818. doi:10.1371/journal.pone.0020818

Acharya, K.R., Sturrock, E.D., Riordan, J.F., Ehlers, M.R.W., 2003. Ace revisited: a new target for structure-based drug design. Nat. Rev. Drug Discov. 2, 891–902. doi:10.1038/nrd1227

Agarwal, D., Dange, R.B., Raizada, M.K., Francis, J., 2013. Angiotensin II causes imbalance between pro- and anti-inflammatory cytokines by modulating GSK-3?? in neuronal culture. Br. J. Pharmacol. 169, 860–874. doi:10.1111/bph.12177

Ahmed, M., Davis, J., Aucoin, D., Sato, T., Ahuja, S., Aimoto, S., Elliott, J.I., Van Nostrand, W.E., Smith, S.O., 2010. Structural conversion of neurotoxic amyloid-beta(1-42) oligomers to fibrils. Nat. Struct. Mol. Biol. 17, 561–567. doi:10.1038/nsmb.1799

Akter, K., Lanza, E.A., Martin, S.A., Myronyuk, N., Rua, M., Raffa, R.B., 2011. Diabetes mellitus and Alzheimer's disease: Shared pathology and treatment? Br. J. Clin. Pharmacol. 71, 365–376. doi:10.1111/j.1365-2125.2010.03830.x

Albiston, A.L., Mustafa, T., McDowall, S.G., Mendelsohn, F.A.O., Lee, J., Chai, S.Y., 2003. AT4 receptor is insulin-regulated membrane aminopeptidase: Potential mechanisms of memory enhancement. Trends Endocrinol. Metab. doi:10.1016/S1043-2760(02)00037-1

Almquist, R.G., Chao, W.R., Ellis, M.E., Johnson, H.L., 1980. Synthesis and biological activity of a ketomethylene analogue of a tripeptide inhibitor of angiotensin converting enzyme. J. Med. Chem. 23, 1392–1398.

Alzheimer, A., 1907. Über eine eigenartige Eskrankung der Nirnrinde. Allg. Zeitschrift fur Psychiatr. 64, 146–148.

Alzheimer's Association, 2013. 2013 Alzheimer ' s disease facts and figures. Alzheimer's Dement. 9, 1–71.

Amor, S., Puentes, F., Baker, D., van der Valk, P., 2010. Inflammation in neurodegenerative diseases. Immunology 129, 154–69. doi:10.1111/j.1365-2567.2009.03225.x

Andreou, L.V., 2013. Preparation of genomic DNA from bacteria. Methods Enzymol. 529, 143–151. doi:10.1016/B978-0-12-418687-3.00011-2

Andújar-Sánchez, M., Cámara-Artigas, A., Jara-Pérez, V., 2004. A calorimetric study of the binding of lisinopril, enalaprilat and captopril to angiotensin-

converting enzyme. Biophys. Chem. 111, 183–9. doi:10.1016/j.bpc.2004.05.011

Andújar-Sánchez, M., Jara-Pérez, V., Cámara-Artigas, A., 2007. Thermodynamic determination of the binding constants of angiotensin-converting enzyme inhibitors by a displacement method. FEBS Lett. 581, 3449–54. doi:10.1016/j.febslet.2007.06.048

Annaert, W., De Strooper, B., 2002. A cell biological perspective on Alzheimer's disease. Annu. Rev. Cell Dev. Biol. 18, 25–51. doi:10.1146/annurev.cellbio.18.020402.142302

Anthony, C.S., Corradi, H.R., Schwager, S.L.U., Redelinghuys, P., Georgiadis, D., Dive, V., Acharya, K.R., Sturrock, E.D., 2010. The N domain of human angiotensin-I-converting enzyme: The role of N-glycosylation and the crystal structure in complex with an N domain-specific phosphinic inhibitor, RXP407. J. Biol. Chem. 285, 35685–35693. doi:10.1074/jbc.M110.167866

Anthony, C.S., Masuyer, G., Sturrock, E.D., Acharya, K.R., 2012. Structure Based Drug Design of Angiotensin-I Converting Enzyme Inhibitors. Curr. Med. Chem. doi:10.2174/092986712799034950

Apelt, J., Ach, K., Schliebs, R., 2003. Aging-related down-regulation of neprilysin, a putative Aβ-amyloid-degrading enzyme, in transgenic Tg2576 Alzheimer-like mouse brain is accompanied by an astroglial upregulation in the vicinity of Aβ-amyloid plaques. Neurosci. Lett. 339, 183–186. doi:10.1016/S0304-3940(03)00030-2

Araujo, M.C., Melo, R.I., Del Nery, E., Alves, M.F., Juliano, M.A., Casarini, D.E., Juliano, L., Carmona, A.K., 1999. Internally quenched fluorogenic substrates for angiotensin I-converting enzyme. J. Hypertens. 17, 665–672. doi:10.1097/00004872-199917050-00010

Araujo, M.C., Melo, R.L., Cesari, M.H., Juliano, M.A., Juliano, L., Carmona, A.K., 2000. Peptidase specificity characterization of C- and N-terminal catalytic sites of angiotensin I-converting enzyme. Biochemistry 39, 8519–8525. doi:10.1021/bi9928905

Arbel-Ornath, M., Hudry, E., Eikermann-Haerter, K., Hou, S., Gregory, J.L., Zhao, L., Betensky, R.A., Frosch, M.P., Greenberg, S.M., Bacskai, B.J., 2013. Interstitial fluid drainage is impaired in ischemic stroke and Alzheimer's disease mouse models. Acta Neuropathol. 126, 353–364. doi:10.1007/s00401-013-1145-2

Arnott, D., Gawinowicz, M.A., Grant, R.A., Neubert, T.A., Packman, L.C., Speicher, K.D., Stone, K., Turck, C.W., 2003. ABRF-PRG03: Phosphorylation site determination. J. Biomol. Tech. 14, 205–215.

Arriagada, P. V, Growdon, J.H., Hedley-Whyte, E.T., Hyman, B.T., 1992. Neurofibrillary tangles but not senile plaques parallel duration and severity of Alzheimer's disease. Neurology 42, 631–639. doi:10.1212/WNL.42.3.631

Ashby, E., Baig, S., Harrison, R., Tayler, H., Speedy, E., Prince, A., Love, S., Kehoe, P.G., 2009. Angiotensin-converting enzyme levels and activity in Alzheimer ' s disease : differences in brain and CSF ACE and association with ACE1 genotypes. Am. J. Transl. Res. Res. 1, 163–177.

Assaf, S.Y., Chung, S.H., 1984. Release of endogenous Zn2+ from brain tissue during

activity. Nature 308, 734–736. doi:10.1038/308734a0

Auerbach, I.D., Vinters, H. V, 2006. Effects of anoxia and hypoxia on amyloid precursor protein processing in cerebral microvascular smooth muscle cells. J. Neuropathol. Exp. Neurol. 65, 610–620. doi:10.1097/00005072-200606000-00009

Aviles, F.X., Vendrell, J., Ventura, S., Sanchez De Groot, N., 2006. Mutagenesis of the central hydrophobic cluster in Ab42 Alzheimer's peptide. FEBS J. 273, 658–668. doi:10.1111/j.1742-4658.2005.05102.x

Azizi, M., Junot, C., Ezan, E., Ménard, J., 2001. Angiotensin I-converting enzyme and metabolism of the haematological peptide N-acetyl-seryl-aspartyl-lysyl-proline, in: Clinical and Experimental Pharmacology and Physiology. Centre d'Investigations Cliniques, Hopital Georges Pompidou, Inserm/Assistance Publique des Hopitaux de Paris, Paris, France. michel.azizi@egp.ap-hop-paris.fr, pp. 1066–1069. doi:10.1046/j.1440-1681.2001.03560.x

Azizi, M., Rousseau, A., Ezan, E., Guyene, T.T., Michelet, S., Grognet, J.M., Lenfant, M., Corvol, P., Ménard, J., 1996. Acute angiotensin-converting enzyme inhibition increases the plasma level of the natural stem cell regulator N-acetyl-seryl-aspartyl-lysyl-proline. J. Clin. Invest. 97, 839–844. doi:10.1172/JCI118484

Backstrom, J.R., Lim, G.P., Cullen, M.J., Tökés, Z.A., 1996. Matrix metalloproteinase-9 (MMP-9) is synthesized in neurons of the human hippocampus and is capable of degrading the amyloid-beta peptide (1-40). J. Neurosci. 16, 7910–7919.

Balyasnikova, I. V, Karran, E.H., Albrecht, R.F., Danilov, S.M., 2002. Epitope-specific antibody-induced cleavage of angiotensin-converting enzyme from the cell surface. Biochem. J. 362, 585–595. doi:10.1042/0264-6021:3620585

Balyasnikova, I. V, Metzger, R., Franke, F.E., Danilov, S.M., 2003. Monoclonal antibodies to denatured human ACE (CD 143), broad species specificity, reactivity on paraffin sections, and detection of subtle conformational changes in the C-terminal domain of ACE. Tissue Antigens 61, 49–62.

Balyasnikova, I. V, Woodman, Z.L., Albrecht, R.F., Natesh, R., Acharya, K.R., Sturrock, E.D., Danilov, S.M., 2005. Localization of an N-domain region of angiotensin-converting enzyme involved in the regulation of ectodomain shedding using monoclonal antibodies. J. Proteome Res. 4, 258–267. doi:10.1021/pr049859w

Barauna, V.G., Campos, L.C.G., Miyakawa, A.A., Krieger, J.E., 2011. ACE as a mechanosensor to shear stress influences the control of its own regulation via phosphorylation of cytoplasmic Ser(1270). PLoS One 6, e22803. doi:10.1371/journal.pone.0022803

Barnes, J.M., Barnes, N.M., Costall, B., Horovitz, Z.P., Ironside, J.W., Naylor, R.J., Williams, T.J., 1990. Angiotensin II inhibits acetylcholine release from human temporal cortex: implications for cognition. Brain Res. 507, 341–343. doi:10.1016/0006-8993(90)90294-L

Barnes, K., Matsas, R., Hooper, N.M., Turner, A.J., Kenny, A.J., 1988. Endopeptidase-24.11 is striosomally ordered in pig brain and, in contrast to aminopeptidase N and peptidyl dipeptidase A ('angiotensin converting enzyme'), is a marker

for a set of striatal efferent fibres. Neuroscience 27, 799–817. doi:10.1016/0306-4522(88)90184-4

Barnes, N.M., Cheng, C.H., Costall, B., Naylor, R.J., Williams, T.J., Wischik, C.M., 1991. Angiotensin converting enzyme density is increased in temporal cortex from patients with Alzheimer's disease. Eur. J. Pharmacol. 200, 289–292.

Bartolini, M., Bertucci, C., Bolognesi, M.L., Cavalli, A., Melchiorre, C., Andrisano, V., 2007. Insight into the kinetic of amyloid β (1-42) peptide self-aggregation: Elucidation of inhibitors' mechanism of action. ChemBioChem 8, 2152–2161. doi:10.1002/cbic.200700427

Baudin, B., Alves, N., Pilon, A., Beneteau-Burnat, B., Giboudeau, J., 1997. Structural and biological roles of glycosylations in pulmonary angiotensin I-converting enzyme. Glycobiology 7, 565–570.

Bayer, T.A., Wirths, O., 2014. Focusing the amyloid cascade hypothesis on N-truncated Abeta peptides as drug targets against Alzheimer's disease. Acta Neuropathol. doi:10.1007/s00401-014-1287-x

Beckett, C., Nalivaeva, N.N., Belyaev, N.D., Turner, A.J., 2012. Nuclear signalling by membrane protein intracellular domains: The AICD enigma. Cell. Signal. doi:10.1016/j.cellsig.2011.10.007

Beher, D., Wrigley, J.D.J., Owens, A.P., Shearman, M.S., 2002. Generation of C-terminally truncated amyloid-beta peptides is dependent on gamma-secretase activity. J. Neurochem. 82, 563–575. doi:0985 [pii]

Belcheva, I., Ternianov, A., Georgiev, V., 2000. Lateralized learning and memory effects of angiotensin II microinjected into the rat CA1 hippocampal area. Peptides 21, 407–411.

Bell, R.D., Zlokovic, B. V, 2009. Neurovascular mechanisms and blood-brain barrier disorder in Alzheimer's disease. Acta Neuropathol. doi:10.1007/s00401-009-0522-3

Ben Khalifa, N., Tyteca, D., Marinangeli, C., Depuydt, M., Collet, J.-F., Courtoy, P.J., Renauld, J.-C., Constantinescu, S., Octave, J.-N., Kienlen-Campard, P., 2012. Structural features of the KPI domain control APP dimerization, trafficking, and processing. FASEB J. doi:10.1096/fj.11-190207

Bennett, J.P., Snyder, S.H., 1976. Angiotensin II binding to mammalian brain membranes. J. Biol. Chem. 251, 7423–7430.

Benseny-Cases, N., Cócera, M., Cladera, J., 2007. Conversion of non-fibrillar beta-sheet oligomers into amyloid fibrils in Alzheimer's disease amyloid peptide aggregation. Biochem. Biophys. Res. Commun. 361, 916–921. doi:10.1016/j.bbrc.2007.07.082

Benzing, T., Fleming, I., Blaukat, A., Müller-Esterl, W., Busse, R., 1999. Angiotensin-Converting Enzyme Inhibitor Ramiprilat Interferes With the Sequestration of the B 2 Kinin Receptor Within the Plasma Membrane of Native Endothelial Cells. Circulation 99, 2034–2040.

Bernier, S.G., Bellemare, J.M., Escher, E., Guillemette, G., 1998. Characterization of AT4 receptor from bovine aortic endothelium with photosensitive analogues of angiotensin IV. Biochemistry 37, 4280–4287. doi:10.1021/bi972863j

Bernstein, K.E., Koronyo, Y., Salumbides, B.C., Sheyn, J., Pelissier, L., Lopes, D.H.J., Shah, K.H., Bernstein, E.A., Fuchs, D., Yu, J.J.-Y., Pham, M., Black, K.L., Shen, X.Z., Fuchs, S., Koronyo-Hamaoui, M., 2014. Angiotensin-converting enzyme overexpression in myelomonocytes prevents Alzheimer's-like cognitive decline. J. Clin. Invest. 124, 1000–12. doi:10.1172/JCI66541

Bernstein, K.E., Martin, B.M., Edwards, A.S., Bernstein, E.A., 1989. Mouse angiotensin-converting enzyme is a protein composed of two homologous domains. J. Biol. Chem. 264, 11945–11951.

Bernstein, K.E., Ong, F.S., Blackwell, W.-L.B., Shah, K.H., Giani, J.F., Gonzalez-Villalobos, R. a, Shen, X.Z., Fuchs, S., Touyz, R.M., 2013. A modern understanding of the traditional and nontraditional biological functions of angiotensin-converting enzyme. Pharmacol. Rev. 65, 1–46. doi:10.1124/pr.112.006809

Bernstein, K.E., Shen, X.Z., Gonzalez-Villalobos, R.A., Billet, S., Okwan-Duodu, D., Ong, F.S., Fuchs, S., 2011. Different in vivo functions of the two catalytic domains of angiotensin-converting enzyme (ACE). Curr. Opin. Pharmacol. 11, 105–111. doi:10.1016/j.coph.2010.11.001

Bertram, L., Mcqueen, M.B., Mullin, K., Blacker, D., Tanzi, R.E., 2007. Systematic meta-analyses of Alzheimer disease genetic association studies: the AlzGene database. Nat. Genet. 39, 17–24. doi:10.1038/ng1934

Biancardi, V.C., Son, S.J., Ahmadi, S., Filosa, J. a, Stern, J.E., 2014. Circulating angiotensin II gains access to the hypothalamus and brain stem during hypertension via breakdown of the blood-brain barrier. Hypertension 63, 572–579. doi:10.1161/HYPERTENSIONAHA.113.01743

Bibl, M., Gallus, M., Welge, V., Esselmann, H., Wolf, S., Rüther, E., Wiltfang, J., 2012. Cerebrospinal fluid amyloid-β 2-42 is decreased in Alzheimer's, but not in frontotemporal dementia. J. Neural Transm. 119, 805–813. doi:10.1007/s00702-012-0801-3

Bicca, M.A., Costa, R., Loch-Neckel, G., Figueiredo, C.P., Medeiros, R., Calixto, J.B., 2015. B_2 receptor blockage prevents Aβ-induced cognitive impairment by neuroinflammation inhibition. Behav. Brain Res. 278, 482–91. doi:10.1016/j.bbr.2014.10.040

Bien, J., Jefferson, T., Čaušević, M., Jumpertz, T., Munter, L., Multhaup, G., Weggen, S., Becker-Pauly, C., Pietrzik, C.U., 2012. The metalloprotease meprin β generates amino terminal-truncated amyloid β peptide species. J. Biol. Chem. 287, 33304–33313. doi:10.1074/jbc.M112.395608

Biffi, A., Sonni, A., Anderson, C.D., Kissela, B., Jagiella, J.M., Schmidt, H., Jimenez-Conde, J., Hansen, B.M., Fernandez-Cadenas, I., Cortellini, L., Ayres, A., Schwab, K., Juchniewicz, K., Urbanik, A., Rost, N.S., Viswanathan, A., Seifert-Held, T., Stoegerer, E.-M., Tomás, M., Rabionet, R., Estivill, X., Brown, D.L., Silliman, S.L., Selim, M., Worrall, B.B., Meschia, J.F., Montaner, J., Lindgren, A., Roquer, J., Schmidt, R., Greenberg, S.M., Slowik, A., Broderick, J.P., Woo, D., Rosand, J., 2010. Variants at APOE influence risk of deep and lobar intracerebral hemorrhage. Ann. Neurol. 68, 934–43. doi:10.1002/ana.22134

Binevski, P. V, Sizova, E.A., Pozdnev, V.F., Kost, O.A., 2003. Evidence for the negative cooperativity of the two active sites within bovine somatic

angiotensin-converting enzyme. FEBS Lett. 550, 84–88. doi:10.1016/S0014-5793(03)00825-1

Blanquet, P.R., 2000. Casein kinase 2 as a potentially important enzyme in the nervous system. Prog. Neurobiol. doi:10.1016/S0301-0082(99)00026-X

Blanquet, P.R., 1998. Neurotrophin-induced activation of casein kinase 2 in rat hippocampal slices. Neuroscience 86, 739–749. doi:10.1016/S0306-4522(98)00087-6

Bloch, S., Obari, D., Girouard, H., 2015. Angiotensin and neurovascular coupling: beyond hypertension. Microcirculation 22, 159–67. doi:10.1111/micc.12193

Bogoyevitch, M.A., Kobe, B., 2006. Uses for JNK: the many and varied substrates of the c-Jun N-terminal kinases. Microbiol. Mol. Biol. Rev. 70, 1061–1095. doi:10.1128/MMBR.00025-06

Bonnet, D., Césaire, R., Lemoine, F., Aoudjhane, M., Najman, A., Guigon, M., 1992. The tetrapeptide AcSDKP, an inhibitor of the cell-cycle status for normal human hematopoietic progenitors, has no effect on leukemic cells. Exp. Hematol. 20, 251–255.

Borsello, T., Forloni, G., 2007. JNK Signalling: A Possible Target to Prevent Neurodegeneration. Curr. Pharm. Des. 13, 1875–1886.

Bourne, K.Z., Ferrari, D.C., Lange-Dohna, C., Rossner, S., Wood, T.G., Perez-Polo, J.R., 2007. Differential regulation of BACE1 promoter activity by nuclear factor-kappaB in neurons and glia upon exposure to beta-amyloid peptides. J. Neurosci. Res. 85, 1194–1204. doi:10.1002/jnr.21252

Boyd-kimball, D., Sultana, R., Mohmmad-Abdul, H., Butterfield, D.A., 2005. Neurotoxicity and oxidative stress in D1M-substituted Alzheimer ' s Aβ(1-42): relevance to N-terminal methionine chemistry in small model peptides. Peptides 26, 665–673. doi:10.1016/j.peptides.2004.11.001

Braak, H., Braak, E., 1991. Neuropathological stageing of Alzheimer-related changes. Acta Neuropathol. 82, 239–59.

Bradford, M.M., 1976. A rapid and sensitive method for the quantitation of microgram quantities of protein utilizing the principle of protein-dye binding. Anal. Biochem. 72, 248–254. doi:10.1016/0003-2697(76)90527-3

Braszko, J.J., 2004. Involvement of D1 dopamine receptors in the cognitive effects of angiotensin IV and des-Phe6 angiotensin IV. Peptides 25, 1195–1203. doi:10.1016/j.peptides.2004.04.014

Braszko, J.J., Kułakowska, A., Karwowska-Polecka, W., 1998. CGP 42112A antagonism of the angiotensin II and angiotensin II(3-7) facilitation of recall in rats. Pharmacol. Res. 38, 461–468. doi:10.1006/phrs.1998.0395

Braszko, J.J., Kułakowska, A., Winnicka, M.M., 2003. Effects of angiotensin II and its receptor antagonists on motor activity and anxiety in rats. J. Physiol. Pharmacol. 54, 271–281.

Braszko, J.J., Kułakowska, A., Wiśniewski, K., 1995. Angiotensin II and its 3-7 fragment improve recognition but not spatial memory in rats. Brain Res. Bull. 37, 627–631. doi:10.1016/0361-9230(95)00056-K

Braszko, J.J., Wiśniewski, K., Kupryszewski, G., Witczuk, B., 1987. Psychotropic effects of angiotensin II and III in rats: locomotor and exploratory vs cognitive behaviour. Behav. Brain Res. 25, 195–203. doi:10.1016/0166-4328(87)90068-4

Braszko, J.J., Własienko, J., Kupryszewski, G., Witczuk, B., Wisniewski, K., 1988. Behavioral effects of angiotensin II and angiotensin II-(4-8)-pentapeptide in rats. Physiol. Behav. 44, 327–332. doi:10.1016/0031-9384(88)90033-9

Bridgewater, J.D., Srikanth, R., Lim, J., Vachet, R.W., 2007. The Effect of Histidine Oxidation on the Dissociation Patterns of Peptide Ions. J. Am. Soc. Mass Spectrom. 18, 553–562. doi:10.1016/j.jasms.2006.11.001

Broder, C., Becker-Pauly, C., 2013. The metalloproteases meprin α and meprin β: unique enzymes in inflammation, neurodegeneration, cancer and fibrosis. Biochem. J. 450, 253–64. doi:10.1042/BJ20121751

Broersen, K., Rousseau, F., Schymkowitz, J., 2010. The culprit behind amyloid beta peptide related neurotoxicity in Alzheimer's disease: oligomer size or conformation? Alzheimers. Res. Ther. 2, 12. doi:10.1186/alzrt36

Bruneval, P., Hinglais, N., Alhenc-Gelas, F., Tricottet, V., Corvol, P., Menard, J., Camilleri, J.P., Bariety, J., 1986. Angiotensin I converting enzyme in human intestine and kidney. Ultrastructural immunohistochemical localization. Histochemistry 85, 73–80.

Bu, G., 2009. Apolipoprotein E and its receptors in Alzheimer's disease: pathways, pathogenesis and therapy. Nat. Rev. Neurosci. 10, 333–344. doi:10.1038/nrn2620

Bueno, V., Palos, M., Ronchi, F.A., Andrade, M.C.C., Ginoza, M., Casarini, D.E., 2004. N-Domain angiotensin I-Converting enzyme expression in renal artery of Wistar, Wistar kyoto, and spontaneously hypertensive rats, in: Transplantation Proceedings. Nephrology Division, Department of Medicine, Paulista School of Medicine, UNIFESP, Sao Paulo, Brazil. valquiriabuerio@hotmail.com, pp. 1001–1003. doi:10.1016/j.transproceed.2004.03.081

Bull, H.G., Thornberry, N.A., Cordes, E.H., 1985. Purification of angiotensin-converting enzyme from rabbit lung and human plasma by affinity chromatography. J. Biol. Chem. 260, 2963–2972.

Bulloj, A., Leal, M.C., Xu, H., Castaño, E.M., Morelli, L., 2010. Insulin-degrading enzyme sorting in exosomes: A secretory pathway for a key brain amyloid-β degrading protease. J. Alzheimer's Dis. 19, 79–95. doi:10.3233/JAD-2010-1206

Bush, A.I., 2003. The metallobiology of Alzheimer's disease. Trends Neurosci. doi:10.1016/S0166-2236(03)00067-5

Böttcher, A., Böttcher, A., Schmitz, G., Schling, P., 2006. Angiotensin-converting enzyme signalling in human preadipocytes and adipocytes. Cent. Eur. J. Biol. 1, 203–220. doi:10.2478/s11535-006-0015-5

Cai, H., Wang, Y., McCarthy, D., Wen, H., Borchelt, D.R., Price, D.L., Wong, P.C., 2001. BACE1 is the major beta-secretase for generation of Abeta peptides by neurons. Nat. Neurosci. 4, 233–234. doi:10.1038/85064

Cai, Z., Yan, L.-J., Li, K., Quazi, S.H., Zhao, B., 2012. Roles of AMP-activated Protein Kinase in Alzheimer's Disease. NeuroMolecular Med. doi:10.1007/s12017-012-8173-2

Caragounis, A., Du, T., Filiz, G., Laughton, K.M., Volitakis, I., Sharples, R.A., Cherny, R.A., Masters, C.L., Drew, S.C., Hill, A.F., Li, Q., Crouch, P.J., Barnham, K.J., White, A.R., 2007. Differential modulation of Alzheimer's disease amyloid beta-peptide accumulation by diverse classes of metal ligands. Biochem. J. 407, 435–450. doi:10.1042/BJ20070579

Carson, J.A., Turner, A.J., 2002. β-amyloid catabolism: Roles for neprilysin (NEP) and other metallopeptidases? J. Neurochem. doi:10.1046/j.1471-4159.2002.00855.x

Carvalho, C., Correia, S.C., Santos, R.X., Cardoso, S., Moreira, P.I., Clark, T.A., Zhu, X., Smith, M.A., Perry, G., 2009. Role of mitochondrial-mediated signaling pathways in Alzheimer disease and hypoxia. J. Bioenerg. Biomembr. doi:10.1007/s10863-009-9247-1

Casarini, D.E., Plavinik, F.L., Zanella, M.T., Marson, O., Krieger, J.E., Hirata, I.Y., Stella, R.C.R., 2001. Angiotensin converting enzymes from human urine of mild hypertensive untreated patients resemble the N-terminal fragment of human angiotensin I-converting enzyme. Int. J. Biochem. Cell Biol. 33, 75–85. doi:10.1016/S1357-2725(00)00072-8

CCP4, 1994. The CCP4 suite: Programs for protein crystallography. Acta Crystallogr. Sect. D Biol. Crystallogr. 50, 760–763. doi:10.1107/S0907444994003112

Chai, S.Y., Fernando, R., Peck, G., Ye, S.-Y., Mendelsohn, F.A.O., Jenkins, T.A., Albiston, A.L., 2004. The angiotensin IV/AT4 receptor. Cell. Mol. Life Sci. 61, 2728–37. doi:10.1007/s00018-004-4246-1

Chai, S.Y., Mendelsohn, F.A., Paxinos, G., 1987. Angiotensin converting enzyme in rat brain visualized by quantitative in vitro autoradiography. Neuroscience 20, 615–627. doi:10.1016/0306-4522(87)90114-X

Chan, S.H.H., Chan, J.Y.H., 2013. Angiotensin-generated reactive oxygen species in brain and pathogenesis of cardiovascular diseases. Antioxid. Redox Signal. 19, 1074–84. doi:10.1089/ars.2012.4585

Chen, V.B., Arendall, W.B., Headd, J.J., Keedy, D.A., Immormino, R.M., Kapral, G.J., Murray, L.W., Richardson, J.S., Richardson, D.C., 2010. MolProbity: All-atom structure validation for macromolecular crystallography. Acta Crystallogr. Sect. D Biol. Crystallogr. 66, 12–21. doi:10.1107/S0907444909042073

Chen, Y.-C., Wu, J.-S., Tsai, H.-D., Huang, C.-Y., Chen, J.-J., Sun, G.Y., Lin, T.-N., 2012. Peroxisome Proliferator-Activated Receptor Gamma (PPAR-γ) and Neurodegenerative Disorders. Mol. Neurobiol. doi:10.1007/s12035-012-8259-8

Chimon, S., Shaibat, M.A., Jones, C.R., Calero, D.C., Aizezi, B., Ishii, Y., 2007. Evidence of fibril-like β-sheet structures in a neurotoxic amyloid intermediate of Alzheimer's β-amyloid. Nat. Struct. Mol. Biol. 14, 1157–1164. doi:10.1038/nsmb1345

Ciaccio, C., Tundo, G.R., Grasso, G., Spoto, G., Marasco, D., Ruvo, M., Gioia, M.,

Rizzarelli, E., Coletta, M., 2009. Somatostatin: A Novel Substrate and a Modulator of Insulin-Degrading Enzyme Activity. J. Mol. Biol. 385, 1556–1567. doi:10.1016/j.jmb.2008.11.025

Clarke, N.E., Fisher, M.J., Porter, K.E., Lambert, D.W., Turner, A.J., 2012. Angiotensin converting enzyme (ACE) and ACE2 bind integrins and ACE2 regulates integrin signalling. PLoS One 7, e34747. doi:10.1371/journal.pone.0034747

Cohen, S.I. a, Linse, S., Luheshi, L.M., Hellstrand, E., White, D. a, Rajah, L., Otzen, D.E., Vendruscolo, M., Dobson, C.M., Knowles, T.P.J., 2013. Proliferation of amyloid-β42 aggregates occurs through a secondary nucleation mechanism. Proc. Natl. Acad. Sci. U. S. A. 110, 9758–63. doi:10.1073/pnas.1218402110

Combs, C.K., Johnson, D.E., Karlo, J.C., Cannady, S.B., Landreth, G.E., 2000. Inflammatory mechanisms in Alzheimer's disease: inhibition of beta-amyloid-stimulated proinflammatory responses and neurotoxicity by PPARgamma agonists. J. Neurosci. 20, 558–567.

Cook, D.G., Leverenz, J.B., McMillan, P.J., Kulstad, J.J., Ericksen, S., Roth, R.A., Schellenberg, G.D., Jin, L.-W., Kovacina, K.S., Craft, S., 2003. Reduced hippocampal insulin-degrading enzyme in late-onset Alzheimer's disease is associated with the apolipoprotein E-epsilon4 allele. Am. J. Pathol. 162, 313–319. doi:10.1016/S0002-9440(10)63822-9

Cooper, S., 2003. Reappraisal of serum starvation, the restriction point, G0, and G1 phase arrest points. FASEB J. 17, 333–340. doi:10.1096/fj.02-0352rev

Corradi, H.R., Chitapi, I., Sewell, B.T., Georgiadis, D., Dive, V., Sturrock, E.D., Acharya, K.R., 2007. The structure of testis angiotensin-converting enzyme in complex with the C domain-specific inhibitor RXPA380. Biochemistry 46, 5473–8. doi:10.1021/bi700275e

Corradi, H.R., Schwager, S.L.U., Nchinda, A.T., Sturrock, E.D., Acharya, K.R., 2006. Crystal structure of the N domain of human somatic angiotensin I-converting enzyme provides a structural basis for domain-specific inhibitor design. J. Mol. Biol. 357, 964–974. doi:10.1016/j.jmb.2006.01.048

Craft, S., Watson, G.S., 2004. Insulin and neurodegenerative disease: Shared and specific mechanisms. Lancet Neurol. doi:10.1016/S1474-4422(04)00681-7

Crawford, D.C., Chobanian, A. V, Brecher, P., 1994. Angiotensin II induces fibronectin expression associated with cardiac fibrosis in the rat. Circ. Res. 74, 727–739. doi:10.1161/01.RES.74.4.727

Curtain, C.C., Ali, F., Volitakis, I., Cherny, R. a, Norton, R.S., Beyreuther, K., Barrow, C.J., Masters, C.L., Bush, a I., Barnham, K.J., 2001. Alzheimer's disease amyloid-beta binds copper and zinc to generate an allosterically ordered membrane-penetrating structure containing superoxide dismutase-like subunits. J. Biol. Chem. 276, 20466–20473. doi:10.1074/jbc.M100175200

Cushman, D.W., Cheung, H.S., 1971a. Concentrations of angiotensin-converting enzyme in tissues of the rat. Biochim. Biophys. Acta 250, 261–265. doi:10.1016/0005-2744(71)90142-2

Cushman, D.W., Cheung, H.S., 1971b. Spectrophotometric assay and properties of the angiotensin-converting enzyme of rabbit lung. Biochem. Pharmacol. 20, 1637–1648. doi:10.1016/0006-2952(71)90292-9

Cushman, D.W., Cheung, H.S., Sabo, E.F., Ondetti, M.A., 1982. Development and design of specific inhibitors of angiotensin-converting enzyme. Am. J. Cardiol. 49, 1390–1394.

Cushman, D.W., Pluscec, J., Williams, N.J., Weaver, E.R., Sabo, E.F., Kocy, O., Cheung, H.S., Ondetti, M.A., 1973. Inhibition of angiotensin-converting enzyme by analogs of peptides from Bothrops jararaca venom. Experientia.

Da Silveira, K., Barroso, L.C., Vieira, A.T., Cisalpino, D., Lima, C.X., Bader, M., Arantes, R.M.E., dos Santos, R.A.S., Simões-e-Silva, A.C., Teixeira, M.M., 2013. Beneficial Effects of the Activation of the Angiotensin-(1-7) Mas Receptor in a Murine Model of Adriamycin-Induced Nephropathy. PLoS One 8. doi:10.1371/journal.pone.0066082

Danser, A.H., Tom, B., de Vries, R., Saxena, P.R., 2000. L-NAME-resistant bradykinin-induced relaxation in porcine coronary arteries is NO-dependent: effect of ACE inhibition. Br. J. Pharmacol. 131, 195–202. doi:10.1038/sj.bjp.0703555

De Felice, F.G., Velasco, P.T., Lambert, M.P., Viola, K., Fernandez, S.J., Ferreira, S.T., Klein, W.L., 2007. Aβ oligomers induce neuronal oxidative stress through an N-methyl-D-aspartate receptor-dependent mechanism that is blocked by the Alzheimer drug memantine. J. Biol. Chem. 282, 11590–11601. doi:10.1074/jbc.M607483200

De Filippis, V., Frasson, R., Fontana, A., 2006. 3-Nitrotyrosine as a spectroscopic probe for investigating protein protein interactions. Protein Sci. 15, 976–986. doi:10.1110/ps.051957006

de Gasparo, M., Catt, K.J., Inagami, T., Wright, J.W., Unger, T., 2000. International union of pharmacology. XXIII. The angiotensin II receptors. Pharmacol. Rev. 52, 415–472. doi:34/848966

de la Monte, S.M., Wands, J.R., 2008. Alzheimer's disease is type 3 diabetes-evidence reviewed. J. Diabetes Sci. Technol. 2, 1101–13.

de la Monte, S.M., Wands, J.R., 2006. Molecular indices of oxidative stress and mitochondrial dysfunction occur early and often progress with severity of Alzheimer's disease. J. Alzheimers. Dis. 9, 167–181.

de la Torre, J.C., Mussivand, T., 1993. Can disturbed brain microcirculation cause Alzheimer's disease? Neurol. Res. 15, 146–153.

de Leeuw, F.-E., de Groot, J.C., Oudkerk, M., Witteman, J.C.M., Hofman, A., van Gijn, J., Breteler, M.M.B., 2002. Hypertension and cerebral white matter lesions in a prospective cohort study. Brain 125, 765–772. doi:10.1093/brain/awf077

De Souza, E.S., Hirata, I.Y., Juliano, L., Ito, A.S., 2000. End-to-end distance distribution in bradykinin observed by Forster resonance energy transfer. Biochim. Biophys. Acta - Gen. Subj. 1474, 251–261. doi:10.1016/S0304-4165(00)00004-0

De Strooper, B., 2010. Proteases and proteolysis in Alzheimer disease: a multifactorial view on the disease process. Physiol. Rev. 90, 465–494. doi:10.1152/physrev.00023.2009

de Tullio, M.B., Morelli, L., Castaño, E.M., 2008. The irreversible binding of amyloid

peptide substrates to insulin-degrading enzyme: a biological perspective. Prion 2, 51–56. doi:10.4161/pri.2.2.6710

Deane, R., Du Yan, S., Submamaryan, R.K., LaRue, B., Jovanovic, S., Hogg, E., Welch, D., Manness, L., Lin, C., Yu, J., Zhu, H., Ghiso, J., Frangione, B., Stern, A., Schmidt, A.M., Armstrong, D.L., Arnold, B., Liliensiek, B., Nawroth, P., Hofman, F., Kindy, M., Stern, D., Zlokovic, B., 2003. RAGE mediates amyloid-beta peptide transport across the blood-brain barrier and accumulation in brain. Nat. Med. 9, 907–913. doi:10.1038/nm890

Deddish, P. a., Marcic, B., Jackman, H.L., Wang, H.Z., Skidgel, R. a., Erdös, E.G., 1998. N-domain-specific substrate and C-domain inhibitors of angiotensin-converting enzyme: angiotensin-(1-7) and keto-ACE. Hypertension 31, 912–917. doi:10.1161/01.hyp.31.4.912

Deddish, P.A., Jackman, H.L., Skidgel, R.A., Erdös, E.G., Erdh, E.G., 1997. Differences in the hydrolysis of enkephalin congeners by the two domains of angiotensin converting enzyme. Biochem. Pharmacol. 53, 1459–1463. doi:10.1016/S0006-2952(97)00087-7

Deddish, P.A., Wang, J., Michel, B., Morris, P.W., Davidson, N.O., Skidgel, R.A., Erdos, E.G., 1994. Naturally occurring active N-domain of human angiotensin I - converting enzyme. Procedings Natl. Acadademy Sci. USA 91, 7807–7811.

Defendini, R., Zimmerman, E.A., Weare, J.A., Alhenc-Gelas, F., Erdös, E.G., 1983. Angiotensin-converting enzyme in epithelial and neuroepithelial cells. Neuroendocrinology 37, 32–40. doi:10.1159/000123512

Delom, F., Chevet, E., 2006. Phosphoprotein analysis: from proteins to proteomes. Proteome Sci. 4, 15. doi:10.1186/1477-5956-4-15

DeNoble, V.J., DeNoble, K.F., Spencer, K.R., Chiu, A.T., Wong, P.C., Timmermans, P.B.M.W.M., 1991. Non-peptide angiotensin II receptor antagonist and angiotensin-converting enzyme inhibitor: Effect on a renin-induced deficit of a passive avoidance response in rats. Brain Res. 561, 230–235. doi:10.1016/0006-8993(91)91599-V

Deshpande, A., Mina, E., Glabe, C., Busciglio, J., 2006. Different conformations of amyloid beta induce neurotoxicity by distinct mechanisms in human cortical neurons. J. Neurosci. 26, 6011–6018. doi:10.1523/JNEUROSCI.1189-06.2006

Dinh, D.T., Frauman, A.G., Johnston, C.I., Fabiani, M.E., 2001. Angiotensin receptors: distribution, signalling and function. Clin. Sci. (Lond). 100, 481–492. doi:10.1042/CS20000263

Dive, V., Cotton, J., Yiotakis, A., Michaud, A., Vassiliou, S., Jiracek, J., Vazeux, G., Chauvet, M.T., Cuniasse, P., Corvol, P., 1999. RXP 407, a phosphinic peptide, is a potent inhibitor of angiotensin I converting enzyme able to differentiate between its two active sites. Proc. Natl. Acad. Sci. U. S. A. 96, 4330–4335. doi:10.1073/pnas.96.8.4330

Dolev, I., Michaelson, D.M., 2006. The nucleation growth and reversibility of Amyloid-β depotistion in vivo. J. Alzheimer's Dis. 10, 291–301.

Dong, Y., Kataoka, K., Tokutomi, Y., Nako, H., Nakamura, T., Toyama, K., Sueta, D., Koibuchi, N., Yamamoto, E., Ogawa, H., Kim-Mitsuyama, S., 2011. Perindopril, a centrally active angiotensin-converting enzyme inhibitor, prevents

cognitive impairment in mouse models of Alzheimer's disease. FASEB J. 25, 2911–20. doi:10.1096/fj.11-182873

Donmez, G., Wang, D., Cohen, D.E., Guarente, L., 2010. SIRT1 Suppresses β-Amyloid Production by Activating the β-Secretase Gene ADAM10. Cell 142, 320–332. doi:10.1016/j.cell.2010.06.020

Donoghue, M., Hsieh, F., Baronas, E., Godbout, K., Gosselin, M., Stagliano, N., Donovan, M., Woolf, B., Robison, K., Jeyaseelan, R., Breitbart, R.E., Acton, S., 2000. A Novel Angiotensin-Converting Enzyme-Related Carboxypeptidase (ACE2) Converts Angiotensin I to Angiotensin 1-9. Circ. Res. 87, 1e–9.

Douglas, R.G., Sharma, R.K., Masuyer, G., Lubbe, L., Zamora, I., Acharya, K.R., Chibale, K., Sturrock, E.D., 2014. Fragment-based design for the development of N-domain-selective angiotensin-1-converting enzyme inhibitors. Clin. Sci. (Lond). 126, 305–13. doi:10.1042/CS20130403

Du, X., Wang, L., Wang, Y., Andreasen, M., Zhan, D., Feng, Y., Li, M., Zhao, M., Otzen, D., Xue, D., Yang, Y., Liu, R., 2011. Aβ1-16 can aggregate and induce the production of reactive oxygen species, nitric oxide, and inflammatory cytokines. J. Alzheimers. Dis. 27, 401–413. doi:10.3233/JAD-2011-110476

Duce, J.A., Tsatsanis, A., Cater, M.A., James, S.A., Robb, E., Wikhe, K., Leong, S.L., Perez, K., Johanssen, T., Greenough, M.A., Cho, H., Galatis, D., Moir, R.D., Masters, C.L., Mclean, C., Tanzi, R.E., Cappai, R., Barnham, K.J., Ciccotosto, G.D., Rogers, J.T., Bush, A.I., 2010. Iron-Export Ferroxidase Activity of β- Amyloid Precursor Protein Is Inhibited by Zinc in Alzheimer ' s Disease. Cell 142, 857–867. doi:10.1016/j.cell.2010.08.014

Dulin, F., Léveillé, F., Ortega, J.B., Mornon, J.P., Buisson, A., Callebaut, I., Colloc'h, N., 2008. p3 peptide, a truncated form of Aβ devoid of synaptotoxic effect, does not assemble into soluble oligomers. FEBS Lett. 582, 1865–1870. doi:10.1016/j.febslet.2008.05.002

Eckman, E.A., Adams, S.K., Troendle, F.J., Stodola, B.A., Kahn, M.A., Fauq, A.H., Xiao, H.D., Bernstein, K.E., Eckman, C.B., 2006. Regulation of steady-state β-amyloid levels in the brain by neprilysin and endothelin-converting enzyme but not angiotensin-converting enzyme. J. Biol. Chem. 281, 30471–30478. doi:10.1074/jbc.M605827200

Eckman, E.A., Watson, M., Marlow, L., Sambamurti, K., Eckman, C.B., 2003. Alzheimer's disease beta-amyloid peptide is increased in mice deficient in endothelin-converting enzyme. J. Biol. Chem. 278, 2081–4. doi:10.1074/jbc.C200642200

Edbauer, D., Willem, M., Lammich, S., Steiner, H., Haass, C., 2002. Insulin-degrading enzyme rapidly removes the β-amyloid precursor protein intracellular domain (AICD). J. Biol. Chem. 277, 13389–13393. doi:10.1074/jbc.M111571200

Ehehalt, R., Keller, P., Haass, C., Thiele, C., Simons, K., 2003. Amyloidogenic processing of the Alzheimer β-amyloid precursor protein depends on lipid rafts. J. Cell Biol. 160, 113–123. doi:10.1083/jcb.200207113

Ehlers, M.R., Chen, Y.N., Riordan, J.F., 1992. The unique N-terminal sequence of testis angiotensin-converting enzyme is heavily O-glycosylated and

unessential for activity or stability. Biochem.Biophys.Res.Commun. 183, 199–205.

Ehlers, M.R., Chen, Y.N., Riordan, J.F., 1991. Purification and characterization of recombinant human testis angiotensin-converting enzyme expressed in Chinese hamster ovary cells. Protein Expr. Purif. 2, 1–9.

Ehlers, M.R., Fox, E.A., Strydom, D.J., Riordan, J.F., 1989. Molecular cloning of human testicular angiotensin-converting enzyme: the testis isozyme is identical to the C-terminal half of endothelial angiotensin-converting enzyme. Proc. Natl. Acad. Sci. U. S. A. 86, 7741–7745. doi:10.1073/pnas.86.20.7741

Ehlers, M.R., Riordan, J.F., 1991. Angiotensin-converting enzyme: zinc- and inhibitor-binding stoichiometries of the somatic and testis isozymes. Biochemistry 30, 7118–26.

Ehlers, M.R., Riordan, J.F., 1989. Angiotensin-converting enzyme: new concepts concerning its biological role. Biochemistry 28, 5311–5318. doi:10.1021/bi00439a001

Ehlers, M.R.W., Schwager, S.L.U., Scholle, R.R., Manji, G.A., Brandt, W.F., Riordan, J.F., 1996. Proteolytic release of membrane-bound angiotensin-converting enzyme: Role of the juxtamembrane stalk sequence. Biochemistry 35, 9549–9559. doi:10.1021/bi9602425

El-Dorry, H.A., Bull, H.G., Iwata, K., Thornberry, N.A., Cordes, E.H., Soffer, R.L., 1982. Molecular and catalytic properties of rabbit testicular dipeptidyl carboxypeptidase. J. Biol. Chem. 257, 14128–14133.

Emanuele, E., D'Angelo, A., Tomaino, C., Binetti, G., Ghidoni, R., Politi, P., Bernardi, L., Maletta, R., Bruni, A.C., Geroldi, D., 2005. Circulating levels of soluble receptor for advanced glycation end products in Alzheimer disease and vascular dementia. Arch. Neurol. 62, 1734–1736. doi:10.1001/archneur.62.11.1734

Emsley, P., Lohkamp, B., Scott, W.G., Cowtan, K., 2010. Features and development of Coot. Acta Crystallogr. Sect. D Biol. Crystallogr. 66, 486–501. doi:10.1107/S0907444910007493

Erdös, E.G., Deddish, P.A., Marcic, B.M., 1999. Potentiation of bradykinin actions by ACE inhibitors. Trends Endocrinol. Metab. doi:10.1016/S1043-2760(99)00156-3

Esther, C.R., Howard, T.E., Marino, E.M., Goddard, J.M., Capecchi, M.R., Bernstein, K.E., 1996. Mice lacking angiotensin-converting enzyme have low blood pressure, renal pathology, and reduced male fertility. Lab. Invest. 74, 953–965.

Fabian, H., Szendrei, G.I., Mantsch, H.H., Greenberg, B.D., Otvös, L., 1994. Synthetic post-translationally modified human A beta peptide exhibits a markedly increased tendency to form beta-pleated sheets in vitro. Eur. J. Biochem. 221, 959–964.

Falcone, C., Emanuele, E., D'Angelo, A., Buzzi, M.P., Belvito, C., Cuccia, M., Geroldi, D., 2005. Plasma levels of soluble receptor for advanced glycation end products and coronary artery disease in nondiabetic men. Arterioscler. Thromb. Vasc. Biol. 25, 1032–1037.

doi:10.1161/01.ATV.0000160342.20342.00

Fantini, J., Yahi, N., 2010. Molecular insights into amyloid regulation by membrane cholesterol and sphingolipids: common mechanisms in neurodegenerative diseases. Expert Rev. Mol. Med. 12, e27. doi:10.1017/S1462399410001602

Farkas, E., Luiten, P.G.M., 2001. Cerebral microvascular pathology in aging and Alzheimer's disease. Prog. Neurobiol. 64, 575–611. doi:10.1016/S0301-0082(00)00068-X

Farris, W., Mansourian, S., Chang, Y., Lindsley, L., Eckman, E.A., Frosch, M.P., Eckman, C.B., Tanzi, R.E., Selkoe, D.J., Guenette, S., 2003. Insulin-degrading enzyme regulates the levels of insulin, amyloid beta-protein, and the beta-amyloid precursor protein intracellular domain in vivo. Proc. Natl. Acad. Sci. U. S. A. 100, 4162–4167. doi:10.1073/pnas.0230450100

Ferguson, A. V., Washburn, D.L.S., 1998. Angiotensin II: A peptidergic neurotransmitter in central autonomic pathways. Prog. Neurobiol. doi:10.1016/S0301-0082(97)00065-8

Fernando, R.N., Albiston, A.L., Chai, S.Y., 2008. The insulin-regulated aminopeptidase IRAP is colocalised with GLUT4 in the mouse hippocampus - Potential role in modulation of glucose uptake in neurones? Eur. J. Neurosci. 28, 588–598. doi:10.1111/j.1460-9568.2008.06347.x

Ferrario, C.M., 2011. ACE2: more of Ang-(1-7) or less Ang II? Curr. Opin. Nephrol. Hypertens. 20, 1–6. doi:10.1097/MNH.0b013e3283406f57

Ferrario, C.M., Chappell, M.C., 2004. Novel angiotensin peptides. Cell. Mol. Life Sci. doi:10.1007/s00018-004-4243-4

Ferrington, L., Palmer, L.E., Love, S., Horsburgh, K.J., Kelly, P.A.T., Kehoe, P.G., 2012. Angiotensin II-inhibition: Effect on Alzheimer's pathology in the aged triple transgenic mouse. Am. J. Transl. Res. 4, 151–164.

Fésüs, G., Dubrovska, G., Gorzelniak, K., Kluge, R., Huang, Y., Luft, F.C., Gollasch, M., 2007. Adiponectin is a novel humoral vasodilator. Cardiovasc. Res. 75, 719–727. doi:10.1016/j.cardiores.2007.05.025

Fogari, R., Zoppi, A., Corradi, L., Lazzari, P., Mugellini, A., Lusardi, P., 1998. Comparative effects of lisinopril and losartan on insulin sensitivity in the treatment of non diabetic hypertensive patients. Br. J. Clin. Pharmacol. 46, 467–471. doi:10.1046/j.1365-2125.1998.00811.x

Fournier, D., Luft, F.C., Bader, M., Ganten, D., Andrade-Navarro, M.A., 2012. Emergence and evolution of the renin-angiotensin-aldosterone system. J. Mol. Med. (Berl). 90, 495–508. doi:10.1007/s00109-012-0894-z

Freund, M., Walther, T., Von Bohlen Und Halbach, O., 2012. Immunohistochemical localization of the angiotensin-(1-7) receptor Mas in the murine forebrain. Cell Tissue Res. 348, 29–35. doi:10.1007/s00441-012-1354-3

Friedland, J., Setton, C., Silverstein, E., 1978. Induction of angiotensin converting enzyme in human monocytes in culture. Biochem. Biophys. Res. Commun. 83, 843–849.

Friedland, J., Silverstein, E., 1977. Sensitive fluorimetric assay for serum angiotensin converting enzyme with the natural substrate angiotensin I. Am.

J. Clin. Pathol. 68, 225–228.

Fryer, J.D., Simmons, K., Parsadanian, M., Bales, K.R., Paul, S.M., Sullivan, P.M., Holtzman, D.M., 2005. Human apolipoprotein E4 alters the amyloid-beta 40:42 ratio and promotes the formation of cerebral amyloid angiopathy in an amyloid precursor protein transgenic model. J. Neurosci. 25, 2803–2810. doi:10.1523/JNEUROSCI.5170-04.2005

Fu, H., Liu, B., Frost, J.L., Hong, S., Jin, M., Ostaszewski, B., Shankar, G.M., Costantino, I.M., Carroll, M.C., Mayadas, T.N., Lemere, C.A., 2012. Complement component C3 and complement receptor type 3 contribute to the phagocytosis and clearance of fibrillar Aβ by microglia. Glia 60, 993–1003. doi:10.1002/glia.22331

Fuchs, S., Frenzel, K., Hubert, C., Lyng, R., Muller, L., Michaud, A., Xiao, H.D., Adams, J.W., Capecchi, M.R., Corvol, P., Shur, B.D., Bernstein, K.E., 2005. Male fertility is dependent on dipeptidase activity of testis ACE. Nat. Med. doi:10.1038/nm1105-1142

Fuchs, S., Xiao, H.D., Cole, J.M., Adams, J.W., Frenzel, K., Michaud, A., Zhao, H., Keshelava, G., Capecchi, M.R., Corvol, P., Bernstein, K.E., 2004. Role of the N-terminal Catalytic Domain of Angiotensin-converting Enzyme Investigated by Targeted Inactivation in Mice. J. Biol. Chem. 279, 15946–15953. doi:10.1074/jbc.M400149200

Fuchs, S., Xiao, H.D., Hubert, C., Michaud, A., Campbell, D.J., Adams, J.W., Capecchi, M.R., Corvol, P., Bernstein, K.E., 2008. Angiotensin-converting enzyme C-terminal catalytic domain is the main site of angiotensin I cleavage in vivo. Hypertension 51, 267–274. doi:10.1161/HYPERTENSIONAHA.107.097865

Fujihara, Y., Tokuhiro, K., Muro, Y., Kondoh, G., Araki, Y., Ikawa, M., Okabe, M., 2013. Expression of TEX101, regulated by ACE, is essential for the production of fertile mouse spermatozoa. Proc. Natl. Acad. Sci. U. S. A. 110, 8111–6. doi:10.1073/pnas.1222166110

Gallien, S., Duriez, E., Crone, C., Kellmann, M., Moehring, T., Domon, B., 2012. Targeted Proteomic Quantification on Quadrupole-Orbitrap Mass Spectrometer. Mol. Cell. Proteomics. doi:10.1074/mcp.O112.019802

Gao, X., He, X., Luo, B., Peng, L., Lin, J., Zuo, Z., 2009. Angiotensin II increases collagen I expression via transforming growth factor-beta 1 and extracellular signal-regulated kinase in cardiac fibroblasts. Eur. J. Pharmacol. 606, 115–120. doi:10.1016/j.ejphar.2008.12.049

Gao, Y., Pimplikar, S.W., 2001. The gamma -secretase-cleaved C-terminal fragment of amyloid precursor protein mediates signaling to the nucleus. Proc. Natl. Acad. Sci. U. S. A. 98, 14979–14984. doi:10.1073/pnas.261463298

Gard, P.R., 2008. Cognitive-enhancing effects of angiotensin IV. BMC Neurosci. 9 Suppl 2, S15. doi:10.1186/1471-2202-9-S2-S15

Gard, P.R., 2002. The role of angiotensin II in cognition and behaviour. Eur. J. Pharmacol. 438, 1–14. doi:10.1016/S0014-2999(02)01283-9

George-Carey, R., Adeloye, D., Chan, K.Y., Paul, A., Kolcic, I., Campbell, H., Rudan, I., 2012. An estimate of the prevalence of dementia in Africa: A systematic analysis. J. Glob. Health 2, 20401. doi:10.7189/jogh.02.020401

Georgiadis, D., Beau, F., Czarny, B., Cotton, J., Yiotakis, A., Dive, V., 2003. Roles of the two active sites of somatic angiotensin-converting enzyme in the cleavage of angiotensin I and bradykinin insights from selective inhibitors. Circ. Res. 93, 148–154. doi:10.1161/01.RES.0000081593.33848.FC

Georgiadis, D., Cuniasse, P., Cotton, J., Yiotakis, A., Dive, V., 2004. Structural determinants of RXPA380, a potent and highly selective inhibitor of the angiotensin-converting enzyme C-domain. Biochemistry 43, 8048–8054. doi:10.1021/bi049504q

Geroldi, D., Falcone, C., Emanuele, E., 2006. Soluble receptor for advanced glycation end products: from disease marker to potential therapeutic target. Curr. Med. Chem. 13, 1971–1978. doi:10.2174/092986706777585013

Girouard, H., Iadecola, C., 2006. Neurovascular coupling in the normal brain and in hypertension, stroke, and Alzheimer disease. J. Appl. Physiol. 100, 328–335. doi:10.1152/japplphysiol.00966.2005

Glabe, C.G., 2008. Structural classification of toxic amyloid oligomers. J. Biol. Chem. 283, 29639–43. doi:10.1074/jbc.R800016200

Glenner, G.G., Wong, C.W., 1984. Alzheimer's disease: Initial report of the purification and characterization of a novel cerebrovascular amyloid protein. Biochem. Biophys. Res. Commun. 120, 885–890.

Godemann, R., Biernat, J., Mandelkow, E., Mandelkow, E.M., 1999. Phosphorylation of tau protein by recombinant GSK-3β: Pronounced phosphorylation at select Ser/Thr-Pro motifs but no phosphorylation at Ser262 in the repeat domain. FEBS Lett. 454, 157–164. doi:10.1016/S0014-5793(99)00741-3

Gohlke, P., Schölkens, B., Henning, R., Urbach, H., Unger, T., 1989. Inhibition of converting enzyme in brain tissue and cerebrospinal fluid of rats following chronic oral treatment with the converting enzyme inhibitors ramipril and Hoe 288. J. Cardiovasc. Pharmacol. 14 Suppl 4, S32–S36. doi:10.1097/00005344-198906144-00008

Goldgaber, D., Lerman, M.I., McBride, O.W., Saffiotti, U., Gajdusek, D.C., 1987. Characterization and chromosomal localization of a cDNA encoding brain amyloid of Alzheimer's disease. Science 235, 877–80.

Gordon, K., 2011. PROTEIN-PROTEIN INTERACTIONS OF HUMAN SOMATIC ANGIOTENSIN-CONVERTING ENZYME. University of Cape Town.

Gordon, K., Redelinghuys, P., Schwager, S.L.U., Ehlers, M.R.W., Papageorgiou, A.C., Natesh, R., Acharya, K.R., Sturrock, E.D., 2003. Deglycosylation, processing and crystallization of human testis angiotensin-converting enzyme. Biochem. J. 371, 437–442. doi:10.1042/BJ20021842

Govoni, S., Mura, E., Racchi, M., Lanni, C., Grilli, M., Zappettini, S., Salamone, A., Olivero, G., Pittaluga, A., Marchi, M., 2014. Dangerous Liaisons between Beta-Amyloid and Cholinergic Neurotransmission. Curr. Pharm. Des. 20, 2525–38.

Gräff, J., Rei, D., Guan, J., Wang, W., Seo, J., Hennig, K.M., Nieland, T.J.F., Fass, D.M., Kao, P.F., Kahn, M., Su, S.C., Samiei, A., Joseph, N., Haggarty, S.J., Delalle, I., Tsai, L., 2012. An epigenetic blockade of cognitive functions in the neurodegenerating brain. Nature 483, 222–6. doi:10.1038/nature10849

Greco, S.J., Hamzelou, A., Johnston, J.M., Smith, M.A., Ashford, J.W., Tezapsidis, N., 2011. Leptin boosts cellular metabolism by activating AMPK and the sirtuins to reduce tau phosphorylation and β-amyloid in neurons. Biochem. Biophys. Res. Commun. 414, 170–174. doi:10.1016/j.bbrc.2011.09.050

Grinshtein, S. V., Levashov, A. V., Kost, O.A., 2001. Unusual Behavior of Membrane Somatic Angiotensin-Converting Enzyme in a Reversed Micelle System. Biochem. 66, 34–41. doi:10.1023/A:1002825527927

Grundke-Iqbal, I., Iqbal, K., Tung, Y.C., Quinlan, M., Wisniewski, H.M., Binder, L.I., 1986. Abnormal phosphorylation of the microtubule-associated protein tau (tau) in Alzheimer cytoskeletal pathology. Proc. Natl. Acad. Sci. U. S. A. 83, 4913–7.

Guimarães, P.B., Alvarenga, É.C., Siqueira, P.D., Paredes-Gamero, E.J., Sabatini, R.A., Morais, R.L.T., Reis, R.I., Santos, E.L., Teixeira, L.G.D., Casarini, D.E., Martin, R.P., Shimuta, S.I., Carmona, A.K., Nakaie, C.R., Jasiulionis, M.G., Ferreira, A.T., Pesquero, J.L., Oliveira, S.M., Bader, M., Costa-Neto, C.M., Pesquero, J.B., 2011. Angiotensin II binding to angiotensin I-converting enzyme triggers calcium signaling. Hypertension 57, 965–72. doi:10.1161/HYPERTENSIONAHA.110.167171

Guo, Q., Wang, Z., Li, H., Wiese, M., Zheng, H., 2012. APP physiological and pathophysiological functions: insights from animal models. Cell Res. 22, 78–89. doi:10.1038/cr.2011.116

Gustafsson, S., Lind, L., Söderberg, S., Ingelsson, E., 2010. Associations of circulating adiponectin with measures of vascular function and morphology. J. Clin. Endocrinol. Metab. 95, 2927–2934. doi:10.1210/jc.2009-2685

Guy, J.L., Jackson, R.M., Acharya, K.R., Sturrock, E.D., Hooper, N.M., Turner, A.J., 2003. Angiotensin-Converting Enzyme-2 (ACE2): Comparative Modeling of the Active Site, Specificity Requirements, and Chloride Dependence. Biochemistry 42, 13185–13192. doi:10.1021/bi035268s

Guzmán, E.A., Bouter, Y., Richard, B.C., Lannfelt, L., Ingelsson, M., Paetau, A., Verkkoniemi-Ahola, A., Wirths, O., Bayer, T.A., 2014. Abundance of $A\beta_5$-x like immunoreactivity in transgenic 5XFAD, APP/PS1KI and 3xTG mice, sporadic and familial Alzheimer's disease. Mol. Neurodegener. 9, 13. doi:10.1186/1750-1326-9-13

Haass, C., Kaether, C., Thinakaran, G., Sisodia, S., 2012. Trafficking and proteolytic processing of APP. Cold Spring Harb. Perspect. Med. 2, a006270. doi:10.1101/cshperspect.a006270

Haass, C., Selkoe, D.J., 2007. Soluble protein oligomers in neurodegeneration: lessons from the Alzheimer's amyloid beta-peptide. Nat. Rev. Mol. Cell Biol. 8, 101–112. doi:10.1038/nrm2101

Hagaman, J.R., Moyer, J.S., Bachman, E.S., Sibony, M., Magyar, P.L., Welch, J.E., Smithies, O., Krege, J.H., O'Brien, D.A., 1998. Angiotensin-converting enzyme and male fertility. Proc. Natl. Acad. Sci. U. S. A. 95, 2552–2557.

Hajjar, I.M., Keown, M., Lewis, P., Almor, A., 2008. Angiotensin converting enzyme inhibitors and cognitive and functional decline in patients with Alzheimer's disease: an observational study. Am. J. Alzheimers. Dis. Other Demen. 23, 77–

83. doi:10.1177/1533317507309803

Halim, A., Brinkmalm, G., Rüetschi, U., Westman-Brinkmalm, A., Portelius, E., Zetterberg, H., Blennow, K., Larson, G., Nilsson, J., 2011. Site-specific characterization of threonine, serine, and tyrosine glycosylations of amyloid precursor protein/amyloid beta-peptides in human cerebrospinal fluid. Proc. Natl. Acad. Sci. U. S. A. 108, 11848–53. doi:10.1073/pnas.1102664108

Hane, F., 2013. Are amyloid fibrils molecular spandrels? FEBS Lett. 587, 3617–9. doi:10.1016/j.febslet.2013.09.048

Hao, G.-H., Niu, X.-L., Gao, D.-F., Wei, J., Wang, N.-P., 2008. Agonists at PPAR-gamma suppress angiotensin II-induced production of plasminogen activator inhibitor-1 and extracellular matrix in rat cardiac fibroblasts. Br. J. Pharmacol. 153, 1409–1419. doi:10.1038/bjp.2008.21

Hardy, J., 1997. Amyloid, the presenilins and Alzheimer's disease. Trends Neurosci. doi:10.1016/S0166-2236(96)01030-2

Hardy, J., Bogdanovic, N., Winblad, B., Portelius, E., Andreasen, N., Cedazo-Minguez, A., Zetterberg, H., 2014. Pathways to Alzheimer's disease. J. Intern. Med. 275, 296–303. doi:10.1111/joim.12192

Hardy, J., Selkoe, D.J., 2002. The amyloid hypothesis of Alzheimer's disease: progress and problems on the road to therapeutics. Science 297, 353–356. doi:10.1126/science.1072994

Hardy, J.A., Higgins, G.A., 1992. Alzheimer's disease: the amyloid cascade hypothesis. Science 256, 184–185. doi:10.1126/science.1566067

Hart, G.W., 1999. The O-GlcNAc Modification, in: Varki, A., Cummings, R., Esko, J. (Eds.), Essentials of Glycobiology. Cold Spring Harbor Laboratory Press, pp. 183–193. doi:NBK1954 [bookaccession]

Hartter, D.E., Barnea, A., 1988. Evidence for release of copper in the brain: depolarization-induced release of newly taken-up 67copper. Synapse 2, 412–5. doi:10.1002/syn.890020408

Hashimoto, Y., Tsuji, O., Niikura, T., Yamagishi, Y., Ishizaka, M., Kawasumi, M., Chiba, T., Kanekura, K., Yamada, M., Tsukamoto, E., Kouyama, K., Terashita, K., Aiso, S., Lint, A., Nishimoto, I., 2003. Involvement of c-Jun N-terminal kinase in amyloid precursor protein-mediated neuronal cell death. J. Neurochem. 84, 864–877. doi:10.1046/j.1471-4159.2003.01585.x

Hausrath, A.C., Matthews, B.W., 2002. Thermolysin in the absence of substrate has an open conformation. Acta Crystallogr. Sect. D Biol. Crystallogr. 58, 1002–1007. doi:10.1107/S090744490200584X

Hawkes, C.A., Gatherer, M., Sharp, M.M., Dorr, A., Yuen, H.M., Kalaria, R., Weller, R.O., Carare, R.O., 2013. Regional differences in the morphological and functional effects of aging on cerebral basement membranes and perivascular drainage of amyloid-β from the mouse brain. Aging Cell 12, 224–236. doi:10.1111/acel.12045

Hawkes, C.A., Härtig, W., Kacza, J., Schliebs, R., Weller, R.O., Nicoll, J.A., Carare, R.O., 2011. Perivascular drainage of solutes is impaired in the ageing mouse brain and in the presence of cerebral amyloid angiopathy. Acta Neuropathol. 121,

431–443. doi:10.1007/s00401-011-0801-7

Hecker, M., Blaukat, A., Bara, A.T., Müller-Esterl, W., Busse, R., 1997. ACE inhibitor potentiation of bradykinin-induced venoconstriction. Br. J. Pharmacol. 121, 1475–1481. doi:10.1038/sj.bjp.0701281

Hecker, M., Pörsti, I., Bara, A.T., Busse, R., 1994. Potentiation by ACE inhibitors of the dilator response to bradykinin in the coronary microcirculation: interaction at the receptor level. Br. J. Pharmacol. 111, 238–244.

Hellner, K., Walther, T., Schubert, M., Albrecht, D., 2005. Angiotensin-(1-7) enhances LTP in the hippocampus through the G-protein-coupled receptor Mas. Mol. Cell. Neurosci. 29, 427–435. doi:10.1016/j.mcn.2005.03.012

Hemming, M.L., Selkoe, D.J., 2005. Amyloid β-protein is degraded by cellular angiotensin-converting enzyme (ACE) and elevated by an ACE inhibitor. J. Biol. Chem. 280, 37644–37650. doi:10.1074/jbc.M508460200

Hemming, M.L., Selkoe, D.J., Farris, W., 2007. Effects of prolonged angiotensin-converting enzyme inhibitor treatment on amyloid beta-protein metabolism in mouse models of Alzheimer disease. Neurobiol. Dis. 26, 273–281. doi:10.1016/j.nbd.2007.01.004

Hilbich, C., Kisters-Woike, B., Reed, J., Masters, C.L., Beyreuther, K., 1992. Substitutions of hydrophobic amino acids reduce the amyloidogenicity of Alzheimer's disease beta A4 peptides. J. Mol. Biol. 228, 460–473. doi:10.1016/0022-2836(92)90835-8

Hilgard, P., Czaja, M.J., Gerken, G., Stockert, R.J., 2004. Proapoptotic function of protein kinase CK2alpha" is mediated by a JNK signaling cascade. Am. J. Physiol. Gastrointest. Liver Physiol. 287, G192–G201. doi:10.1152/ajpgi.00507.2003

Holland, D.R., Hausrath, A.C., Juers, D., Matthews, B.W., 1995. Structural analysis of zinc substitutions in the active site of thermolysin. Protein Sci. 4, 1955–1965. doi:10.1002/pro.5560041001

Hooijmans, C.R., Kiliaan, A.J., 2008. Fatty acids, lipid metabolism and Alzheimer pathology. Eur. J. Pharmacol. doi:10.1016/j.ejphar.2007.11.081

Hooper, N.M., Turner, A.J., 2000. Protein processing mechanisms: from angiotensin-converting enzyme to Alzheimer's disease. Biochem. Soc. Trans. 28, 441–446. doi:10.1042/0300-5127:0280441

Hornig, B., Kohler, C., Drexler, H., 1997. Role of bradykinin in mediating vascular effects of angiotensin-converting enzyme inhibitors in humans. Circulation 95, 1115–1118. doi:10.1161/01.CIR.95.5.1115

Hovius, R., Vallotton, P., Wohland, T., Vogel, H., 2000. Fluorescence techniques: shedding light on ligand-receptor interactions. Trends Pharmacol. Sci. doi:10.1016/S0165-6147(00)01503-0

Howard, T.E., Shai, S.Y., Langford, K.G., Martin, B.M., Bernstein, K.E., 1990. Transcription of testicular angiotensin-converting enzyme (ACE) is initiated within the 12th intron of the somatic ACE gene. Mol. Cell. Biol. 10, 4294–4302. doi:10.1128/MCB.10.8.4294

Howell, G.A., Welch, M.G., Frederickson, C.J., 1984. Stimulation-induced uptake and

release of zinc in hippocampal slices. Nature 308, 736–738. doi:10.1038/308736a0

Howell, S., Nalbantoglu, J., Crine, P., 1995. Neutral endopeptidase can hydrolyze beta-amyloid(1-40) but shows no effect on beta-amyloid precursor protein metabolism. Peptides 16, 647–652. doi:0196-9781(95)00021-B [pii]

Hu, J., Igarashi, A., Kamata, M., Nakagawa, H., 2001. Angiotensin-converting Enzyme Degrades Alzheimer Amyloid Aβ-Peptide (Aβ); Retards Aβ Aggregation, Deposition, Fibril Formation; and Inhibits Cytotoxicity. J. Biol. Chem. 276, 47863–47868. doi:10.1074/jbc.M104068200

Huang, X., Atwood, C.S., Hartshorn, M.A., Multhaup, G., Goldstein, L.E., Scarpa, R.C., Cuajungco, M.P., Gray, D.N., Lim, J., Moir, R.D., Tanzi, R.E., Bush, A.I., 1999. The Aβ peptide of Alzheimer's disease directly produces hydrogen peroxide through metal ion reduction. Biochemistry 38, 7609–7616. doi:10.1021/bi990438f

Hubert, C., Houot, A.M., Corvol, P., Soubrier, F., 1991. Structure of the angiotensin I-converting enzyme gene: Two alternate promoters correspond to evolutionary steps of a duplicated gene. J. Biol. Chem. 266, 15377–15383.

Hughes, K., Nikolakaki, E., Plyte, S.E., Totty, N.F., Woodgett, J.R., 1993. Modulation of the glycogen synthase kinase-3 family by tyrosine phosphorylation. EMBO J. 12, 803–808.

Hunter, T., 2000. Signaling--2000 and beyond. Cell 100, 113–127. doi:10.1016/j.surg.2006.06.009

Hureau, C., 2012. Coordination of redox active metal ions to the amyloid precursor protein and to amyloid-β peptides involved in Alzheimer disease. Part 1: An overview. Coord. Chem. Rev. 256, 2164–2174. doi:10.1016/j.ccr.2012.03.037

Iadecola, C., 2004. Neurovascular regulation in the normal brain and in Alzheimer's disease. Nat. Rev. Neurosci. 5, 347–360. doi:10.1038/nrn1387

Igbavboa, U., Sun, G.Y., Weisman, G.A., He, Y., Wood, W.G., 2009. Amyloid beta-protein stimulates trafficking of cholesterol and caveolin-1 from the plasma membrane to the Golgi complex in mouse primary astrocytes. Neuroscience 162, 328–38. doi:10.1016/j.neuroscience.2009.04.049

Ihara, Y., Egashira, K., Nakano, K., Ohtani, K., Kubo, M., Koga, J. ichiro, Iwai, M., Horiuchi, M., Gang, Z., Yamagishi, S. ichi, Sunagawa, K., 2007. Upregulation of the ligand-RAGE pathway via the angiotensin II type I receptor is essential in the pathogenesis of diabetic atherosclerosis. J. Mol. Cell. Cardiol. 43, 455–464. doi:10.1016/j.yjmcc.2007.07.044

Ill-Raga, G., Ramos-Fernández, E., Guix, F.X., Tajes, M., Bosch-Morató, M., Palomer, E., Godoy, J., Belmar, S., Cerpa, W., Simpkins, J.W., Inestrosa And, N.C., Muoz, F.J., 2010. Amyloid-β peptide fibrils induce nitro-oxidative stress in neuronal cells. J. Alzheimer's Dis. 22, 641–652. doi:10.3233/JAD-2010-100474

Inoue, K., Hosaka, D., Mochizuki, N., Akatsu, H., Tsutsumiuchi, K., Hashizume, Y., Matsukawa, N., Yamamoto, T., Toyo'oka, T., 2014. Simultaneous Determination of Post-Translational Racemization and Isomerization of N-Terminal Amyloid-beta in Alzheimer's Brain Tissues by Covalent Chiral Derivatized Ultraperformance Liquid Chromatography Tandem Mass

Spectrometry. Anal. Chem. 86, 797–804. doi:Doi 10.1021/Ac403315h

Inoue, K., Nakagawa, A., Hino, T., Oka, H., 2009. Screening assay for metal-catalyzed oxidation inhibitors using liquid chromatography-mass spectrometry with an N-terminal beta-amyloid peptide. Anal. Chem. 81, 1819–1825. doi:10.1021/ac802162n

Israel, M.A., Yuan, S.H., Bardy, C., Reyna, S.M., Mu, Y., Herrera, C., Hefferan, M.P., Van Gorp, S., Nazor, K.L., Boscolo, F.S., Carson, C.T., Laurent, L.C., Marsala, M., Gage, F.H., Remes, A.M., Koo, E.H., Goldstein, L.S.B., 2012. Probing sporadic and familial Alzheimer's disease using induced pluripotent stem cells. Nature 482, 216–220. doi:10.1038/nature10821

Istrate, A.N., Tsvetkov, P.O., Mantsyzov, A.B., Kulikova, A.A., Kozin, S.A., Makarov, A.A., Polshakov, V.I., 2012. NMR solution structure of rat Aβ(1-16): Toward understanding the mechanism of rats' resistance to Alzheimer's disease. Biophys. J. 102, 136–143. doi:10.1016/j.bpj.2011.11.4006

Iwabu, M., Yamauchi, T., Okada-Iwabu, M., Sato, K., Nakagawa, T., Funata, M., Yamaguchi, M., Namiki, S., Nakayama, R., Tabata, M., Ogata, H., Kubota, N., Takamoto, I., Hayashi, Y.K., Yamauchi, N., Waki, H., Fukayama, M., Nishino, I., Tokuyama, K., Ueki, K., Oike, Y., Ishii, S., Hirose, K., Shimizu, T., Touhara, K., Kadowaki, T., 2010. Adiponectin and AdipoR1 regulate PGC-1alpha and mitochondria by Ca(2+) and AMPK/SIRT1. Nature 464, 1313–1319. doi:10.1038/nature08991

Iwata, N., Mizukami, H., Shirotani, K., Takaki, Y., Muramatsu, S., Lu, B., Gerard, N.P., Gerard, C., Ozawa, K., Saido, T.C., 2004. Presynaptic localization of neprilysin contributes to efficient clearance of amyloid-beta peptide in mouse brain. J. Neurosci. 24, 991–998. doi:10.1523/JNEUROSCI.4792-03.2004

Iwata, N., Sekiguchi, M., Hattori, Y., Takahashi, A., Asai, M., Ji, B., Higuchi, M., Staufenbiel, M., Muramatsu, S., Saido, T.C., 2013. Global brain delivery of neprilysin gene by intravascular administration of AAV vector in mice. Sci. Rep. 3, 1472. doi:10.1038/srep01472

Iwata, N., Takaki, Y., Fukami, S., Tsubuki, S., Saido, T.C., 2002. Region-specific reduction of Aβ-degrading endopeptidase, neprilysin, in mouse hippocampus upon aging. J. Neurosci. Res. 70, 493–500. doi:10.1002/jnr.10390

Iwata, N., Tsubuki, S., Takaki, Y., Shirotani, K., Lu, B., Gerard, N.P., Gerard, C., Hama, E., Lee, H.J., Saido, T.C., 2001. Metabolic regulation of brain Abeta by neprilysin. Science 292, 1550–1552. doi:10.1126/science.1059946

Iwata, N., Tsubuki, S., Takaki, Y., Watanabe, K., Sekiguchi, M., Hosoki, E., Kawashima-Morishima, M., Lee, H.J., Hama, E., Sekine-Aizawa, Y., Saido, T.C., 2000. Identification of the major Abeta1-42-degrading catabolic pathway in brain parenchyma: suppression leads to biochemical and pathological deposition. Nat. Med. 6, 143–150. doi:10.1038/72237

Jaspard, E., Wei, L., Alhenc-Gelas, F., 1993. Differences in the properties and enzymatic specificities of the two active sites of angiotensin I-converting enzyme (kininase II). Studies with bradykinin and other natural peptides. J. Biol. Chem. 268, 9496–9503.

Jawhar S, Wirths O, B.T., 2011. Pyroglutamate Abeta -- a hatchet man in Alzheimer

disease. J. Biol. Chem. 286, 38825–38832. doi:10.1074/jbc.R111.288308

Jiang, D., Li, X., Williams, R., Patel, S., Men, L., Wang, Y., Zhou, F., 2009. Ternary complexes of iron, amyloid-beta, and nitrilotriacetic acid: binding affinities, redox properties, and relevance to iron-induced oxidative stress in Alzheimer's disease. Biochemistry 48, 7939–47. doi:10.1021/bi900907a

Jiang, T., Zhang, Y.-D., Zhou, J.-S., Zhu, X.-C., Tian, Y.-Y., Zhao, H.-D., Lu, H., Gao, Q., Tan, L., Yu, J.-T., 2015. Angiotensin-(1-7) is Reduced and Inversely Correlates with Tau Hyperphosphorylation in Animal Models of Alzheimer's Disease. Mol. Neurobiol. doi:10.1007/s12035-015-9260-9

Jin, M., Shepardson, N., Yang, T., Chen, G., Walsh, D., Selkoe, D.J., 2011. Soluble amyloid beta-protein dimers isolated from Alzheimer cortex directly induce Tau hyperphosphorylation and neuritic degeneration. Proc. Natl. Acad. Sci. U. S. A. 108, 5819–5824. doi:10.1073/pnas.1017033108

Johns, E.J., 2005. Angiotensin II in the brain and the autonomic control of the kidney. Exp. Physiol. 90, 163–168. doi:10.1113/expphysiol.2004.029025

Johnson, S.A., Hunter, T., 2005. Kinomics: methods for deciphering the kinome. Nat. Methods 2, 17–25. doi:10.1038/nmeth731

Johnstone, M., Gearing, A.J.H., Miller, K.M., 1999. A central role for astrocytes in the inflammatory response to β-amyloid; chemokines, cytokines and reactive oxygen species are produced. J. Neuroimmunol. 93, 182–193.

Jullien, N.D., Cuniasse, P., Georgiadis, D., Yiotakis, A., Dive, V., 2006. Combined use of selective inhibitors and fluorogenic substrates to study the specificity of somatic wild-type angiotensin-converting enzyme. FEBS J. 273, 1772–1781. doi:10.1111/j.1742-4658.2006.05196.x

Junot, C., Gonzales, M.F., Ezan, E., Cotton, J., Vazeux, G., Michaud, A., Azizi, M., Vassiliou, S., Yiotakis, A., Corvol, P., Dive, V., 2001. RXP 407, a selective inhibitor of the N-domain of angiotensin I-converting enzyme, blocks in vivo the degradation of hemoregulatory peptide acetyl-Ser-Asp-Lys-Pro with no effect on angiotensin I hydrolysis. J. Pharmacol. Exp. Ther. 297, 606–611.

Kalra, J., Prakash, A., Kumar, P., Majeed, A.B.A., 2015. Cerebroprotective effects of RAS inhibitors: Beyond their cardio-renal actions. J. Renin. Angiotensin. Aldosterone. Syst. 1470320315583582–. doi:10.1177/1470320315583582

Kanekiyo, T., Bu, G., 2014. The low-density lipoprotein receptor-related protein 1 and amyloid-β clearance in Alzheimer's disease. Front. Aging Neurosci. doi:10.3389/fnagi.2014.00093

Kang, J., Lemaire, H.G., Unterbeck, A., Salbaum, J.M., Masters, C.L., Grzeschik, K.H., Multhaup, G., Beyreuther, K., Müller-Hill, B., 1987. The precursor of Alzheimer's disease amyloid A4 protein resembles a cell-surface receptor. Nature 325, 733–736. doi:10.1097/00002093-198701030-00032

Kang, J., Rivest, S., 2012. Lipid metabolism and neuroinflammation in alzheimer's disease: A role for liver X receptors. Endocr. Rev. doi:10.1210/er.2011-1049

Kang, J.-E., Lim, M.M., Bateman, R.J., Lee, J.J., Smyth, L.P., Cirrito, J.R., Fujiki, N., Nishino, S., Holtzman, D.M., 2009. Amyloid-beta dynamics are regulated by orexin and the sleep-wake cycle. Science 326, 1005–1007.

doi:10.1126/science.1180962

Karr, J.W., Kaupp, L.J., Szalai, V.A., 2004. Amyloid-beta binds Cu2+ in a mononuclear metal ion binding site. J. Am. Chem. Soc. 126, 13534–8. doi:10.1021/ja0488028

Katzov, H., Bennet, A.M., Kehoe, P., Wiman, B., Gatz, M., Blennow, K., Lenhard, B., Pedersen, N.L., de Faire, U., Prince, J.A., 2004. A cladistic model of ACE sequence variation with implications for myocardial infarction, Alzheimer disease and obesity. Hum. Mol. Genet. 13, 2647–2657. doi:10.1093/hmg/ddh286

Kehoe, P.G., Katzov, H., Feuk, L., Bennet, A.M., Johansson, B., Wilman, B., de Faire, U., Cairns, N.J., Wilcock, G.K., Brookes, A.J., Blennow, K., Prince, J.A., 2003. Haplotypes extending across ACE are associated with Alzheimer's disease. Hum. Mol. Genet. 12, 859–867. doi:10.1093/hmg/ddg094

Kehoe, P.G., Passmore, P.A., 2012. The Renin-Angiotensin system and antihypertensive drugs in Alzheimer's disease: Current standing of the angiotensin hypothesis? J. Alzheimer's Dis. doi:10.3233/JAD-2012-111376

Kehoe, P.G., Russ, C., McIlory, S., Williams, H., Holmans, P., Holmes, C., Liolitsa, D., Vahidassr, D., Powell, J., McGleenon, B., Liddell, M., Plomin, R., Dynan, K., Williams, N., Neal, J., Cairns, N.J., Wilcock, G., Passmore, P., Lovestone, S., Williams, J., Owen, M.J., 1999. Variation in DCP1, encoding ACE, is associated with susceptibility to Alzheimer disease. Nat. Genet. doi:10.1038/5009

Kehoe, P.G., Wilcock, G.K., 2007. Is inhibition of the renin-angiotensin system a new treatment option for Alzheimer's disease? Lancet Neurol. 6, 373–378. doi:10.1016/S1474-4422(07)70077-7

Kelstrup, C.D., Hekmat, O., Francavilla, C., Olsen, J. V, 2011. Pinpointing phosphorylation sites: Quantitative filtering and a novel site-specific x-ion fragment. J. Proteome Res. 10, 2937–48. doi:10.1021/pr200154t

Kenny, A.J., Bourne, A., Ingram, J., 1993. Hydrolysis of human and pig brain natriuretic peptides, urodilatin, C-type natriuretic peptide and some C-receptor ligands by endopeptidase-24.11. Biochem. J. 291 (Pt 1, 83–88.

Kerr, D.S., Bevilaqua, L.R.M., Bonini, J.S., Rossato, J.I., Köhler, C.A., Medina, J.H., Izquierdo, I., Cammarota, M., 2005. Angiotensin II blocks memory consolidation through an AT2 receptor-dependent mechanism. Psychopharmacology (Berl). 179, 529–535. doi:10.1007/s00213-004-2074-5

Khachaturian, A.S., Zandi, P.P., Lyketsos, C.G., Hayden, K.M., Skoog, I., Norton, M.C., Tschanz, J.T., Mayer, L.S., Welsh-Bohmer, K.A., Breitner, J.C.S., 2006. Antihypertensive medication use and incident Alzheimer disease: the Cache County Study., Archives of neurology. doi:10.1001/archneur.63.5.noc60013

Kim, H.S., Krege, J.H., Kluckman, K.D., Hagaman, J.R., Hodgin, J.B., Best, C.F., Jennette, J.C., Coffman, T.M., Maeda, N., Smithies, O., 1995. Genetic control of blood pressure and the angiotensinogen locus. Proc. Natl. Acad. Sci. U. S. A. 92, 2735–2739. doi:10.1073/pnas.92.7.2735

Kisanuki, Y.Y., Emoto, N., Ohuchi, T., Widyantoro, B., Yagi, K., Nakayama, K., Kedzierski, R.M., Hammer, R.E., Yanagisawa, H., Williams, S.C., Richardson, J.A., Suzuki, T., Yanagisawa, M., 2010. Low blood pressure in endothelial cell-

specific endothelin 1 knockout mice. Hypertension 56, 121–128. doi:10.1161/HYPERTENSIONAHA.109.138701

Kivipelto, M., Solomon, A., 2006. Cholesterol as a risk factor for Alzheimer's disease - Epidemiological evidence. Acta Neurol. Scand. doi:10.1111/j.1600-0404.2006.00685.x

Klumpp, S., Mäurer, A., Zhu, Y., Aichele, D., Pinna, L.A., Krieglstein, J., 2004. Protein kinase CK2 phosphorylates BAD at threonine-117. Neurochem. Int. 45, 747–752. doi:10.1016/j.neuint.2004.02.006

Knight, C.G., 1995. Active-site titration of peptidases. Methods Enzymol. 248, 85–104. doi:10.1016/0076-6879(95)48008-0

Kohlstedt, K., Brandes, R.P., Müller-Esterl, W., Busse, R., Fleming, I., 2004. Angiotensin-Converting Enzyme Is Involved in Outside-in Signaling in Endothelial Cells. Circ. Res. 94, 60–67. doi:10.1161/01.RES.0000107195.13573.E4

Kohlstedt, K., Busse, R., Fleming, I., 2005. Signaling via the angiotensin-converting enzyme enhances the expression of cyclooxygenase-2 in endothelial cells. Hypertension 45, 126–132. doi:10.1161/01.HYP.0000150159.48992.11

Kohlstedt, K., Gershome, C., Friedrich, M., Müller-Esterl, W., Alhenc-Gelas, F., Busse, R., Fleming, I., 2006a. Angiotensin-converting enzyme (ACE) dimerization is the initial step in the ACE inhibitor-induced ACE signaling cascade in endothelial cells. Mol. Pharmacol. 69, 1725–1732. doi:10.1124/mol.105.020636

Kohlstedt, K., Gershome, C., Trouvain, C., Hofmann, W.-K., Fichtlscherer, S., Fleming, I., 2009. Angiotensin-converting enzyme (ACE) inhibitors modulate cellular retinol-binding protein 1 and adiponectin expression in adipocytes via the ACE-dependent signaling cascade. Mol. Pharmacol. 75, 685–692. doi:10.1124/mol.108.051631

Kohlstedt, K., Kellner, R., Busse, R., Fleming, I., 2006b. Signaling via the angiotensin-converting enzyme results in the phosphorylation of the nonmuscle myosin heavy chain IIA. Mol. Pharmacol. 69, 19–26. doi:10.1124/mol.105.016733.The

Kohlstedt, K., Shoghi, F., Müller-Esterl, W., Busse, R., Fleming, I., 2002. CK2 phosphorylates the angiotensin-converting enzyme and regulates its retention in the endothelial cell plasma membrane. Circ. Res. 91, 749–56. doi:10.1161/01.RES.0000038114.17939.C8

Kohlstedt, K., Trouvain, C., Boettger, T., Shi, L., Fisslthaler, B., Fleming, I., 2013. AMP-activated protein kinase regulates endothelial cell angiotensin-converting enzyme expression via p53 and the post-transcriptional regulation of microRNA-143/145. Circ. Res. 112, 1150–8. doi:10.1161/CIRCRESAHA.113.301282

Kohlstedt, K., Trouvain, C., Namgaladze, D., Fleming, I., 2011. Adipocyte-derived lipids increase angiotensin-converting enzyme (ACE) expression and modulate macrophage phenotype. Basic Res. Cardiol. 106, 205–15. doi:10.1007/s00395-010-0137-9

Koka, V., Huang, X.R., Chung, A.C.K., Wang, W., Truong, L.D., Lan, H.Y., 2008.

Angiotensin II up-regulates angiotensin I-converting enzyme (ACE), but down-regulates ACE2 via the AT1-ERK/p38 MAP kinase pathway. Am. J. Pathol. 172, 1174–1183. doi:10.2353/ajpath.2008.070762

Kost, O.A., Balyasnikova, I. V, Chemodanova, E.E., Nikolskaya, I.I., Albrecht, R.F., Danilov, S.M., 2003. Epitope-dependent blocking of the angiotensin-converting enzyme dimerization by monoclonal antibodies to the N-terminal domain of ACE: Possible link of ACE dimerization and shedding from the cell surface. Biochemistry 42, 6965–6976. doi:10.1021/bi034645y

Kost, O.A., Orth, T.A., Nikolskaya, I.I., Nametkin, S.N., Levashov, A. V, 1998. Carbohydrates regulate the dimerization of angiotensin-converting enzyme. Biochem. Mol. Biol. Int. 44, 535–542.

Kowalik-Jankowska, T., Ruta-Dolejsz, M., Wiśniewska, K., Łankiewicz, L., 2001. Cu(II) interaction with N-terminal fragments of human and mouse beta-amyloid peptide. J. Inorg. Biochem. 86, 535–545. doi:S0162-0134(01)00226-4 [pii]

Kozin, S.A., Mezentsev, Y. V, Kulikova, A.A., Indeykina, M.I., Golovin, A. V, Ivanov, A.S., Tsvetkov, P.O., Makarov, A.A., 2011. Zinc-induced dimerization of the amyloid-β metal-binding domain 1-16 is mediated by residues 11-14. Mol. Biosyst. 7, 1053–1055. doi:10.1039/c0mb00334d

Krege, J.H., John, S.W., Langenbach, L.L., Hodgin, J.B., Hagaman, J.R., Bachman, E.S., Jennette, J.C., O'Brien, D.A., Smithies, O., 1995. Male-female differences in fertility and blood pressure in ACE-deficient mice. Nature 375, 146–148. doi:10.1038/375146a0

Kröger, W.L., 2009. A Molecular Basis for the C-Domain Selectivity of Angiotensin-Converting Enzyme.

Kröger, W.L., Douglas, R.G., O'Neill, H.G., Dive, V., Sturrock, E.D., 2009. Investigating the domain specificity of phosphinic inhibitors RXPA380 and RXP407 in angiotensin-converting enzyme. Biochemistry 48, 8405–8412. doi:10.1021/bi9011226

Kukkola, P.J., Savage, P., Sakane, Y., Berry, J.C., Bilci, N.A., Ghai, R.D., Jeng, A.Y., 1995. Differential structure-activity relationships of phosphoramidon analogues for inhibition of three metalloproteases: endothelin-converting enzyme, neutral endopeptidase, and angiotensin-converting enzyme. J. Cardiovasc. Pharmacol. 26 Suppl 3, S65–8.

Kumar, S., Rezaei-Ghaleh, N., Terwel, D., Thal, D.R., Richard, M., Hoch, M., Mc Donald, J.M., Wüllner, U., Glebov, K., Heneka, M.T., Walsh, D.M., Zweckstetter, M., Walter, J., 2011. Extracellular phosphorylation of the amyloid β-peptide promotes formation of toxic aggregates during the pathogenesis of Alzheimer's disease. EMBO J. 30, 2255–65. doi:10.1038/emboj.2011.138

Kumar, S., Singh, S., Hinze, D., Josten, M., Sahl, H.G., Siepmann, M., Walter, J., 2012. Phosphorylation of amyloid-β peptide at serine 8 attenuates its clearance via insulin-degrading and angiotensin-converting enzymes. J. Biol. Chem. 287, 8641–8651. doi:10.1074/jbc.M111.279133

Kummer, M.P., Heneka, M.T., 2014. Truncated and modified amyloid-beta species. Alzheimers. Res. Ther. 6, 28. doi:10.1186/alzrt258

Kummer, M.P., Hermes, M., Delekarte, A., Hammerschmidt, T., Kumar, S., Terwel, D., Walter, J., Pape, H.C., König, S., Roeber, S., Jessen, F., Klockgether, T., Korte, M., Heneka, M.T., 2011. Nitration of tyrosine 10 critically enhances amyloid β aggregation and plaque formation. Neuron 71, 833–844. doi:10.1016/j.neuron.2011.07.001

Kurochkin, I. V, Goto, S., 1994. Alzheimer's beta-amyloid peptide specifically interacts with and is degraded by insulin degrading enzyme. FEBS Lett. 345, 33–37. doi:10.1016/0014-5793(94)00387-4

Kurochkin, I. V., 1998. Amyloidogenic determinant as a substrate recognition motif of insulin-degrading enzyme. FEBS Lett. doi:10.1016/S0014-5793(98)00422-0

Ladu, M.J., Reardon, C., Van Eldik, L., Fagan, A.M., Bu, G., Holtzman, D., Getz, G.S., 2000. Lipoproteins in the central nervous system. Ann. N. Y. Acad. Sci. 903, 167–175. doi:10.1111/j.1749-6632.2000.tb06365.x

LaDu, M.J., Shah, J.A., Reardon, C.A., Getz, G.S., Bu, G., Hu, J., Guo, L., van Eldik, L.J., 2000. Apolipoprotein E receptors mediate the effects of beta-amyloid on astrocyte cultures. J. Biol. Chem. 275, 33974–33980. doi:10.1074/jbc.M000602200

Laemmli, U.K., 1970. Cleavage of structural proteins during the assembly of the head of bacteriophage T4. Nature 227, 680–685. doi:10.1038/227680a0

LaFerla, F.M., Green, K.N., Oddo, S., 2007. Intracellular amyloid-β in Alzheimer's disease. Nat. Rev. Neurosci. doi:10.1038/nrn2168

Langford, K.G., Shai, S.Y., Howard, T.E., Kovac, M.J., Overbeek, P.A., Bernstein, K.E., 1991. Transgenic mice demonstrate a testis-specific promoter for angiotensin-converting enzyme. J. Biol. Chem. 266, 15559–62.

Larson, M., Sherman, M. a, Amar, F., Nuvolone, M., Schneider, J. a, Bennett, D. a, Aguzzi, A., Lesné, S.E., 2012. The complex PrP(c)-Fyn couples human oligomeric Aβ with pathological tau changes in Alzheimer's disease. J. Neurosci. 32, 16857–71a. doi:10.1523/JNEUROSCI.1858-12.2012

Laskowski, R.A., Swindells, M.B., 2011. LigPlot+: Multiple ligand-protein interaction diagrams for drug discovery. J. Chem. Inf. Model. 51, 2778–2786. doi:10.1021/ci200227u

Launer, L.J., 2009. Diabetes: Vascular or Neurodegenerative: An epidemiologic perspective, in: Stroke. doi:10.1161/STROKEAHA.108.533075

Launer, L.J., Ross, G.W., Petrovitch, H., Masaki, K., Foley, D., White, L.R., Havlik, R.J., 2000. Midlife blood pressure and dementia: The Honolulu-Asia aging study. Neurobiol. Aging 21, 49–55. doi:10.1016/S0197-4580(00)00096-8

Lawrence, J.L.M., Tong, M., Alfulaij, N., Sherrin, T., Contarino, M., White, M.M., Bellinger, F.P., Todorovic, C., Nichols, R.A., 2014. Regulation of Presynaptic Ca2+, Synaptic Plasticity and Contextual Fear Conditioning by a N-terminal -Amyloid Fragment. J. Neurosci. 34, 14210–14218. doi:10.1523/JNEUROSCI.0326-14.2014

Lee, E.H., Ma, Y.L., Wayner, M.J., Armstrong, D.L., 1995. Impaired retention by angiotensin II mediated by the AT1 receptor. Peptides 16, 1069–1071.

doi:10.1016/0196-9781(95)00073-S

Lehmann, D.J., Cortina-Borja, M., Warden, D.R., Smith, A.D., Sleegers, K., Prince, J.A., Van Duijn, C.M., Kehoe, P.G., 2005. Large meta-analysis establishes the ACE insertion-deletion polymorphism as a marker of Alzheimer's disease. Am. J. Epidemiol. 162, 305–317. doi:10.1093/aje/kwi202

Leissring, M.A., 2008. The AbetaCs of Abeta-cleaving proteases. J. Biol. Chem. 283, 29645–29649. doi:10.1074/jbc.R800022200

Leissring, M.A., Farris, W., Chang, A.Y., Walsh, D.M., Wu, X., Sun, X., Frosch, M.P., Selkoe, D.J., 2003a. Enhanced proteolysis of β-amyloid in APP transgenic mice prevents plaque formation, secondary pathology, and premature death. Neuron 40, 1087–1093. doi:10.1016/S0896-6273(03)00787-6

Leissring, M.A., Farris, W., Wu, X., Christodoulou, D.C., Haigis, M.C., Guarente, L., Selkoe, D.J., 2004. Alternative translation initiation generates a novel isoform of insulin-degrading enzyme targeted to mitochondria. Biochem. J. 383, 439–446. doi:10.1042/BJ20041081

Leissring, M.A., Lu, A., Condron, M.M., Teplow, D.B., Stein, R.L., Farris, W., Selkoe, D.J., 2003b. Kinetics of amyloid β-protein degradation determined by novel fluorescence- and fluorescence polarization-based assays. J. Biol. Chem. 278, 37314–37320. doi:10.1074/jbc.M305627200

Leslie, A.G.W., Powell, H.R., 2007. Processing diffraction data with MOSFLM, in: Evolving Methods for Macromolecular Crystallography. pp. 41–51. doi:10.1007/978-1-4020-6316-9_4

Lesné, S., Docagne, F., Gabriel, C., Liot, G., Lahiri, D.K., Buée, L., Plawinski, L., Delacourte, A., MacKenzie, E.T., Buisson, A., Vivien, D., 2003. Transforming growth factor-beta 1 potentiates amyloid-beta generation in astrocytes and in transgenic mice. J. Biol. Chem. 278, 18408–18418. doi:10.1074/jbc.M300819200

Lesné, S., Koh, M.T., Kotilinek, L., Kayed, R., Glabe, C.G., Yang, A., Gallagher, M., Ashe, K.H., 2006. A specific amyloid-beta protein assembly in the brain impairs memory. Nature 440, 352–357. doi:10.1038/nature04533

Lesné, S.E., Sherman, M.A., Grant, M., Kuskowski, M., Schneider, J.A., Bennett, D.A., Ashe, K.H., 2013. Brain amyloid-β oligomers in ageing and Alzheimer's disease. Brain 136, 1383–1398. doi:10.1093/brain/awt062

Lew, R.A., Mustafa, T., Ye, S., McDowall, S.G., Chai, S.Y., Albiston, A.L., 2003. Angiotensin AT4 ligands are potent, competitive inhibitors of insulin regulated aminopeptidase (IRAP). J. Neurochem. 86, 344–350. doi:10.1046/j.1471-4159.2003.01852.x

Li, H., Wang, Z., Wang, B., Guo, Q., Dolios, G., Tabuchi, K., Hammer, R.E., Südhof, T.C., Wang, R., Zheng, H., 2010. Genetic dissection of the amyloid precursor protein in developmental function and amyloid pathogenesis. J. Biol. Chem. 285, 30598–605. doi:10.1074/jbc.M110.137729

Li, J.-M., Mogi, M., Tsukuda, K., Tomochika, H., Iwanami, J., Min, L.-J., Nahmias, C., Iwai, M., Horiuchi, M., 2007. Angiotensin II-induced neural differentiation via angiotensin II type 2 (AT2) receptor-MMS2 cascade involving interaction between AT2 receptor-interacting protein and Src homology 2 domain-

containing protein-tyrosine phosphatase 1. Mol. Endocrinol. 21, 499–511. doi:10.1210/me.2006-0005

Li, N., Lee, A., Whitmer, R.A., Kivipelto, M., Lawler, E., Kazis, L.E., Wolozin, B., 2010. Use of angiotensin receptor blockers and risk of dementia in a predominantly male population: prospective cohort analysis. BMJ 340, b5465. doi:10.1136/bmj.b5465

Li, P., Xiao, H.D., Xu, J., Ong, F.S., Kwon, M., Roman, J., Gal, A., Bernstein, K.E., Fuchs, S., 2010. Angiotensin-converting enzyme N-terminal inactivation alleviates bleomycin-induced lung injury. Am. J. Pathol. 177, 1113–21. doi:10.2353/ajpath.2010.081127

Li, S., Jin, M., Zhang, D., Yang, T., Koeglsperger, T., Fu, H., Selkoe, D.J., 2013. Environmental novelty activates β2-adrenergic signaling to prevent the impairment of hippocampal LTP by Aβ oligomers. Neuron 77, 929–941. doi:10.1016/j.neuron.2012.12.040

Li, S., Shankar, G.M., Selkoe, D.J., 2010. How do Soluble Oligomers of Amyloid beta-protein Impair Hippocampal Synaptic Plasticity? Front. Cell. Neurosci. 4, 5. doi:10.3389/fncel.2010.00005

Liao, M.Q., Tzeng, Y.J., Chang, L.Y.X., Huang, H.B., Lin, T.H., Chyan, C.L., Chen, Y.C., 2007. The correlation between neurotoxicity, aggregative ability and secondary structure studied by sequence truncated Aβ peptides. FEBS Lett. 581, 1161–1165. doi:10.1016/j.febslet.2007.02.026

Liao, T.D., Yang, X.P., D'Ambrosio, M., Zhang, Y., Rhaleb, N.E., Carretero, O.A., 2010. N-acetyl-seryl-aspartyl-lysyl-proline attenuates renal injury and dysfunction in hypertensive rats with reduced renal mass: council for high blood pressure research. Hypertension 55, 459–467.

Lichtenthaler, S.F., Haass, C., Steiner, H., 2011. Regulated intramembrane proteolysis - Lessons from amyloid precursor protein processing. J. Neurochem. doi:10.1111/j.1471-4159.2011.07248.x

Lin, C., Datta, V., Okwan-Duodu, D., Chen, X., Fuchs, S., Alsabeh, R., Billet, S., Bernstein, K.E., Shen, X.Z., 2011. Angiotensin-converting enzyme is required for normal myelopoiesis. FASEB J. 25, 1145–1155. doi:10.1096/fj.10-169433

Lin, C.-X., Rhaleb, N.-E., Yang, X.-P., Liao, T.-D., D'Ambrosio, M.A., Carretero, O.A., 2008. Prevention of aortic fibrosis by N-acetyl-seryl-aspartyl-lysyl-proline in angiotensin II-induced hypertension. Am. J. Physiol. Heart Circ. Physiol. 295, H1253–H1261. doi:10.1152/ajpheart.00481.2008

Lindgren, M., Hammarström, P., 2010. Amyloid oligomers: Spectroscopic characterization of amyloidogenic protein states. FEBS J. doi:10.1111/j.1742-4658.2010.07571.x

Liu, S., Liu, J., Miura, Y., Tanabe, C., Maeda, T., Terayama, Y., Turner, A.J., Zou, K., Komano, H., 2014. Conversion of Aβ43 to Aβ40 by the successive action of angiotensin-converting enzyme 2 and angiotensin-converting enzyme. J. Neurosci. Res. 92, 1178–1186. doi:10.1002/jnr.23404

Liu, Y., Kati, W., Chen, C.M., Tripathi, R., Molla, A., Kohlbrenner, W., 1999. Use of a fluorescence plate reader for measuring kinetic parameters with inner filter effect correction. Anal. Biochem. 267, 331–335. doi:10.1006/abio.1998.3014

Louis, W.J., Mander, A.G., Dawson, M., O'Callaghan, C., Conway, E.L., 1999. Use of computerized neuropsychological tests (CANTAB) to assess cognitive effects of antihypertensive drugs in the elderly. Cambridge Neuropsychological Test Automated Battery., Journal of hypertension.

Lue, L.F., Walker, D.G., Brachova, L., Beach, T.G., Rogers, J., Schmidt, A.M., Stern, D.M., Yan, S.D., 2001. Involvement of microglial receptor for advanced glycation endproducts (RAGE) in Alzheimer's disease: identification of a cellular activation mechanism. Exp. Neurol. 171, 29–45. doi:10.1006/exnr.2001.7732

MacLean, B., Tomazela, D.M., Shulman, N., Chambers, M., Finney, G.L., Frewen, B., Kern, R., Tabb, D.L., Liebler, D.C., MacCoss, M.J., 2010. Skyline: An open source document editor for creating and analyzing targeted proteomics experiments. Bioinformatics 26, 966–968. doi:10.1093/bioinformatics/btq054

Magara, F., Muller, U., Li, Z.-W., Lipp, H.-P., Weissmann, C., Stagljar, M., Wolfer, D.P., 1999. Genetic background changes the pattern of forebrain commissure defects in transgenic mice underexpressing the -amyloid-precursor protein. Proc. Natl. Acad. Sci. 96, 4656–4661. doi:10.1073/pnas.96.8.4656

Mahley, R.W., Weisgraber, K.H., Huang, Y., 2009. Apolipoprotein E: structure determines function, from atherosclerosis to Alzheimer's disease to AIDS. J. Lipid Res. 50 Suppl, S183–S188. doi:10.1194/jlr.R800069-JLR200

Maianti, J.P., McFedries, A., Foda, Z.H., Kleiner, R.E., Du, X.Q., Leissring, M. a, Tang, W.-J., Charron, M.J., Seeliger, M. a, Saghatelian, A., Liu, D.R., 2014. Anti-diabetic activity of insulin-degrading enzyme inhibitors mediated by multiple hormones. Nature 511, 94–98. doi:10.1038/nature13297

Mairet-Coello, G., Polleux, F., 2014. Involvement of "stress-response" kinase pathways in Alzheimer's disease progression. Curr. Opin. Neurobiol. doi:10.1016/j.conb.2014.03.011

Malito, E., Hulse, R.E., Tang, W.J., 2008. Amyloid β-degrading cryptidases: Insulin degrading enzyme, presequence peptidase, and neprilysin. Cell. Mol. Life Sci. doi:10.1007/s00018-008-8112-4

Marcic, B., Deddish, P.A., Jackman, H.L., Erdös, E.G., 1999. Enhancement of bradykinin and resensitization of its B2 receptor. Hypertension 33, 835–843. doi:10.1161/01.HYP.33.3.835

Marcic, B., Deddish, P.A., Jackman, H.L., Erdös, E.G., Tan, F., 2000. Effects of the N-terminal sequence of ACE on the properties of its C-domain. Hypertension 36, 116–121. doi:10.1161/01.HYP.36.1.116-a

Margraf-Schönfeld, S., Böhm, C., Watzl, C., 2011. Glycosylation affects ligand binding and function of the activating natural killer cell receptor 2B4 (CD244) protein. J. Biol. Chem. 286, 24142–24149. doi:10.1074/jbc.M111.225334

Marques, G.D.M., Quinto, B.M.R., Plavinik, F.L., Krieger, J.E., Marson, O., Casarini, D.E., 2003. N-domain angiotensin I-converting enzyme with 80 kDa as a possible genetic marker of hypertension, in: Hypertension. Departamento de Medicina, Disciplina de Nefrologia, UNIFESP, Escola Paulista de Medicina, INCOR, Sao Paulo, SP, Brazil, pp. 693–701. doi:10.1161/01.HYP.0000085784.18572.CB

Marr, R.A., Rockenstein, E., Mukherjee, A., Kindy, M.S., Hersh, L.B., Gage, F.H., Verma, I.M., Masliah, E., 2003. Neprilysin gene transfer reduces human amyloid pathology in transgenic mice. J. Neurosci. 23, 1992–1996. doi:23/6/1992 [pii]

Marrero, M.B., Fulton, D., Stepp, D., Stern, D.M., 2004. Angiotensin II-induced insulin resistance and protein tyrosine phosphatases. Arterioscler. Thromb. Vasc. Biol. doi:10.1161/01.ATV.0000140059.04717.f3

Masselon, C., Anderson, G.A., Harkewicz, R., Bruce, J.E., Pasa-Tolic, L., Smith, R.D., 2000. Accurate mass multiplexed tandem mass spectrometry for high-throughput polypeptide identification from mixtures. Anal. Chem. 72, 1918–1924. doi:10.1021/ac991133+

Masters, C.L., Multhaup, G., Simms, G., Pottgiesser, J., Martins, R.N., Beyreuther, K., 1985. Neuronal origin of a cerebral amyloid: neurofibrillary tangles of Alzheimer's disease contain the same protein as the amyloid of plaque cores and blood vessels. EMBO J. 4, 2757–2763.

Masuyer, G., Schwager, S.L.U., Sturrock, E.D., Isaac, R.E., Acharya, K.R., 2012. Molecular recognition and regulation of human angiotensin-I converting enzyme (ACE) activity by natural inhibitory peptides. Sci. Rep. doi:10.1038/srep00717

Matsas, R., Kenny, A.J., Turner, A.J., 1984. The metabolism of neuropeptides. The hydrolysis of peptides, including enkephalins, tachykinins and their analogues, by endopeptidase-24.11. Biochem. J. 223, 433–440.

Mattson, M.P., 2004. Pathways towards and away from Alzheimer's disease. Nature 430, 631–9. doi:10.1038/nature02621

Mattson, M.P., 1997. Cellular actions of beta-amyloid precursor protein and its soluble and fibrillogenic derivatives. Physiol. Rev. 77, 1081–1132.

Mawuenyega, K.G., Sigurdson, W., Ovod, V., Munsell, L., Kasten, T., Morris, J.C., Yarasheski, K.E., Bateman, R.J., 2010. Decreased clearance of CNS beta-amyloid in Alzheimer's disease. Science 330, 1774. doi:10.1126/science.1197623

Maynard, C.J., Cappai, R., Volitakis, I., Cherny, R.A., White, A.R., Beyreuther, K., Masters, C.L., Bush, A.I., Li, Q.X., 2002. Overexpression of Alzheimer's disease amyloid-β opposes the age-dependent elevations of brain copper and iron. J. Biol. Chem. 277, 44670–44676. doi:10.1074/jbc.M204379200

Mc Donald, J.M., Savva, G.M., Brayne, C., Welzel, A.T., Forster, G., Shankar, G.M., Selkoe, D.J., Ince, P.G., Walsh, D.M., 2010. The presence of sodium dodecyl sulphate-stable Aβ dimers is strongly associated with Alzheimer-type dementia. Brain 133, 1328–1341. doi:10.1093/brain/awq065

McAlister, G.C., Berggren, W.T., Griep-Raming, J., Horning, S., Makarov, A., Phanstiel, D., Stafford, G., Swaney, D.L., Syka, J.E.P., Zabrouskov, V., Coon, J.J., 2008. A proteomics grade electron transfer dissociation-enabled hybrid linear ion trap-orbitrap mass spectrometer. J. Proteome Res. 7, 3127–36. doi:10.1021/pr800264t

McCord, L. a, Liang, W.G., Dowdell, E., Kalas, V., Hoey, R.J., Koide, A., Koide, S., Tang, W.-J., 2013. Conformational states and recognition of amyloidogenic peptides

of human insulin-degrading enzyme. Proc. Natl. Acad. Sci. U. S. A. 110, 13827–32. doi:10.1073/pnas.1304575110

McCoy, A.J., Grosse-Kunstleve, R.W., Adams, P.D., Winn, M.D., Storoni, L.C., Read, R.J., 2007. Phaser crystallographic software. J. Appl. Crystallogr. 40, 658–674. doi:10.1107/S0021889807021206

McFarlane, S.I., Kumar, A., Sowers, J.R., 2003. Mechanisms by which angiotensin-converting enzyme inhibitors prevent diabetes and cardiovascular disease. Am. J. Cardiol. 91, 30H–37H. doi:10.1016/S0002-9149(03)00432-6

McKinley, M.J., Albiston, A.L., Allen, A.M., Mathai, M.L., May, C.N., McAllen, R.M., Oldfield, B.J., Mendelsohn, F.A.O., Chai, S.Y., 2003. The brain renin-angiotensin system: Location and physiological roles. Int. J. Biochem. Cell Biol. doi:10.1016/S1357-2725(02)00306-0

McLean, C.A., Cherny, R.A., Fraser, F.W., Fuller, S.J., Smith, M.J., Beyreuther, K., Bush, A.I., Masters, C.L., 1999. Soluble pool of Aβ amyloid as a determinant of severity of neurodegeneration in Alzheimer's disease. Ann. Neurol. 46, 860–866. doi:10.1002/1531-8249(199912)46:6<860::AID-ANA8>3.0.CO;2-M

Mechaeil, R., Gard, P., Jackson, A., Rusted, J., 2011. Cognitive enhancement following acute losartan in normotensive young adults. Psychopharmacology (Berl). 217, 51–60. doi:10.1007/s00213-011-2257-9

Melo, J.C., Graeff, F.G., 1975. Effect of intracerebroventricular bradykinin and related peptides on rabbit operant behavior. J. Pharmacol. Exp. Ther. 193, 1–10.

Michalski, A., Damoc, E., Hauschild, J.-P., Lange, O., Wieghaus, A., Makarov, A., Nagaraj, N., Cox, J., Mann, M., Horning, S., 2011. Mass Spectrometry-based Proteomics Using Q Exactive, a High-performance Benchtop Quadrupole Orbitrap Mass Spectrometer. Mol. Cell. Proteomics 10, M111.011015. doi:10.1074/mcp.M111.011015

Michaud, A., Chauvet, M.T., Corvol, P., 1999. N-domain selectivity of angiotensin I-converting enzyme as assessed by structure-function studies of its highly selective substrate, N-acetyl-seryl-aspartyl-lysyl-proline. Biochem. Pharmacol. 57, 611–618. doi:10.1016/S0006-2952(98)00336-0

Michaud, A., Williams, T.A., Chauvet, M.T., Corvol, P., 1997. Substrate dependence of angiotensin I-converting enzyme inhibition: captopril displays a partial selectivity for inhibition of N-acetyl-seryl-aspartyl-lysyl-proline hydrolysis compared with that of angiotensin I. Mol. Pharmacol. 51, 1070–1076.

Milton, N.G., 2001. Phosphorylation of amyloid-beta at the serine 26 residue by human cdc2 kinase. Neuroreport 12, 3839–3844. doi:10.1097/00001756-200112040-00047

Miners, J.S., Ashby, E., Van Helmond, Z., Chalmers, K.A., Palmer, L.E., Love, S., Kehoe, P.G., 2008. Angiotensin-converting enzyme (ACE) levels and activity in Alzheimer's disease, and relationship of perivascular ACE-1 to cerebral amyloid angiopathy. Neuropathol. Appl. Neurobiol. 34, 181–193. doi:10.1111/j.1365-2990.2007.00885.x

Miners, J.S., Baig, S., Palmer, J., Palmer, L.E., Kehoe, P.G., Love, S., 2008. Aβ-degrading enzymes in Alzheimer's disease, in: Brain Pathology. pp. 240–252.

doi:10.1111/j.1750-3639.2008.00132.x

Miners, J.S., Kehoe, P., Love, S., 2011. Neprilysin protects against cerebral amyloid angiopathy and Aβ-induced degeneration of cerebrovascular smooth muscle cells. Brain Pathol. 21, 594–605. doi:10.1111/j.1750-3639.2011.00486.x

Miners, J.S., Palmer, J.C., Tayler, H., Palmer, L.E., Ashby, E., Kehoe, P.G., Love, S., 2014. Aβ degradation or cerebral perfusion? Divergent effects of multifunctional enzymes. Front. Aging Neurosci. 6, 1–13. doi:10.3389/fnagi.2014.00238

Miners, J.S., Van Helmond, Z., Chalmers, K., Wilcock, G., Love, S., Kehoe, P.G., 2006. Decreased expression and activity of neprilysin in Alzheimer disease are associated with cerebral amyloid angiopathy. J. Neuropathol. Exp. Neurol. 65, 1012–1021. doi:10.1097/01.jnen.0000240463.87886.9a

Minicozzi, V., Stellato, F., Comai, M., Serra, M.D., Potrich, C., Meyer-klaucke, W., Morante, S., 2008. Identifying the Minimal Copper- and Zinc-binding Site Sequence in Amyloid- β Peptides. J. Biol. Chem. 283, 10784 –10792. doi:10.1074/jbc.M707109200

Minshall, R.D., Tan, F., Nakamura, F., Rabito, S.F., Becker, R.P., Marcic, B., Erdös, E.G., 1997. Potentiation of the actions of bradykinin by angiotensin I-converting enzyme inhibitors. The role of expressed human bradykinin B2 receptors and angiotensin I-converting enzyme in CHO cells. Circ. Res. 81, 848–856. doi:10.1161/01.RES.81.5.848

Miyazaki, T., Bub, J.D., Uzuki, M., Iwamoto, Y., 2005. Adiponectin activates c-Jun NH2-terminal kinase and inhibits signal transducer and activator of transcription 3. Biochem. Biophys. Res. Commun. 333, 79–87. doi:10.1016/j.bbrc.2005.05.076

Mogi, M., Li, J.M., Iwanami, J., Min, L.J., Tsukuda, K., Iwai, M., Horiuchi, M., 2006. Angiotensin II type-2 receptor stimulation prevents neural damage by transcriptional activation of methyl methanesulfonate sensitive 2. Hypertension 48, 141–148. doi:10.1161/01.HYP.0000229648.67883.f9

Moore, B.D., Chakrabarty, P., Levites, Y., Kukar, T.L., Baine, A.-M., Moroni, T., Ladd, T.B., Das, P., Dickson, D.W., Golde, T.E., 2012. Overlapping profiles of Abeta peptides in the Alzheimer's disease and pathological aging brains. Alzheimers. Res. Ther. doi:10.1186/alzrt121

Morgan, J.M., Routtenberg, A., 1977. Angiotensin injected into the neostriatum after learning disrupts retention performance. Science 196, 87–89. doi:10.1126/science.402696

Morice, A.H., Lowry, R., Brown, M.J., Higenbottam, T., 1987. Angiotensin-converting enzyme and the cough reflex., Lancet. Clinical Pharmacology Unit, Addenbrooke's Hospital, Cambridge.

Morimoto, A., Irie, K., Murakami, K., Masuda, Y., Ohigashi, H., Nagao, M., Fukuda, H., Shimizu, T., Shirasawa, T., 2004. Analysis of the secondary structure of beta-amyloid (Abeta42) fibrils by systematic proline replacement. J. Biol. Chem. 279, 52781–52788. doi:10.1074/jbc.M406262200

Morishima, Y., Gotoh, Y., Zieg, J., Barrett, T., Takano, H., Flavell, R., Davis, R.J., Shirasaki, Y., Greenberg, M.E., 2001. Beta-amyloid induces neuronal apoptosis

via a mechanism that involves the c-Jun N-terminal kinase pathway and the induction of Fas ligand. J. Neurosci. 21, 7551–7560. doi:21/19/7551 [pii]

Morrison, J.F., 1982. The slow-binding and slow, tight-binding inhibition of enzyme-catalysed reactions. Trends Biochem. Sci. doi:10.1016/0968-0004(82)90157-8

Morrison, J.F., 1969. Kinetics of the reversible inhibition of enzyme-catalysed reactions by tight-binding inhibitors. Biochim. Biophys. Acta 185, 269–286. doi:10.1016/0005-2744(69)90420-3

Murasawa, S., Mori, Y., Nozawa, Y., Masaki, H., Maruyama, K., Tsutsumi, Y., Moriguchi, Y., Shibasaki, Y., Tanaka, Y., Iwasaka, T., Inada, M., Matsubara, H., 1998. Role of calcium-sensitive tyrosine kinase Pyk2/CAKbeta/RAFTK in angiotensin II induced Ras/ERK signaling. Hypertension 32, 668–75.

Murshudov, G.N., Vagin, A.A., Dodson, E.J., 1997. Refinement of macromolecular structures by the maximum-likelihood method. Acta Crystallogr. Sect. D Biol. Crystallogr. doi:10.1107/S0907444996012255

Musiek, E.S., Xiong, D.D., Holtzman, D.M., 2015. Sleep, circadian rhythms, and the pathogenesis of Alzheimer Disease. Exp. Mol. Med. 47, e148. doi:10.1038/emm.2014.121

Nalivaeva, N.N., Beckett, C., Belyaev, N.D., Turner, A.J., 2012. Are amyloid-degrading enzymes viable therapeutic targets in Alzheimer's disease? J. Neurochem. doi:10.1111/j.1471-4159.2011.07510.x

Nalivaeva, N.N., Belyaev, N.D., Lewis, D.I., Pickles, A.R., Makova, N.Z., Bagrova, D.I., Dubrovskaya, N.M., Plesneva, S.A., Zhuravin, I.A., Turner, A.J., 2012. Effect of sodium valproate administration on brain neprilysin expression and memory in rats. J. Mol. Neurosci. 46, 569–577. doi:10.1007/s12031-011-9644-x

Nalivaeva, N.N., Turner, A.J., 2013. The amyloid precursor protein: A biochemical enigma in brain development, function and disease. FEBS Lett. doi:10.1016/j.febslet.2013.05.010

Natesh, R., Schwager, S.L.U., Sturrock, E.D., Acharya, K.R., 2003. Crystal structure of the human angiotensin-converting enzyme-lisinopril complex. Nature 421, 551–554.

Nchinda, A.T., Chibale, K., Redelinghuys, P., Sturrock, E.D., 2006. Synthesis of novel keto-ACE analogues as domain-selective angiotensin I-converting enzyme inhibitors. Bioorganic Med. Chem. Lett. 16, 4612–4615. doi:10.1016/j.bmcl.2006.06.003

Ng, K.K., Vane, J.R., 1968. Fate of angiotensin I in the circulation. Nature 218, 144–150. doi:10.1038/218144a0

Ng, K.K., Vane, J.R., 1967. Conversion of angiotensin I to angiotensin II. Nature 216, 762–766.

Nguyen, G., Contrepas, A., 2008. Physiology and pharmacology of the (pro)renin receptor. Curr. Opin. Pharmacol. doi:10.1016/j.coph.2007.12.009

Nguyen, G., Delarue, F., Burcklé, C., Bouzhir, L., Giller, T., Sraer, J.D., 2002. Pivotal role of the renin/prorenin receptor in angiotensin II production and cellular responses to renin. J. Clin. Invest. 109, 1417–1427.

doi:10.1172/JCI200214276

Nhan, H.S., Chiang, K., Koo, E.H., 2014. The multifaceted nature of amyloid precursor protein and its proteolytic fragments: friends and foes. Acta Neuropathol. 129, 1–19. doi:10.1007/s00401-014-1347-2

Nilsson, B.L., Nilsson, B.L., Soellner, M.B., Soellner, M.B., Raines, R.T., Raines, R.T., 2005. Chemical Synthesis of Proteins. Annu. Rev. Biophys. Biomol. Struct. 34, 91–118. doi:10.1146/annurev.biophys.34.040204.144700

Nishino, S., Nishida, Y., 2001. Oxygenation of amyloid beta-peptide (1-40) by copper(II) complex and hydrogen peroxide system. Inorg. Chem. Commun. 4, 86–89. doi:10.1016/S1387-7003(00)00213-6

Noinaj, N., Bhasin, S.K., Song, E.S., Scoggin, K.E., Juliano, M.A., Juliano, L., Hersh, L.B., Rodgers, D.W., 2011. Identification of the allosteric regulatory site of insulysin. PLoS One 6. doi:10.1371/journal.pone.0020864

O'Neill, H.G., Redelinghuys, P., Schwager, S.L.U., Sturrock, E.D., 2008. The role of glycosylation and domain interactions in the thermal stability of human angiotensin-converting enzyme. Biol. Chem. 389, 1153–1161. doi:10.1515/BC.2008.131

Oba, R., Igarashi, A., Kamata, M., Nagata, K., Takano, S., Nakagawa, H., 2005. The N-terminal active centre of human angiotensin-converting enzyme degrades Alzheimer amyloid β-peptide. Eur. J. Neurosci. 21, 733–340. doi:10.1111/j.1460-9568_2005.03912.x

Oefner, C., D'Arcy, A., Hennig, M., Winkler, F.K., Dale, G.E., 2000. Structure of human neutral endopeptidase (Neprilysin) complexed with phosphoramidon. J. Mol. Biol. 296, 341–349. doi:10.1016/S0887-7963(01)80062-6

Ohrui, T., Matsui, T., Yamaya, M., Arai, H., Ebihara, S., Maruyama, M., Sasaki, H., 2004. Angiotensin-converting enzyme inhibitors and incidence of Alzheimer's disease in Japan. J. Am. Geriatr. Soc. doi:10.1111/j.1532-5415.2004.52178_7.x

Ohrui, T., Tomita, N., Sato-Nakagawa, T., Matsui, T., Maruyama, M., Niwa, K., Arai, H., Sasaki, H., 2004. Effects of brain-penetrating ACE inhibitors on Alzheimer disease progression., Neurology. doi:10.1212/01.WNL.0000140705.23869.E9

Olivares-Reyes, J.A., Arellano-Plancarte, A., Castillo-Hernandez, J.R., 2009. Angiotensin II and the development of insulin resistance: Implications for diabetes. Mol. Cell. Endocrinol. doi:10.1016/j.mce.2008.12.011

Olsen, J. V, Macek, B., Lange, O., Makarov, A., Horning, S., Mann, M., 2007. Higher-energy C-trap dissociation for peptide modification analysis. Nat. Methods 4, 709–712. doi:10.1038/nmeth1060

Ondetti, M.A., Rubin, B., Cushman, D.W., 1977. Design of specific inhibitors of angiotensin-converting enzyme: new class of orally active antihypertensive agents. Science 196, 441–444. doi:10.1126/science.191908

Ongali, B., Nicolakakis, N., Tong, X.K., Aboulkassim, T., Papadopoulos, P., Rosa-Neto, P., Lecrux, C., Imboden, H., Hamel, E., 2014. Angiotensin II type 1 receptor blocker losartan prevents and rescues cerebrovascular, neuropathological and cognitive deficits in an Alzheimer's disease model. Neurobiol. Dis. 68, 126–136. doi:10.1016/j.nbd.2014.04.018

Origlia, N., Bonadonna, C., Rosellini, A., Leznik, E., Arancio, O., Yan, S.S., Domenici, L., 2010. Microglial receptor for advanced glycation end product-dependent signal pathway drives beta-amyloid-induced synaptic depression and long-term depression impairment in entorhinal cortex. J. Neurosci. 30, 11414–11425. doi:10.1523/JNEUROSCI.2127-10.2010

Palumbo, A.M., Reid, G.E., 2008. Evaluation of gas-phase rearrangement and competing fragmentation reactions on protein phosphorylation site assignment using collision induced dissociation-MS/MS and MS3. Anal. Chem. 80, 9735–9747. doi:10.1021/ac801768s

Pang, S., Chubb, A.J., Schwager, S.L., Ehlers, M.R., Sturrock, E.D., Hooper, N.M., 2001. Roles of the juxtamembrane and extracellular domains of angiotensin-converting enzyme in ectodomain shedding. Biochem. J. 358, 185–192. doi:10.1042/0264-6021:3580185

Pannee, J., Törnqvist, U., Westerlund, A., Ingelsson, M., Lannfelt, L., Brinkmalm, G., Persson, R., Gobom, J., Svensson, J., Johansson, P., Zetterberg, H., Blennow, K., Portelius, E., 2014. The amyloid-β degradation pattern in plasma-A possible tool for clinical trials in Alzheimer's disease. Neurosci. Lett. 573, 7–12. doi:10.1016/j.neulet.2014.04.041

Parker, B.L., Yang, G., Humphrey, S.J., Chaudhuri, R., Ma, X., Peterman, S., James, D.E., 2015. Targeted phosphoproteomics of insulin signaling using data-independent acquisition mass spectrometry. Sci. Signal. 8, rs6. doi:10.1126/scisignal.aaa3139

Parkin, E., Gough, M., Parr-Sturgess, C., 2011. Zinc metalloproteinases and amyloid beta-peptide metabolism: The positive side of proteolysis in Alzheimer's disease. Biochem. Res. Int. doi:10.1155/2011/721463

Passos-Silva, D.G., Verano-Braga, T., Santos, R. a S., 2013. Angiotensin-(1-7): beyond the cardio-renal actions. Clin. Sci. (Lond). 124, 443–56. doi:10.1042/CS20120461

Patton, R.L., Kalback, W.M., Esh, C.L., Kokjohn, T.A., Van Vickle, G.D., Luehrs, D.C., Kuo, Y.-M., Lopez, J., Brune, D., Ferrer, I., Masliah, E., Newel, A.J., Beach, T.G., Castaño, E.M., Roher, A.E., 2006. Amyloid-beta peptide remnants in AN-1792-immunized Alzheimer's disease patients: a biochemical analysis. Am. J. Pathol. 169, 1048–63.

Peng, H., Carretero, O.A., Raij, L., Yang, F., Kapke, A., Rhaleb, N.E., 2001. Antifibrotic effects of N-acetyl-seryl-aspartyl-Lysyl-proline on the heart and kidney in aldosterone-salt hypertensive rats. Hypertension 37, 794–800. doi:10.1161/01.HYP.37.2.794

Peng, H., Carretero, O.A., Vuljaj, N., Liao, T.-D., Motivala, A., Peterson, E.L., Rhaleb, N.-E., 2005. Angiotensin-converting enzyme inhibitors: a new mechanism of action. Circulation 112, 2436–2445. doi:10.1161/CIRCULATIONAHA.104.528695

Pflanzner, T., Janko, M.C., André-Dohmen, B., Reuss, S., Weggen, S., Roebroek, A.J.M., Kuhlmann, C.R.W., Pietrzik, C.U., 2011. LRP1 mediates bidirectional transcytosis of amyloid-β across the blood-brain barrier. Neurobiol. Aging 32. doi:10.1016/j.neurobiolaging.2010.05.025

Phillips, M.I., 1987. Functions of angiotensin in the central nervous system. Annu. Rev. Physiol. 49, 413–435. doi:10.1146/annurev.physiol.49.1.413

Phillips, M.I., De Oliveira, E.M., 2008. Brain renin angiotensin in disease. J. Mol. Med. doi:10.1007/s00109-008-0331-5

Phillips, M.I., Sumners, C., 1998. Angiotensin II in central nervous system physiology. Regul. Pept. doi:10.1016/S0167-0115(98)00122-0

Piersma, S.R., Knol, J.C., de Reus, I., Labots, M., Sampadi, B.K., Pham, T. V, Ishihama, Y., Verheul, H.M.W., Jimenez, C.R., 2015. Feasibility of label-free phosphoproteomics and application to base-line signaling of colorectal cancer cell lines. J. Proteomics. doi:10.1016/j.jprot.2015.03.019

Pike, C.J., Overman, M.J., Cotman, C.W., 1995. Amino-terminal deletions enhance aggregation of Aβ-amyloid peptides in vitro. J. Biol. Chem. 270, 23895–23898. doi:10.1074/jbc.270.41.23895

Pooler, A.M., Noble, W., Hanger, D.P., 2014. A role for tau at the synapse in Alzheimer's disease pathogenesis. Neuropharmacology. doi:10.1016/j.neuropharm.2013.09.018

Portelius, E., Bogdanovic, N., Gustavsson, M.K., Volkmann, I., Brinkmalm, G., Zetterberg, H., Winblad, B., Blennow, K., 2010a. Mass spectrometric characterization of brain amyloid beta isoform signatures in familial and sporadic Alzheimer's disease. Acta Neuropathol. 120, 185–193. doi:10.1007/s00401-010-0690-1

Portelius, E., Brinkmalm, G., Tran, A., Andreasson, U., Zetterberg, H., Westman-Brinkmalm, A., Blennow, K., Ohrfelt, A., 2010b. Identification of novel N-terminal fragments of amyloid precursor protein in cerebrospinal fluid. Exp. Neurol. 223, 351–358. doi:10.1016/j.expneurol.2009.06.011

Portelius, E., Price, E., Brinkmalm, G., Stiteler, M., Olsson, M., Persson, R., Westman-Brinkmalm, A., Zetterberg, H., Simon, A.J., Blennow, K., 2011. A novel pathway for amyloid precursor protein processing. Neurobiol. Aging 32, 1090–1098. doi:10.1016/j.neurobiolaging.2009.06.002

Portelius, E., Zetterberg, H., Andreasson, U., Brinkmalm, G., Andreasen, N., Wallin, A., Westman-Brinkmalm, A., Blennow, K., 2006. An Alzheimer's disease-specific β-amyloid fragment signature in cerebrospinal fluid. Neurosci. Lett. 409, 215–219. doi:10.1016/j.neulet.2006.09.044

Potter, L.R., 2011. Natriuretic peptide metabolism, clearance and degradation. FEBS J. doi:10.1111/j.1742-4658.2011.08082.x

Preston, S.D., Steart, P. V., Wilkinson, A., Nicoll, J.A.R., Weller, R.O., 2003. Capillary and arterial cerebral amyloid angiopathy in Alzheimer's disease: Defining the perivascular route for the elimination of amyloid ?? from the human brain. Neuropathol. Appl. Neurobiol. doi:10.1046/j.1365-2990.2003.00424.x

Qiao, L., Lee, B., Kinney, B., Yoo, H.S., Shao, J., 2011. Energy intake and adiponectin gene expression. Am. J. Physiol. Endocrinol. Metab. 300, E809–E816. doi:10.1152/ajpendo.00004.2011

Qi-Takahara, Y., Morishima-Kawashima, M., Tanimura, Y., Dolios, G., Hirotani, N., Horikoshi, Y., Kametani, F., Maeda, M., Saido, T.C., Wang, R., Ihara, Y., 2005.

Longer forms of amyloid beta protein: implications for the mechanism of intramembrane cleavage by gamma-secretase. J. Neurosci. 25, 436–45. doi:10.1523/JNEUROSCI.1575-04.2005

Qiu, W.Q., Mwamburi, M., Besser, L.M., Zhu, H., Li, H., Wallack, M., Phillips, L., Qiao, L., Budson, A.E., Stern, R., Kowall, N., 2013. Angiotensin converting enzyme inhibitors and the reduced risk of Alzheimer's disease in the absence of apolipoprotein E4 allele. J. Alzheimers. Dis. 37, 421–8. doi:10.3233/JAD-130716

Qiu, W.Q., Walsh, D.M., Ye, Z., Vekrellis, K., Zhang, J., Podlisny, M.B., Rosner, M.R., Safavi, A., Hersh, L.B., Selkoe, D.J., 1998. Insulin-degrading enzyme regulates extracellular levels of amyloid β- protein by degradation. J. Biol. Chem. 273, 32730–32738. doi:10.1074/jbc.273.49.32730

Radi, R., 2004. Nitric oxide, oxidants, and protein tyrosine nitration. Proc. Natl. Acad. Sci. U. S. A. 101, 4003–4008. doi:10.1073/pnas.0307446101

Raghavendra, V., Chopra, K., Kulkarni, S.K., 1999. Brain renin angiotensin system (RAS) in stress-induced analgesia and impaired retention. Peptides 20, 335–342. doi:10.1016/S0196-9781(99)00040-6

Ramteke, S.N., Walke, G.R., Joshi, B.N., Rapole, S., Kulkarni, P.P., 2014. Effects of oxidation on redox and cytotoxic properties of copper complex of Aβ1-16 peptide. Free Radic. Res. 48, 1417–1425. doi:10.3109/10715762.2014.960412

Rapoport, M., Dawson, H.N., Binder, L.I., Vitek, M.P., Ferreira, A., 2002. Tau is essential to beta -amyloid-induced neurotoxicity. Proc. Natl. Acad. Sci. U. S. A. 99, 6364–6369. doi:10.1073/pnas.092136199

Rappsilber, J., Ishihama, Y., Mann, M., 2003. Stop And Go Extraction tips for matrix-assisted laser desorption/ionization, nanoelectrospray, and LC/MS sample pretreatment in proteomics. Anal. Chem. 75, 663–670. doi:10.1021/ac026117i

Rawlings, N.D., Barrett, A.J., Bateman, A., 2010. MEROPS: the peptidase database. Nucleic Acids Res. 38, D227–D233.

Redelinghuys, P., 2006. Structure function relationship of angiotensin converting enyme 1: Glycosylation and domain selectivity. University of Cape Town.

Rice, G.I., Thomas, D.A., Grant, P.J., Turner, A.J., Hooper, N.M., 2004. Evaluation of angiotensin-converting enzyme (ACE), its homologue ACE2 and neprilysin in angiotensin peptide metabolism. Biochem. J. 383, 45–51. doi:10.1042/BJ20040634

Riddell, D.R., Zhou, H., Atchison, K., Warwick, H.K., Atkinson, P.J., Jefferson, J., Xu, L., Aschmies, S., Kirksey, Y., Hu, Y., Wagner, E., Parratt, A., Xu, J., Li, Z., Zaleska, M.M., Jacobsen, J.S., Pangalos, M.N., Reinhart, P.H., 2008. Impact of apolipoprotein E (ApoE) polymorphism on brain ApoE levels. J. Neurosci. 28, 11445–11453. doi:10.1523/JNEUROSCI.1972-08.2008

Rigat, B., Hubert, C., Alhenc-Gelas, F., Cambien, F., Corvol, P., Soubrier, F., 1990. An insertion/deletion polymorphism in the angiotensin I-converting enzyme gene accounting for half the variance of serum enzyme levels. J. Clin. Invest. 86, 1343–6. doi:10.1172/JCI114844

Rigat, B., Hubert, C., Corvol, P., Soubrier, F., 1992. PCR detection of the insertion/deletion polymorphism of the human angiotensin converting enzyme gene (DCP1) (dipeptidyl carboxypeptidase 1). Nucleic Acids Res. 20, 1433. doi:10.1093/nar/20.6.1433-a

Riordan, J.F., 2003. Angiotensin-I-converting enzyme and its relatives. Genome Biol. 4, 225. doi:10.1186/gb-2003-4-8-225

Ripka, J.E., Ryan, J.W., Valido, F.A., Chung, A.Y., Peterson, C.M., Urry, R.L., 1993. N-glycosylation of forms of angiotensin converting enzyme from four mammalian species. Biochem. Biophys. Res. Commun. 196, 503–508. doi:10.1006/bbrc.1993.2278

Roberson, E.D., Scearce-Levie, K., Palop, J.J., Yan, F., Cheng, I.H., Wu, T., Gerstein, H., Yu, G.-Q., Mucke, L., 2007. Reducing endogenous tau ameliorates amyloid beta-induced deficits in an Alzheimer's disease mouse model. Science 316, 750–754. doi:10.1126/science.1141736

Rodriguez-Rivera, J., Denner, L., Dineley, K.T., 2011. Rosiglitazone reversal of Tg2576 cognitive deficits is independent of peripheral gluco-regulatory status. Behav. Brain Res. 216, 255–61. doi:10.1016/j.bbr.2010.08.002

Rogers, J.T., Bush, A.I., Cho, H.-H., Smith, D.H., Thomson, A.M., Friedlich, A.L., Lahiri, D.K., Leedman, P.J., Huang, X., Cahill, C.M., 2008. Iron and the translation of the amyloid precursor protein (APP) and ferritin mRNAs: riboregulation against neural oxidative damage in Alzheimer's disease. Biochem. Soc. Trans. 36, 1282–1287. doi:10.1042/BST0361282

Roher, A.E., Lowenson, J.D., Clark, S., Wang, R., Cotter, R.J., Reardon, I.M., Zürcher-neely, H.A., Heinriksonss, R.L., Balltiv, M.J., Greenberg, B.D., 1993a. Structural Alterations in the Peptide Backbone of β-Amyloid Core Protein May Account for Its Deposition and Stability in Alzheimer ' s Disease. J. Biol. Chem. 268, 3072–3083.

Roher, A.E., Lowenson, J.D., Clarke, S., Woods, A.S., Cotter, R.J., Gowing, E., Ball, M.J., 1993b. beta-Amyloid-(1-42) is a major component of cerebrovascular amyloid deposits: implications for the pathology of Alzheimer disease. Proc. Natl. Acad. Sci. U. S. A. 90, 10836–10840. doi:10.1073/pnas.90.22.10836

Ronchi, F.A., Andrade, M.C.C., Carmona, A.K., Krieger, J.E., Casarini, D.E., 2005. N-domain angiotensin-converting enzyme isoform expression in tissues of Wistar and spontaneously hypertensive rats. J. Hypertens. 23, 1869–1878. doi:10.1097/01.hjh.0000183523.66123.95

Rosenberg, G.A., 2009. Matrix metalloproteinases and their multiple roles in neurodegenerative diseases. Lancet Neurolology 8, 205–216.

Rosenblum, W.I., 2014. Why Alzheimer trials fail: removing soluble oligomeric beta amyloid is essential, inconsistent, and difficult. Neurobiol. Aging 35, 969–74. doi:10.1016/j.neurobiolaging.2013.10.085

Roßner, S., Sastre, M., Bourne, K., Lichtenthaler, S.F., 2006. Transcriptional and translational regulation of BACE1 expression-Implications for Alzheimer's disease. Prog. Neurobiol. doi:10.1016/j.pneurobio.2006.06.001

Rothman, S.M., Herdener, N., Camandola, S., Texel, S.J., Mughal, M.R., Cong, W.N., Martin, B., Mattson, M.P., 2012. 3xTgAD mice exhibit altered behavior and

elevated Aβ after chronic mild social stress. Neurobiol. Aging 33. doi:10.1016/j.neurobiolaging.2011.07.005

Rousseau, A., Michaud, A., Chauvet, M.-T., Lenfant, M., Corvol, P., 1995. The Hemoregulatory Peptide N-Acetyl-Ser-Asp-Lys-Pro Is a Natural and Specific Substrate of the N-terminal Active Site of Human Angiotensin-converting Enzyme. J. Biol. Chem. 270, 3656–3661.

Roychaudhuri, R., Yang, M., Condron, M.M., Teplow, D.B., 2012. Structural dynamics of the amyloid β-protein monomer folding nucleus. Biochemistry 51, 3957–9. doi:10.1021/bi300350p

Rozzini, L., Chilovi, B.V., Bertoletti, E., Conti, M., Del Rio, I., Trabucchi, M., Padovani, A., 2006. Angiotensin Converting Enzyme (ACE) inhibitors modulate the rate of progression of amnestic mild cognitive impairment. Int. J. Geriatr. Psychiatry 21, 550–555. doi:10.1002/gps.1523

Ruitenberg, A., Skoog, I., Ott, A., Aevarsson, O., Witteman, J.C.M., Lernfelt, B., Van Harskamp, F., Hofman, A., Breteler, M.M.B., 2001. Blood pressure and risk of dementia: Results from the Rotterdam study and the Gothenburg H-70 study. Dement. Geriatr. Cogn. Disord. 12, 33–39. doi:10.1159/000051233

Rushworth, C.A., Guy, J.L., Turner, A.J., 2008. Residues affecting the chloride regulation and substrate selectivity of the angiotensin-converting enzymes (ACE and ACE2) identified by site-directed mutagenesis. FEBS J. 275, 6033–42. doi:10.1111/j.1742-4658.2008.06733.x

Ryan, J.W., Valido, F.A., Chung, A.Y., Ripka, J.E., Peterson, C.M., Urry, R.L., 1993. A comparison of guinea pig serum angiotensin converting enzyme with forms of angiotensin converting enzyme from human, rat and rabbit tissues. Biochem. Biophys. Res. Commun. 196, 509–514. doi:10.1006/bbrc.1993.2279

Rylatt, D.B., Aitken, A., Bilham, T., Condon, G.D., Embi, N., Cohen, P., 1980. Glycogen synthase from rabbit skeletal muscle. Amino acid sequence at the sites phosphorylated by glycogen synthase kinase-3, and extension of the N-terminal sequence containing the site phosphorylated by phosphorylase kinase. Eur. J. Biochem. 107, 529–537. doi:10.1111/j.1432-1033.1980.tb06059.x

Saavedra, J.M., Sánchez-Lemus, E., Benicky, J., 2011. Blockade of brain angiotensin II AT1 receptors ameliorates stress, anxiety, brain inflammation and ischemia: Therapeutic implications. Psychoneuroendocrinology. doi:10.1016/j.psyneuen.2010.10.001

Saito, T., Iwata, N., Tsubuki, S., Takaki, Y., Takano, J., Huang, S.-M., Suemoto, T., Higuchi, M., Saido, T.C., 2005. Somatostatin regulates brain amyloid beta peptide Abeta42 through modulation of proteolytic degradation. Nat. Med. 11, 434–439. doi:10.1038/nm1206

Sakaguchi, K., Chai, S.Y., Jackson, B., Johnston, C.I., Mendelsohn, F.A., 1987. Blockade of angiotensin converting enzyme in circumventricular organs of the brain after oral lisinopril administration demonstrated by quantitative in vitro autoradiography. Clin. Exp. Pharmacol. Physiol. 14, 155–158.

Sakono, M., Zako, T., 2010. Amyloid oligomers: Formation and toxicity of Aβ oligomers. FEBS J. doi:10.1111/j.1742-4658.2010.07568.x

Sambrook, J., Fritsch, E.F., Maniatis, T., 1989. Molecular Cloning: A Laboratory Manual (2nd ed.). Cold Spring Harb. Lab. Press.

Sancho, J., Re, R., Burton, J., Barger, A.C., Haber, E., 1976. The role of the renin-angiotensin-aldosterone system in cardiovascular homeostasis in normal human subjects. Circulation 53, 400–405. doi:10.1161/01.CIR.53.3.400

Santos, R.A.S., Simoes e Silva, A.C., Maric, C., Silva, D.M.R., Machado, R.P., de Buhr, I., Heringer-Walther, S., Pinheiro, S.V.B., Lopes, M.T., Bader, M., Mendes, E.P., Lemos, V.S., Campagnole-Santos, M.J., Schultheiss, H.-P., Speth, R., Walther, T., 2003. Angiotensin-(1-7) is an endogenous ligand for the G protein-coupled receptor Mas. Proc. Natl. Acad. Sci. U. S. A. 100, 8258–8263. doi:10.1073/pnas.1432869100

Sastre, M., Dewachter, I., Landreth, G.E., Willson, T.M., Klockgether, T., van Leuven, F., Heneka, M.T., 2003. Nonsteroidal anti-inflammatory drugs and peroxisome proliferator-activated receptor-gamma agonists modulate immunostimulated processing of amyloid precursor protein through regulation of beta-secretase. J. Neurosci. 23, 9796–9804. doi:23/30/9796 [pii]

Sato, T., Dohmae, N., Qi, Y., Kakuda, N., Misonou, H., Mitsumori, R., Maruyama, H., Koo, E.H., Haass, C., Takio, K., Morishima-Kawashima, M., Ishiura, S., Ihara, Y., 2003. Potential link between amyloid beta-protein 42 and C-terminal fragment gamma 49-99 of beta-amyloid precursor protein. J. Biol. Chem. 278, 24294–301. doi:10.1074/jbc.M211161200

Savaskan, E., 2005. The role of the brain renin-angiotensin system in neurodegenerative disorders. Curr. Alzheimer Res. 2, 29–35. doi:10.2174/1567205052772740

Savaskan, E., Hock, C., Olivieri, G., Bruttel, S., Rosenberg, C., Hulette, C., Müller-Spahn, F., 2001. Cortical alterations of angiotensin converting enzyme, angiotensin II and AT1 receptor in Alzheimer's dementia. Neurobiol. Aging 22, 541–546. doi:10.1016/S0197-4580(00)00259-1

Schley, D., Carare-Nnadi, R., Please, C.P., Perry, V.H., Weller, R.O., 2006. Mechanisms to explain the reverse perivascular transport of solutes out of the brain. J. Theor. Biol. 238, 962–974. doi:10.1016/j.jtbi.2005.07.005

Schnegg, C.I., Kooshki, M., Hsu, F.C., Sui, G., Robbins, M.E., 2012. PPAR delta prevents radiation-induced proinflammatory responses in microglia via transrepression of NF-kappa B and inhibition of the PK alpha/MEK1/2/ERK1/2/AP-1 pathway. Free Radic. Biol. Med. doi:10.1016/j.freeradbiomed.2012.02.032

Schwager, S.L., Carmona, A.K., Sturrock, E.D., 2006. A high-throughput fluorimetric assay for angiotensin I-converting enzyme. Nat. Protoc. 1, 1961–1964. doi:10.1038/nprot.2006.305

Scott Miners, J., Van Helmond, Z., Raiker, M., Love, S., Kehoe, P.G., 2011. Ace variants and association with brain aβ levels in alzheimer's disease. Am. J. Transl. Res. 3, 73–80.

Sefton, B.M., Shenolikar, S., 2001. Overview of protein phosphorylation. Curr. Protoc. Mol. Biol. Chapter 18, Unit 18.1. doi:10.1002/0471140864.ps1301s00

Sergeant, N., Bombois, S., Ghestem, A., Drobecq, H., Kostanjevecki, V., Missiaen, C.,

Wattez, A., David, J.P., Vanmechelen, E., Sergheraert, C., Delacourte, A., 2003. Truncated beta-amyloid peptide species in pre-clinical Alzheimer's disease as new targets for the vaccination approach. J. Neurochem. 85, 1581–1591. doi:10.1046/j.1471-4159.2003.01818.x

Serot, J.M., Zmudka, J., Jouanny, P., 2012. A possible role for CSF turnover and choroid plexus in the pathogenesis of late onset alzheimer's disease. J. Alzheimer's Dis. doi:10.3233/JAD-2012-111964

Serpell, L., 2000. Alzheimer's amyloid fibrils: structure and assembly. Biochim. Biophys. Acta - Mol. Basis Dis. 1502, 16–30. doi:10.1016/S0925-4439(00)00029-6

Seubert, P., Oltersdorf, T., Lee, M.G., Barbour, R., Blomquist, C., Davis, D.L., Bryant, K., Fritz, L.C., Galasko, D., Thal, L.J., 1993. Secretion of beta-amyloid precursor protein cleaved at the amino terminus of the beta-amyloid peptide. Nature 361, 260–263. doi:10.1038/361260a0

Shapiro, R., Riordan, J.F., 1984. Inhibition of angiotensin converting enzyme: dependence on chloride. Biochemistry 23, 5234–5240.

Shapiro, R., Riordan, J.F., 1983. Critical lysine residue at the chloride binding site of angiotensin converting enzyme. Biochemistry 22, 5315–21. doi:10.1021/bi00285a021

Shen, X.Z., Billet, S., Lin, C., Okwan-Duodu, D., Chen, X., Lukacher, A.E., Bernstein, K.E., 2011. The carboxypeptidase ACE shapes the MHC class I peptide repertoire. Nat. Immunol. doi:10.1038/ni.2107

Shen, X.Z., Ong, F.S., Bernstein, E.A., Janjulia, T., Blackwell, W.B., Shah, K.H., Taylor, B.L., Gonzalez-Villalobos, R.A., Fuchs, S., Bernstein, K.E., 2012. Nontraditional roles of angiotensin-converting enzyme. Hypertension 59, 763–8. doi:10.1161/HYPERTENSIONAHA.111.188342

Shen, Y., Joachimiak, A., Rosner, M.R., Tang, W.-J., 2006. Structures of human insulin-degrading enzyme reveal a new substrate recognition mechanism. Nature 443, 870–874. doi:10.1038/nature05143

Shepherd, J., Bill, D.J., Dourish, C.T., Grewal, S.S., McLenachan, A., Stanhope, K.J., 1996. Effects of the selective angiotensin II receptor antagonists losartan and PD123177 in animal models of anxiety and memory. Psychopharmacology (Berl). 126, 206–218. doi:10.1007/BF02246450

Shi, H., Kang, B., Lee, J.Y., 2014. Zn(2+) Effect on Structure and Residual Hydrophobicity of Amyloid β-peptide Monomers. J. Phys. Chem. B. doi:10.1021/jp504779m

Shibata, M., Yamada, S., Ram Kumar, S., Calero, M., Bading, J., Frangione, B., Holtzman, D.M., Miller, C.A., Strickland, D.K., Ghiso, J., Zlokovic, B. V., 2000. Clearance of Alzheimer's amyloid-β1-40 peptide from brain by LDL receptor-related protein-1 at the blood-brain barrier. J. Clin. Invest. 106, 1489–1499. doi:10.1172/JCI10498

Shoji, M., Golde, T.E., Ghiso, J., Cheung, T.T., Estus, S., Shaffer, L.M., Cai, X.D., McKay, D.M., Tintner, R., Frangione, B., 1992. Production of the Alzheimer amyloid beta protein by normal proteolytic processing. Science 258, 126–129.

Sickmann, A., Meyer, H.E., 2001. Review Phosphoamino acid analysis. Proteomics 49, 200–206. doi:10.1002/1615-9861(200102)1:2<200::AID-PROT200>3.0.CO;2-V

Simões E Silva, A.C., Silveira, K.D., Ferreira, A.J., Teixeira, M.M., 2013. ACE2, angiotensin-(1-7) and Mas receptor axis in inflammation and fibrosis. Br. J. Pharmacol. doi:10.1111/bph.12159

Sink, K.M., Leng, X., Williamson, J., Kritchevsky, S.B., Yaffe, K., Kuller, L., Yasar, S., Atkinson, H., Robbins, M., Psaty, B., Goff, D.C., 2009. Angiotensin-converting enzyme inhibitors and cognitive decline in older adults with hypertension: results from the Cardiovascular Health Study. Arch. Intern. Med. 169, 1195–202. doi:10.1001/archinternmed.2009.175

Skidgel, R.A., Engelbrecht, S., Johnson, A.R., Erdös, E.G., 1984. Hydrolysis of substance p and neurotensin by converting enzyme and neutral endopeptidase. Peptides 5, 769–776. doi:10.1016/0196-9781(84)90020-2

Skidgel, R.A., Erdös, E.G., 1985. Novel activity of human angiotensin I converting enzyme: release of the NH2- and COOH-terminal tripeptides from the luteinizing hormone-releasing hormone. Proc. Natl. Acad. Sci. U. S. A. 82, 1025–1029. doi:10.1073/pnas.82.4.1025

Skirgello, O.E., Binevski, P. V, Pozdnev, V.F., Kost, O.A., 2005. Kinetic probes for inter-domain co-operation in human somatic angiotensin-converting enzyme. Biochem. J. 391, 641–647. doi:10.1042/BJ20050702

Skrbic, R., Igic, R., 2009. Seven decades of angiotensin (1939-2009). Peptides. doi:10.1016/j.peptides.2009.07.003

Sokol, S.I., Portnay, E.L., Curtis, J.P., Nelson, M.A., Hebert, P.R., Setaro, J.F., Foody, J.M., 2004. Modulation of the renin-angiotensin-aldosterone system for the secondary prevention of stroke. Neurology 63, 208–213. doi:10.1212/01.WNL.0000130360.21618.D0

Sokolovsky, M., Riordan, J.F., Vallee, B.L., 1966. Tetranitromethane. A reagent for the nitration of tyrosyl residues in proteins. Biochemistry 5, 3582–3589. doi:10.1021/bi00875a029

Solfrizzi, V., Scafato, E., Frisardi, V., Seripa, D., Logroscino, G., Kehoe, P.G., Imbimbo, B.P., Baldereschi, M., Crepaldi, G., Di Carlo, A., Galluzzo, L., Gandin, C., Inzitari, D., Maggi, S., Pilotto, A., Panza, F., 2011. Angiotensin-converting enzyme inhibitors and incidence of mild cognitive impairment. The Italian Longitudinal Study on Aging. Age (Dordr). 35, 441–53. doi:10.1007/s11357-011-9360-z

Song, J., Lee, W.T., Park, K.A., Lee, J.E., 2014. Association between risk factors for vascular dementia and Adiponectin. Biomed Res. Int. doi:10.1155/2014/261672

Soubrier, F., Alhenc-Gelas, F., Hubert, C., Allegrini, J., John, M., Tregear, G., Corvol, P., 1988. Two putative active centers in human angiotensin I-converting enzyme revealed molecular cloning. Procedings Natl. Acadademy Sci. USA 85, 9386–9390.

Spyroulias, G.A., Galanis, A.S., Pairas, G., Manessi-Zoupa, E., Cordopatis, P., 2004. Structural features of angiotensin-I converting enzyme catalytic sites:

conformational studies in solution, homology models and comparison with other zinc metallopeptidases. Curr. Top. Med. Chem. 4, 403–429. doi:10.2174/1568026043451294

Stergachis, A.B., MacLean, B., Lee, K., Stamatoyannopoulos, J.A., MacCoss, M.J., 2011. Rapid empirical discovery of optimal peptides for targeted proteomics. Nat. Methods. doi:10.1038/nmeth.1770

Stern, D., Du Yan, S., Fang Yan, S., Marie Schmidt, A., 2002. Receptor for advanced glycation endproducts: A multiligand receptor magnifying cell stress in diverse pathologic settings. Adv. Drug Deliv. Rev. doi:10.1016/S0169-409X(02)00160-6

Sturrock, E.D., Anthony, C.S., Danilov, S.M., 2012. Peptidyl-Dipeptidase A/Angiotensin I-Converting Enzyme. Handb. Proteolytic Enzym. Vol. 1.

Sturrock, E.D., Danilov, S.M., Riordan, J.F., 1997. Limited proteolysis of human kidney angiotensin-converting enzyme and generation of catalytically active N- and C-terminal domains. Biochem. Biophys. Res. Commun. 236, 16–19. doi:10.1006/bbrc.1997.6841

Sudilovsky, A., Cutler, N.R., Sramek, J.J., Wardle, T., Veroff, A.E., Mickelson, W., Markowitz, J., Repetti, S., 1993. A pilot clinical trial of the angiotensin-converting enzyme inhibitor ceranapril in Alzheimer disease., Alzheimer disease and associated disorders.

Sun, X., Becker, M., Pankow, K., Krause, E., Ringling, M., Beyermann, M., Maul, B., Walther, T., Siems, W.-E.E., 2008a. Catabolic attacks of membrane-bound angiotensin-converting enzyme on the N-terminal part of species-specific amyloid-β peptides. Eur. J. Pharmacol. 588, 18–25. doi:10.1016/j.ejphar.2008.03.058

Sun, X., Rentzsch, B., Gong, M., Eichhorst, J., Pankow, K., Papsdorf, G., Maul, B., Bader, M., Siems, W.-E., 2010. Signal transduction in CHO cells stably transfected with domain-selective forms of murine ACE. Biol. Chem. 391, 235–44. doi:10.1515/BC.2010.020

Sun, X., Wiesner, B., Lorenz, D., Papsdorf, G., Pankow, K., Wang, P., Dietrich, N., Siems, W.E., Maul, B., 2008b. Interaction of angiotensin-converting enzyme (ACE) with membrane-bound carboxypeptidase M (CPM) - A new function of ACE. Biol. Chem. 389, 1477–1485. doi:10.1515/BC.2008.168

Sunderland, T., Linker, G., Mirza, N., Putnam, K.T., Friedman, D.L., Kimmel, L.H., Bergeson, J., Manetti, G.J., Zimmermann, M., Tang, B., Bartko, J.J., Cohen, R.M., 2003. Decreased beta-amyloid1-42 and increased tau levels in cerebrospinal fluid of patients with Alzheimer disease. JAMA 289, 2094–2103. doi:10.1001/jama.289.16.2094

Syková, E., Nicholson, C., 2008. Diffusion in brain extracellular space. Physiol. Rev. 88, 1277–340. doi:10.1152/physrev.00027.2007

Szentistványi, I., Patlak, C.S., Ellis, R.A., Cserr, H.F., 1984. Drainage of interstitial fluid from different regions of rat brain. Am. J. Physiol. 246, F835–F844.

Tabaton, M., Zhu, X., Perry, G., Smith, M.A., Giliberto, L., 2009. Signaling effect of amyloid-β42 on the processing of AβPP. Exp. Neurol. doi:10.1016/j.expneurol.2009.09.002

Takai, S., Jin, D., Kimura, M., Kirimura, K., Sakonjo, H., Tanaka, K., Miyazaki, M., 2007. Inhibition of vascular angiotensin-converting enzyme by telmisartan via the peroxisome proliferator-activated receptor gamma agonistic property in rats. Hypertens. Res. 30, 1231–1237. doi:10.1291/hypres.30.1231

Takami, M., Nagashima, Y., Sano, Y., Ishihara, S., Morishima-Kawashima, M., Funamoto, S., Ihara, Y., 2009. gamma-Secretase: successive tripeptide and tetrapeptide release from the transmembrane domain of beta-carboxyl terminal fragment. J. Neurosci. 29, 13042–13052. doi:10.1523/JNEUROSCI.2362-09.2009

Takeda, S., Sato, N., Takeuchi, D., Kurinami, H., Shinohara, M., Niisato, K., Kano, M., Ogihara, T., Rakugi, H., Morishita, R., 2009. Angiotensin receptor blocker prevented beta-amyloid-induced cognitive impairment associated with recovery of neurovascular coupling. Hypertension 54, 1345–1352. doi:10.1161/HYPERTENSIONAHA.109.138586

Tambo, K., Yamaguchi, T., Kobayashi, K., Terauchi, E., Ichi, I., Kojo, S., 2013. Racemization of the aspartic acid residue of amyloid-β peptide by a radical reaction. Biosci. Biotechnol. Biochem. 77, 416–8. doi:10.1271/bbb.120797

Tan, J., Wang, J.M., Leenen, F.H.H., 2005. Inhibition of brain angiotensin-converting enzyme by peripheral administration of trandolapril versus lisinopril in Wistar rats. Am. J. Hypertens. 18, 158–164. doi:10.1016/j.amjhyper.2004.09.004

Tanzi, R.E., Gusella, J.F., Watkins, P.C., Bruns, G.A., St George-Hyslop, P., Van Keuren, M.L., Patterson, D., Pagan, S., Kurnit, D.M., Neve, R.L., 1987. Amyloid beta protein gene: cDNA, mRNA distribution, and genetic linkage near the Alzheimer locus. Science 235, 880–4.

Taylor, B.M., Sarver, R.W., Fici, G., Poorman, R.A., Lutzke, B.S., Molinari, A., Kawabe, T., Kappenman, K., Buhl, A.E., Epps, D.E., 2003. Spontaneous aggregation and cytotoxicity of the beta-amyloid Abeta1-40: a kinetic model. J. Protein Chem. 22, 31–40. doi:10.1023/A:1023063626770

Taylor, W.J., Ott, J., Eckstein, F., 1985. The rapid generation of oligonucleotide-directed mutations at high frequency using phosphorothioate-modified DNA. Nucleic Acids Res. 13, 8765–8785. doi:10.1093/nar/13.24.8765

Thornton, C., Bright, N.J., Sastre, M., Muckett, P.J., Carling, D., 2011. AMP-activated protein kinase (AMPK) is a tau kinase, activated in response to amyloid β-peptide exposure. Biochem. J. 434, 503–512. doi:10.1042/BJ20101485

Tipnis, S.R., Hooper, N.M., Hyde, R., Karran, E., Christie, G., Turner, A.J., 2000. A human homolog of angiotensin-converting enzyme: Cloning and functional expression as a captopril-insensitive carboxypeptidase. J. Biol. Chem. 275, 33238–33243. doi:10.1074/jbc.M002615200

Tomic, J.L., Pensalfini, A., Head, E., Glabe, C.G., 2009. Soluble fibrillar oligomer levels are elevated in Alzheimer's disease brain and correlate with cognitive dysfunction. Neurobiol. Dis. 35, 352–358. doi:10.1016/j.nbd.2009.05.024

Toropygin, I.Y., Kugaevskaya, E. V, Mirgorodskaya, O.A., Elisseeva, Y.E., Kozmin, Y.P., Popov, I.A., Nikolaev, E.N., Makarov, A.A., Kozin, S.A., 2008. The N-domain of angiotensin-converting enzyme specifically hydrolyzes the Arg-5-His-6

bond of Alzheimer's Aβ-(1-16) peptide and its isoAsp-7 analogue with different efficiency as evidenced by quantitative matrix-assisted laser desorption/ionization time-o. Rapid Commun. Mass Spectrom. 22, 231–239. doi:10.1002/rcm

Tota, S., Kamat, P.K., Awasthi, H., Singh, N., Raghubir, R., Nath, C., Hanif, K., 2009. Candesartan improves memory decline in mice: Involvement of AT1 receptors in memory deficit induced by intracerebral streptozotocin. Behav. Brain Res. 199, 235–240. doi:10.1016/j.bbr.2008.11.044

Towler, P., Staker, B., Prasad, S.G., Menon, S., Tang, J., Parsons, T., Ryan, D., Fisher, M., Williams, D., Dales, N.A., Patane, M.A., Pantoliano, M.W., 2004. ACE2 X-Ray Structures Reveal a Large Hinge-bending Motion Important for Inhibitor Binding and Catalysis. J. Biol. Chem. 279, 17996–18007. doi:10.1074/jbc.M311191200

Tucker, H.M., Kihiko, M., Caldwell, J.N., Wright, S., Kawarabayashi, T., Price, D., Walker, D., Scheff, S., McGillis, J.P., Rydel, R.E., Estus, S., 2000. The plasmin system is induced by and degrades amyloid-beta aggregates. J. Neurosci. 20, 3937–3946. doi:20/11/3937 [pii]

Tundo, G., Ciaccio, C., Sbardella, D., Boraso, M., Viviani, B., Coletta, M., Marini, S., 2012. Somatostatin modulates insulin-degrading-enzyme metabolism: Implications for the regulation of microglia activity in AD. PLoS One 7. doi:10.1371/journal.pone.0034376

Turner, A.J., 2003. Exploring the structure and function of zinc metallopeptidases: old enzymes and new discoveries. Biochem. Soc. Trans. 31, 723–727. doi:10.1042/BST0310723

Turner, A.J., Hooper, N.M., 2002. The angiotensin-converting enzyme gene family: genomics and pharmacology. Trends Pharmacol. Sci. 23, 177–83.

Turner, A.J., Isaac, R.E., Coates, D., 2001. The neprilysin (NEP) family of zinc metalloendopeptidases: genomics and function. Bioessays 23, 261–9. doi:10.1002/1521-1878(200103)23:3<261::AID-BIES1036>3.0.CO;2-K

Tzakos, A.G., Galanis, A.S., Spyroulias, G. a, Cordopatis, P., Manessi-Zoupa, E., Gerothanassis, I.P., 2003. Structure-function discrimination of the N- and C-catalytic domains of human angiotensin-converting enzyme: implications for Cl- activation and peptide hydrolysis mechanisms. Protein Eng. 16, 993–1003. doi:10.1093/protein/gzg122

Uversky, V.N., 2010. Mysterious oligomerization of the amyloidogenic proteins. FEBS J. 277, 2940–2953. doi:10.1111/j.1742-4658.2010.07721.x

Varadarajan, S., Yatin, S., Aksenova, M., Butterfield, D.A., 2000. Review: Alzheimer's amyloid beta-peptide-associated free radical oxidative stress and neurotoxicity. J. Struct. Biol. 130, 184–208. doi:10.1006/jsbi.2000.4274

Vasilevko, V., Passos, G.F., Quiring, D., Head, E., Kim, R.C., Fisher, M., Cribbs, D.H., 2010. Aging and cerebrovascular dysfunction: contribution of hypertension, cerebral amyloid angiopathy, and immunotherapy. Ann. N. Y. Acad. Sci. 1207, 58–70. doi:10.1111/j.1749-6632.2010.05786.x

Vassar, R., Bennett, B.D., Babu-Khan, S., Kahn, S., Mendiaz, E.A., Denis, P., Teplow, D.B., Ross, S., Amarante, P., Loeloff, R., Luo, Y., Fisher, S., Fuller, J., Edenson, S.,

Lile, J., Jarosinski, M.A., Biere, A.L., Curran, E., Burgess, T., Louis, J.C., Collins, F., Treanor, J., Rogers, G., Citron, M., 1999. Beta-secretase cleavage of Alzheimer's amyloid precursor protein by the transmembrane aspartic protease BACE. Science 286, 735–741. doi:10.1126/science.286.5440.735

Vazeux, G., Cotton, J., Cuniasse, P., Dive, V., 2001. Potency and selectivity of RXP407 on human, rat, and mouse angiotensin-converting enzyme. Biochem. Pharmacol. 61, 835–841. doi:10.1016/S0006-2952(01)00550-0

Vekrellis, K., Ye, Z., Qiu, W.Q., Walsh, D., Hartley, D., Chesneau, V., Rosner, M.R., Selkoe, D.J., 2000. Neurons regulate extracellular levels of amyloid beta-protein via proteolysis by insulin-degrading enzyme. J. Neurosci. 20, 1657–65.

Velazquez, P., Cribbs, D.H., Poulos, T.L., Tenner, A.J., 1997. Aspartate residue 7 in amyloid beta-protein is critical for classical complement pathway activation: implications for Alzheimer's disease pathogenesis. Nat. Med. 3, 77–79. doi:10.1038/nm0197-77

Verbeek, M.M., Kremer, B.P.H., Rikkert, M.O., Van Domburg, P.H.M.F., Skehan, M.E., Greenberg, S.M., 2009. Cerebrospinal fluid amyloid beta(40) is decreased in cerebral amyloid angiopathy. Ann. Neurol. 66, 245–249. doi:10.1002/ana.21694

Viel, T.A., Buck, H.S., 2011. Kallikrein-kinin system mediated inflammation in Alzheimer's disease in vivo. Curr. Alzheimer Res. 8, 59–66. doi:10.2174/156720511794604570

Vijayaraghavan, J., Scicli, A.G., Carretero, O.A., Slaughter, C., Moomaw, C., Hersh, L.B., 1990. The hydrolysis of endothelins by neutral endopeptidase 24.11 (enkephalinase). J. Biol. Chem. 265, 14150–14155.

Villard, E., 1998. Induction of Angiotensin I-converting Enzyme Transcription by a Protein Kinase C-dependent Mechanism in Human Endothelial Cells. J. Biol. Chem. 273, 25191–25197. doi:10.1074/jbc.273.39.25191

Vinh, A., Widdop, R.E., Drummond, G.R., Gaspari, T.A., 2008. Chronic angiotensin IV treatment reverses endothelial dysfunction in ApoE-deficient mice. Cardiovasc. Res. 77, 178–187. doi:10.1093/cvr/cvm021

Vishnu, V.Y., 2013. Can tauopathy shake the amyloid cascade hypothesis? Nat. Rev. Neurol. 9, 356. doi:10.1038/nrneurol.2013.21-c1

Volpe, M., Rubattu, S., Burnett, J., 2014. Natriuretic peptides in cardiovascular diseases: Current use and perspectives. Eur. Heart J. doi:10.1093/eurheartj/eht466

von Koch, C.S., Zheng, H., Chen, H., Trumbauer, M., Thinakaran, G., van der Ploeg, L.H., Price, D.L., Sisodia, S.S., 1997. Generation of APLP2 KO mice and early postnatal lethality in APLP2/APP double KO mice. Neurobiol. Aging 18, 661–9. doi:10.1016/S0197-4580(97)00151-6

Vyazovskiy, V. V, Cirelli, C., Pfister-Genskow, M., Faraguna, U., Tononi, G., 2008. Molecular and electrophysiological evidence for net synaptic potentiation in wake and depression in sleep. Nat. Neurosci. 11, 200–8. doi:10.1038/nn2035

Wang, D.-S., Dickson, D.W., Malter, J.S., 2006. β-Amyloid Degradation and

Alzheimer's Disease. J. Biomed. Biotechnol. 1–12. doi:10.1155/JBB/2006/58406

Wang, G.T., Chung, C.C., Holzman, T.F., Krafft, G.A., 1993. A continuous fluorescence assay of renin activity. Anal. Biochem. 210, 351–359. doi:10.1006/abio.1993.1207

Wang, J., Ho, L., Chen, L., Zhao, Z., Zhao, W., Qian, X., Humala, N., Seror, I., Bartholomew, S., Rosendorff, C., Pasinetti, G.M., 2007. Valsartan lowers brain ??-amyloid protein levels and improves spatial learning in a mouse model of Alzheimer disease. J. Clin. Invest. 117, 3393–3402. doi:10.1172/JCI31547

Watermeyer, J.M., Kroger, W.L., O'Neill, H.G., Sewell, B.T., Sturrock, E.D., 2008. Probing the basis of domain-dependent inhibition using novel ketone inhibitors of angiotensin-converting enzyme. Biochemistry 47, 5942–5950. doi:10.1021/bi8002605

Watermeyer, J.M., Kröger, W.L., O'Neill, H.G., Sewell, B.T., Sturrock, E.D., 2010. Characterization of domain-selective inhibitor binding in angiotensin-converting enzyme using a novel derivative of lisinopril. Biochem. J. 428, 67–74. doi:10.1042/BJ20100056

Watermeyer, J.M., Kroger, W.L., Sturrock, E.D., Ehlers, M.R.W., 2009. Angiotensin-Converting Enzyme - New Insights into Structure, Biological Significance and Prospects for Domain-Selective Inhibitors. Curr. Enzym. Inhib. doi:10.2174/157340809789071155

Watermeyer, J.M., Sewell, B.T., Schwager, S.L., Natesh, R., Corradi, H.R., Acharya, K.R., Sturrock, E.D., 2006. Structure of testis ACE glycosylation mutants and evidence for conserved domain movement. Biochemistry 45, 12654–12663. doi:10.1021/bi061146z

Webb, R.L., Yasay, G.D., McMartin, C., McNeal, R.B., Zimmerman, M.B., 1989. Degradation of atrial natriuretic peptide: pharmacologic effects of protease EC 24.11 inhibition. J. Cardiovasc. Pharmacol. 14, 285–293.

Webster, C.I., Burrell, M., Olsson, L.-L., Fowler, S.B., Digby, S., Sandercock, A., Snijder, A., Tebbe, J., Haupts, U., Grudzinska, J., Jermutus, L., Andersson, C., 2014. Engineering neprilysin activity and specificity to create a novel therapeutic for Alzheimer's disease. PLoS One 9, e104001. doi:10.1371/journal.pone.0104001

Wei, L., Alhenc-Gelas, F., Corvol, P., Clauser, E., 1991. The two homologous domains of human angiotensin I-converting enzyme are both catalytically active. J. Biol. Chem. 266, 9002–9008.

Wei, L., Clauser, E., Alhenc-Gelas, F., Corvol, P., 1992. The two homologous domains of human angiotensin I-converting enzyme interact differently with competitive inhibitors. J. Biol. Chem. 267, 13398–13405.

Wei, W., 2002. Abeta 17-42 in Alzheimer's disease activates JNK and caspase-8 leading to neuronal apoptosis. Brain 125, 2036–2043. doi:10.1093/brain/awf205

Weiner, M.F., Bonte, F.J., Tintner, R., Ford, N., Svetlik, D., Riall, T., 1992. ACE Inhibitor lacks acute effect on cognition or brain blood flow in Alzheimer's

disease. Drug Dev. Res. 26, 467–471.

Weller, R.O., Galea, I., Carare, R.O., Minagar, A., 2010. Pathophysiology of the lymphatic drainage of the central nervous system: Implications for pathogenesis and therapy of multiple sclerosis. Pathophysiology 17, 295–306. doi:10.1016/j.pathophys.2009.10.007

Weller, R.O., Preston, S.D., Subash, M., Carare, R.O., 2009. Cerebral amyloid angiopathy in the aetiology and immunotherapy of Alzheimer disease. Alzheimer's Res. Ther. 1, 1–13. doi:10.1186/alzrt6

Wildhaber, B.E., Yang, H., Haxhija, E.Q., Spencer, A.U., Teitelbaum, D.H., 2005. Intestinal intraepithelial lymphocyte derived angiotensin converting enzyme modulates epithelial cell apoptosis. Apoptosis 10, 1305–1315. doi:10.1007/s10495-005-2138-y

Williams, A.D., Portelius, E., Kheterpal, I., Guo, J.T., Cook, K.D., Xu, Y., Wetzel, R., 2004. Mapping Aβ amyloid fibril secondary structure using scanning proline mutagenesis. J. Mol. Biol. 335, 833–842. doi:10.1016/j.jmb.2003.11.008

Wilquet, V., Strooper, B. De, 2004. Amyloid-beta precursor protein processing in neurodegeneration. Curr. Opin. Neurobiol. doi:10.1016/j.conb.2004.08.001

Wolf, B.B., Lopes, M.B., VandenBerg, S.R., Gonias, S.L., 1992. Characterization and immunohistochemical localization of alpha 2-macroglobulin receptor (low-density lipoprotein receptor-related protein) in human brain. Am. J. Pathol. 141, 37–42.

Woltjer, R.L., Sonnen, J.A., Sokal, I., Rung, L.G., Yang, W., Kjerulf, J.D., Klingert, D., Johnson, C., Rhew, I., Tsuang, D., Crane, P.K., Larson, E.B., Montine, T.J., 2009. Quantitation and mapping of cerebral detergent-insoluble proteins in the elderly. Brain Pathol. 19, 365–374. doi:10.1111/j.1750-3639.2008.00190.x

Woodman, Z.L., Oppong, S.Y., Cook, S., Hooper, N.M., Schwager, S.L., Brandt, W.F., Ehlers, M.R., Sturrock, E.D., 2000. Shedding of somatic angiotensin-converting enzyme (ACE) is inefficient compared with testis ACE despite cleavage at identical stalk sites. Biochem. J. 347 Pt 3, 711–718. doi:10.1042/0264-6021:3470711

Woodman, Z.L., Schwager, S.L.U., Redelinghuys, P., Carmona, A.K., Ehlers, M.R.W., Sturrock, E.D., 2005. The N domain of somatic angiotensin-converting enzyme negatively regulates ectodomain shedding and catalytic activity. Biochem. J. 389, 739–744. doi:10.1042/BJ20050187

Woodman, Z.L., Schwager, S.L.U., Redelinghuys, P., Chubb, A.J., Van Der Merwe, E.L., Ehlers, M.R.W., Sturrock, E.D., 2006. Homologous substitution of ACE C-domain regions with N-domain sequences: Effect on processing, shedding, and catalytic properties. Biol. Chem. 387, 1043–1051. doi:10.1515/BC.2006.129

World Health Organization, 2012. Dementia: A public health priority, WHO Report. WHO Press, Geneva.

Wright, J.W., Harding, J.W., 2013. The brain renin-angiotensin system: A diversity of functions and implications for CNS diseases. Pflugers Arch. Eur. J. Physiol. doi:10.1007/s00424-012-1102-2

Wright, J.W., Harding, J.W., 2010. The brain RAS and Alzheimer's disease. Exp. Neurol. doi:10.1016/j.expneurol.2009.09.012

Wright, J.W., Harding, J.W., 2008. The angiotensin AT4 receptor subtype as a target for the treatment of memory dysfunction associated with Alzheimer's disease. J. Renin. Angiotensin. Aldosterone. Syst. 9, 226–237. doi:10.1177/1470320308099084

Wright, J.W., Harding, J.W., 2004. The brain angiotensin system and extracellular matrix molecules in neural plasticity, learning, and memory. Prog. Neurobiol. doi:10.1016/j.pneurobio.2004.03.003

Wright, J.W., Harding, J.W., 1997. Important role for angiotensin III and IV in the brain renin-angiotensin system. Brain Res. Brain Res. Rev. 25, 96–124.

Wright, J.W., Kawas, L.H., Harding, J.W., 2013. A Role for the Brain RAS in Alzheimer's and Parkinson's Diseases. Front. Endocrinol. (Lausanne). 4, 158. doi:10.3389/fendo.2013.00158

Wright, J.W., Miller-Wing, A. V, Shaffer, M.J., Higginson, C., Wright, D.E., Hanesworth, J.M., Harding, J.W., 1993. Angiotensin II(3-8) (ANG IV) hippocampal binding: potential role in the facilitation of memory. Brain Res. Bull. 32, 497–502. doi:10.1016/0361-9230(93)90297-O

Wyss-Coray, T., Masliah, E., Mallory, M., McConlogue, L., Johnson-Wood, K., Lin, C., Mucke, L., 1997. Amyloidogenic role of cytokine TGF-beta1 in transgenic mice and in Alzheimer's disease. Nature 389, 603–606. doi:10.1038/39321

Xiao, H.D., Fuchs, S., Frenzel, K., Teng, L., Li, P., Shen, X.Z., Adams, J., Zhao, H., Keshelava, G.T., Bernstein, K.E., Cole, J.M., 2004. The use of knockout mouse technology to achieve tissue selective expression of angiotensin converting enzyme. J. Mol. Cell. Cardiol. doi:10.1016/j.yjmcc.2004.02.013

Xie, L., Helmerhorst, E., Taddei, K., Plewright, B., Van Bronswijk, W., Martins, R., 2002. Alzheimer's beta-amyloid peptides compete for insulin binding to the insulin receptor. J. Neurosci. 22, RC221. doi:20026383

Xu, P., Sriramula, S., Lazartigues, E., 2011. ACE2/ANG-(1-7)/Mas pathway in the brain: the axis of good. Am. J. Physiol. Regul. Integr. Comp. Physiol. 300, R804–R817. doi:10.1152/ajpregu.00222.2010

Yagishita, S., Morishima-Kawashima, M., Ishiura, S., Ihara, Y., 2008. Abeta46 is processed to Abeta40 and Abeta43, but not to Abeta42, in the low density membrane domains. J. Biol. Chem. 283, 733–8. doi:10.1074/jbc.M707103200

Yamauchi, T., Kamon, J., Waki, H., Terauchi, Y., Kubota, N., Hara, K., Mori, Y., Ide, T., Murakami, K., Tsuboyama-Kasaoka, N., Ezaki, O., Akanuma, Y., Gavrilova, O., Vinson, C., Reitman, M.L., Kagechika, H., Shudo, K., Yoda, M., Nakano, Y., Tobe, K., Nagai, R., Kimura, S., Tomita, M., Froguel, P., Kadowaki, T., 2001. The fat-derived hormone adiponectin reverses insulin resistance associated with both lipoatrophy and obesity. Nat. Med. 7, 941–946. doi:10.1038/90984

Yan, P., Hu, X., Song, H., Yin, K., Bateman, R.J., Cirrito, J.R., Xiao, Q., Hsu, F.F., Turk, J.W., Xu, J., Hsu, C.Y., Holtzman, D.M., Lee, J.M., 2006. Matrix metalloproteinase-9 degrades amyloid-β fibrils in vitro and compact plaques in situ. J. Biol. Chem. 281, 24566–24574. doi:10.1074/jbc.M602440200

Yan, S.D., Chen, X., Fu, J., Chen, M., Zhu, H., Roher, A., Slattery, T., Zhao, L., Nagashima, M., Morser, J., Migheli, A., Nawroth, P., Stern, D., Schmidt, A.M., 1996. RAGE and amyloid-beta peptide neurotoxicity in Alzheimer's disease. Nature 382, 685–691. doi:10.1038/382685a0

Yanai, K., Saito, T., Kakinuma, Y., Kon, Y., Hirota, K., Taniguchi-Yanai, K., Nishijo, N., Shigematsu, Y., Horiguchi, H., Kasuya, Y., Sugiyama, F., Yagami, K.I., Murakami, K., Fukamizu, A., 2000. Renin-dependent cardiovascular functions and renin-independent blood- brain barrier functions revealed by renin-deficient mice. J. Biol. Chem. 275, 5–8. doi:10.1074/jbc.275.1.5

Yang, Y., Song, W., 2013. Molecular links between Alzheimer's disease and diabetes mellitus. Neuroscience. doi:10.1016/j.neuroscience.2013.07.009

Yasojima, K., McGeer, E.G., McGeer, P.L., 2001. Relationship between beta amyloid peptide generating molecules and neprilysin in Alzheimer disease and normal brain. Brain Res. 919, 115–121. doi:10.1016/S0006-8993(01)03008-6

Yates, C.J., Masuyer, G., Schwager, S.L.U., Akif, M., Sturrock, E.D., Acharya, K.R., 2014. Molecular and thermodynamic mechanisms of the chloride-dependent human angiotensin-I-converting enzyme (ACE). J. Biol. Chem. 289, 1798–1814. doi:10.1074/jbc.M113.512335

Yokosawa, H., Endo, S., Ogura, Y., Ishii, S., 1983. A new feature of angiotensin-converting enzyme in the brain: hydrolysis of substance P. Biochem. Biophys. Res. Commun. 116, 735–742. doi:10.1016/0006-291X(83)90586-7

Yoon, S.O., Park, D.J., Ryu, J.C., Ozer, H.G., Tep, C., Shin, Y.J., Lim, T.H., Pastorino, L., Kunwar, A.J., Walton, J.C., Nagahara, A.H., Lu, K.P., Nelson, R.J., Tuszynski, M.H., Huang, K., 2012. JNK3 Perpetuates Metabolic Stress Induced by Aβ Peptides. Neuron 75, 824–837. doi:10.1016/j.neuron.2012.06.024

Youssef, I., Florent-Béchard, S., Malaplate-Armand, C., Koziel, V., Bihain, B., Olivier, J.L., Leininger-Muller, B., Kriem, B., Oster, T., Pillot, T., 2008. N-truncated amyloid-β oligomers induce learning impairment and neuronal apoptosis. Neurobiol. Aging 29, 1319–1333. doi:10.1016/j.neurobiolaging.2007.03.005

Yu, X.C., Sturrock, E.D., Wu, Z., Biemann, K., Ehlers, M.R., Riordan, J.F., 1997. Identification of N-linked glycosylation sites in human testis angiotensin-converting enzyme and expression of an active deglycosylated form. J. Biol. Chem. 272, 3511–3519.

Zaman, M.A., Oparil, S., Calhoun, D.A., 2002. Drugs targeting the renin-angiotensin-aldosterone system. Nat. Rev. Drug Discov. 1, 621–636. doi:10.1038/nrd873

Zhao, J., Li, L., Leissring, M.A., 2009. Insulin-degrading enzyme is exported via an unconventional protein secretion pathway. Mol. Neurodegener. 4, 4. doi:10.1186/1750-1326-4-4

Zhao, W.-Q., De Felice, F.G., Fernandez, S., Chen, H., Lambert, M.P., Quon, M.J., Krafft, G.A., Klein, W.L., 2008. Amyloid beta oligomers induce impairment of neuronal insulin receptors. FASEB J. 22, 246–260. doi:10.1096/fj.06-7703com

Zheng, H., Chordia, M.D., Cooper, D.R., Chruszcz, M., Müller, P., Sheldrick, G.M., Minor, W., 2014. Validation of metal-binding sites in macromolecular structures with the CheckMyMetal web server. Nat. Protoc. 9, 156–170.

doi:10.1038/nprot.2013.172

Zheng, H., Jiang, M., Trumbauer, M.E., Sirinathsinghji, D.J., Hopkins, R., Smith, D.W., Heavens, R.P., Dawson, G.R., Boyce, S., Conner, M.W., Stevens, K. a, Slunt, H.H., Sisoda, S.S., Chen, H.Y., Van der Ploeg, L.H., 1995. beta-Amyloid precursor protein-deficient mice show reactive gliosis and decreased locomotor activity. Cell 81, 525–31. doi:0092-8674(95)90073-X [pii]

Zhu, D., Shi, J., Zhang, Y., Wang, B., Liu, W., Chen, Z., Tong, Q., 2011. Central angiotensin II stimulation promotes β-amyloid production in Sprague Dawley rats. PLoS One 6, e16037. doi:10.1371/journal.pone.0016037

Zhu, X., Smith, M.A., Honda, K., Aliev, G., Moreira, P.I., Nunomura, A., Casadesus, G., Harris, P.L.R., Siedlak, S.L., Perry, G., 2007. Vascular oxidative stress in Alzheimer disease. J. Neurol. Sci. 257, 240–246. doi:10.1016/j.jns.2007.01.039

Zhu, Y., Nwabuisi-Heath, E., Dumanis, S.B., Tai, L.M., Yu, C., Rebeck, G.W., Ladu, M.J., 2012. APOE genotype alters glial activation and loss of synaptic markers in mice. Glia 60, 559–569. doi:10.1002/glia.22289

Zhu, Y., Shan, X., Yuzwa, S.A., Vocadlo, D.J., 2014. The emerging link between O-GlcNAc and Alzheimer disease. J. Biol. Chem. 289, 34472–81. doi:10.1074/jbc.R114.601351

Zhu, Y.Z., Chimon, G.N., Zhu, Y.C., Lu, Q., Li, B., Hu, H.Z., Yap, E.H., Lee, H.S., Wong, P.T., 2000. Expression of angiotensin II AT2 receptor in the acute phase of stroke in rats. Neuroreport 11, 1191–1194. doi:10.1097/00001756-200004270-00009

Zigman, W.B., Devenny, D.A., Krinsky-McHale, S.J., Jenkins, E.C., Urv, T.K., Wegiel, J., Schupf, N., Silverman, W., 2008. Alzheimer's Disease in Adults with Down Syndrome. Int. Rev. Res. Ment. Retard. 36, 103–145. doi:10.1016/S0074-7750(08)00004-9

Zirah, S., Kozin, S. a, Mazur, A.K., Blond, A., Cheminant, M., Ségalas-Milazzo, I., Debey, P., Rebuffat, S., 2006. Structural changes of region 1-16 of the Alzheimer disease amyloid β-peptide upon zinc binding and in vitro aging. J. Biol. Chem. 281, 2151–2161. doi:10.1074/jbc.M504454200

Zlokovic, B. V., 2004. Clearing amyloid through the blood-brain barrier. J. Neurochem. doi:10.1111/j.1471-4159.2004.02385.x

Zolezzi, J.M., Inestrosa, N.C., 2013. Peroxisome proliferator-activated receptors and alzheimer's disease: Hitting the blood-brain barrier. Mol. Neurobiol. doi:10.1007/s12035-013-8435-5

Zou, K., Kim, D., Kakio, A., Byun, K., Gong, J.S., Kim, J., Kim, M., Sawamura, N., Nishimoto, S.I., Matsuzaki, K., Lee, B., Yanagisawa, K., Michikawa, M., 2003. Amyloid β-protein (Aβ)1-40 protects neurons from damage induced by Aβ1-42 in culture and in rat brain. J. Neurochem. 87, 609–619. doi:10.1046/j.1471-4159.2003.02018.x

Zou, K., Maeda, T., Watanabe, A., Liu, J., Liu, S., Oba, R., Satoh, Y.I., Komano, H., Michikawa, M., 2009. Aβ42-to-Aβ40- and angiotensin-converting activities in different domains of angiotensin-converting enzyme. J. Biol. Chem. 284, 31914–31920. doi:10.1074/jbc.M109.011437

Zou, K., Yamaguchi, H., Akatsu, H., Sakamoto, T., Ko, M., Mizoguchi, K., Gong, J.-S., Yu, W., Yamamoto, T., Kosaka, K., Yanagisawa, K., Michikawa, M., 2007. Angiotensin-converting enzyme converts amyloid beta-protein 1-42 (Abeta(1-42)) to Abeta(1-40), and its inhibition enhances brain Abeta deposition. J. Neurosci. 27, 8628–8635. doi:10.1523/JNEUROSCI.1549-07.2007

Zubenko, G.S., Volicer, L., Direnfeld, L.K., Freeman, M., Langlais, P.J., Nixon, R.A., 1985. Cerebrospinal fluid levels of angiotensin-converting enzyme in Alzheimer's disease, Parkinson's disease and progressive supranuclear palsy. Brain Res. 328, 215–221.